Co-expression of GAD67 and Choline Acetyltransferase in Neurones in the Mouse Spinal Cord and Medulla Oblongata

Jittima Gotts

Submitted in accordance with the requirements for the degree of Doctor of Philosophy

University of Leeds

School of Biomedical Sciences

September 2015

The candidate confirms that the work submitted is her own, except where work which has formed part of jointly authored publications has been included. The contribution of the candidate and the other authors to this work has been explicitly indicated below. The candidate confirms that appropriate credit has been given within the thesis where reference has been made to the work of others.

Chapter 4 incorporates material from a jointly authored publication, the details of which are as follows:

> Gotts, J., Atkinson, L., Edwards, I.J., Yanagawa, Y., Deuchars, S.A. & Deuchars, J. 2015 Co-expression of GAD67 and choline acetyltransferase reveals a novel phenotype in the mouse medulla oblongata. *Auton Neurosci.* 2015 May 16. pii: S1566-0702(15)00053-3. doi: 10.1016/j.autneu.2015.05.003.

All the experimental work (including preparation and analysis), plus the original figures and text upon which the publication was based, were directly and solely attributable to myself, J. Gotts.

L. Atkinson developed the publication manuscript, plus selected and optimised the final figures from those provided by J. Gotts.

I.J. Edwards taught J. Gotts the experimental techniques that she used in the publication.

Y. Yanagawa provided the GAD67-GFP knock-in mice used in the publication.

J. Deuchars and S.A. Deuchars devised the experiments and proofed the publication manuscript.

Acknowledgements

I would like to thank Jim and Sue for their patience, support and endless guidance over the last four years.

Special thanks to Ian, the master of everything; Brenda, the queen of immuno; Yusoff, my PhD buddy and GP; Aaron, my lovely Uni brother and job forwarder; Kaisan, the endnote specialist; plus Calvin, Yazi and Kinon, spinal cord gurus. I would like to thank all the members of the Deuchars group who have been present during the course of my studies, both past and current, who although I have not mentioned by name have all helped me in different ways.

I would like to thank my mum and dad who have given me tremendous support in my pursuit of a PhD, and have been patiently waiting (for over 3 years) for our reunion upon completion of my PhD studies. Thank you for being such wonderful parents who love me unconditionally and inspire me to believe in what I love to do. I would like to thank my wonderful brother, sister and friends, Pepsi, X, Nigel, Nat, Katie, Roger, Lih Tyng, Nazlah, Karoliina, Gareth, Mukti, Farid, Kirati, Tommy, Muay, Fah, Kai, Tira, Gib, Olin, Teay, Piying and Yam who have always been there and given me support. I would like to thank all the staff in the anatomy group plus all the anatomy demonstrators at the University of Leeds who I have worked with. It has been a great pleasure working with such lovely people.

Finally I would like to thank the Faculty of Biological Sciences, who provided me with an anatomy demonstrating PhD studentship. Without this funding I would not be in the position of writing my PhD thesis now.

Abstract

GABAergic and cholinergic interneurones play an important role in modulating activity of neuronal circuits within the spinal cord and medulla oblongata. This study investigates the spatial distribution of co-localisation of the synthesising enzymes for ACh/GABA in the spinal cord and medulla oblongata. Immunohistochemistry, retrograde neuronal tracing and juxtacellular labelling were employed in combination with mice in which a green fluorescent protein (GFP) is expressed under the control of the promoter of the GABA synthesising enzyme, glutamic acid decarboxylase 67 (GAD67-GFP mice). Within the cervical, thoracic and lumbar spinal cord the majority of GAD67-GFP neurones co-localising with the ACh synthesising enzyme choline acetyltransferase (ChAT) were observed in lamina X. Located primarily ventral to the central canal, they were neither motoneurones nor preganglionic neurones since they were negative for Fluorogold transported retrogradely following intraperitoneal injections. On application of juxtacellular labelling to neurones in spinal cord slices from young mice, the processes of the ChAT/GAD67-GFP neurone were located in lamina X. Investigations into synaptic inputs indicated that ChAT/GAD67-GFP neurones in lamina X received inputs from terminals immunoreactive for vesicular glutamate transporter 1, vesicular glutamate transporter 2, glycine transporter 2 and GAD67. Co-expression of ChAT/GAD67-GFP was also observed in the medulla oblongata in the nucleus of tractus solitarius, area postrema and reticular formation. Although the function of these ChAT/GAD67-GFP neurones is currently unknown, this study has furthered knowledge regarding their morphology, location, possible projections and inputs.

Table of Contents

List of Tables

List of Figures

Lists of Abbreviations

AChE	Acetylcholinesterase
AP	Area postrema
AS-ODN	Antisense oligodeoxynucleotide
AU	Arbitrary Unit
CAA	Central autonomic area
CB-HRP	Cholera Toxin B chain conjugated to HRP
CC	Central canal
Ce	Central subnucleus of the NTS
ChAT	Choline acetyltransferase
com	Commissural subnucleus of the NTS
CSFcCs	Cerebrospinal fluid contacting cells
CTB	Cholera toxin subunit B
Cu	Cuneate nucleus
DHβE	Dihydro-β-erythoidine
dl	Dorsolateral subnucleus of the NTS
dm	Dorsomedial subnucleus of the NTS
DMPP	1, 1 – dimethyl-4-phenyl-piperazinium
DRG	Dorsal root ganglion
EGFP	Enhanced GFP
GAD	Glutamic acid decarboxylase
GAD65	Glutamic acid decarboxylase isoform 65

GAD67	Glutamic acid decarboxylase isoform 67
GFP	Green fluorescent protein
GIN	GFP-expressing inhibitory neurones
GlyT2	Glycine transporter 2
GPCR	G protein-coupled receptor
Gr	Gracile nucleus
HRP	Horseradish Peroxidase
IHC	Immunohistochemistry
IML	Intermediolateral cell column
IMLf	Funicular intermediolateral nucleus
IMLp	Principal intermediolateral nucleus
IMM	Intermediomedial nucleus
ins	Interstitial subnucleus of the NTS
int	Intermediate subnucleus of the NTS
IR	Immunoreactive
ISH	In Situ Hybridization
Isl1	Islet-1
IV	Fourth ventricle
lat	Lateral subnucleus of the NTS
LGIC	Ligand gated ion channel
LHA	Lateral hypothalamic area
Lhx3	LIM homeobox 3 transcription factor
LPGN	Lateral paragigantocellular nucleus

m	Medial subnucleus of the NTS
mAChRs	Muscarinic ACh receptors
MCH	Melanin-concentrating hormone
n	Number of animals used
N	Number of neurones counted
nAChRs	Nicotinic ACh receptors
nNOS	Neuronal nitric oxide synthase
NOS	Nitric oxide synthase
nsc	Number of sections counted
NTS	Nucleus of tractus solitarius
PBN	Lateral parabrachial nucleus
PHA-L	Phaseolus vulgaris leucoagglutinin
PPG	Pre-proglucagon
PRV	Pseudorabies virus
PVN	Hypothalamic paraventricular nucleus
Shh-N	Sonic hedgehog N-terminus recombinant protein
SPGN	Sympathetic postganglionic neurones
SPNs	Sympathetic preganglionic neurones
ST	Solitary tract
v	Ventral subnucleus of the NTS
VAChT	Vesicular acetylcholine transporter
VGAT	Vesicular GABA transporter
VGLUT1	Vesicular glutamate transporter 1

VGLUT2	Vesicular glutamate transporter 2
VIAAT	Vesicular inhibitory amino acid transporter
vl	Ventrolateral subnucleus of the NTS
WGA	Wheat germ agglutinin
WGA-HRP	Wheat germ agglutinin-conjugated HRP
X	Dorsal vagal nucleus
XII	Hypoglossal nucleus
YFP	Yellow fluorescent protein

Publications

Gotts, J., Atkinson, L., Edwards, I.J., Yanagawa, Y., Deuchars, S.A. & Deuchars, J. 2015 Co-expression of GAD67 and choline acetyltransferase reveals a novel phenotype in the mouse medulla oblongata. *Auton Neurosci.* 2015 May 16. pii: S1566-0702(15)00053-3. doi: 10.1016/j.autneu.2015.05.003.

1 General Introduction

1.1 General Introductory paragraph

This introductory chapter will describe the gross anatomy of the spinal cord, the laminar structure of the spinal grey matter, development of the various neuronal populations in the spinal cord with an emphasis on those that develop within the ventral neural tube, the neurochemical classification of spinal neurones with a focus on acetylcholine (ACh) and gamma amino butyric acid (GABA), plus a general introduction to the autonomic nervous system with particular emphasis on the sympathetic nervous system. In addition, since the nucleus of tractus solitarius (NTS) of the medulla oblongata has a significant role as the primary integration site for the autonomic nervous system (Loewy and Burton, 1978, Ross et al., 1985, Zoccal et al., 2014) , an introduction to the NTS will be provided in detail within this chapter.

1.2 Gross anatomy of the spinal cord: segmental variation

The mouse spinal cord is a near cylindrical shaped structure. Rostrally, it starts at the level of foramen magnum (extending from the inferior end of the hindbrain) and runs down to terminate at the inferior aspect of the vertebral column. The caudal end of the spinal cord, termed the conus medullaris, gives rise to a structure called the filum terminale; a thread of fibrous tissue originating from the pia and enclosed by arachnoid mater. Distally, the spinal cord is attached to the vertebral column by the filum terminale (Sengul and Watson, 2012). Commonly, there are 7 cervical, 13 thoracic, 6 lumbar, 4 sacral and 28 caudal vertebrae in a mouse. This gives rise to a total of 34 spinal cord segments, which comprise 8 cervical segments (C1 to C8), 13 thoracic segments (T1 to T13), 6 lumbar segments (L1 to L6), 4 sacral segments (S1 to S4) and 3 coccygeal segments (Co1 to Co3) (Sengul et al., 2012, Sengul and Watson, 2012). The gross outline of the cord is not the same along its entirety. The width of the cord is greater in the cervical (C5-T1) and lumbosacral (L2-L6) enlargements, where increased numbers of motoneurones are located for the innervation of the forelimbs and hindlimbs respectively (Watson and Kayalioglu, 2009, Sengul and Watson, 2012, Sengul et al., 2012, Harrison et al., 2013).

The spinal cord is primarily comprised of grey matter and white matter. For the most part, the grey matter is encased by the white matter (Watson and Kayalioglu, 2009).

The white matter predominantly contains axons and glial cells, while the grey matter mostly contains the cell bodies and processes of neurones and glial cells. In a transverse section, the grey matter appears to resemble a butterfly or the capital “H” in shape; consisting of two ventral (anterior) horns and two dorsal (posterior) horns, linked together (at each side) via intermediate grey matter. Commissural grey matter constitutes the cross connection between the two sides or uprights of the “H”. In two regions of the spinal cord, specifically the thoracic and upper lumbar areas, an area termed the intermediolateral horn (lateral horn) is present (Watson and Kayalioglu, 2009, Snell, 2010) (see Figure 1.1).

The gross morphology of transverse cord sections for each region in mice differs from one another. Segmental variations of the cervical, thoracic and lumbar cord regions will be described in due course as they are the regions of interest. The cervical cord has an oval transverse sectional profile. The ventral horns at the cervical enlargements (C5-T1) contain a large number of motoneurone clusters which innervate the forelimbs and the axial muscles (Watson et al., 2009, Sengul and Watson, 2012, Sengul et al., 2012, Harrison et al., 2013, Allen Brain Atlas: Mouse Spinal Cord). Transverse sections from the thoracic region exhibit a round profile and are smaller in size than sections taken from either of the cervical and lumbar cord segments. The grey matter of the ventral and dorsal horns are slender in comparison to those in the cervical and lumbar regions. The ventral horn contains smaller clusters of motoneurones which innervate only the axial and intercostal muscles (Watson et al., 2009, Harrison et al., 2013, Allen Brain Atlas: Mouse Spinal Cord). The lateral horn is found throughout the thoracic cord and is where the sympathetic preganglionic neurones (SPNs) of the intermediolateral cell column (IML) are located (Petras and Cummings, 1972, Anderson et al., 2009, Watson and Kayalioglu, 2009, Sengul et al., 2012). The transverse section of the lumbar region has an oval profile similar to that of the cervical region but smaller in diameter and more rounded. The H-shaped grey matter in the lumbar cord sections is large, of which the ventral horns contain motoneurones clusters that innervate the hindlimbs and the axial muscles. This leads to the lumbosacral enlargement at L2-L6 segments (Watson et al., 2009, Sengul and Watson, 2012, Sengul et al., 2012, Harrison et al., 2013, Allen Brain Atlas: Mouse Spinal Cord). The lateral horns, containing SPNs of the IML, are also found in L1-L2 cord segments (Anderson et al., 2009, Sengul and Watson, 2012). Transverse sections taken from the sacral and coccygeal regions have a round profile, the diameter of which rapidly reduces as the cord progresses caudally (Watson et al., 2009, Harrison et al., 2013, Allen Brain Atlas: Mouse Spinal Cord). The grey matter constitutes most of the cross-sectional area for both of these cord regions, with a much

smaller volume of white matter surrounding it (Watson et al., 2009, Allen Brain Atlas: Mouse Spinal Cord).

Since our study only focuses on the distribution of neurones in the cervical, thoracic and lumbar cord segments, a diagram representing the segmental variation of these regions for transverse section is presented in Figure1.1.

The spinal cord in mice, in similarity with that for humans and rats, receives its arterial supply from a single anterior spinal artery, two posterior spinal arteries, and radicular arteries (Lang-Lazdunski et al., 2000, Bilgen and Al-Hafez, 2006). The anterior spinal artery, which arises from a union of two branches originating from the two vertebral arteries (Lang-Lazdunski et al., 2000, Scremin, 2009, Sengul and Watson, 2012), descends caudally on the anterior surface of the cord to the conus medullaris. The anterior spinal artery is joined by anterior radicular arteries, which run transversely to enter the spinal canal via the intervertebral foraminae (Lang-Lazdunski et al., 2000, Scremin, 2009). The two posterior spinal arteries originate from the vertebral arteries (Sengul and Watson, 2012), and descend longitudinally on the posterior surface of the cord (Bilgen and Al-Hafez, 2006). They are joined by numerous posterior radicular arteries (Lang-Lazdunski et al., 2000, Scremin, 2009). The radicular arteries derive from various origins, including the vertebral, deep cervical, intercostals, sacral and hypogastric arteries (Lang-Lazdunski et al., 2000). The venous system of the cord reflects the arterial system. It includes three anterior spinal and three posterior spinal veins which are interconnected and drained by anterior and posterior radicular veins. The radicular veins drain into the internal vertebral venous plexus occupying the epidural space. The internal vertebral venous plexus additionally interconnects with the external vertebral venous plexus along the external vertebral surfaces (Scremin, 2009, Sengul and Watson, 2012, Farrar et al., 2015).

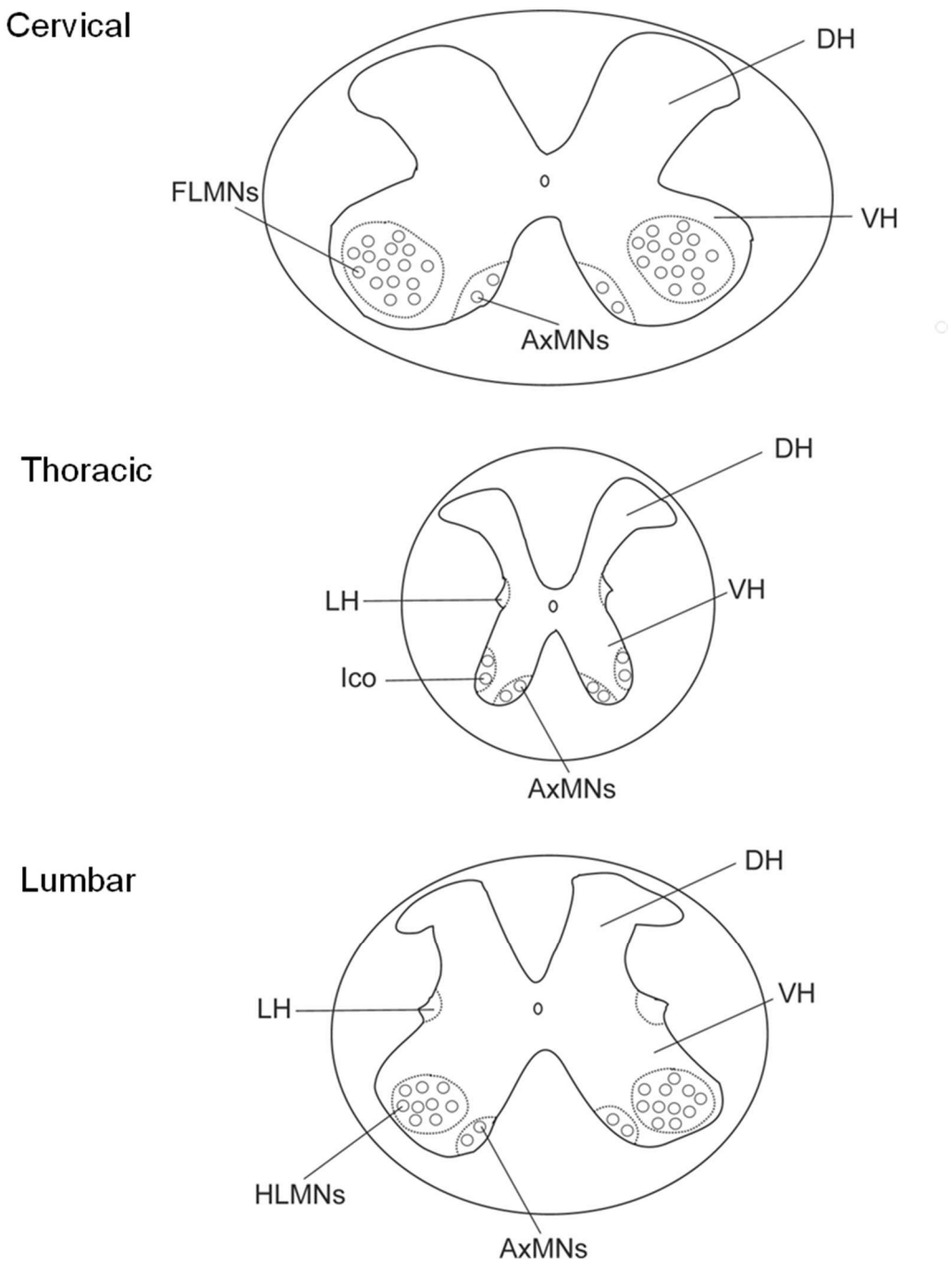

Figure 1.1: Diagramatic representation of the segmental variations of the mouse cervical, thoracic and lumbar transverse cord sections (Figure adapted from Watson et al., 2009, Harrison et al., 2013, Allen Brain Atlas: Mouse Spinal Cord). VH: ventral horn; DH: dorsal horn; LH: lateral horn, FLMNs: forelimb motoneurones; HLMNs: hindlimb motoneurones; AxMNs: Axial motoneurones; Ico: intercostal motoneurones.

1.3 The laminae of Rexed

The laminal organization of the spinal cord is defined based on the cytological features, cell body dimension, cell orientation and density of packing of the neurones present in the grey matter of the spinal cord. Accordingly the grey matter is classified into 10 regions or laminae. These were first described by Rexed (Rexed, 1952) from their investigations of cat spinal cord utilising the toluidine blue staining technique and are briefly described below. With the exception of lamina X, which is located about the central canal, the numbering scheme used for the laminae relates to their dorsal to ventral order across the grey matter (see Figure 1.2). Since this study is concerned with investigating cell types within the laminae, with a particular focus on those in lamina X, a brief summary of the known cell-types in specific laminae are also described.

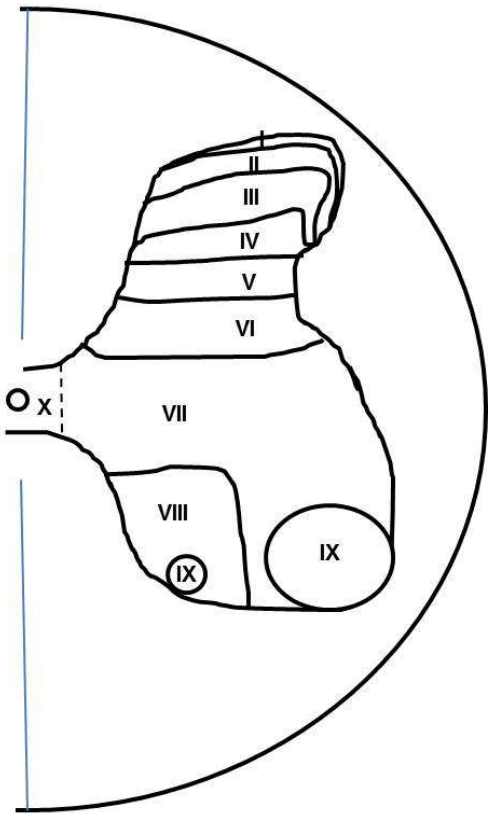

Figure 1.2: The laminae of Rexed. The lamination of the grey matter of the spinal cord can be organised into ten laminae based on morphology (shape and size) and cytoarchitectural arrangement. Figure adapted from Rexed, 1952.

Lamina I

Lamina I is the most dorsal section of the grey matter in the dorsal horn. It occupies a narrow area lying parallel to the curvature of the dorsal horn. Within lamina I the cells possess different shapes (triangular and spindle) and sizes (small, medium and relatively large; the smallest are 5 μm x 8-10 μm and the largest are 15-25 μm x 30 μm, with the majority of neurones in the range 8-10 μm x 12-15 μm) and are loosely scattered (Rexed, 1952, Rexed, 1954). In mouse spinal cord, various cell shapes and sizes are also observed in lamina I, including large elongated, smaller triangular, multipolar and fusiform (Sengul and Watson, 2012).

Lamina II

Lamina II is thicker in appearance than lamina I (Rexed, 1952) and, due to the high density of its constituent cells, forms a distinct feature across the dorsal horn. Lamina II is also known as the substantia gelatinosa Rolandi. The cells in lamina II are small in size (ranging from 5 μm x 5 μm to 10 μm x 10 μm) (Rexed, 1952, Rexed, 1954).

With regard to the mouse spinal cord, the neurones in lamina II are similarly small sized cells and possess either rounded or elongated shapes. Due to the lack of myelinated nerve fibres within the region, lamina II appears as a semi-transparent area. Lamina II can be divided into 2 zones, a ventral inner zone (lamina IIi) and a dorsal outer zone (lamina IIo). The neurones of the dorsal outer zone are smaller than those in the ventral inner zone and more crowded (Sengul and Watson, 2012).

Lamina II interneurones are classified into islet, central, vertical, radial and medio-lateral cells based on their morphology and the orientation of their process arborization (Grudt and Perl, 2002, Lu and Perl, 2003, Hantman et al., 2004, Lu and Perl, 2005). Islet cells possess dendrites and axons that extend more rostro-caudally than any other lamina II cell type. Central cells have a morphology similar to the islet cells, but with less extensive dendritic branching in the rostro-caudal axia. Vertical cells exhibit a dendritic arbour which, relatively, has a significant extension along the dorso-ventral orientation. Radial cells possess soma which are located adjacent to the border of lamina IIo and IIi. The medio-lateral cells possess dendrites that extend in the medio-lateral orientation (Grudt and Perl, 2002).

Lamina III

The cells in lamina III are relatively small in size (most cells are 7-8 μm x 10-12 μm in size, with the smallest being 5 μm x 7-8 μm and the largest approximately 10-12 μm x 15-18 μm), although slightly larger than those comprising lamina II. Like laminae I and II, lamina III also curves laterally, however the degree of curvature in Lamina III is not as pronounced (Rexed, 1952).

In relation to the mouse spinal cord a differentiating feature between lamina III and lamina II is that the former contains myelinated nerve fibres, while the latter is devoid of such fibres. A variety of cell shapes are observed within lamina III, including round, elongate, and spindle (Sengul and Watson, 2012). The majority of cells in the lamina have diameters ranging from 7 μm to 12 μm (Sengul et al., 2012).

A large number of neurones in laminae I-III have axons that project within the spinal cord, and so are termed interneurones. Nearly all neurones in lamina II and the majority of those in laminae I and III are interneurones (Todd, 2010). Interneurones of the dorsal horn are either excitatory, using glutamate, or inhibitory, using GABA and/or glycine as their primary neurotransmitter. In rat approximately 25%, 30% and 40% of interneurones in laminae I, II and III respectively, contain GABA (Polgar et al., 2003, Todd, 2010). Moreover, for laminae I-III cells that contain glycine typically also contain GABA (Todd and Sullivan, 1990, Polgar et al., 2013). By contrast, while the majority of ChAT-IR neurones in lamina III are found to contain GABA (Todd, 1991, Mesnage et al., 2011), those neurones do not contain glycine (Todd, 1991). Projection neurones are primarily concentrated within lamina I plus scattered across laminae III – VI, with a limited number to be found in lamina II (Todd, 2010). Many of the axons from the projection neurones in the dorsal horn project across the midline and ascend rostrally within the white matter, terminating in nuclei of the brainstem and thalamus which are involved in pain and temperature perception.

Lamina IV

A distinguishable feature between lamina IV and lamina III is that the former contains cells of various sizes (small – ranging between 7-9 μm x 10-12 μm – medium – generally 10-12 μm x 15-18 μm – and large – 35 μm x 45 μm), while the latter generally contains cells that are of the smaller sizes (Rexed, 1952, Rexed, 1954).

With respect to the mouse, in appearance lamina IV is more substantial than laminae I-III. However, the concentration of neurones within it is less. Moreover, only a limited number of large neurones are observed. Even so, a considerable variance in cell size is also apparent in lamina IV of mice, with the smallest being 7-10 μm in diameter and the largest being 35-45 μm (Sengul and Watson, 2012, Sengul et al., 2012).

Lamina V

In comparison to laminae I to IV, lamina V contains fewer cells but a greater abundance of nerve fibres; in fact the nerve bundles are both numerous and sizeable in the lateral region of lamina V (Rexed, 1952, Rexed, 1954). Lamina V can be divided into medial and lateral zones (Rexed, 1954). The cells of the medial zone tend to be medium in size (10-13 μm x 15-20 μm), while those of the lateral zone include a higher abundance of larger cells (up to 30 μm x 45 μm) in cat (Rexed, 1952, Rexed, 1954) .

Similarly, in mouse the lateral part of lamina V also contains sizeable groups of nerve fibres and neurones which are large in size (diameters ranging from 30-45 μm) (Sengul and Watson, 2012, Sengul et al., 2012), while the medial part is absent of such fibre groups and consists of neurones that are relatively small to medium in size. Moreover, in mouse the shapes of the neurones found in lamina V are triangular, multipolar and spindle (Sengul and Watson, 2012).

Lamina VI

Lamina VI is located at the base of the dorsal horn (Rexed, 1954). It is comprised of medial and lateral zones. The medial zone contains cells that are relatively densely congregated and these are typically small (8 μm x 8 μm at a minimum) or medium (10-12 μm x 12-15 μm) in size; the majority being in the medium range. By contrast, the cells of the lateral zone are generally less densely distributed and include cells of larger size (30 μm x 35 μm) exhibiting a star shape (Rexed, 1952, Rexed, 1954).

In regard to the mouse spinal cord, the neurones found in this lamina possess elongated, spindle, triangular and multipolar shapes. Similar to cat, lamina VI in mouse is composed of a medial part whose form appears compact, and a lateral part whose form appears reticulated (Sengul and Watson, 2012).

GAD65 expressing inhibitory interneurones located in the medial portions of laminae V and VI are the origin of P boutons in lamina IX, which provide presynaptic inhibition of Ia afferent terminals (Hughes et al., 2005); where the term Ia indicates a primary muscle spindle afferent.

Lamina VII

Lamina VII covers an area in the middle part of the grey matter that was previously recognized as the zona intermedia (Rexed, 1952) and is alternatively termed as the intermediate grey (Sengul and Watson, 2012). The cells in lamina VII are typically medium in size (13-15 μm x 15-20 μm), although some can be relatively large in size (up to 40 μm x 50 μm), possess a star shape and are uniformly though not densely distributed, giving the lamina a homogeneous aspect (Rexed, 1952, Rexed, 1954).

In the mouse spinal cord, the neurones (possessing multipolar, triangular and fusiform in shapes) of this lamina are likewise uniformly dispersed. Moreover, the lamina contains several nuclei that have been given specific names depending on their cord levels; from C1 to C4 there is the central cervical nucleus, from T1 to L2 there are the intermediolateral, intercalated and intermediomedial nuclei, from L1 to L2 there is the lumbar dorsal commissural nucleus, from L6 to S4 there is the sacral dorsal commissural nucleus, from S1 to S4 there is the sacral precerebellar nucleus, and from S1 to S2 there is the sacral parasympathetic nucleus (Sengul and Watson, 2012).

Renshaw cells are found in lamina VII (Lagerback and Kellerth, 1985, Song et al., 2006) and are glycinergic (Curtis et al., 1976). Renshaw cells receive excitatory innervation from motoneurones and then subsequently inhibit motoneurones plus also Ia inhibitory interneurones (Sapir et al., 2004). Ia inhibitory interneurones are located in lamina VII, particularly dorsal or dorsomedial to the motoneurones (Jankowska and Lindstrom, 1972).

Lamina VIII

In the thoracic cord region lamina VIII occupies an area which encompasses both the base and the core of the ventral horn. However in other regions, due to the presence of increased numbers of motoneurones within the ventral horn, lamina VIII is only found in the medial half of the ventral horn. Lamina VIII contains cells of various sizes (for cats

the range spans from the smallest at 10 μm x 10 μm to the largest at 50 μm x 60 μm, and while there is no particularly dominant size present, an appreciable number of cells exhibit sizes in the range 10-15 μm x 15-20 μm) and as a result seems heterogeneous in feature in the spinal cord of both cats (Rexed, 1952) and mice (Sengul and Watson, 2012).

With respect to mouse spinal cord the large cells in lamina VIII closely resemble motoneurones in form. Furthermore, a large proportion of neurones in the lamina notably possess dendrites which exhibit a dorsoventral orientation. The commissural fibres from some of the neurones in the lamina are contralateral projecting fibres, since they extend to the ventral horn on the opposite side (Sengul and Watson, 2012).

Commissural interneurones have been observed within laminae VI, VII and VIII, and are either excitatory using glutamate, or inhibitory using glycine. These interneurones may excite or inhibit contralateral motoneurones in the ventral horn (Bannatyne et al., 2003).

Lamina IX

Lamina IX contains large sized motoneurones (Rexed, 1952, Heise and Kayalioglu, 2009a), the most commonly observed size appearing to be around 30 μm x 40 μm. In some spinal cord segments two distinct groups of motoneurones are discerned, corresponding to medial and lateral cell columns (Rexed, 1952, Rexed, 1954).

Mouse lamina IX contains α-motoneurones (involved in the innervation of skeletal muscles and which are relatively large (Weber et al., 1997, Sengul and Watson, 2012)), possessing diameters of more than 30 μm (Wootz et al., 2013), and γ-motoneurones (involved in the innervation of muscle spindles), which are relatively smaller in size. Whereas most alpha motoneurones receive direct input from Ia-derived proprioceptive sensory afferents, gamma motoneurones do not receive such direct input (Friese et al., 2009). In addition, interneurones and a limited quantity of β-motoneurones can also be found in the lamina (Sengul and Watson, 2012). It should be noted that the designation of motoneuron classification based on size in the literature is inconsistent, with different groups utilising diameter, cross-sectional area or estimated volume (Weber et al., 1997, d'Errico et al., 2013).

Lamina X

Lamina X, also termed area X or the central grey of the spinal cord (Rexed, 1952, Rexed, 1954, Watson and Kayalioglu, 2009, Heise and Kayalioglu, 2009a, Deuchars, 2015), is the area surrounding the central canal containing the grey commissures and the substantia gelatinosa centralis. The abundance of nerve fibres in the lamina is relatively low (Rexed, 1954).

The neurones found in lamina X of mice are triangular, multipolar and spindle shaped; the lamina contains two named nuclei, these being the paraependymal part of the intercalated nucleus (central autonomic area (CAA)) plus the cholinergic central canal cluster neurones (Sengul and Watson, 2012).

In rats, lamina X contains large cells of 40-50 μm in diameter as well as smaller cells possessing diameters of 20-30 μm (Nicholas et al., 1999). For mice, cells within lamina X are reported to typically range about two diameters, 7 μm and 20 μm, while the ependymal cells which line the central canal are indicated as being 6-7 μm in diameter (Fornai et al., 2014).

1.4 The arborisaton of primary afferent inputs in various laminae

Primary afferent fibres of various modalities arborise in the dorsal horn laminae. Generally, the majority of the large myelinated cutaneous (Aβ) afferents are low-threshold mechanoreceptors which respond to touch or hair movement, while most of the finely myelinated (Aδ) and unmyelinated (C) afferent fibres convey nociceptive or thermoreceptive information (Todd, 2010, Abraira and Ginty, 2013).

The primary afferent axons of mechanoreceptors involved in the detection of the discriminative touch and tactile perception (such as pressure, vibration, stretch of the skin and hair deflection air) can be categorised based on the morphology of the peripheral mechanosensory end organs that they innervate (Luo et al., 2009). Conduction velocity, which is a property of fibre size and degree of myelination, plus physiological properties are also used to categorise the primary afferent axons (Luo et al., 2009, Todd, 2010). The majority of the primary afferents of mechanoreceptors are low-threshold large diameter fibres (Luo et al., 2009). Although Woolf and Fitzgerald

mapped the termination of Aβ low-threshold afferents in laminae III and IV (Woolf and Fitzgerald, 1986), the arborisation of myelinated low-threshold mechanoreceptive afferent fibres responding to touch or hair movement can be observed to terminate in an area which spans from laminae IIi to VI (LaMotte, 1977, Todd, 2010). Myelinated Aδ hair afferent fibres terminate in lamina III with extensions into laminae IIi and IV (Light and Perl, 1979, Djouhri, 2016). Mechanoreceptors can be further categorised into two groups dependent upon the rate of their adaptation to sustained mechanical stimuli. These two groups are the rapidly adapting (RA) and slowly adapting (SA) mechanoreceptors (Brown and Iggo, 1967, Luo et al., 2009). The RA mechanoreceptors are reported to terminate in laminae III to V (Luo et al., 2009), similarly, the axon arborisation of SA mechanorectors are to be found in laminae III and IV, plus the dorsal part of lamina V (Brown et al., 1978). Ia muscle spindle afferents are found to terminate in various laminae; including V, VI, VII and IX with the largest distribution in lamina IX (Ishizuka et al., 1979). GABAergic neurones in laminae V and VI have been identified as the source of ventral horn P boutons that form axo-axonic synapse with Ia afferent terminals involved in motor output regulation (Maxwell et al., 1990, Hughes et al., 2005). These GABAergic P boutons can be distinguished from other GABAergic terminals in the ventral horn by their strong expression of the GAD65 isoform, which is in contrast to the majority of GABAergic terminals in the ventral horn that possess strong GAD67 and low GAD65 immunoreactivity (Hughes et al., 2005).

Aδ and C afferents fibres, which can be nociceptive or thermoreceptive, predominantly terminate in lamina I and II (Todd, 2010). Aδ nociceptive afferents have additionally been observed in laminae I and V (Light and Perl, 1979, Djouhri, 2016). Nociceptive C afferent fibres can be divided into 2 neurochemical subgroups, those that express neuropeptides and those that are devoid of neuropeptides, peptidergic and nonpeptidergic respectively (Hunt and Rossi, 1985, Todd, 2010). The peptidergic afferents predominantly terminate in lamina I and IIo, while non-peptidergic afferents largely terminate in lamina IIi (Hunt and Rossi, 1985).

1.5 Development of the various neuronal populations in the spinal cord with a focus on those that develop within the ventral neural tube

An alternative way to describe neuronal cell types within the spinal cord is through the application of knowledge in relation to spinal cord development and cell differentiation. This section will discuss the neuronal types that develop within the spinal cord, focusing on those that generate within the ventral neural tube.

The nervous system of vertebrates develops from what is termed the neural plate (Pituello, 1997) and starts with the plate induction (Tanabe and Jessell, 1996); the plate subsequently folds during maturation to form the neural tube. Determination of cell patterning in the CNS is largely dependent on where a given induced neural cell is located relative to a network formed by two signalling systems, one of which operates along the anteroposterior axis of the neural tube, while the other acts along the dorsoventral axis (originally the mediolateral axis of the neural plate) (Simon et al., 1995, Tanabe and Jessell, 1996); the nature of the inductive signal experienced by the precursor cells from the signalling systems being dependent on where the cells are situated in relation to the network axes (Roelink et al., 1995, Simon et al., 1995). Signals from the anteroposterior axis give rise to the various sections of the neural tube, while those relating to the dorsoventral axis generate the various cell types within each section (Simon et al., 1995, Tanabe and Jessell, 1996).

During the initial stages of spinal cord development, the ventral neural tube produces floor plate cells (around the ventral midline), motoneurones (about ventrolateral locations) and ventral interneurones (from locations that are more dorsal) (Tanabe and Jessell, 1996). With particular regard to ventral interneurones four classes have been identified to derive from the neural tube corresponding to types V0, V1, V2 and V3 (Ericson et al., 1997a, Ericson et al., 1997b, Jessell, 2000, Briscoe and Ericson, 2001)(see Figure 1.3). During cell development a protein termed sonic hedgehog has been shown to be strongly expressed in the notochord and floor plate cells; discernible through immunohistochemistry (Roelink et al., 1995). Sonic hedgehog facilitates notochord and floor plate signalling events to induce cell differentiation in the ventral neural tube (Roelink et al., 1995, Ericson et al., 1997b). This has been confirmed via the incubation of stage 10 ventral neural tube/floor plate explants with an antibody raised against sonic hedgehog (Ericson et al., 1997b). In comparison to the control

explants, those grown in the presence of the anti-sonic hedgehog antibody generated <3 motoneurones, while in the control the number totalled ~250 motoneurones. Ventral interneurones were also discerned to be greatly affected by the presence of the anti-sonic hedgehog antibody with ~10 V1 and V2 interneurones generated in the test explants compared to ~60 V1 and ~100 V2 in the control (Ericson et al., 1997b).

Ericson et al. (Ericson et al., 1997b) additionally demonstrated the concentration gradient dependence of different ventral cell types on sonic hedgehog using applications of the sonic hedgehog N-terminus recombinant protein (Shh-N) on *in vitro* stage 10 chick intermediate neural plate explants. In the absence of the recombinant protein the explanted tissue failed to produce both interneurones of types V1 and V2, or indeed motoneurones. The amount of sonic hedgehog required for signal induction of the ventral cell types located in different locations is varied. For example, induction of V1 interneurones requires a lower concentration of sonic hedgehog than is necessary for V2 interneurones (by around a factor of 2), while the sonic hedgehog concentration required for motoneurone induction is greater than that for V2 interneurones (by approximately a further factor of 2). This suggests that cell types generated at more ventral locations apparently require higher levels of sonic hedgehog for their formation.

Neuronal cells in the ventral spinal cord also express a variety of homeodomain transcription factors. These factors have subsequently been used not only as an alternative way to identify neuronal subtype (Roelink et al., 1995, Ericson et al., 1997a, Ericson et al., 1997b) but also as an aid in establishing the sources of extrinsic and intrinsic signals that affect the diversity of such neurones (Jessell, 2000, Pierani et al., 2001).

The development of the dorsal neural tube is dependent upon dorsalising signals from the roof plate, particularly from bone morphogenetic proteins (BMP) (Helms and Johnson, 2003, Lu et al., 2015) and what are termed Wnts (members of Wingless +MMTV integrants, *Int* family) (Lu et al., 2015). Eight dorsal horn neuronal subtypes have been identified, termed dI1- dI6, dIL_A and dIL_B (Gross et al., 2002, Muller et al., 2002, Helms and Johnson, 2003, Caspary and Anderson, 2003, Wilson and Maden, 2005, Xu et al., 2013, Lu et al., 2015). These neurones can be distinguished from one another via the homeodomain transcription factors which they express (Caspary and Anderson, 2003, Helms and Johnson, 2003). Since the neurones of interest to this study are located in the area generated from the ventral neural tube, only the locations

of ventral interneuronal subtypes (V0-V3) and motoneurones during embryonic and postnatal developments have been represented in Figure 1.3.

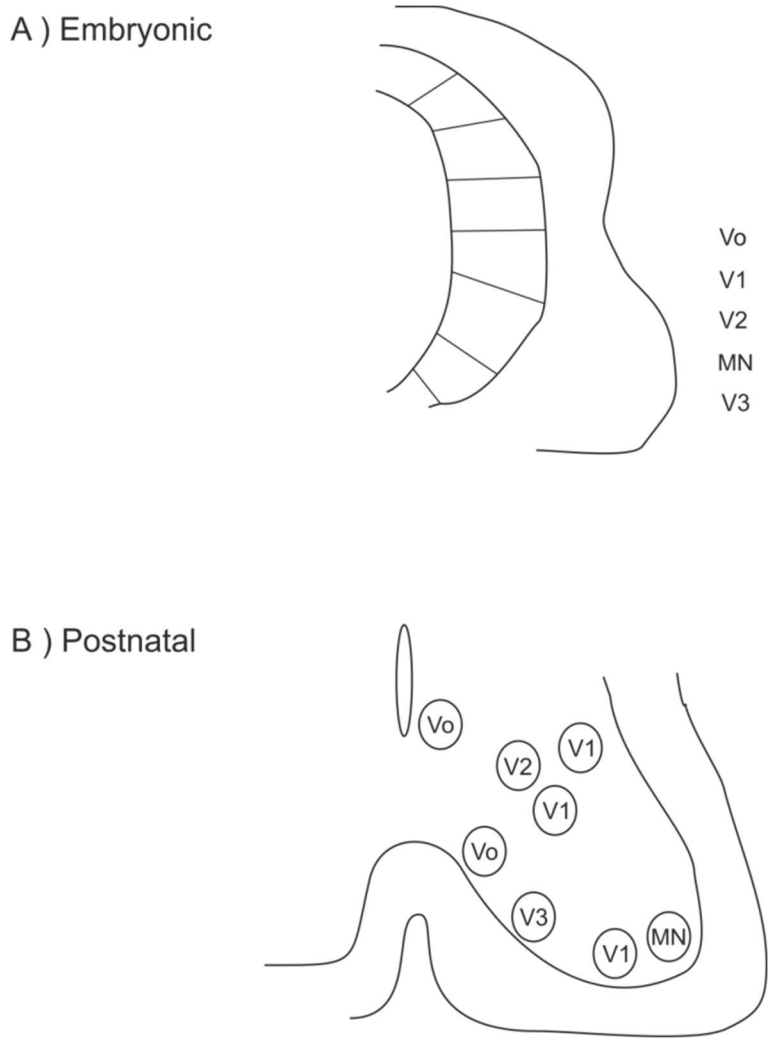

Figure 1.3: The location of ventral interneurone subtypes (V0-V3) and motoneurones (MN) during embryonic and postnatal development
(Figures adapted from Grossmann et al., 2010).

1.6 Neurochemical classification of spinal neurons (laminae I-X): with focus on ACh and GABA

1.6.1 The synthesis of acetylcholine (ACh) and GABA

1.6.1.1 ACh: Synthesis and Immunohistochemical markers

The first suggestion that nerves might release substances that were either the same as or acted similar to drugs which were being used in a given experiment came from Elliott in 1904 (Elliott, 1904). However, it was not until Loewi published results on experiments with isolated frog hearts in 1921 (Loewi, 1921) – using what was subsequently established to be ACh -- that such was confirmed; as outlined in Dale's address to the Physiological Society in 1935 (Dale, 1935). Following the isolation and identification of ACh from ergot by Ewins (Ewins, 1914), Dale subsequently identified the similarity of the effect of ACh to both muscarine and certain divisions of the autonomic nervous system (Dale, 1914).

The process of ACh biosynthesis requires choline (Lipton and Barron, 1946). It is initiated by the uptake of extracellular choline into the nerve terminals of cholinergic neurones via a high-affinity system that is dependent on sodium (Yamamura and Snyder, 1972, Yamamura and Snyder, 1973). In addition to choline, the synthesis process also requires an acetyl group (attached to a coenzyme). Although initial studies were unable to establish the source of the acetyl group (Lipton and Barron, 1946, Nachmansohn and Berman, 1946) later work proved to be more successful at identifying the compound as acetyl coenzyme A (acetyl-CoA); with Lipmann having been the first to name the source as coenzyme A (Lipmann, 1953). Biosynthesis of ACh from choline and acetyl-CoA subsequently occurs within the cytoplasm of neuronal nerve terminals (Feldberg and Vogt, 1948, Roghani et al., 1994, Usdin et al., 1995), and is facilitated by the key enzyme currently known as choline acetyltransferase (ChAT) (Perry et al., 1978, Erickson et al., 1994); this enzyme originally being termed as choline acetylase (Nachmansohn and Machado, 1943).The manufactured ACh is subsequently packed into synaptic vesicles via a vesicular acetylcholine transporter (VAChT) (Erickson et al., 1994, Roghani et al., 1994)(see Figure 1.4).

The neurotransmission activity of ACh typically terminates at the synaptic cleft, where it is hydrolysed by the enzyme acetylcholinesterase (AChE) (originally known as choline

esterase) (Stedman and Stedman, 1937, Marnay and Nachmansohn, 1937) into acetate and choline (Fagerlund and Eriksson, 2009).

The most reliable method for localising cholinergic neurones histochemically has proved to be via the use of antisera raised against ChAT (Bradford, 1986) which has been widely used by many researchers in the field (Barber et al., 1984, Ruggiero et al., 1990, Stornetta et al., 2013, Gotts et al., 2015).

Because ACh is packed into synaptic vesicles by VAChT, antisera raised against VAChT has also been used as a marker to label cholinergic neurones and their processes, particularly their nerve terminals (Arvidsson et al., 1997, Maeda et al., 2004). Another marker for cholinergic neurones in the CNS is the ACh hydrolysing enzyme, AChE, however, its use is unreliable since AChE has been observed to be present in some non-cholinergic cells (Wallace, 1981, Eckenstein and Sofroniew, 1983).

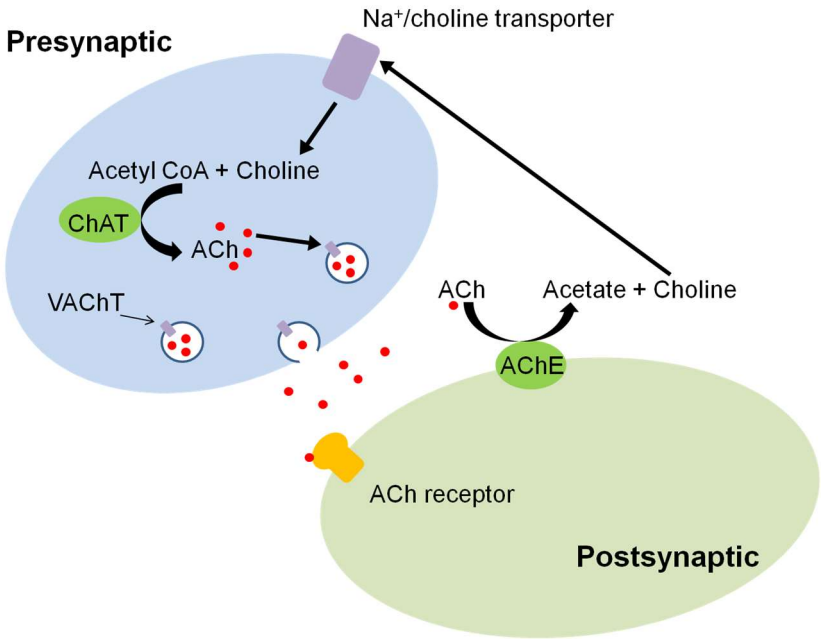

Figure 1.4: Illustration summarising the various stages in the biochemistry for the synthesis of Ach. Figure based on information in Zimmermann, 2008.

1.6.1.2 GABA: Synthesis, Immunohistochemical markers and In Situ Hybridization (ISH)

Aside from the neurotransmitter glycine (Kish et al., 1989), GABA is a major inhibitory neurotransmitter in the CNS (Krnjevic and Schwartz, 1967, Iversen and Kelly, 1975, Clark et al., 1992, Liu et al., 1993, Gadea and Lopez-Colome, 2001); more than 40 % of the inhibitory synapses occurring in the brain use GABA (Bowery and Smart, 2006). Neurones using GABA are generally found to be linked to local circuits across the CNS (Benes and Berretta, 2001, Briatore et al., 2010, Watanabe et al., 2015, Lin et al., 2015, Voytenko et al., 2015).

The main precursor to GABA synthesis is glutamate, which is catalysed by the enzyme glutamic acid decarboxylase (GAD) to produce GABA (Costa et al., 1979). According to the history of its discovery, GABA was first reportedly identified in the brain of various animals and humans in 1950 (Roberts and Frankel, 1950, Awapara et al., 1950, Udenfriend, 1950). The results from an experiment carried out by Roberts and Frankel (Roberts and Frankel, 1950) suggested glutamic acid as being a likely precursor of GABA, since increased levels of GABA were observed in every instance when homogenate containing mouse brain had been incubated with glutamic acid. The authors also hypothesized that the enzyme responsible for GABA synthesis in bacteria and plants via decarboxylation of glutamic acid, GAD, could also be responsible for its occurrence in the brains of mammals. GAD was subsequently reported to be present in the brain tissue of rats shortly thereafter (Wingo and Awapara, 1950); in the brain it is now established that there are two major isoforms of GAD, these being GAD67 (GAD1) and GAD65 (GAD2) (Bradford, 1986, Erlander et al., 1991). Transportation of GABA into synaptic vesicles requires the actions of a vesicular inhibitory amino acid transporter (VIAAT), and occurs in a manner that is ATP dependent (Hell et al., 1988, Kish et al., 1989, Fykse et al., 1989, Hell et al., 1990, Hell et al., 1991, McIntire et al., 1997, Sagne et al., 1997, Chessler et al., 2002)(see Figure 1.5).

With respect to GABA removal from the synaptic cleft, high-affinity GABA transporters (known as GATs), dependent on Na^+, can be found in both neurones and glia (Schon and Kelly, 1975, Clark et al., 1992, Liu et al., 1993, Borden et al., 1994). There are 3 subtypes of GAT expressed in the CNS. The predominant forms are GAT1 and GAT3, which are primarily found at the neuronal nerve terminals and glial processes, respectively (Radian et al., 1990, Ikegaki et al., 1994, Itouji et al., 1996, Su et al., 2015). GAT2 is also expressed in the CNS, but only to a limited extent, seemingly in leptomeninges and blood vessels (Lopez-Corcuera et al., 1992, Ikegaki et al., 1994,

Zhou et al., 2012). GABA degradation then requires the combined action of mitochondrial enzymes, specifically GABA transaminase and succinic semialdehyde dehydrogenase (Bouche et al., 2003).

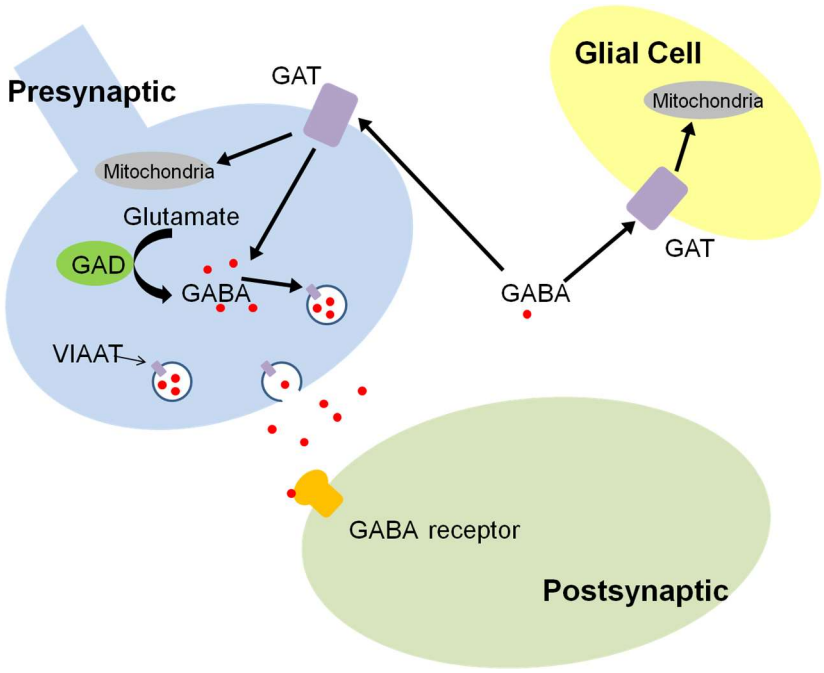

Figure 1.5: Illustration summarising the various stages in the biochemistry for the synthesis of GABA. Figure based on information in Brekke et al., 2015.

In the 1970s-1980s, GABAergic neurones in rat and mice had been detected utilising immunohistochemistry (IHC) for GABA (Davidoff and Schulze, 1988, Kosaka et al., 1988, Caffe et al., 1996) or GAD (not specific to any particular GAD isoform) (Ruggiero et al., 1985, Kosaka et al., 1988, Gritti et al., 1993, Belin et al., 1983, Caffe et al., 1996, Meeley et al., 1985).

However, the GAD enzyme seems to be concentrated in nerve terminals compared to cell bodies. Therefore, the labelling of GABAergic neurone cell bodies has proven to be a challenge. To overcome this problem, some studies have avoided use of a permeabilizing agent and utilised enzymatic visualisation to boost the low signal intensity (Fong et al., 2005), or injected colchicine (Kosaka et al., 1988, Meeley et al., 1985) into studied animals which disrupts axoplasmic transport and leads to accumulation of GAD in cell bodies (Ribak et al., 1978, Whatley et al., 1994, Sardella et

al., 2011). Additionally, ISH for GAD67 and/or GAD65 has been utilised by studies investigating the distribution of GABAergic neurones (Stornetta and Guyenet, 1999, Tillakaratne et al., 2000, Tillakaratne et al., 2002, Fong et al., 2005, Deuchars et al., 2005, Edwards et al., 2007, Trifonov et al., 2012).

1.6.2 ACh and GABA receptor subunits

The effects of neurotransmitters such as ACh and GABA are mediated by the protein structures they bind to. These effectors of neurotransmitter action undergo conformational changes upon agonist binding resulting in an effect that is either direct or indirect. Based on their structure and function, such effectors, which are generally termed as receptors, can be placed into two broad classes. The first class directly mediates the flow of ions into the cell when bound by an agonist and is called a ligand gated ion channel (LGIC) (Miller and Smart, 2010). The second class triggers a cascade of intracellular signalling which modulates the activity of ion channels (Audet and Bouvier, 2012). The effects of the latter are determined by the type of G-protein they are associated with and are known as G-protein coupled receptors (GPCRs) (Caulfield and Birdsall, 1998, Alexander et al., 2015a). Both these classes of receptor have their own subdivisions and variations; for the purpose of this thesis those appropriate to ACh and GABA will be addressed below.

As a receptor class, LGIC has several subdivisions that can be defined according to receptor structure homology. In the case of ACh and GABA, they belong to the same subdivision, the Cys-loop ligand gated ion channel superfamily, that are characterised by the existence of a disulphide-bridged loop in the extracellular domain (Miller and Smart, 2010). GPCRs are often referred to as 7TM receptors due to their possessing 7 hydrophobic regions identified as being transmembrane (TM) domains (Alexander et al., 2015a).

1.6.2.1 Receptor structure of nicotinic acetylcholine receptor: the prototypical receptor for the Cys-loop ligand gated ion channel superfamily

The nicotinic acetylcholine receptor (nAChR) belongs to the Cys-loop superfamily of LGICs (Miller and Smart, 2010). This member has its structure resolved due to the rich

source of these receptors found in the electric organ of *Torpedo marmorata* (Unwin et al., 1988, Unwin, 2005). Each functional receptor is a pentameric structure consisting of 5 individually coded subunits, arranged in a ring-like configuration (Miller and Smart, 2010, Unwin, 2013). Each subunit is a single protein containing 4 hydrophobic regions (M1 to M4) that pass through the cell membrane with the second transmembrane region (M2) forming the channel pore and gate (Unwin et al., 1988, Miller and Smart, 2010, Unwin, 2013)(see Figure 1.6a and 1.6b). The ion channel is selective for Na^+ and K^+ ions, plus also limited amounts of Ca^{2+} ions which varies according to the subunits present (Unwin, 2013).

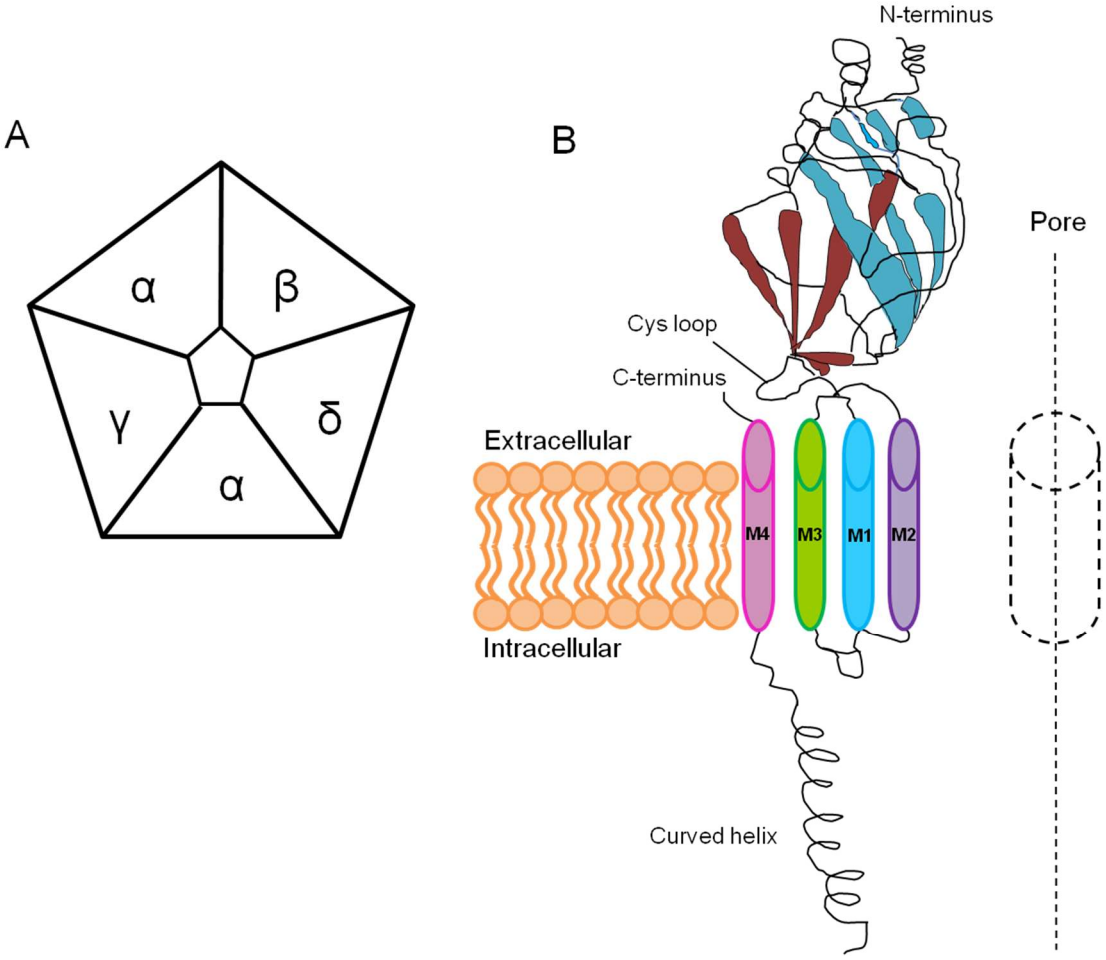

Figure 1.6: Structure of the nicotinic acetylcholine receptor. Figure based on information in Unwin, 2013.

A) Diagramatic representation of top down view of a nicotinic acetylcholine receptor with identified subunits.

B) Side view of an individual nicotinic acetylcholine receptor subunit illustrated as a ribbon diagram with key features labelled.

1.6.2.2 Receptor stoichiometry and pharmacology of nicotinic acetylcholine receptors

Of the 17 gene encoded functional nAChR subunits that have been identified, 16 can be found in mammals; the α8 subunit expression being restricted to avian species (Lukas et al., 1999, Alexander et al., 2015b). The subunits fall within 5 families (α, β, γ, δ and ε), with the largest being the α family which is distinguishable from the other subunit forms through its having two tandem cysteine residues located near the ACh binding site (Alexander et al., 2015b). The stoichiometry of functional channels is dependent upon their anatomical expression. For example, in adult animals the somatic neuromuscular junction contains hetero-oligomeric channels with a conserved assembly of $(\alpha1)_2\beta1\delta\varepsilon$. In contrast, both embryonic and denervated skeletal muscle contain nAChR assembled from $(\alpha1)_2\beta1\gamma\delta$ (Alexander et al., 2015b). Most functional nAChRs are hetero-oligomeric combinations of α and β subunits. Occasionally, a third subunit is present which leads to a modification of the channels biophysical or pharmacological properties (Alexander et al., 2015b). Some α-subunits (α7-9) can form functional homomeric channels with distinct pharmacological properties (Alexander et al., 2015b). The ACh binding site forms at the interface of the α subunit (the principal component) and a neighbouring subunit (the complementary component), with two binding sites per receptor, the individual affinities of which are determined by the constituent subunits (Sine and Engel, 2006, Alexander et al., 2015b).

Experiments by Dale (1914) functionally described the agonist action of ACh in comparative terms to muscarine and nicotine. Ultimately this lead to the two classes of ACh receptor being defined according to their prototypical selective agonist: muscarinic and nicotinic, respectively (Dale, 1914), although the potent effect of ACh is transient due to its rapid hydrolysis by cholinesterase (Dale, 1914, Brucke, 1937). nAChRs can be divided into two classes (Gotti et al., 2006) depending on their sensitivity to the snake venom, α-bungarotoxin (Changeux et al., 1970). Those channels sensitive to this toxin include α7, α8 and α9 homo-pentameric arrangements as well as hetero-pentameric α7α8 and α9α10 combinations (Gotti et al., 2006). Insensitivity to α-bungarotoxin is exhibited by hetero-pentameric receptors which are combinations of subunits α2-α6 and β2-4. The use of nonselective agonists for functional assays include nicotine, 1,1-dimethyl-4-phenylpiperazinium (DMPP), epibatidine and ACh (Gotti et al., 2006, Alexander et al., 2015b). Antagonists of nAChR such as tubocurarine and pancuronium are potent neuromuscular blockers with a long history of clinical use during surgery (Wenningmann and Dilger, 2001). More selective nAChR

antagonists are available and provide a useful tool in discerning the roles of different receptor subtypes in physiological processes (see review by Alexander et al. 2015b) (Rousseau et al., 2005, Alexander et al., 2015b). In contrast to ligands that bind at the classic ACh binding site (also referred to as the orthosteric binding site), more recent advances have led to the discovery of receptor modulators that bind at alternative sites to that used by ACh, termed allosteric sites (Chatzidaki and Millar, 2015). The ligands binding at these alternative sites can potentiate (positive allosteric modulator) the effects of orthosteric ligand binding or inhibit (negative allosteric modulator) thus acting as a non-competitive antagonist.

1.6.2.3 Receptor structure of $GABA_A$ receptor

Schofield et al., (Schofield et al., 1987) suggested on the basis of sequence homology that $GABA_A$ receptors and nAChRs belonged to the same superfamily of ligand gated ion channels. This was the beginning of the Cys-loop ligand-gated ion channel superfamily to which glycine and 5-hydroxytryptamine type 3 (5-HT_3) receptors also belong (Miller and Smart, 2010). Having the same ultrastructural composition as the nAChR, $GABA_A$ receptors are a pentameric arrangement of individually coded subunits (each subunit containing 4 transmembrane domains) (Alexander et al., 2015b)(see Figure 1.7). To date for mammals, there have been 19 $GABA_A$ receptor genes identified collected into the subunit groups α1-6, β1-3, γ1-3, π, δ, ε, θ and ρ1-3 accordingly (Collingridge et al., 2009, Alexander et al., 2015b). All functional $GABA_A$ receptor assemblies are anion selective channels, which under most physiological conditions leads to hyperpolarisation of the cell membrane potential through an influx of Cl^- (Olsen and Sieghart, 2008). The effect of $GABA_A$ receptor activation is therefore inhibitory in most scenarios. By contrast, in the immature brain a higher quantity of $Na^+/K^+/Cl^-$ cotransporters are present, which control intracellular Cl^- concentrations and effectively act to drive Cl^- into the neurones, resulting in higher Cl^- concentrations within the cell compared to outside (Plotkin et al., 1997). In this latter situation, activation of the $GABA_A$ receptors results in depolarization of the postsynaptic cells and excitation (Mueller et al., 1983, Gaiarsa et al., 1995), since Cl^- passes out of the cell via the receptor so making the inside of the cell less negatively charged (Plotkin et al., 1997). This also happens in some mature sensory neurones (Price et al., 2006). The channel pore is formed by the second transmembrane (M2) region of each subunit, the structural features of which define the channel gate and ion selectivity filter (Olsen and Sieghart, 2008, Miller and Smart, 2010).

1.6.2.4 Receptor stoichiometry and pharmacology of $GABA_A$ receptors

Most $GABA_A$ receptors are heteropentameric constructs of stoichiometry 2α, 2β and 1γ; in respect of which variants contain a single α subtype, a single β subtype and the γ subunit may be substituted with either a π, δ, ε or θ subunit (Olsen and Sieghart, 2008, Alexander et al., 2015b). The stoichiometric subunit arrangement of 2α.2β.1γ is supported by recombinant receptor studies of the most common hetero-oligomer, α1β2γ2, which conclude that the functional receptor is an arrangement of $(\alpha1)_2(\beta2)_2\gamma2$ (Chang et al., 1996, Collingridge et al., 2009, Alexander et al., 2015b). The ρ subunit generally does not co-assemble to form heteropentamers but instead forms homopentameric channels (Bormann, 2000, Alexander et al., 2015b). Initially identified and characterised by their unique pharmacology, these channels were originally termed "$GABA_C$", however use of this term has subsequently been discouraged, since on the basis of sequence homology, structure, and functionality, they are more appropriately classified as $GABA_A$ subunits (Milligan et al., 2004, Olsen and Sieghart, 2008).

The GABA binding site is found at the interface of the α and β subunits (β+α-) (see Figure 1.7c) with two binding sites present in the typical αβγ heteropentameric channel (Smith and Olsen, 1995, Ramerstorfer et al., 2011). This is also the site of action for the classical $GABA_A$ competitive antagonist, bicuculline (Bormann, 2000, Alexander et al., 2015b). Observations of bicuculline insensitive responses to GABA led to the discovery of GABA ρ receptors; although, despite their insensitivity to bicuculline, barbiturates and lack of modulation by benzodiazepines, GABA ρ receptors are still sensitive to neurosteroids and picrotoxin like other $GABA_A$ receptors (Olsen and Sieghart, 2008).

Benzodiazepines (BZs) are important modulators of relevance to the vast majority of $GABA_A$ receptors with continuing clinical application (Rudolph and Knoflach, 2011). As allosteric modulators of $GABA_A$ receptors, BZs do not activate the channel opening directly but instead potentiate the actions of GABA when it binds to its orthosteric site. The BZ-binding site is located at the interface between the γ and α subunit extracellular domains (α+γ-), in a region containing a conserved histidine residue (see Figure 1.7c) (Rudolph and Knoflach, 2011, Ramerstorfer et al., 2011); though the absence of this histidine residue in α4 and α6 subunits renders the $GABA_A$ receptors containing them insensitive to BZs. As a result, studies into the contribution different α subunits make to the pharmacological effects observed with BZ administration have been facilitated

through the adoption of point mutation experiments involving the histidine residue (Rudolph and Knoflach, 2011).

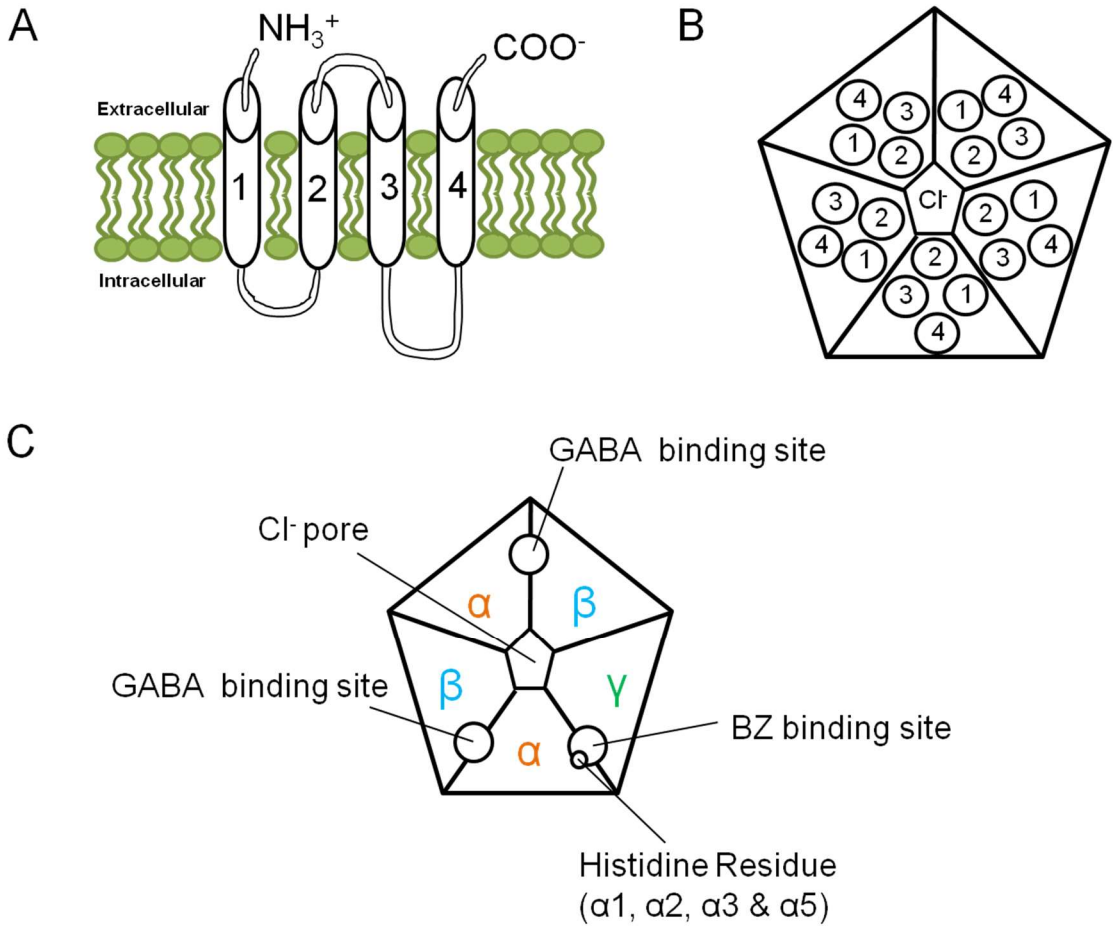

Figure 1.7: Diagramatic representation of the $GABA_A$ receptor and its binding sites.

A) Each subunit is a single protein with 4 transmembrane spanning regions (TM1-4), a large extracellular N-terminus domain, and also an intracellular loop linking the M3 and M4 parts. Diagram based on information in Bormann, 2000.

B) The arrangement of each subunit within the pentameric receptor, with the channel pore being formed from the alignment of the M2 regions. Diagram based on information in Bormann, 2000.

Figure 1.7 (continued):

C) The two orthosteric GABA binding sites are located on the interface between α and β subunits (β+α-). The allosteric benzodiazepine (BZ) binding site is located at the interface between the γ and α subunits (α+γ-) with the conserved histidine residues required for BZ activity found on the extracellular domain of the α subunit (with the exceptions of α4 and α6). Diagram based on information in Rudolph and Knoflach, 2011.

1.6.2.5 Receptor structure of GPCRs: Muscarinic acetylcholine receptor

Dale's initial observations of the effects of ACh were compared to the actions of muscarine, a description that has continued to this day to define the family of receptors that mediate the non-nicotinic actions of ACh. Only upon blockade of muscarine with atropine were the "nicotine-like" actions of ACh revealed (Dale, 1914). The muscarinic acetylcholine receptor (mAChR) belongs to the Class A, rhodopsin-like family of GPCRs. GPCRs are comprised of single polypeptide chains with 7 hydrophobic regions which form transmembrane domains (TM1 to TM7); giving rise to their alternative terminology as "7TM receptors" (Alexander et al., 2015a). They possess an extracellular N-terminus, 3 extracellular loops (ECL1-ECL3) and 3 intracellular loops (ICL1-ICL3) which link the TM domains (Audet and Bouvier, 2012, Alexander et al., 2015a), plus a C-terminus containing an eighth helix (H8) which lies parallel to the cell membrane intracellularly (see Figure 1.8) (Moreira, 2014). Operating as part of a transduction unit, the GPCR binds with a soluble signal before activating a heterotrimeric (αβγ) G protein, which subsequently leads to the modulation of an effector that may be in the form of an enzyme or an ion channel (Audet and Bouvier, 2012, Moreira, 2014). The G protein is bound to the intracellular surface of the GPCR, with the regions TM3/ICL2, TM5/ICL3 and ICL3/TM6, plus also the C-terminus, being of particular importance to this process (Kaye et al., 2011, Moreira, 2014).

1.6.2.6 Receptor subtypes and pharmacology of muscarinc acetylcholine receptors

The genes for 5 muscarinic acetylcholine receptors have been discovered and are referred to as $M_{1\text{-}5}$ in accordance with NC-IUPHAR recommendations (NC-IUPHAR :

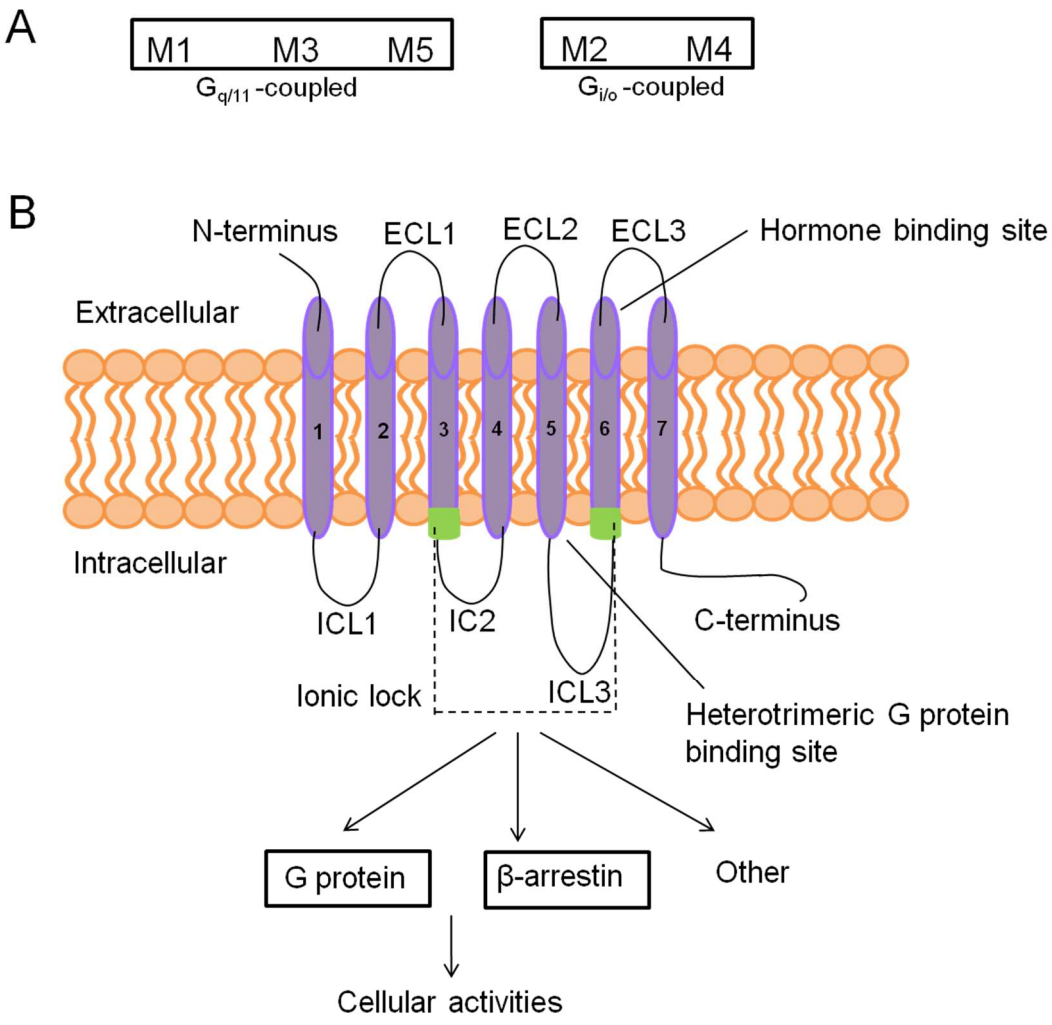

Figure 1.8: Structure of the muscaric acetylcholine receptor

A) Sequence homology and G-protein coupling on muscarinic acetylcholine receptor. Diagram based on information in Kruse et al., 2012.

B) Illustration of the topological organisation of GPCRs showing conserved structural features. Also illustrated are the G protein dependent and G protein independent signalling. Diagram based on information in Audet and Bouvier, 2012.

The International Union of Basic and Clinical Pharmacology Committee on Receptor Nomenclature and Drug Classification) (Caulfield and Birdsall, 1998). These 5 receptors divide into two groups based on the G protein that they preferentially couple with; the $M_1/M_3/M_5$ receptors acting through $G_{q/11}$, while the M_2/M_4 receptors act through

$G_{i/o}$ (Caulfield and Birdsall, 1998). This preference correlates with differences between the ICL3 regions in each of the two groups, which suggests that the structural sequence of the ICL3 region is likely an important determinant in the selective coupling of G protein subtypes to the receptor (Caulfield and Birdsall, 1998, Moreira, 2014).

The $M_1/M_3/M_5$ receptors activate phospholipase Cβ via $G_{q/11}$ to bring about increases in inositol 1,4,5-trisphosphate (IP_3) and diacylglycerol (DAG) (Caulfield, 1993, Caulfield and Birdsall, 1998). The increase in IP_3 leads to a rise in $[Ca^{2+}]_i$ via release of the ion from IP_3-sensitive intracellular stores, whilst the increase in DAG is believed to bring about protein kinase C (PKC) activation. Conversely, the M_2/M_4 receptors act to inhibit adenylyl cyclase (AC) via their coupled G protein, so reducing intracellular cAMP levels and counteracting the effects of G_s-coupled GPCRs such as β-adrenoceptors (Caulfield, 1993).

There are no subtype selective agonists for muscarinic receptors. As a result the physiological effects from the action of such agonist are determined by the type of tissue in which the action occurs (Caulfield and Birdsall, 1998). Broad acting agonists for mAChRs include carbachol and bethanechol. In contrast, some muscarinic receptor antagonists do demonstrate receptor selectivity, such as biperidin (M_1), tripitramine (M_2) and ML381 (M_5) (Alexander et al., 2015a).

1.6.2.7 Receptor structure and pharmacology of $GABA_B$ receptors

First reported as a bicuculline-insensitive, baclofen-sensitive GABA receptor (Bowery et al., 1981), $GABA_B$ receptors have since been cloned (Kaupmann et al., 1997) and were the first GPCR to be identified as a heterodimer (Marshall et al., 1999, Alexander et al., 2015a)(see Figure 1.9). They are classified as belonging to the metabotropic glutamate family of GPCRs (Class C), share the 7TM structure common to all GPCRs and utilise the $G_{i/o}$ protein subunit for signal transduction (Bowery et al., 2002, Alexander et al., 2015a). In their native heterodimeric form, $GABA_{B1}$ and $GABA_{B2}$ allosterically couple, mutually enhancing the affinity of the former for agonists and the ability of the latter to couple to G proteins (Alexander et al., 2015a). Transduction through the pertussis toxin sensitive $G_{i/o}$ protein leads to inhibition of adenylate cyclase and a reduction in intracellular cAMP. Presynaptic $GABA_B$ activation reduces Ca^{2+} conductance through P/Q- and N-type voltage gated calcium channels. Postsynaptic effects of $GABA_B$ activation include an increase in K^+ conductance, plus possibly also

the induction of Ca^{2+} spiking in thalamocortical neurones upon their being subject to long-duration hyperpolarisation (Bowery et al., 2002).

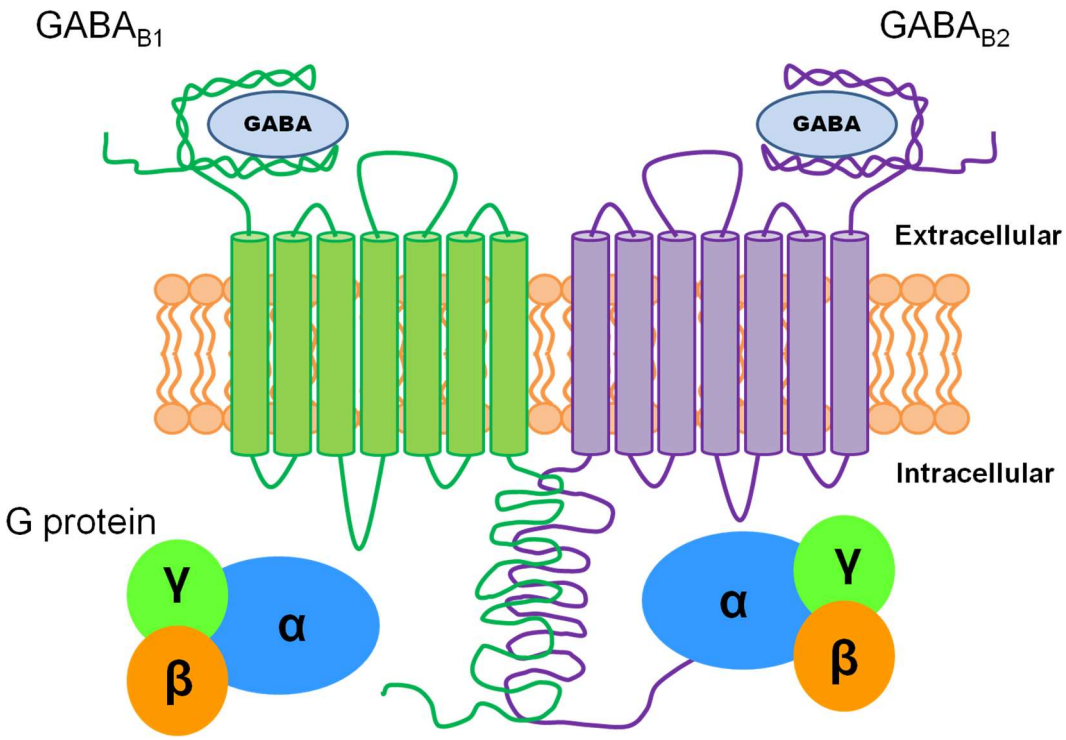

Figure 1.9: Schematic representation of the $GABA_B$ heterodimeric receptor. Figure based on information in Marshall et al., 1999.

The first specific agonist reported for $GABA_B$ was the β-p-chlorophenyl GABA derivative, baclofen (Bowery et al., 1981). Since then, additional equally effective specific agonists have been developed, including CGP 44532 (Alexander et al., 2015a). The first selective antagonists for $GABA_B$ were phaclofen, saclofen and 2-hydroxysaclofen, however their expressed affinity for $GABA_B$ was low. Subsequent research into selective antagonists included development of an agonist capable of crossing the blood-brain barrier, CGP35348 (Bowery et al., 2002).

1.6.3 The laminar and segmental distribution of cells that express GABA and cells that express ACh, with particular emphasis on thoracic regions

In the spinal cord five major groups of cholinergic neurones have been identified in rat by Barber et al. utilising IHC for ChAT. These are ventral horn motoneurones, sympathetic preganglionic and parasympathetic preganglionic neurones, partition neurones in the intermediate grey matter, central canal cluster cells, plus dorsal horn neurones (Barber et al., 1984). The identifications by Barber et al. (1984) are consistent with the observations of Eckenstein and Thoenen, who localised the cholinergic neurones in the CNS through the use of ChAT antibodies (Eckenstein and Thoenen, 1982, Eckenstein and Thoenen, 1983)(see Figure 1.10).

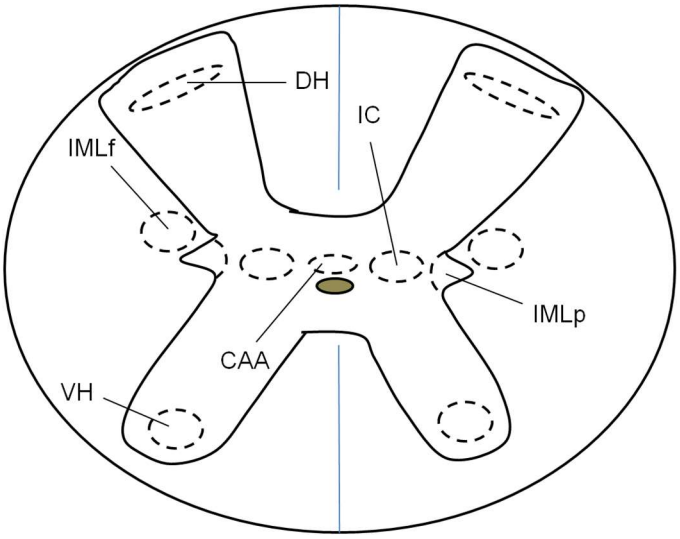

Figure 1.10: Diagramatic distribution of cholinergic neurones in the thoracic transverse cord sections of rats utilising IHC for ChAT. Sympathetic cholinergic preganglionic neurones are found in four locations, specifically the principal intermediolateral nucleus (IMLp), the intercalated nucleus (IC), the central autonomic area (CAA) and the funicular intermediolateral nucleus (MILf). The dorsal horn (DH) and ventral horn (VH) also contain cholinergic neurones. Figure based on information in Barber et al., 1984 and Eckenstein and Thoenen, 1982.

Within this section only three groups of cholinergic neurones will be the subject of discussion; specifically those of the motoneurones, SPNs (though the parasympathetic preganglionic neurones will not be the subject of further discussion in this thesis because they are not present in the thoracic spinal cord) and the dorsal horn neurones. While the groups relating to partition neurones in lamina VII and central canal cluster cells in lamina X are located in the areas of our interest, they are not pertinent and so are discussed separately in section 1.6.4

It is well established that ACh is used in motor circuits by somatic motoneurones in the ventral horn of the spinal cord (Barber et al., 1984, Johann et al., 2011). Somatic motoneurones innervate the voluntary skeletal muscles of the neck, trunk and limbs. They mainly consist of two types, specifically α-motoneurones and γ-motoneurones. α-motoneurones are the main population and innervate the skeletal muscle extrafusal fibres. γ-motoneurones are of lower abundance and innervate the intrafusal muscle fibres belonging to muscle spindles (McHanwell and Watson, 2009) .

Regarding SPNs, four sub-groups of ChAT immunoreactive (ChAT-IR) neurones are reported (Barber et al., 1984)(Figure 1.10). The major group is in the principal intermediolateral nucleus (IMLp) (Heise and Kayalioglu, 2009b) of the lateral horn, which extends from the first segment of thoracic cord to upper lumbar segments (Barber et al., 1984, McHanwell and Watson, 2009). The second group of ChAT-IR neurones are found dorsal to the central canal (Barber et al., 1984, Seddik et al., 2007, Anderson et al., 2009), in an area termed the central autonomic area (also known as CA (Barber et al., 1984) or CAA (Deuchars et al., 2005)). The third group of ChAT-IR neurones are found in the area between CAA and IMLp, termed the intercalated nucleus (Barber et al., 1984, Anderson et al., 2009). The last group has been termed the funicular intermediolateral nucleus (IMLf (Heise and Kayalioglu, 2009b)) and is located lateral to the IMLp within the white matter of the lateral funiculus (Barber et al., 1984, Anderson et al., 2009).

In 1996, Bordey et al. (Bordey et al., 1996a) utilised electrophysiology to study neurones in lamina X of the thoracolumbar cord dorsal to the central canal. These neurones were identified as SPNs in CAA based on observations made in respect to their morphology and location. In the study, application of 1,1-dimethyl-4-phenyl-piperazinium (DMPP), a selective nAChR agonist, gave rise to a direct depolarization of CAA neurones, so suggesting nicotinic excitation of these neurones could influence sympathetic outflow. Given their results, plus other (Barber et al., 1984) observations of cholinergic neurone populations within lamina X, Bordey et al. concluded that

interneurones in lamina X might be potential candidates for the source of cholinergic input to the CAA SPNs (Bordey et al., 1996a), much like they are for intermediomedial nucleus (IMM) SPNs as reported by Borges and Iversen (Borges and Iversen, 1986).

The distribution of ChAT immunoreactivity in rat spinal cord has been subject to study utilising peroxidase anti-peroxidase IHC for ChAT (Barber et al., 1984). Results indicated that in some horizontal sections, for the region adjacent to the ependymal layer (ventral to the central canal being the most frequently observed location), the presence of ChAT-IR varicosities could be discerned, stemming from central canal cluster cells. Furthermore, ChAT-IR fibres possessing a terminal-like appearance were observed in the central grey matter in proximity to non-ChAT immunoreactive (ChAT-IR) cells of the ependymal layer.

It has been suggested that dorsal horn cholinergic neurones are involved in the moderation of sensory circuits, particularly nociceptive transmission (Mesnage et al., 2011, Pawlowski et al., 2013). When treating mice with an antisense oligodeoxynucleotide (AS-ODN) against ChAT (a technique in which the sequence constituting the AS-ODN effectively binds to the mRNA to prevent the subsequent expression of ChAT and so block the process of genetic information transfer from DNA to protein (Dias and Stein, 2002)), ChAT levels in the dorsal horn decreases; though the levels of ChAT in motoneurones are seemingly unaffected. As a result of the reduced amount of ACh produced in the region, a substantial drop in nociceptive thresholds can be discerned in paw pressure and thermal paw withdrawal tests for the mice (Matsumoto et al., 2007). In addition, in keeping with an inhibitory cholinergic role, approximately 94-95% of the dorsal horn cholinergic neurones are immunoreactive for GABA (Todd, 1991, Mesnage et al., 2011).

Barber's group have also reported on extensive studies into the presence of GABAergic neurones within the rat spinal cord, finding that such neurones can be found throughout most of the spinal cord grey matter. They were present in all laminae of Rexed, including laminae I to VIII and X, except for lamina IX. Small sized GABAergic neurones were observed in lamina I – III, while larger GABAergic neurones were additionally apparent in laminae located more ventrally (see Figure 1.11) (Barber et al., 1982). In addition, some GAD-IR or GABA-IR neurones in three major groups or areas within the spinal cord also expressed ChAT immunoreactivity; these being central canal cluster cells, partition cells and the dorsal horn (Kosaka et al., 1988). A novel subgroup of GABAergic interneurones within the CAA of the thoracic cord were shown by Deuchars et al. (Deuchars et al., 2005) to have a role in the inhibitory control

of SPNs of the IML. In 2007 Al-Mosawie et al. reported on the subtypes of V2-derived interneurones in the spinal cord of adult mice, with reference to their location and possible neurochemistry (Al-Mosawie et al., 2007). During development, without the presence of Islet-1 (Isl1) the cell fate of V2 interneurones was dependent upon LIM homeobox 3 (Lhx3) transcription factor expression (Ericson et al., 1997b, Zhou et al., 2000, Karunaratne et al., 2002). YFP expression in the double-transgenic offspring of Lhx3cre/+ x thy1-loxP-stop-loxP-YFP mice was used to mark postnatal interneurones which were V2-derived; while intraperitoneal injection (IP) of Fluorogold was used to label the motoneurones. Spinal cord sections (from the cervical, thoracic, lumbar and sacral cord levels) were then used to quantify the distribution of V2-derived interneurones. Al-Mosawie et al. found that approximately 88% of all YFP^+ V2-derived neurones were interneurones (approximately 12% were motoneurones). For all the examined cord levels, V2-derived interneurones predominantly resided in lamina VII, though some neurones could also be discerned in laminae V, VI and X. Using fluorescent ISH for vesicular glutamate transporter 2 (VGLUT2), it was discerned that an appreciable portion (in excess of 50% from the observed sections of 2 animals) of YFP^+ V2-derived interneurones were glutamatergic. Moreover, on studying the co-labelled YFP and VGLUT2 terminals via IHC, results suggested that projections from the glutamatergic V2-derived interneurones mainly traverse to the ventral horn, particularly at the lumbar cord levels. In addition, Al-Mosawie et al. found that some YFP^+ boutons exhibited co-expression for the neuronal glycine transporter 2 (GlyT2) or GABA synthesising enzymes (GAD65 or GAD67), suggesting that V2-derived interneurones could also be glycinergic or GABAergic. The YFP^+/GlyT2 immunoreactive (YFP^+/GlyT2-IR) boutons were found predominantly in the dorsal horn plus laminae IX and X. The YFP^+/GAD67-IR boutons were discerned in the dorsal spinal cord, and the YFP^+/GAD65-IR boutons were observed throughout the grey matter of the spinal cord.

Given the literature reports on the discovery of GABAergic and cholinergic neurones within lamina X and/or its adjacent laminae, a discussion detailing the findings from such studies in relation to GABAergic and cholinergic interneurones is provided in section 1.6.4.

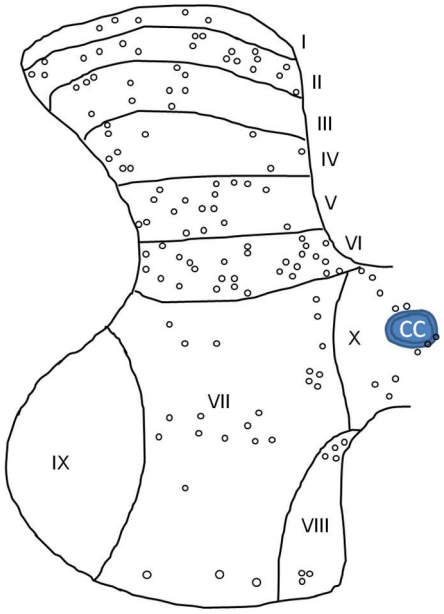

Figure 1.11: The distribution of GAD-IR neurones in the lumbar spinal cord of rats. Figure based on information in Barber et al., 1982.

1.6.4 Identified cell types and reported cholinergic and GABAergic receptor mediated effects in lamina X and adjacent regions

As previously mentioned, lamina X contains central canal cluster cells which are cholinergic as well as cholinergic SPNs in the CAA (Barber et al., 1984). However, further cell types, in relation to functionality and neurochemistry, have also been discovered and reported within lamina X and its adjacent regions. These neurones will be described here (see Figure 1.12).

The role of lamina X cholinergic interneurones in the modulation of motor circuitry was indicated since they are the source of the C bouton (terminal) input onto motoneurones in the ventral horn. In 1972, McLaughlin reported that the origin of cholinergic C boutons may stem from such interneurones in the spinal cord since the number of cholinergic C boutons projecting to the motoneurones in the ventral horn did not decrease after spinal transection (McLaughlin, 1972). However, the specific location of these neurones remained unidentified. In 2007 Miles et al. (Miles et al., 2007) indicated that for mice in which ChAT promoter controlled expression of GFP, all motoneurones of the lumbar spinal cord expressed GFP, but C boutons and some groups of cholinergic interneurones (in the dorsal horn, lamina VII and lamina X) did not; therefore suggesting that C boutons possibly originate from cholinergic interneurone

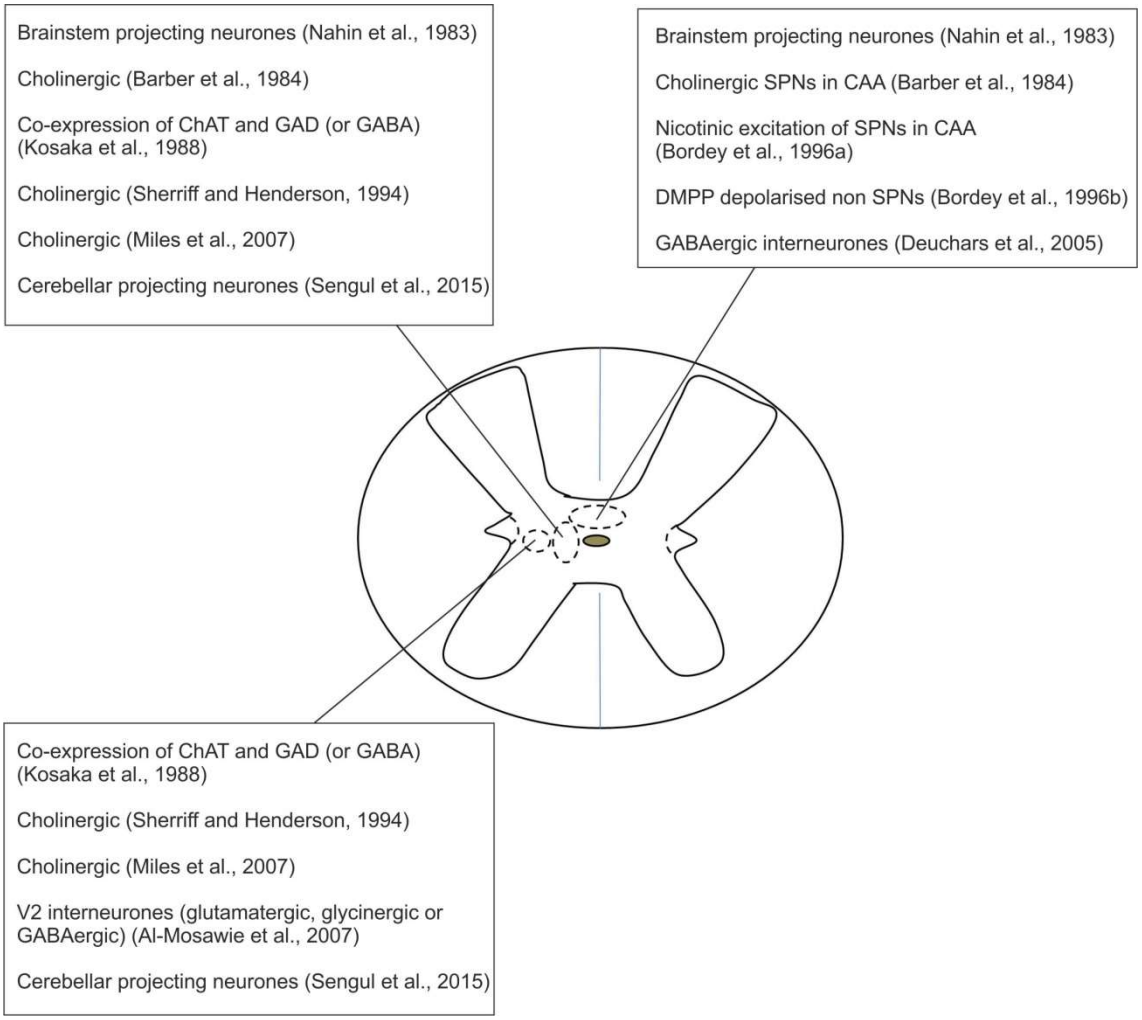

Figure 1.12: Locations of cell types and cholinergic receptor mediated effects reported in lamina X and its adjacent regions based on literature.

groups. Miles and his colleagues extended their investigations to transgenic mice in which yellow fluorescent protein (YFP) expression had been controlled by the transcription factor Dbx1, termed Dbx1-YFP mice (where Dbx is a developmentally defined V0 interneuronal marker) (Jessell, 2000). In the mouse line C boutons were found to be positive for YFP. On applying immunohistochemical analysis to the lumbar spinal cord sections of the Dbx1-YFP mice, it was determined that C boutons exhibited a profile of $ChAT^{+}/YFP^{+}/NOS^{-}$ (where NOS is nitric oxide synthase) and that the interneurones with such a profile were largely located lateral to the central canal (in lamina X and the medial section of lamina VII). These neurones giving rise to C boutons are termed as medial partition neurones. Moreover, upon investigating C

bouton functionality through the application of electrophysiology in relation to motoneurone response, results indicated that M_2 receptor activation increases motoneurone activity (Miles et al., 2007, Wilson et al., 2004, Muennich and Fyffe, 2004).

With regard to autonomic control, ACh plays a significant role in cardiovascular regulation, as evidenced by studies involving anaesthetised rats, where injecting ACh into the IML of the thoracic cord resulted in increased heart rate (McKitrick and Calaresu, 1991). However, in seeming contrast to the results from rats, initial experiments using microelectrophoretic application of ACh to SPNs in anaesthetised cats failed to produce a response (Coote et al., 1981). The weak effect of ACh was specifically remarked upon by Gibson & Logan (Gibson and Logan, 1995) in their rat thoracolumbar spinal cord slice experiments, which they suggested may due to rapid metabolism of ACh by endogenous cholinesterase. By instead using the enzyme-resistant ACh analogue carbachol, hyperpolarising responses in SPNs were subsequently observed and attributed to M_2 muscarinic receptor activation. Unexpectedly, in the presence of a complete muscarinic receptor blockade by atropine, no nicotinic response to carbachol was observed, leading the authors to theorise that the two receptor types could be differentially expressed by SPNs dependent upon their target organ.

In addition to studies on SPNs in the IML, the effects of ACh on other autonomic nuclei in the spinal cord have also been performed, particularly in respect of the CAA. Bordey et al. (Bordey et al., 1996a) observed that all thoracolumbar lamina X neurones in the region dorsal to the central canal, which corresponds to the CAA, depolarised in response to application of nAChR agonist, DMPP. In addition to this direct depolarisation, their results also suggested that increased presynaptic glutamate release was involved in facilitating excitatory transmission onto these cells. Further evidence of nAChR on SPNs in the CAA was provided by Bradaia et al. when they pharmacologically identified α7-containing receptors on these cells. Using choline (10 mM) as a selective α7 nAChR agonist (Papke et al., 1996, Bradaia et al., 2005) in combination with selective α7 nAChR antagonists α bungarotoxin (α-BgT, 50 nM) and strychnine (1 μM), the subunit composition of CAA SPN nAChRs were investigated. Choline-induced inward currents were highly sensitive to α-BgT and strychnine. They were also apparently insensitive to dihydro-β-erythoidine (DHβE, 1 μM), which is a non-α7 nAChR antagonist. Conversely the inward currents produced upon application of the broad nicotinic agonist, DMPP (100 μM), were not significantly affected by α-BgT

and strychnine but were blocked by the non-α7 nAChR antagonist, DHβE. The partial recovery of choline-induced inward currents from α-BgT blockade also suggests that these receptors may not be homomeric α7 but heteromeric nAChRs, thus indicating a role for these receptors in fast cholinergic transmission (Bradaia et al., 2005). Members of the same group later demonstrated that presynaptic non α7 nAChR activation on GABAergic terminals innervating SPNs in the CAA plays a role in facilitating inhibitory transmission (Seddik et al., 2006).

As well as SPNs in lamina X, non-SPN neurones are also present (Bordey et al., 1996b). Bordey et al. (Bordey et al., 1996b) undertook whole-cell patch-clamp recording on thoracolumbar spinal cord slices from neonate rats. Comparing the location of these lamina X neurones, situated at a more dorsal location to the central canal, with the location of the previously discerned SPNs, predominantly in the ventral part of the dorsal commissure (Hosoya et al., 1994) and also in the pericanal region, indicated that these neurones were not SPNs. Application of DMPP depolarised the neurones, which suggested that the neurones possessed nAChRs. The source of their cholinergic input is unknown.

In 2005 Deuchars et al. reported a newly identified group of GABAergic interneurones in the CAA of the rat thoracic spinal cord. Employing trans-synaptic labelling via injection of the pseudorabies virus (PRV) into the rat adrenal gland, in combination with ISH for GAD67 mRNA, some infected neurones observed dorsal and lateral to the central canal (in the CAA) were also identified as being GABAergic, since they expressed mRNA encoding for GAD67. This suggested that these particular GABAergic neurones in the CAA were presympathetic neurones. Utilising electrophysiology, stimulation of the CAA in the region containing these GABAergic interneurones produced monosynaptic IPSPs in SPNs. Subsequent bicuculline antagonism of these IPSPs indicated that they were mediated via activation of $GABA_A$ receptors. Moreover, upon glutamate microinjection into the CAA, to activate neuronal cell bodies, the degree of hyperpolarization observed was found to greatly diminish on application of bicuculline. In combination, the results from the study suggested these GABAergic interneurones in the CAA play a direct role in the inhibitory regulation of SPNs (Deuchars et al., 2005).

Kosaka et al. (Kosaka et al., 1988) investigated the co-expression of ChAT and GAD (or GABA) in the adult rat cervical spinal cord. The experiment involved intracerebroventricular injection of colchicine into the animal one day prior to perfusion. Utilising peroxidise-antiperoxidase IHC for ChAT, GAD or GABA, one of the two paired

surfaces from adjacent sections (40 μm thick) was incubated with ChAT antibody while the other paired surface was incubated with GAD (or GABA) antibody. The approach taken therefore allowed for the observation of co-localisation in individual cell bodies which as a result of the sectioning process had been cleaved, and so were present in adjacent slices. Co-expression of ChAT and GAD (or GABA) was found in central canal cluster cells and partition cells; at a level of 37%, corresponding to 18 of the 49 ChAT-IR neurones examined. In addition, co-expression was also observed in the dorsal horn (10 co-localised neurones among the 16 examined ChAT-IR neurones). A similar observation was reported by Todd, where 94% of ChAT-IR neurones within lamina III were also immunoreactive to GABA (Todd, 1991).

There is little evidence that cholinergic innervation of the spinal cord is supraspinal. In 1991, Sherriff et al. (Sherriff et al., 1991) investigated the possible existence of a cholinergic projection from the brainstem to the spinal cord. In their study, rats were injected with retrograde tracers (Horseradish Peroxidase (HRP), wheat germ agglutinin-conjugated HRP (WGA-HRP) or true blue) into the lumbar enlargement, or in one instance into the mid thoracic spinal cord. The brain and spinal cord sections were subsequently processed according to IHC protocols in order to visualise the tracers (through the use of tetramethylbenzidine and cobalt intensified diaminobenzidine (DAB)) and also cholinergic neurones (utilising IHC for ChAT). Although they did observe the presence of descending projections from the brainstem to the spinal cord none of these labelled cells were cholinergic, so indicating that cholinergic innervation to the spinal cord is from within the spinal cord itself. Sheriff and Henderson (Sherriff and Henderson, 1994) extended the investigation by studying sources of spinal cholinergic neurones innervating the rat spinal cord through the use of retrograde tracing methods, via True blue or cholera toxin subunit B (CTB) injection into the spinal cord at the level of first lumbar vertebra, in combination with IHC for ChAT and CTB. The presence of neurones exhibiting ChAT and tracer double labelling was only observed in sections up to 6 segments rostrally and caudally distant from the injection site. These double labelled neurones were identified as being partition cells (predominantly belonging to the medial group) and central canal cluster cells; with each 50 μm thick spinal cord section containing a few double labelled neurones from each group. Based on the evidence from their study Sheriff and Henderson determined that some cholinergic partition and central canal cluster cells contribute short range intersegmental propriospinal projections.

A neuronal group in lamina X that could be a potential source of ascending projections to the brainstem was investigated by Nahin et al. (Nahin et al., 1983). Rats were injected with HRP as a retrograde tracer into several regions of the medulla, pons and midbrain. While injections into all parts of the brainstem resulted in neurones within lamina X being retrogradely labelled, so suggesting that lamina X neurones give rise to long ascending projections across all subdivisions of the brainstem, those applied specifically into the paramedian medullar and/or pontine reticular formation generated the largest number of labelled lamina X neurones (mainly on the side contralateral to that of the injection site). However, Nahin et al. did not investigate the neurochemistry of the studied neuronal population.

Retrograde tracer Fluorogold and/or CTB was injected into the cerebellum of mice. The cerebellar and spinal cord sections were subsequently processed using IHC to observe spinal neurones which projected to the cerebellum. The results suggested that the central cervical nucleus, located lateral to the central canal, and other scattered neurones within laminae VII (at all spinal cord levels) sent projections to the cerebellum (Sengul et al., 2015). However, the neurochemistry of these cerebellar projecting neurones was not investigated.

1.6.4.1 Inputs to lamina X and its adjacent regions

In order to understand neuronal circuits and their function, a knowledge of the possible associated inputs and outputs for these circuits within the regions of interest is important. To reveal this aspect a number of research investigations have been undertaken utilising various techniques including IHC, tracing studies and electrophysiology. This section will describe the evidence of possible inputs reported within lamina X plus adjacent regions in the spinal cord of various species.

The distribution of punctate GAD-IR structures, presumed to be terminals, has been reported in the rat lumbosacral spinal cord using peroxidase IHC (McLaughlin et al., 1975). According to the light microscopic analysis, moderate accumulation of GAD-IR puncta was observed in laminae VII and lamina X. Puncta located in the ventral horn and the dorsal horn were additionally revealed by electron microscopy to correspond to GAD-IR synaptic terminals. Although the puncta observed within laminae VII and X were not investigated under an electron microscope, it may be suggested that the puncta found in these laminae also correspond to GAD-IR terminals which make

contact with local neurones within these regions. A similar finding was reported in monkey lumbar cord where peroxidase anti-peroxidase IHC for GABA revealed that lamina X contained a moderate concentration of GABA-IR fibres and terminals (Carlton and Hayes, 1990).

Neurones in the lateral hypothalamic area (LHA) that are immunoreactive to melanin-concentrating hormone (MCH), plus the projections from such neurones into the rat spinal cord, have been the subject of past investigation (Bittencourt and Elias, 1998). In the study, one group of rats were injected at the thoracic cord level with the retrograde tracer diamidino yellow. To improve neurone immunostaining these animals were also injected with colchicine 20-25 days after tracer injection and 48 hours before perfusion. Adjacent serial sections of forebrain, brainstem and spinal cord were then stained using IHC for the retrograde tracer and MCH. A second group of rats were injected with *Phaseolus vulgaris* leucoagglutinin (PHA-L), an anterograde tracer, into either their LHA or zona incerta; since MCH and neuropeptide EI generally co-localise within neurones of these regions (Bittencourt et al., 1992), the purpose of this group was to confirm both the distribution of co-localised MCH and neuropeptide EI projecting neurones and determine the terminal projections of such neurones into the spinal cord. Both MCH and neuropeptide EI are processed from a precursor which is also responsible for producing a hormone that affects adaptive changes of pigmentation. Results from the study showed that large numbers of MCH-IR terminals project into lamina X, predominantly around the central canal, from the LHA at all spinal cord levels. This suggests that lamina X is enriched by MCH innervations from descending projection neurones in the LHA. Moreover, since co-localisation between MCH and neuropeptide EI was observed to be prevalent in neurones of the LHA, Bittencourt and Elias proposed that the MCH-IR terminals projecting to the spinal cord from the LHA were also likely to be immunoreactive for neuropeptide EI (Bittencourt and Elias, 1998)

Major contributions of serotonergic (5-HT or 5-hydroxytryptamine) projections to the spinal cord arise from the raphe nuclei, particularly from the nucleus raphe magnus, the nucleus raphe pallidus and the nucleus raphe obscurus (Ballion et al., 2002). According to a study on mice, utilising both immunoperoxidase and immunofluorescence techniques to localise serotonin (Ballion et al., 2002), at zero days postnatal the dorsal region of the peri-ependymal area of the spinal cord possessed commissural 5-HT-IR fibres (5-HT), while at 10 days postnatal the region received high levels of 5-HT innervation. In adult rat, the distribution of descending serotonergic fibres projecting to the spinal cord has been investigated utilising peroxidise antiperoxidase IHC (Newton

and Hamill, 1989). The whole spinal cord from C1 to the conus medullaris was examined for the presence of 5-HT-IR terminals. Results indicated that large amounts of 5-HT-IR fibres were present in both laminae VII and X (particularly in the dorsal commissural nucleus). The authors additionally noted that the areas within lamina VII and X that possessed most of the 5-HT-IR fibres also contained SPNs. Ten days after transection of the spinal cord (at the junction of T4-T5) a significant decrease in serotonergic descending fibres was discerned caudal to the transection, in the IMLp, intercalated nucleus and dorsal commissural nucleus. Furthermore, results obtained from spinal cord hemisection indicated that laminae VII and X received innervation from both crossed and uncrossed descending serotonergic projections.

An investigation into the co-localisation of serotonin (5-HT) with nine individual substances within the axons of adult rat spinal cord has further suggested that these 5-HT pathways are neurochemically heterogeneous. Markers tested were GAD and eight neuropeptides (specifically calcitonin, gene-related peptide, dynorphin, enkephalin, galanin, neuropeptide Y, neurotensin, substance P and somatostantin) (Maxwell et al., 1996). In the study fluorescent IHC in combination with confocal microscopy was used to examine the L4 spinal cord segments. The results indicated that a moderate level of co-localisation between serotonin and substance P was present within axon terminals in lamina X. Furthermore, the only other substances for which serotonin co-localisation could be discerned within lamina X axon terminals were dynorphin and galanin, both in limited numbers. Therefore they may be a small subgroup of serotonergic inputs with potentially different functions.

An investigation into dopaminergic distributions across all regions of the spinal cord (for rats, cats and monkeys) revealed that lamina X received considerable dopaminergic innervation, though essentially confined to the area encircling the central canal plus a region spreading out in an apparently dorsolateral direction (Holstege et al., 1996).

Met-Enkephalin, substance P and somatostatin synaptic terminals were also investigated in the cervical cord lamina X region of monkey utilising electron microscopy in combination with IHC (LaMotte and Shapiro, 1991). Met-enkephalin terminals were largely observed lateral to the central canal. Similarly, substance P terminals were also predominantly observed lateral to the central canal and in the dorsal commissural nucleus, though some terminals could additionally be found dorsal and ventral to the pericanal region. Relative to Met-enkephalin and substance P terminals, the number of observed somatostatin terminals in lamina X was more

limited, with the majority of those discerned being lateral to the central canal and along the dorsal commissure.

Utilising PHA-L (an anterograde tracer) injection into the locus coeruleus nucleus of rat spinal cord in combination with IHC for PHA-L and dopamine-β-hydroxylase (Clark and Proudfit, 1991), noradrenergic projections from the locus coeruleus were predominantly observed to terminate in lamina X (particularly in the area adjacent to the central canal) and lamina VII (ipsilateral side to the injection site).

The existence of a monosynaptic pathway between SPNs and cells in the raphe pallidus and/or caudal raphe magnus of rat has been ultrastructurally studied (Bacon et al., 1990). PHA-L retrograde tracer was injected into the raphe pallidus and the raphe magnus. The adrenal gland was later injected unilaterally with cholera B chain conjugated to HRP (CB-HRP), which subsequently retrogradely labelled SPNs in the IMLp, IMLf and a few in the intercalated nucleus on the ipsilateral site, predominantly in T7-T11 cord segments. Synaptic contacts between the retrogradely labelled SPNs and PHA-L containing terminals were observed, suggesting the presence of a monosynaptic pathway between these SPNs and cells in the raphe pallidus and/or the caudal raphe magnus.

Cholinergic V0-derived interneurones, of interest due to their location in close proximity to the central canal, were studied through the use of transgenic mice, IHC and electrophysiology (Zagoraiou et al., 2009). Focusing on Pitx2 positive V0 interneurones in the upper lumbar spinal cord levels, synaptic inputs to transgenically labelled neurones (Pitx2::Cre;Thy1.lsl.YFP) were investigated via immunofluorescence. Their results indicated the presence of strong synaptic input (based on the numbers of boutons in close apposition to somata) from VGLUT2 and GAD67 containing neurones; each contributing more than 50 boutons per cholinergic V0 soma. Suggested sources of the glutamatergic input included interneurones (Alvarez et al., 2004) and descending projections (Du Beau et al., 2012). Some serotonergic (20 boutons per soma) inputs were detected and attributed to serotonergic innervation from the brainstem (Ballion et al., 2002). In addition a few VGLUT1 (vesicular glutamate transporter 1) (approximately 10 boutons per soma) inputs were observed, likely originating from primary afferents (Alvarez et al., 2004) and/or the corticospinal tract (Du Beau et al., 2012). Electrophysiological recordings from the hemisected spinal cords of Pitx2::Cre;Thy1.lsl.YFP mice subjected to a rhythmogenic drug cocktail (NMDA 5 μM, 5-HT 10 μM, dopamine 50 μM) showed most fluorescent protein-labelled V0 interneurones to be tonically active, with a small number showing distinct bursting

activity. Among the tonically active fluorescent protein-labelled neurones, while they lack intrinsic rhythmic activity, most (80%) increased their firing rate in phase with motor burst activity. Under voltage clamp conditions, while inhibitory postsynaptic currents (IPSCs) were detected throughout the motor burst cycle, barrages of excitatory postsynaptic currents (EPSCs) in phase with ventral root bursts were also observed. Indirect input from sensory afferents was additionally demonstrated. The study concluded that the rhythmic activity exhibited by Pitx2^{+} V0 interneurones was largely dependent on local excitatory interneurone inputs (Zagoraiou et al., 2009).

1.6.4.2 Output from lamina X and its adjacent regions

A background knowledge of projections from the area of interest is important in order to understand the circuits involved within the region. This section will describe studies carried out to investigate possible projections from lamina X and its adjacent regions to various CNS areas.

The connection between spinal cord neurones and both the midbrain periaqueductal grey and the medullary reticular formation were studied in rat using fluorescent retrograde tracers, Fast Blue plus either Nuclear yellow or Diamidino yellow dihydrochloride. Injections made into the periaqueductal grey (Fast Blue) and the medullary reticular formation (one of the two yellow dyes), gave rise to double labelled neurones in instances where neurones provided projections to both regions. Laminae VII and X contained prominent levels of the observed double labelled neurones, so indicating that some neurones within these laminae provide ascending projections to both the periaqueductal grey and the medullary reticular formation (Pechura and Liu, 1986).

In rats which had been injected into various areas of the brain with a gold complex retrograde tracer made of WGA-apohorseradish peroxidase conjugate coupled to colloidal gold, neurones situated close to the CAA (dorsal commissural nucleus) of lamina X were discerned to project to the nucleus of tractus solitarius (NTS) and the parabrachial area via the spinosolitary and spinoparabrachial tracts respectively. In addition neurones in lamina VII of the lower thoracic and upper lumbar cord were observed to project to the hypothalamus and amygdala. Furthermore, investigations were also undertaken using c-fos immunohistochemistry as a marker to label active spinal neurones activated by noxious visceral stimulation via acidified (acetic acid) IP

injection. Results suggested that spinal neurones which contributed to the spinoparabrachial and spinosolitary tracts might play a major role in visceronociceptive transmission. A limited number of such neurones were discerned to be in lamina X at the thoracolumbar junction (Menetrey and de Pommery, 1991).

Another site of projection from neurones in lamina X is to the ventral horn of the spinal cord. Medial partition neurones, interneurones located lateral to the central canal within lamina X and the medial section of lamina VII, have been reported to be the neuronal source of cholinergic C boutons which project to motoneurones in the ventral horn (Miles et al., 2007). Details on the experimental procedures involved to establish this determination are described within section 1.6.4.

One target for the efferent projections from lamina X neurones is within lamina X itself. According to the study by Barber et al. on rat spinal cord sections, involving the application of peroxidase anti-peroxidase immunohistochemical techniques for ChAT (Barber et al., 1984), such local projections have been identified in relation to the neuronal origins for some ChAT-IR varicosities observed in the region adjacent to the ependymal layer (ventral to the central canal being the most frequently observed location). In these instances the ChAT-IR varicosities were seen to extend from central canal cluster cells.

As mentioned previously, evidence also exists that lamina X interneurones target SPNs in the IML (Deuchars et al., 2005) (see section 1.6.4).

1.7 The Autonomic nervous system with particular emphasis on sympathetic nervous system

Homeostasis is strongly influenced by the autonomic nervous system. Cardiac muscle, smooth muscle and glands are governed by the efferent (motor) aspect of the autonomic nervous system. However, in addition there is also an afferent aspect to the autonomic nervous system. The afferent system is concerned with the feedback of sensory information from receptors present in the organs to the CNS. Such information is then integrated by various neuronal pathways in the CNS to influence the autonomic motor outflow (Loewy, 1990a, Deuchars and Lall, 2015).

The autonomic nervous system was first described by Langley (Langley, 1921). In the body, the autonomic nervous system can be split into three components. These are the sympathetic, parasympathetic and enteric nervous system. Various internal organs are controlled through the joint, but opposing, actions of the sympathetic and parasympathetic components. For instance, activation of sympathetic fibres in the heart causes tachycardia, whereas bradycardia occurs as a result of parasympathetic fibres being stimulated (Loewy, 1990a). Further effects of the sympathetic nervous system include pupillary dilation, vasoconstriction of blood vessels, sweat secretion, piloerection, bronchial dilation, plus relaxation of the bladder wall muscle and contraction of the internal sphincter, while those of the parasympathetic nervous system include pupillary constriction, vasodilation, bronchial constriction, plus contraction of the bladder wall muscle and inhibition of the internal sphincter (Purves, 2008). By contrast, glandular secretion and motility in the gut are controlled by a group of neurones in the gut wall which is termed the enteric nervous system (Loewy, 1990a).

The efferents of the sympathetic nervous system arise from the spinal cord and innervate ganglionic cells in the sympathetic chains which in turn project to the thoracic viscera (including lung and heart), various abdominopelvic viscera, the muscles in vascular walls, hair follicles and sweat glands (Snell, 2010). Its activation gives rise to responses which are associated with “Fright, fight and flight”, causing the heart, blood vessels, airways and liver to work in such ways as to result in increased cardiac output, changes to blood flow, increased lung airflow and raised concentrations of blood glucose respectively. These changes contribute to increasing the chances of survival when subjects are placed in stressful situations (Longstaff, 2005).

The efferents of the parasympathetic nervous system arise from brainstem nuclei and the sacral spinal grey matter (Snell, 2010, Longstaff, 2005). Activation of the parasympathetic nervous system is associated with the body being in a “rest and digest” condition. It is involved in the stimulation of exocrine gland secretion and anabolic processes (Longstaff, 2005).

The enteric nervous system is located exclusively outside the CNS. It consists of both the myenteric and the submucosal plexus, which lie within the gut wall. The enteric nervous system primarily regulates the rhythm and coordination of the gut contraction (Langley, 1921, Kingsley, 2000).

1.7.1 Sympathetic nervous system

1.7.1.1 Location of the sympathetic preganglionic cell column

In mice, lamina VII contains the sympathetic preganglionic cell columns, including the intermediolateral nucleus (forming two IMLs) – which constitutes the lateral horn (Anderson et al., 2009, Sengul et al., 2012) – and the intercalated nucleus. The IML is situated at the lateral border of lamina VII, between the first thoracic and second lumbar segments (T1-L2) (Anderson et al., 2009, Sengul and Watson, 2012). By comparison for the majority of mammalian species the IML is to be found between the C8 and L3 segments (Strack et al., 1988, Deuchars and Lall, 2015). In addition to the IML and the intercalated nucleus, detailed studies within these segments have indicated that sympathetic preganglionic neurones (SPNs) also reside in the lateral funiculus and the central autonomic nucleus (Barber et al., 1984, Deuchars and Lall, 2015).

1.7.1.2 Anatomical organisation of the sympathetic nervous system

The axons of SPNs exit the spinal cord via the ventral nerve roots and then travel to the sympathetic chain, which lies along both sides of the vertebral column. From the sympathetic chain, there are three possible modes of distribution for these preganglionic axons. Firstly, they may form a synapse, using ACh as their neurotransmitter, onto sympathetic postganglionic neurones within the sympathetic chain. The postganglionic axons then travel out of the sympathetic chain to reach the thoracic spinal nerves, at which point they subsequently accompany the spinal nerves to reach smooth muscle within the vascular walls, sweat glands and arrector pili muscles. Secondly, after leaving the spinal cord the preganglionic axons of SPNs may travel rostrally within the sympathetic chain to synapse onto sympathetic postganglionic neurones in the cervical segments of the chain. The postganglionic axons then leave the sympathetic chain and distribute to the cervical spinal nerves.

Several axons of SPNs also travel caudally within the sympathetic chain to synapse with sympathetic postganglionic neurones in the lower lumbar and sacral regions of the chain. The postganglionic axons from these neurones then travel to join the lumbar, sacral and coccygeal spinal nerves. Thirdly, the preganglionic axons of SPNs travel to the sympathetic chain and then leave the chain without synapsing with any ganglionic neurones. These preganglionic axons then travel to synapse with postganglionic

neurones which are located outside the sympathetic chain (such as prevertebral ganglion). After synapsing, the postganglionic axons subsequently travel to the glands and smooth muscle of the viscera. A limited number of preganglionic axons of SPNs also reach the adrenal medulla of the adrenal gland. Cells in the adrenal medulla are considered to be modified sympathetic neurones involved in adrenaline and noradrenaline secretion (Snell, 2010, Deuchars and Lall, 2015)(see Figure 1.13). In an alternative to the local reflex pathway, some central axons from the dorsal root ganglia neurones connect to ascending neurones which in turn send axons to make links with regions in higher centres which are responsible for the modulation of autonomic, limbic and endocrine functions (Snell, 2010, Deuchars and Lall, 2015).

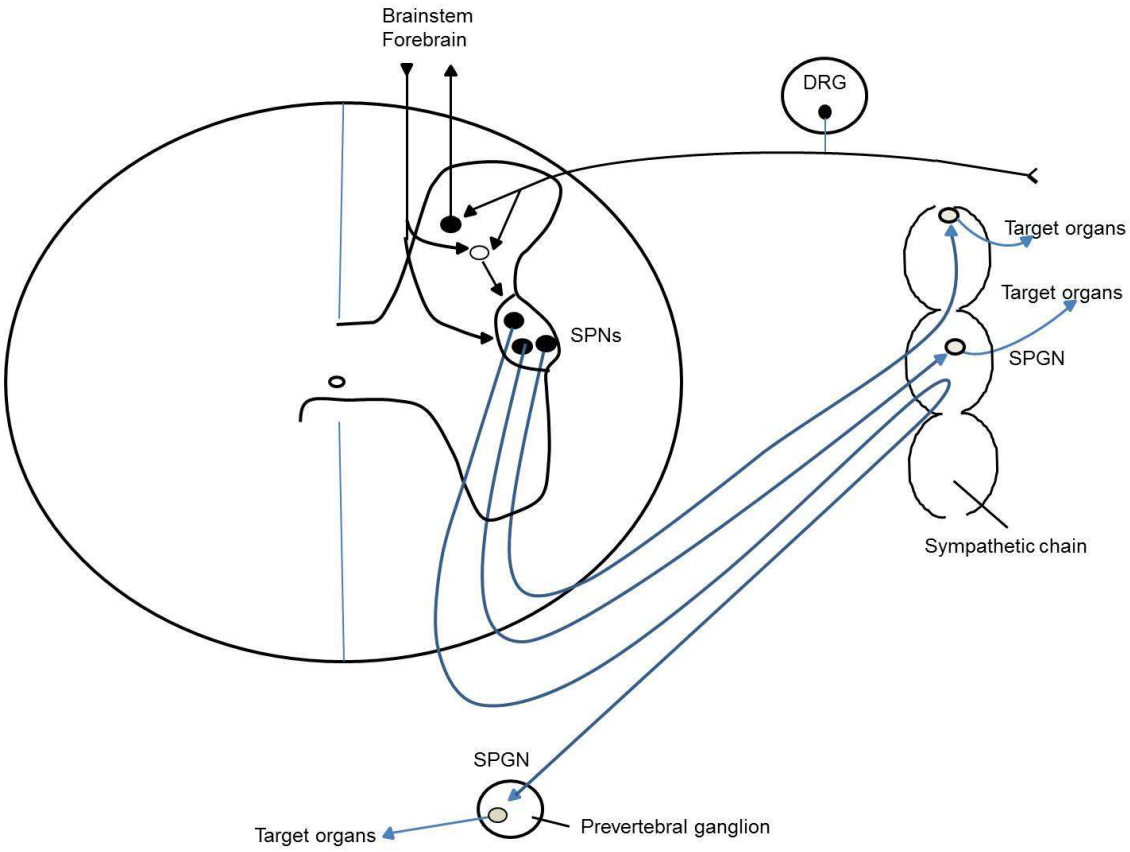

Figure 1.13: Anatomical organisation of the sympathetic nervous system (Figure adapted from Loewy, 1990a, Deuchars and Lall, 2015). SPNs: sympathetic preganglionic neurones; DRG: dorsal root ganglion; SPGN: sympathetic postganglionic neurone.

Sympathetic outflow from the spinal cord originates from SPNs, the last common central pathway of the sympathetic nervous system and interface between the CNS and peripheral nervous system (Deuchars, 2007). SPNs receive supraspinal inputs from various regions of the brain including paraventricular hypothalamic nucleus, A5 noradrenergic cell groups, caudal raphe region, rostral ventrolateral medulla, and ventromedial medulla (Strack et al., 1989a, Strack et al., 1989b, Deuchars, 2007). Some circuits utilise interneurones in order to establish contact onto SPNs. The locations of interneurones controlling sympathetic activity in laminae V, VII, X, and the IML (Strack et al., 1989a, Cabot et al., 1994, Deuchars, 2007) have only been established in the last few decades but details pertaining to their role and neurochemistry is still not well reported. Along with supraspinal innervation, sympathetic interneurones additionally receive innervation from local afferent pathways; each innervation path playing a crucial role in the maintenance of sympathetic outflow (Deuchars, 2007). The contribution of motoneurones to the modulation of sympathetic activity may be mediated by an undefined population of interneurones. Chizh et al. (1998) suggested that sympathomotor coordination could occur through a common central pattern generator projecting to both the somatic motoneurones and sympathetic neurones however they could only demonstrate unidirectional integration of activity from motorneurons to SPNs (Chizh et al., 1998).

1.7.2 Parasympathetic nervous system

1.7.2.1 Locations of parasympathetic preganglionic neurones

The cells that give rise to parasympathetic preganglionic axons have their origins within both the brainstem and also the sacral spinal grey matter (Snell, 2010, Longstaff, 2005); an aspect termed craniosacral outflow.

Several cranial nerves originate from brainstem parasympathetic nuclei. These are the oculomotor nerve (via the Edinger-Westphal nucleus), the facial nerve (via the superior salivary nucleus and lacrimatory nucleus), the glossopharyngeal nerve (via the inferior salivatory nucleus) and the vagus nerve (via the dorsal vagal nucleus) (Snell, 2010). As regards the spinal cord of mice, preganglionic parasympathetic neurones are located in the L6-S1 cord segments (Anderson et al., 2009).

1.7.2.2 Anatomical organisation of the parasympathetic nervous system

The cells that give rise to the afferent fibres of the parasympathetic system have their origins in both cranial nerve sensory ganglia and also the sacral dorsal root ganglia. The afferent fibres related to these cells extend from the viscera. Central axons then pass into the CNS where they establish an afferent element to a local reflex arc or ascend to make connections with higher centres associated with the autonomic nervous system (Snell, 2010).

The preganglionic axons leave the brainstem and spinal cord via their associated cranial nerves and ventral spinal nerve roots respectively. The preganglionic axons target visceral structures, establishing synapses with neurones in peripheral ganglia that are in close proximity to their target structure; the neurotransmitter associated with these synapses being ACh (Snell, 2010).

1.8 Nucleus of tractus solitarius (NTS)

1.8.1 Gross Morphology of the NTS

The NTS is constituted from an assortment of neurones in the dorsomedial medulla, and stretches from the lower end of the facial motor nucleus to the lower end of the pyramidal decussation (Ciriello, 1994). Afferent projections from the facial (CN VII), glossopharyngeal (CN IX) and vagus (CN X) nerves (Torvik, 1956, Kalia and Mesulam, 1980, Loewy, 1990b) constitute a bundle of nerve fibres termed the solitary tract, which in turn is encircled by the group of neurones comprising the NTS (see Figure 1.14).

At the rostral level the NTS appears as two columns situated alongside the fourth ventricle. The two columns subsequently unite to establish a single component at the level inferior to obex (Ciriello, 1994) – the obex is the lower border of the fourth ventricle (Burt, 1993). The NTS is generally divided into three regions, defined by their location relative to the area postrema, which are termed rostral, intermediate and caudal (Loewy, 1990b) (see Figure 1.15).

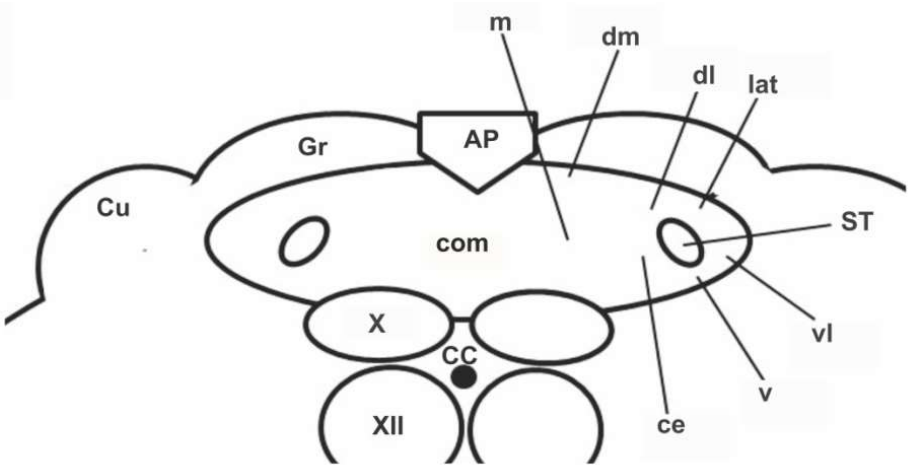

Figure 1.14: Diagram of a transvese section of mouse medulla oblongata at the level of the area postrema showing the location of the NTS. Afferent projections from the facial (CN VII), glossopharyngeal (CN IX) and vagus (CN X) nerves (Torvik, 1956, Kalia and Mesulam, 1980, Loewy, 1990b) constitute a bundle of nerve fibres termed the solitary tract (ST). The neurones comprising the NTS subnuclei surround the solitary tract (Figure adapted from Ciriello, 1994, Okada et al., 2008, Ganchrow et al., 2014, Allen Brain Atlas: Mouse Brain).

NTS subnuclei; com: commissural subnucleus; ce: central subnucleus; dl: dorsolateral subnucleus; dm: dorsomedial subnucleus; lat: lateral subnucleus; m: medial subnucleus; v: ventral subnucleus; vl: ventrolateral subnucleus.

Other structures; AP: area postrema; CC: central canal; Cu: cuneate nucleus; Gr: gracile nucleus; X: dorsal vagal nucleus; XII: hypoglossal nucleus.

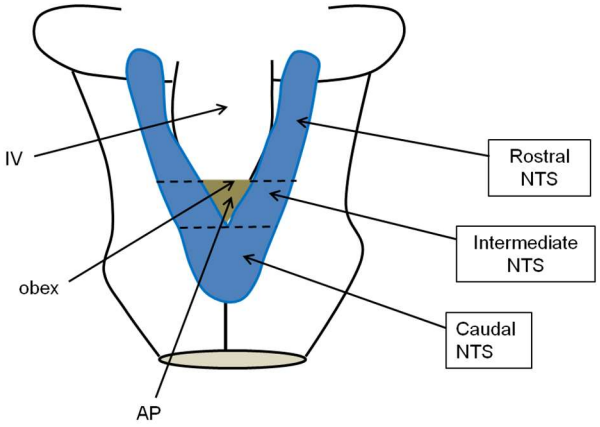

Figure 1.15: Morphology and sub-regions of the NTS. Rostrally, the NTS (marked in blue) appears as two columns situated alongside the fourth ventricle (IV). These two columns subsequently unite to establish a single component at the level inferior to obex (Ciriello, 1994). The intermediate NTS region lies in the same plane and adjacent to the area postrema (AP), whereas the rostral and caudal NTS regions respectively lie rostral and caudal to this plane (Figure adapted from Loewy, 1990b).

1.8.2 Functions of the NTS: why it is important to study?

Afferent information to the NTS comes from baroreceptors, chemoreceptors, cardiac receptors, gastrointestinal and pulmonary receptors plus also the gustatory sense (Kalia et al., 1984, Altschuler et al., 1989, Loewy, 1990b)(see Figure 1.16). The NTS is therefore a primary integration location for the autonomic nervous system (Loewy, 1990b).

To form reflex pathways efferent outputs from the NTS are subsequently sent via mono- or multi-synaptic pathways to vagal or SPNs, which control target structures. In contrast, the integrative function involves more complex alterations. Information from the NTS makes several connections with various systems in the brainstem and forebrain so that the autonomic, neuroendocrine and behavioural response is regulated within a range that still maintains homeostasis (Loewy, 1990b).

Determining the constituent cell types in the NTS is therefore important for a full understanding of the circuits involved in central autonomic control. Two of the major neurotransmitters in the NTS are GABA (Walberg and Ottersen, 1992, Fong et al.,

2005) and ACh (Tago et al., 1989, Ruggiero et al., 1990), but their co-localisation has not been reported.

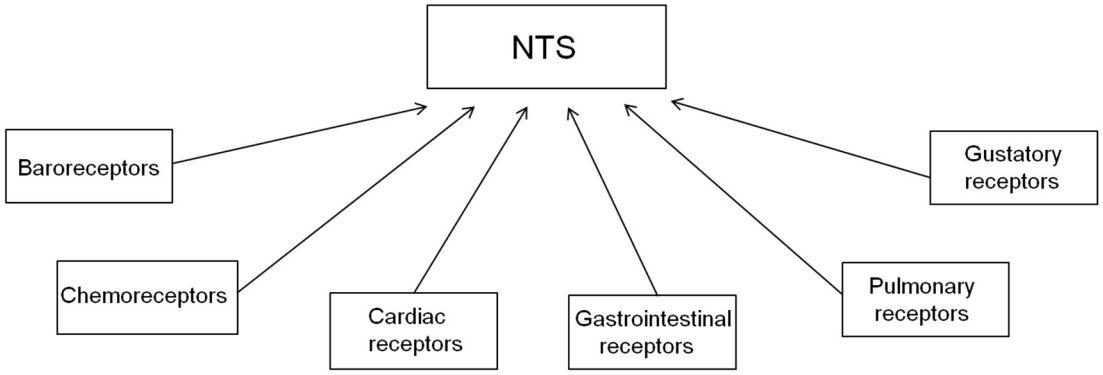

Figure 1.16: The projection of afferent information from various visceral receptors to the NTS (Figure adapted from Loewy and Burton, 1978, Loewy, 1990b).

1.8.3 The subdivision of the NTS

The NTS is very heterogeneous in neuronal types. For over half of a century, numbers of researchers have actively attempted to classify the NTS neurones into subdivisions. In general, most of these subnuclei are named after their location relative to the solitary tract (Ciriello, 1994).

A simple system used to categorise the NTS neurones into two major groups based on cytoarchitectural aspects was described by Torvik, whose best observations were obtained upon application of the silver impregnation method. According to his study the NTS could be divided into two regions, the medial and the lateral; the boundary between the two regions being located somewhat medial to the solitary tract. The medial group was defined by a uniform yellow appearance and contained heavily crowded neurones plus a few delicate intrinsic nerve fibres, similar to the substantia gelatinosa of the spinal dorsal horn. In contrast, the lateral group possessed large numbers of nerve fibres plus neurones which were more sparsely distributed (Torvik, 1956). Kalia and Sullivan (Kalia and Sullivan, 1982) extended the number of defined NTS subdivisions to six, specifically the medial, intermediate, ventral, ventrolateral, interstitial and commissural subnuclei, based on results obtained utilising the Nissl-stain technique on rat brainstem sections. Results from other research studies have

indicated even more NTS subdivisions including dorsolateral, dorsal (Kalia et al., 1984) and subnucleus gelatinosus (Kalia and Mesulam, 1980). The subnucleus gelatinosus is a subgroup situated in proximity to the area postrema, and is comprised of neurones which exhibit a gelatinous appearance due to the total absence of myelinated nerve fibres (Kalia and Mesulam, 1980). In addition, Ross et al. carried out a study on rats to observe the efferent projections from the NTS to the rostral regions of the ventrolateral medulla (Ross et al., 1985). From their study, the subnucleus centralis (or the central subnucleus) is named and described as a roughly circular grouping of cells located medial to the ventral part of the solitary tract within the middle third of the NTS column. The locations of the various NTS subnuclei are shown in Chapter 4.

1.8.4 Afferent inputs of NTS subnuclei

A single subnucleus of the NTS may obtain afferent inputs (see Table 1.1) from more than one specific organ (Baptista et al., 2005).

In addition to receiving afferent inputs from various organs, the NTS neurones also receive inputs from the area postrema (Loewy, 1990b); which is classified as a circumventricular organ since the endothelial cells in the capillaries of the area postrema are fenestrated, enabling substances such as proteins to cross the blood brain barrier (van der Kooy and Koda, 1983, Wuchert et al., 2008). The area postrema is a significant component in circuits involved in autonomic regulation, for example, it receives afferent inputs from the hypothalamic paraventricular nucleus (PVN), lateral parabrachial nucleus (PBN), the NTS (Shapiro and Miselis, 1985) and vagus nerve (Contreras et al., 1982) and projects to the PBN, the dorsal motor nucleus of the vagus, the NTS (van der Kooy and Koda, 1983, Shapiro and Miselis, 1985) and the nucleus ambiguus (Shapiro and Miselis, 1985). Other CNS areas involved in autonomic integration similarly provide projections to the NTS, including the hypothalamus (Geerling et al., 2010) and the amygdala (Saha, 2005).

The NTS is innervated by projections from spinal neurones (Menetrey and Basbaum, 1987). Neurones in lamina I have been observed to project to the NTS through the application of tracing methods (Gamboa-Esteves et al., 2001a, Gamboa-Esteves et al., 2001b, Gamboa-Esteves et al., 2001c). Moreover, by utilising Fluorogold injections into

Table 1.1: A summary of afferent input to NTS subnuclei

NTS subnucleus	Afferent input
Commissural	Cardiac afferent (Kalia et al., 1984)
Central	Oesophagus (Altschuler et al., 1989, Baptista et al., 2005)
Dorsolateral	Baroreceptor and chemoreceptor (Kalia et al., 1984)
Dorsal	Baroreceptor and chemoreceptor (Kalia et al., 1984)
Subnucleus gelatinosus (also term parvocellular NTS or subpostrema NTS (Loewy, 1990b))	Stomach (Altschuler et al., 1989)
Intermediate	Palate, pharynx (Altschuler et al., 1989) Major respiratory nucleus (Kalia et al., 1984) Tracheal afferent (Kalia et al., 1984)
Interstitial	Palate, pharynx (Altschuler et al., 1989), Major respiratory nucleus (Kalia et al., 1984) Laryngeal afferent (Kalia et al., 1984)
Medial	Gastrointestinal afferents (Kalia et al., 1984)
Ventral	Major respiratory nucleus (Kalia et al., 1984) Pulmonary afferent (Kalia et al., 1984)
Ventrolateral	Major respiratory nucleus (Kalia et al., 1984) Pulmonary afferent (Kalia et al., 1984)

the NTS of rats in combination with substance P receptor IHC, Guan et al. observed that some trigeminal and spinal substance P receptor expressing neurones sent projections to the NTS; those neurones that did so were primarily located in lamina I of the spinal cord. The observations made from such studies suggest that lamina I spinal neurones projecting to the NTS may therefore be involved in the regulation of somatic and also visceral nociceptive information, individually or in combination (Guan et al., 1998). As previously mentioned (see Section 1.6.4.2), in rats, neurones in the superficial layers of the dorsal horn (Menetrey and de Pommery, 1991) as well as neurones situated close to the CAA of lamina X have been discerned to project to the NTS, via the spinosolitary tract . Besides laminae I and X, projections to the NTS also arise from neurones in other areas of the spinal cord, including lamina V, the lateral spinal nucleus of the dorsolateral funiculus, and the autonomic cell columns of both the thoracic and sacral regions (Menetrey and Basbaum, 1987)(see Figure 1.17).

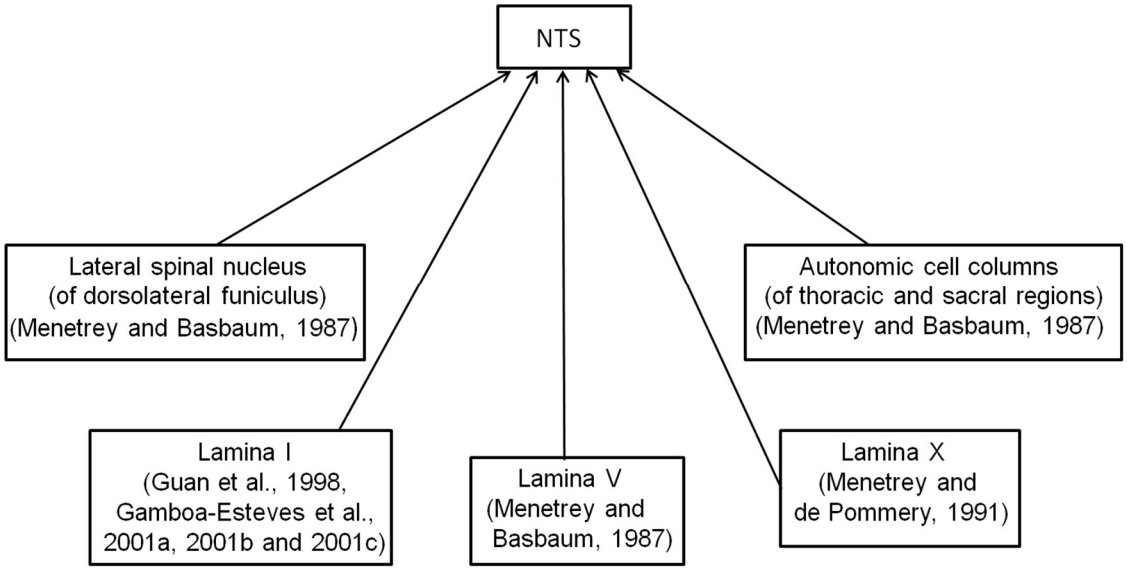

Figure 1.17: Ascending projections from the spinal cord to the NTS based on literature.

1.8.5 Efferent projections and central autonomic connections of the NTS

Studies have been carried out utilising both tracing methods and/or IHC to investigate projections from the NTS to the spinal cord.

Through the application of an autoradiographic anterograde axonal transport technique (involving injections directly into the NTS) and a retrograde HRP technique (involving injections into several regions including the parabrachial region in the pons, the inferior olivary complex, ventrolateral portions of the reticular formation, the ambiguus complex and the spinal cord), neurones from various subnuclei of the NTS of cats were observed to project to the spinal cord. These NTS subnuclei include the intermediate, ventrolateral, commissural and medial subnuclei (Loewy and Burton, 1978). Injection of CTB into laminae I-III of the C4-C7 spinal cord segments of rats caused retrograde labelling that indicated that the commissural subnucleus of the NTS sends descending projections to the superficial laminae of the dorsal horn (Tavares and Lima, 1994). In cats, retrograde tracing using fluorescent tracers revealed that the targeting of thoracic levels by projections from respiratory related neurones in the ventrolateral subnucleus of the NTS was entirely contralateral, while for cervical levels the targeting was predominantly contralateral (Portillo et al., 1986).

Following bilateral injection of WGA-HRP into the midcervical cord of rats (Mtui et al., 1993), labelled NTS neurones were primarily observed at caudal NTS levels in an area ventral to the solitary tract (within ventral and ventrolateral subnuclei). Moreover, for levels which were caudal to the obex, labelled neurones were discerned in the intermediate division. Similarly, upon injection of WGA-HRP into the upper thoracic cord of rats, NTS neurones in an area located close to the ventral border of the solitary tract were retrogradely labelled, although seemingly only at the level of the area postrema. Subsequent unilateral iontophoretic injection of the anterograde tracer PHA-L into the caudal NTS, in combination with IHC, showed decussation of labelled NTS axons in lamina X, plus also projection of labelled NTS axons to the ventral horn, lamina VII and superficial lamina of the dorsal horn.

Pre-proglucagon (PPG) neurones are to be found predominantly in the NTS and the reticular formation of the medulla. Research using transgenic mice (where YFP had been expressed under control of a glucagon promoter) along with IHC techniques, produced results which suggested that PPG neurones in the NTS and the reticular formation contribute abundant projections to SPNs and interneurones in the spinal cord. Since the densest PPG innervation was discerned to project to SPNs, it was subsequently indicated that such connections may be involved in the modulation of sympathetic function (Llewellyn-Smith et al., 2015).

Based on the literature, neurones from various NTS subnuclei (including intermediate, ventrolateral, ventral, commissural and medial subnuclei) send supraspinal projections

to the spinal cord. Nearly all the areas within the spinal cord, including the dorsal horn, ventral horn, lamina VII and lamina X, receive projections from the NTS. In addition, SPNs and interneurones in the spinal cord are innervated by projections from the NTS.

Apart from sending projections to the spinal cord (Loewy and Burton, 1978)(see Table 1.2), the NTS also sends projections to various important nuclei in the brainstem and forebrain regions which are related to the regulation of autonomic and endocrine functions (Loewy and Burton, 1978, Ross et al., 1985, Loewy, 1990b) (see Figure 1.18).

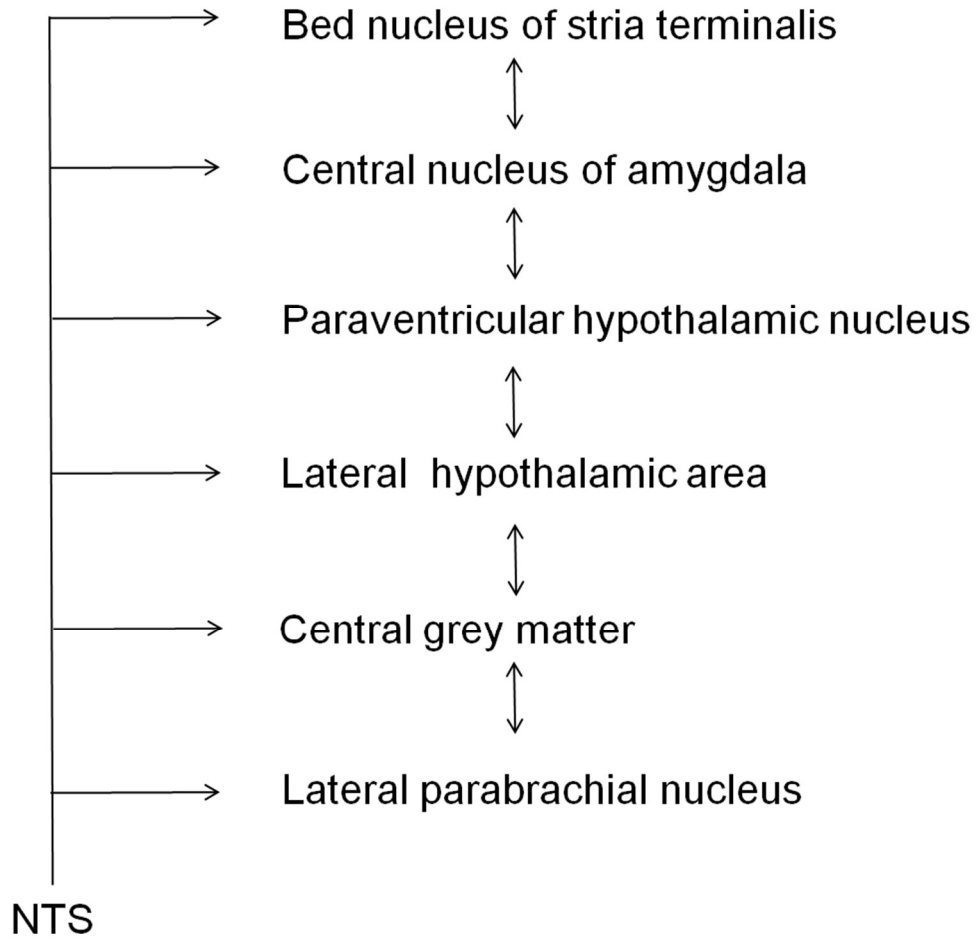

Figure 1.18: Diagram showing the efferent projections from NTS to the central autonomic network of the brain (Figure adapted from Loewy, 1990b).

Table 1.2: A summary of efferent projections from NTS subnuclei to the spinal cord and brainstem regions

NTS Subnucleus	Efferent projection
Commissural	Nucleus reticularis rostroventrolateralis (RVL) (Ross et al., 1985) Parabrachial nuclei & Kölliker-Fuse nuclei (Loewy and Burton, 1978) Cervical spinal cord (Loewy and Burton, 1978) Thoracic spinal cord (Loewy and Burton, 1978) Lumbar & sacral spinal cord (Loewy and Burton, 1978)
Central	Retrofacial nucleus and nucleus ambiguus (Ross et al., 1985)
Dorsal	RVL (Ross et al., 1985)
Intermediate	RVL (Ross et al., 1985) Cervical spinal cord (Loewy and Burton, 1978) Thoracic spinal cord (Loewy and Burton, 1978) Lumbar & sacral spinal cord (Loewy and Burton, 1978)
Interstitial	RVL (Ross et al., 1985)
Lateral	Medial accessory olive (Loewy and Burton, 1978)
Medial	Parabrachial nuclei & Kölliker-Fuse nuclei (Loewy and Burton, 1978)
Parvocellular	Parabrachial nuclei & Kölliker-Fuse nuclei (Loewy and Burton, 1978)
Ventral	RVL (Ross et al., 1985)
Ventrolateral	RVL (Ross et al., 1985) Cervical spinal cord (Loewy and Burton, 1978) Thoracic spinal cord (Loewy and Burton, 1978)

1.9 Summary

GABAergic and cholinergic interneurones play an important role in modulating afferent and efferent neurones within the spinal cord, particularly in lamina X, and within the NTS of the medulla oblongata. The co-localisation of these two neurotransmitters within a population of interneurones could represent an important subgroup of interneurones that may function to integrate different systems or provide antagonistic feedback within a single system.

1.10 Aim

The neurotransmitters GABA and ACh play important functional roles in various pathways of the spinal cord. GABAergic and cholinergic interneurones have been reported to play a crucial role in sensory (Maxwell et al., 1990, Todd, 1991, Mesnage et al., 2011), motor (Miles et al., 2007, Al-Mosawie et al., 2007) and autonomic circuits (Bordey et al., 1996a, Deuchars et al., 2005). Some sources of cholinergic and GABAergic inputs which modulate these circuits are still unknown. Some neurones in various CNS regions including cerebral cortex, basal forebrain, retina (Kosaka et al., 1988), laterodorsal, pedunculopontine tegmental nuclei (Jia et al., 2003), the NTS, area postrema, reticular formation and lateral paragigantocellular nucleus (Gotts et al., 2015) are reported to co-express ChAT and GABA or GAD. In the spinal cord the dorsal horn (Kosaka et al., 1988, Todd, 1991, Mesnage et al., 2011) and lamina X cervical cord (Kosaka et al., 1988) are observed to contain neurones co-expressing ChAT and GABA (or GAD). It is suggested that lamina X and adjacent regions may contain many unidentified interneurones which may have a key involvement in several pathways (Barber et al., 1984, Strack et al., 1989a, Sherriff and Henderson, 1994, Bordey et al., 1996a, Deuchars, 2007). Indeed, newly identified interneurones in lamina X and VII have been increasingly reported over the last decade (Deuchars et al., 2005, Miles et al., 2007, Al-Mosawie et al., 2007, Zagoraiou et al., 2009). Therefore lamina X is an attractive area for the observation of new neuronal subgroups. Since ACh and GABA play crucial roles in numerous circuits of the spinal cord, this study focuses on the presence of a neuronal group in lamina X and adjacent regions that potentially uses both ACh and GABA.

The aim of this study is to determine the spatial distribution of ACh/GABA co-localisation within neurones of lamina X and lamina VII, with a particular focus on the

thoracic spinal cord, because evidence suggests that these areas are heterogeneous in cell type. There is also evidence to suggest that SPNs and various neuronal groups in the spinal cord are modulated through cholinergic and GABAergic receptors. The source of these cholinergic and GABAergic inputs are not well established, and so could potentially arise from the projections of ACh/GABA co-localised neurones located within lamina X and VII. Other cord regions including the cervical and lumbar and various areas within the medulla oblongata focusing on the NTS will also be investigated for the co-localisation. Building upon initial observations from Kosaka (Kosaka et al., 1988) in relation to the cervical spinal cord, we wish to deduce the distribution of ChAT/GAD67-GFP co-localised neurones throughout the spinal cord and regions of the medulla oblongata. In order to investigate ChAT/GAD67-GFP co-localised neurones, GAD67-GFP knock-in mice (Tamamaki et al., 2003) will be used in combination with IHC. A thorough knowledge regarding the distribution of these co-localised neurones will aid the necessary physiological studies needed to elucidate their role. To this end determination of the inputs and outputs of these cells will be made utilising IHC and/or juxtacellular labelling under electrophysiological conditions.

1.11 Hypothesis

The ChAT/GAD67-GFP co-localised neurones form a subgroup within the spinal cord with a distinct spatial distribution that may correspond to the role they perform in the modulation of neurones within the spinal cord. A study performed by Chizh et al., (1998) demonstrated the ability of sympathetic outflow to synchronise with somatic motor output independent of supraspinal structures; as determined via the tested animals having been bisected at the upper thoracic level, which meant that responses were not influenced by supraspinal levels (Chizh et al., 1998). In discussing the theoretical explanations for their observations, Chizh et al. suggested that only a subgroup of each neuronal population were coupled, sharing inputs from the same central pattern generator or oscillator. Given the apparent unidirectional nature of the coupling between somatic motor outflow and associated sympathetic activity (whereas sympathetic outflow seemingly does not correlate to associated somatic motor outflow), shared input from a common source seems unlikely and the cellular pathways underlying this relationship remain unresolved. There is a possibility that ChAT/GAD co-localised neurones have a role in autonomic-efferent modulation. The co-localisation also extends rostrally, plus reaches the medulla oblongata region.

This study is an important first step in the identification and characterisation of a subgroup of interneurones within the spinal cord. Co-localisation of ChAT and GABA (or GAD) in central canal cluster cells in cervical spinal cord sections of the rat has been demonstrated (Kosaka et al., 1988). Here a population of ChAT/GAD67-GFP co-expressing neurones located ventral to the central canal in cervical, thoracic and lumbar regions of the spinal cord was described. A detailed description of the anatomical location of these neurones is necessary so that physiological studies to determine their role can be performed. A thorough understanding of the physiological role and pharmacological properties of ChAT/GAD67-GFP co-expressing neurones may then establish their viable potential as a therapeutic target.

2 General Methods

The experiments in this thesis have utilised neuroanatomical techniques for investigating the organisation and morphology of ChAT-IR, GAD67-GFP-IR and ChAT/GAD67-GFP co-localised neurones within the spinal cord and medulla oblongata. The chemistry, possible projections and synaptic inputs of these neurones have also been explored. The investigative techniques utilised for the work involved retrograde tracing via Fluorogold injection, IHC and electrophysiology.

This chapter defines the basic methodology, plus the technical considerations and all the preparative procedures applied for the experiments encompassed by this thesis. Supplemental details to these basic methods are provided in the relevant chapters.

2.1 Animals

The animal work detailed in this thesis has been carried out in line with the Animals (Scientific Procedures) Act 1986 and the ethical standards set out by the University of Leeds Ethical Review Committee by individuals with UK Home Office approval.

The Animals were kept in a 12 hour light/dark cycle with free access to food and water. They were phenotyped at P1-4 days and weaned at P19-21 days. No more than 5 animals were housed per cage. Animal stocks were maintained by harem breeding using wild type C57/BL6 mates with one male and two females.

Due to difficulty in localising the labelled cell bodies of GABAergic neurones using GAD or GABA antibodies (Fong et al., 2005, Zhao et al., 2013) without colchicine injection (Barber et al., 1982, Kosaka et al., 1988), GAD67-GFP knock-in mice expressing green fluorescent protein (GFP) under control of the endogenous promoter for GAD67 (Tamamaki et al., 2003) were used in this study. The details of GAD67-GFP knock-in mice and their suitability over other transgenic mouse lines are discussed in section 2.1.1.

Wild type mice (C57BL/6) were also used in this study.

2.1.1 Transgenic mice

The details of relevant transgenic mice and the reason for choosing GAD67-GFP knock-in mice over other mice lines are discussed below.

In GIN (GFP-expressing inhibitory neurones) mice (Oliva et al., 2000), the selective expression of GAD67-EGFP in a subpopulation of GAD67-IR neurones has been demonstrated. The authors took advantage of this to investigate the distribution of a somatostatin-expressing subpopulation of GABAergic interneurones in the hippocampus. However, the absence of expression in other brain areas, particularly the cerebellum, striatum and hypothalamus, effectively limits the use of this line for other studies.

An alternative strategy which has been used is to couple GFP expression with GAD65 expression, to produce GAD65-GFP mice. However, for this transgenic mouse line, while it is expected that GABAergic neurones in many regions of brain (such as the hippocampus and neocortex) will express GFP (Lopez-Bendito et al., 2004), it appears that during development only low numbers of GAD65-GFP cells are positive for GABA; around 50% of GAD65-GFP cells in this mouse line indicate the presence of GABA during the embryonic period, increasing to approximately 70% at 21 days postnatal. Therefore, this mouse line appears to have limitations in regards to its viability for studies into GABAergic neurones during development.

In recent years, transgenic mice in which a green fluorescent protein (GFP) expressed under control of a GAD67 promoter (GAD67-GFP knock-in mice) (Tamamaki et al., 2003) have become widely used to study the structures and functions associated with the GABAergic system in the CNS (Edwards et al., 2014, Gotts et al., 2015). According to Tamamaki et al., within various regions of the CNS the distribution of GFP positive cell bodies (detected from IHC) in this transgenic mouse line is comparable to that of the GAD67 signals (obtained from ISH). Furthermore, non-GAD67 cells demonstrate no ectopic expression of GFP, while cells which are positive for GAD67 always exhibit GFP expression (Tamamaki et al., 2003).

2.1.2 Validation of GAD67-GFP knock in mice in the spinal cord

2.1.2.1 Preparation of animals

Three GAD67-GFP knock-in mice (males) were perfused with 100 ml of 2% glutaraldehyde in 4% paraformaldehyde (PFA) in 0.1% phosphate buffer (PB), and then postfixed with 4% PFA overnight. Cervical, thoracic and lumbar cords of the mice were sectioned transversely at 20 µm with a vibrating microtome (Leica VT1000S, UK) and cryostat. Since preliminary data suggested that the staining apparent in the cryostat sections was not as good as that observed for tissue sectioned using the microtome, cryosectioning was subsequently avoided in this study. To detect GAD67 the use of Triton X-100 and ethanol as permeablising agents was not included in the protocols since our preliminary data demonstrated that these reduced the number of GAD67-IR cell bodies labelled. The IHC protocol used was as follows:

2.1.2.2 Double labelling IHC for GAD67 and GFP

The sections were incubated in 1% bovine serum albumin (BSA) blocking serum (Molecular Probes) (10 mg of BSA/10ml of phosphate buffer saline (PBS; 0.876% NaCl, 0.02% KCl in 0.1 M PB, pH 7.2) for thirty minutes and then washed with PBS. Next, the sections were simultaneously incubated with the GFP and GAD67 primary antibodies diluted in 1% BSA in PBS for 4 nights, following which they were rinsed with PBS before being incubated in biotinylated horse anti-mouse (see Table 2.1) overnight. After being rinsed with PBS the sections were incubated in Alexa Fluor ® 488 and Streptavidin Alexa Fluor ® 555 (see Table 2.1) for 1-2 hours. Subsequent to a final rinse with PBS the sections were mounted.

Since only the cells on the surface of the tissue section were labelled, a single plane of image was taken under a confocal microscope. Images were acquired of three sections each at the cervical, thoracic and lumbar cord levels for all test animals (n = 3 animals) and the degree of co-localisation between GAD67 and GFP within the cell bodies noted.

Table 2.1: Combinations of antibodies used for double labelling for GAD67 and GFP IHC.

Target Marker	Primary			Secondary			Tertiary		
	Antibody	Conc	Source	Antibody	Conc	Source	Antibody	Conc	Source
GAD67	Mouse anti-GAD67	1:500	Chemicon International	Biotinylated hourse anti-mouse	1 : 500	Vector Laboratories	Streptavidin Alexa Fluor ® 555	1 : 1000	Invitrogen
GFP	Rabbit anti-GFP	1: 1000	Invitrogen	Alexa Fluor ® 488 donkey anti-rabbit	1: 1000	Invitrogen			

Co-localisation of GFP and GAD67 can be observed (Figure 2.1) in cells throughout the spinal grey matter particularly in the areas known to contain GABAergic neurones, particularly the dorsal horn (Figure 2.1 B), lamina VII (Figure 2.1 C) and lamina X (Figure 2.1 D). Since lamina X is the main focus of our study, validation of GAD67-GFP knock-in mice with respect to their use in lamina X spinal cord research has additionally been carried out in this study since it has not previously been reported in literature. Results indicate that in lamina X, 100% of GAD-IR cells of the cervical, thoracic and lumbar cords contain GFP, while 76.19%, 84.57% and 85.79% of the GFP positive cells of the cervical, thoracic and lumbar cords respectively are GAD67-IR. This suggests that GFP positive cells in the spinal cord are GAD67-IR cells; with the fact that not all GFP positive cells are observed as GAD67-IR being likely due to the difficulty of using IHC for GAD67 in order to obtain exact numbers of labelled GAD67-IR cell bodies (Fong et al., 2005).

Our preliminary data suggested that using Triton X-100 and cryosectioning decreased the efficiency of GAD67-IR soma labelling; a finding consistent with other studies (Fong et al., 2005, Zhao et al., 2013). However, since Triton X-100 was not used in our study, the extent of antibody penetration was therefore limited to the surface of the tissue sections, and so only cells on the surface were labelled. It is well known that GABAergic neurones are difficult to detect. Other improved immunohistochemical approach has been introduced to mitigate the difficulty of GAD/GABA immunostaining. These include the use of fixative agents which contain high concentrations of glutaraldehyde (0.5-2.5%), which preserves GAD/GABA immunoreactivity by switfly binding GAD/GABA to the cell (Zhao et al., 2013), plus colchicine injections, which can enhance cell body labelling of GABAergic neurones as it blocks axonal transport of

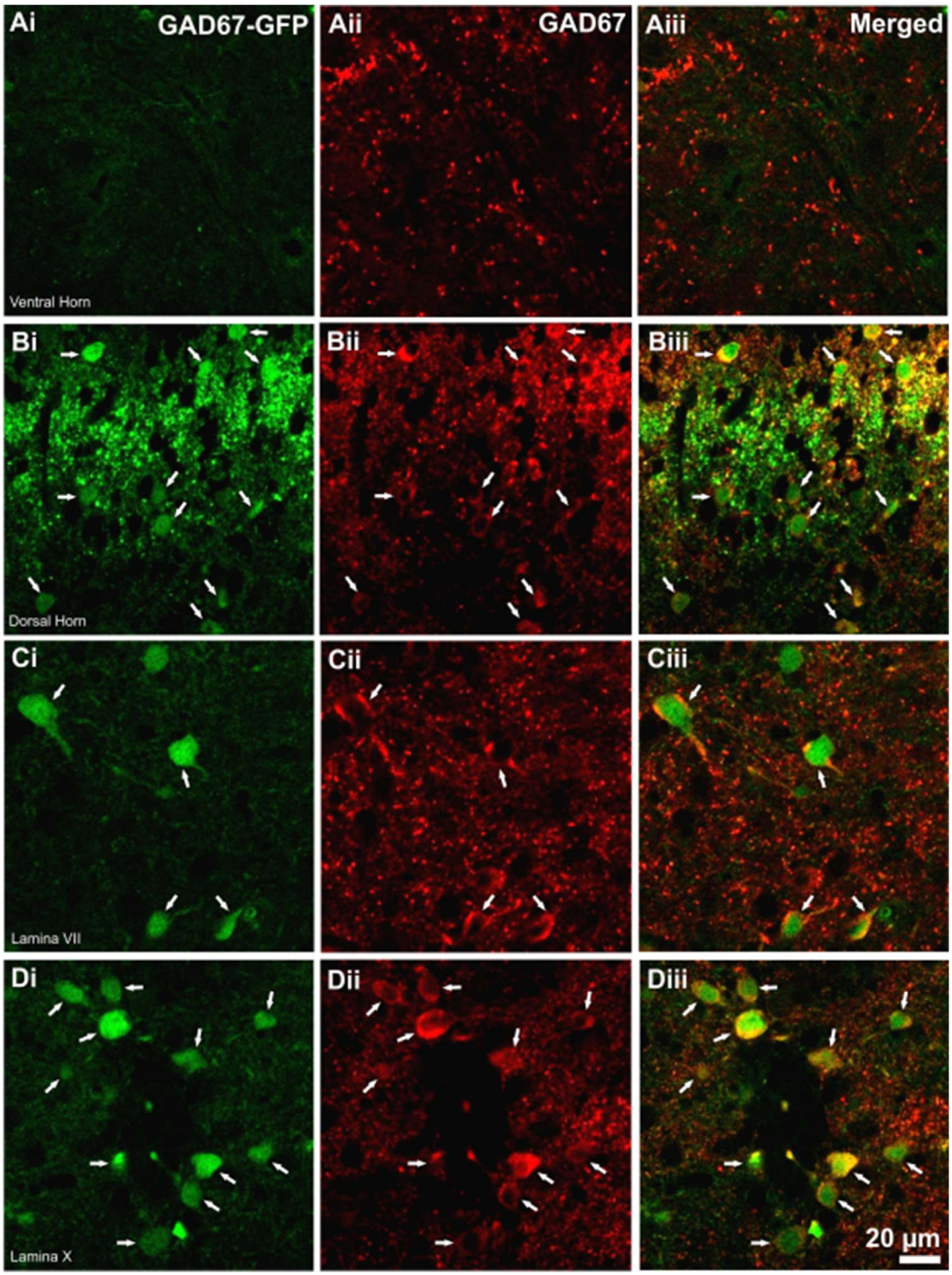

Figure 2.1: The co-localisation of GAD67 and GFP in cells within the grey matter of lumbar spinal cord. Confocal images show the co-localisation of GAD67 and GFP immunoreactivity within the cells of the dorsal horn (Bi to Biii), lamina VII (Ci to Ciii) and lamina X (Di to Diii). Few co-localised cells are present in the ventral horn and none were observed in this section (Ai to Aiii). Cells which exhibit co-localisation are indicated by arrows.

GAD/GABA. Despite these improved methods, insufficient numbers of labelled cell bodies were still observed (Zhao et al., 2013).

Given the above observations, the GAD67-GFP knock-in mouse line was accepted to constitute a suitable animal group for the research described in this text, where the intention was to observe the labelled cell bodies of GAD67-IR neurones in the lamina X of the spinal cord.

2.2 Tracing techniques

To observe the connections between neurones and other structures (both within the CNS and outside of the CNS) procedures involving the introduction of chemicals or agents into the brain areas have been developed, which are now termed tracing techniques. Depending on the direction that these chemicals are transported, the tracing techniques can be categorised into two types; retrograde tracing and anterograde tracing (Purves, 2008).

Retrograde tracing is utilised to investigate connections from their terminations to their neuronal points of origin, and is achieved via the tracing agents first being absorbed by axons and terminals in proximity to the injection site and then transported toward the cell body. Conversely, anterograde tracing is used to trace connections from their neuronal points of origin to their terminations, and is achieved through the tracing agents first being absorbed by the cell bodies of neurones and then transported to the axon terminals of those neurones (Purves, 2008).

2.3 Retrograde labelling of motoneurones and preganglionic neurones

Work undertaken by Ambalavanar and Morris previously found that when injecting animals subcutaneously (into the right vibrissal pad and the middle of the back) or intravascularly (into the right carotid artery and right femoral vein), Fluorogold was absorbed into the nerve terminals located in the periphery and then transported retrogradely to their cell bodies. Their results indicated that this technique facilitated retrograde labelling of motoneurones, autonomic nervous system preganglionic

neurones, plus also pituitary projecting neurones of the hypothalamus (Ambalavanar and Morris, 1989). Fluorogold can also be taken up into axons indirectly from IP injection via endocytosis at nerve terminals (Catapano et al., 2008) and may also be visualised without using IHC. Fluorogold has been widely used to distinguish motoneurones and autonomic motoneurones from interneurones in the CNS (Anderson and Edwards, 1994, Deuchars et al., 2001, Brooke et al., 2002, Al-Mosawie et al., 2007, Llewellyn-Smith et al., 2015).

In this study, Fluorogold injections were selected to be used, via the retrograde tracing method, to distinguish motoneurones and SPNs from interneurones. The major disadvantage to the use of Fluorogold is that it is non specific to a particular group of neurones; readily diffusing from the injection site, Fluorogold will be endocytosed by any neurones whose terminals it makes contact with (Catapano et al., 2008). However, this is not a limitation in this study as the IP injection results only in labelling of CNS neurones with axons that project to the periphery and not neurones intrinsic to the CNS.

2.4 Immunohistochemistry (IHC)

Although often used interchangeably, the terms immunohistochemistry (IHC) and immunocytochemistry (ICC) refer to the application of similar techniques to different preparations. Both techniques make use of the explicit attraction that exists between an antigen and a relevant antibody (Polak and Van Noorden, 2003). In the case of ICC, antibodies are used to detect antigens on isolated cells devoid of the extracellular matrices and architecture found in vivo, such as in cultured cell monolayers. Immunohistochemistry refers to the same process but applied to sections of tissue and the cells within (Matos et al., 2010).

From the early 1940s until mid-1950s, Coons and his collaborators played a critical role in developing knowledge concerning the use of IHC. Most notably, they pioneered the procedure of labelling antibodies with fluorescent dyes and subsequently using these labelled antibodies to locate the presence of antigens within selected tissue sections; the results from such applications being visualised via fluorescent microscopy (Coons et al., 1941, Coons and Kaplan, 1950, Coons et al., 1955).

The development of enzyme-linked antibodies opened up the technique to those laboratories lacking fluorescent microscopes and so helped to popularise the use of IHC (Nakane and Pierce, 1966, Matos et al., 2010). The use of diaminobenzidine to produce an electron dense precipitate for use in electron microscopy (Singer, 1959, Matos et al., 2010), peroxidase anti-peroxidase (PAP) (Sternberger et al., 1970) and alkaline phosphatase-antialkaline phosphatase (APAAP) (Mason and Sammons, 1978) further broadened the application of IHC (Matos et al., 2010). Additional advances led to antigen retrieval methods (Huang et al., 1976), and systems for labelling cells in fresh samples such as avidin-biotin-complex (ABC) (Hsu and Raine, 1981, Matos et al., 2010).

2.5 Preparation of animals

2.5.1 Retrograde tracing utilising Fluorogold injection

Three adult GAD67-GFP knock-in mice (4-6 weeks in age, approximately 30 grams in weight, both sexes), plus three GAD67-GFP knock-in young mice (7-14 days in age, both sexes) used for quantitative analysis, were intraperitoneally injected with Fluorogold (0.1 ml of 1% Fluorogold per adult animal and 0.05 ml of 1% Fluorogold for the young mice).

2.5.2 Perfusion and fixation

One to three days after the Fluorogold injection, the mice were anaesthetised with an IP injection of 60 mg/kg sodium pentobarbitone. The depth of anaesthesia was assessed by the pinch reflex. When the pinch reflex was absent the ribcage was opened to expose the heart. The right atrium was cut and 100 ml of 4% PFA in 0.1M PB for the adult mice, or 50 ml of 4% PFA in 0.1M PB for the young mice, then perfused through the left ventricle. After the perfusion, the skulls and vertebral columns were dissected and the brainstem and spinal cords removed and then postfixed with 4% PFA for up to 24 hours. The tissues were subsequently kept in PB.

2.5.3 Tissue sectioning

The meninges were carefully removed using fine forceps and spinal cords and brainstems sectioned transversely or sagittally at 30 µm to 50 µm with a vibrating microtome (Leica VT1000S, UK), and free floating sections collected in 0.1 M PB.

2.5.4 Gelatin embedding for IHC on longitudinal sections

In instances where the tissue was fragile and needed support, or sagittal sections were required, gelatin embedding was required. 10% gelatin in 50 ml of deionised water was placed on a hot plate stirrer until the gelatin melted. The gelatin solution was then left to cool until it was warm but not yet set. The spinal cord was then embedded by the gelatin using a 35 mm tissue culture dish. The culture dish sat upon a copper plate previously cooled in a -20 C freezer. Once the gelatine had begun to show signs of setting the dish was transferred to a freezer to expedite the process, but using caution to avoid any freezing of the tissue. Once set, the block of gelatine surrounding the cord was excised and then postfixed with 0.2% - 1% glutaraldehyde in 4% PFA for up to 24 hours before sectioning was undertaken via a vibrating microtome.

2.6 Antigen retrieval

Cross-linking of proteins can occur when using fixative agents. This may prevent antibodies from binding to the antigenic sites. In formaldehyde fixed tissue, the use of high temperature, pH and suitable solutions (Shi et al., 1997) can be used as an aid to the antigen retrieval process. While experimenting to determine the optimal conditions for immunostaining we explored the use of antigen retrieval using 10 mM sodium citrate. Tissue was incubated with sodium citrate in 80 °C water for thirty minutes prior to primary antibody incubation. However it was found that the procedure compromised the GFP immunoreactivity. As a result is was decided to not use this protocol for the subsequent investigations.

An alternative fixative which produces a stronger reaction with better tissue preservation than formaldehyde is glutaraldehyde. However it also possesses many of the disadvantages that are seen with formaldehyde but more accentuated due to its increased reactivity. This includes loss of antigenicity due to cross-linking; which can

be overcome by diluting it in another fixative, such as formaldehyde. In this situation the more rapid action of formaldehyde initiates the fixation process, stabilising the molecules, and thus gives time for the relatively slowly diffusing glutaraldehyde to strengthen the reaction (Stradleigh and Ishida, 2015).

2.7 Fluorescence IHC

The first time each antibody was used (see Table 2.2), the optimal concentration for its use was determined by performing serial dilutions of the antibody in PBS containing 0.1% - 0.3% Triton X-100 (Sigma) (to increase cell permeability) and 5% donkey serum (blocking for non-specific immunoreactivity) at 4 °C for a minimum of 18 hours. The sections were washed with PBS for 3 x 10 minutes before application of a suitable Alexa Fluor secondary antibody (1:1000, 1-3 hours, room temperature). This was followed by further 3 x 10 minutes PBS washes.

For double labelling fluorescent IHC, tissue sections were incubated as previously described but with both primary antibodies simultaneously. After repeated washing of the tissue in PBS solution the sections were then incubated in Alexa Fluor secondary antibodies diluted in PBS (see Table 2.3) for 1-3 hours before being washed with PBS for 3 x 10 minutes.

For triple labelling, tissue sections were simultaneously incubated with all three primary antibodies following the method described for single labelling. After repeated washes in PBS solution the sections were incubated in biotinylated antibody (see Table 2.3) for either 4 hours (dilution; 1:200) or overnight (dilution; 1:500) prior to being washed with PBS again for 3 x 10 minutes. Subsequently, the sections were incubated with streptavidin-conjugated fluorophore and secondary antibodies (see Table 2.3) for one to three hours before being washed with PBS for 3 x 10 minutes.

Once the washes post secondary antibody incubation were complete the tissue sections were mounted as described in Section 2.9.

Due to the difficulty of GAD detection in cell bodies, the use of GAD67 antibody required special consideration to facilitate effective immunostaining, as discussed below.

Table 2.2: Determination of optimal primary antibody concentration and characterisation of primary antibodies used.

Antibody	Immunogen	Manufacturer and details	Concentration	Ref/control
Goat anti-ChAT	Human placental enzyme	Millipore Cat# AB144P-1ML, RRID:AB_262156, polyclonal antibody	1:500	(Chapman et al., 2013)
Rabbit anti-GFP	GFP isolated directly from Aequorea Victoria	Invitrogen Cat# A11122, RRID:AB_221569, polyclonal antibody	1:1000	(Chapman et al., 2013)
Mouse anti GFP	GFP isolated directly from Aequorea Victoria	Invitrogen Cat# A11120, RRID:AB_221568, monoclonal antibody	1:1000	The labelling was only observed in cells that expressed GFP
Mouse anti-GAD67	Recombinant GAD67 protein	Chemicon International Cat# MAB5406, RRID:AB_2278725, monoclonal antibody	1:500	(Chapman et al., 2013)
Rabbit anti-GABA	GABA-BSA	Sigma Cat# A2052, RRID:AB_477652, polyclonal antibody	1:500	Staining reveals identical patterns to those previously documented (Kosaka et al., 1988, Todd 1991)
Mouse anti-NOS1 (nNOS)	Amino acids 2-300 of NOS1 of human origin	Santa Cruz Biotechnology, Inc Cat# sc-5302, RRID:AB_626757, monoclonal antibody	1:250	Staining reveals identical patterns to those previously documented (Wiedner et al., 1995)
Guinea pig anti-VGLUT1	Synthetic peptide from rat VGLUT1 protein	Millipore Cat# AB5905, RRID:AB_2301751, polyclonal antibody	1:30,000	Staining reveals identical patterns to those previously documented (Todd et al., 2003)
Guinea pig anti-VGLUT 2	Synthetic peptide from rat VGLUT2 protein	Millipore Cat# AB2251, RRID:AB_1587626, polyclonal antibody	1:10,000	Staining reveals identical patterns to those previously documented (Todd et al., 2003)
Guinea pig anti-GlyT2	Synthetic peptide from the carboxy terminus as predicted from cloned rat GlyT2	Millipore Cat# AB1773, RRID:AB_90953), raised in guinea pig, polyclonal antibody	1:15,000	Staining reveals identical patterns to those previously documented (Jursky and Nelson, 1995)

Table 2.3: Determination of optimal secondary antibody and conjugate concentrations.

Antibody	Manufacturer and details	Concentration
Alexa Fluor ® 555 donkey anti-goat	Invitrogen	1: 1000
Alexa Fluor ® 488 donkey anti-rabbit	Invitrogen	1: 1000
Alexa Fluor ® 488 donkey anti-mouse	Invitrogen	1: 1000
Alexa Fluor ® 555 donkey anti-rabbit	Invitrogen	1: 1000
Streptavidin Alexa Fluor ® 555	Life Technologies	1: 1000
Streptavidin pacific blue	Invitrogen	1: 1000
Biotinylated donkey anti- goat	Jackson Immuno-Research Laboratories	1:200 for 4 hrs or 1:500 overnight
Biotinylated donkey anti- rabbit	Jackson Immuno-Research Laboratories	1:200 for 4 hrs or 1:500 overnight
Biotinylated horse anti- mouse	Vector Laboratories	1:200 for 4 hrs or 1:500 overnight
Biotinylated donkey anti- guinea pig	Jackson Immuno-Research Laboratories	1:200 for 4 hrs or 1:500 overnight
ExtrAvidin® Peroxidase (EAP)	Sigma	1 : 1500 for IHC 1 : 250 for cell recovery
DAB solution	Sigma	5 mg in 10 ml in Tris buffer with 0.01% H_2O_2
DAB SK-4100	Vector Laboratories	5 ml of distilled water containing buffer solution (2 drops), DAB (4 drops) and H_2O_2 (2 drops)

The spinal cord was sectioned using a vibrating microtome as it resulted in better staining for labelled GAD67-IR cell bodies than those sectioned using cryosectioning, per our preliminary data. Initially spinal cord sections were washed for 3 x 10 minutes in PBS before a 30 minute incubation with 50% ethanol to permeabilise the tissue (Fong et al., 2005) . However, our results suggested that this method provided lower numbers of labelled GAD67-IR cell bodies in comparison to sections which had been prepared without incorporating ethanol incubation. Consequently the use of ethanol incubation was subsequently avoided. Sections were incubated in primary antibody using the protocol described in section 2.1.2.2 The use of Triton X-100 was avoided at all stages since it reduced the cell body labelling (Fong et al., 2005).

2.8 Peroxidase IHC

Peroxidase cytochemistry was first introduced by Graham and Karnovsky (Graham and Karnovsky, 1966). For the purposes of the studies in this thesis the following procedure was followed:

To provide a permanent reaction product, tissue sections were incubated with 1% H_2O_2 for thirty minutes to quench endogenous peroxidase. The sections were washed three times with PBS before being incubated in primary antibody for a minimum of 18 hours at 4 °C (in PBS containing 0.1% - 0.3% Triton X-100). The sections were washed three times with PBS before being incubated in biotinylated antibody overnight at 4 °C. The sections were then washed three times with PBS before being incubated in ExtrAvidin® Peroxidase (EAP; 1:1500 in PBS, Sigma) overnight at 4 °C. Next, one of two options for continued tissue preparation was selected. The first option was to wash the sections three times with PBS prior to incubation in diaminobenzidine (DAB) solution (Sigma) (5 mg in 10 ml in Tris buffer with 0.01% H_2O_2) for ten minutes in a dark cold room at 4 °C. The reaction was subsequently precipitated through the continued addition of 1% H_2O_2 until brown colour labelling was observed. To halt the reaction the sections were then washed with Tris twice (10 minutes each). In the second option, the sections were washed three times with PBS before being incubated at room temperature in DAB solution using peroxidase substrate kit (DAB SK-4100, Vector Laboratories; 5 ml of distilled water containing buffer solution (2 drops), DAB (4 drops) and H_2O_2 (2 drops))(see Table 2.3) until brown colour labelling occurred. The final concentration of H_2O_2 in the reaction mixture was 0.01%. To stop the reaction, the sections were washed with deionised water and then kept in PBS. Details on peroxidise IHC in

relation to cell recovery for juxtacellular labelling will not be mentioned here but will be detailed in Chapter 3.

2.9 Preparation of sections for viewing under the fluorescence, confocal and light microscope

For viewing under a fluorescence and/or confocal microscope, the sections were air dried on glass slides (Academy Science Limited) and mounted under a coverslip (Scientific Laboratory Supplies) using Vectashield mounting medium (Vector laboratories, UK). The edges of the coverslips were sealed by applying nail varnish to prevent evaporation of the mounting medium.

For viewing sections that had been processed using peroxidase IHC under a light microscope, the sections were air dried on gelatinised glass slides overnight. The tissue sections were then dehydrated through an ethanol concentration series of 50%, 70%, 95%, 100% and 100% for two to five minutes at each stage. Finally, the sections were cleared through xylene and mounted in DPX under a coverslip (BDH Laboratory Supplies, UK).

2.10 Image capture

A Nikon Eclipse E600 microscope equipped with epifluorescence and a Q-Imaging Micropublishing 5.0 camera was used, with the images being visualised and captured using Acquis image capture software (Acquis Images Capture system, Synoptics, UK).

Some tissue sections from fluorescence IHC were selected to be alternatively visualised and captured using a confocal microscope (Zeiss LSM 510 Meta Confocal Microscope) in conjunction with Zen software.

2.11 Image manipulation and figure making

A combination of confocal and epifluorescent microscopy was used to study the data, selection being dependent upon the desired objectives. For gross counting and initial observations epifluorescent microscopy was sufficient and readily available. Some situations required higher resolution images however, such as when a precise determination of co-localisation was necessary, or there was close apposition, or methodological considerations led to sub-optimal staining. In these instances, confocal microscopy was used.

Fluorescent images in Figures 3.4, 3.11, 3.12, 4.3, 4.6, 4.8 and 4.9 B were obtained using epifluorescent microscopy. All other fluorescent images were obtained via confocal microscopy. The captured images were only adjusted minimally for brightness and contrast and then labelled using CorelDraw x5 and x6 software.

2.12 Quantification of co-localisation

2.12.1 Spinal cord study

ChAT-IR and/or GAD67-GFP-IR neurones in lamina X, VII, ventral horn, dorsal horn and lateral horn of the adult (n =3) and young mice (n = 3) were manually quantified from both sides of the cord across 50 µm thick sections under an epiflorescence microscope. Each area was identified by its location based on literature reports (Rexed, 1952, Rexed, 1954, Watson and Kayalioglu, 2009, Sengul and Watson, 2012, Sengul et al., 2012, Allen Brain Atlas: Mouse Spinal Cord), as depicted in Figure 1.1 and 1.2.

To avoid double counting cells in adult animals, every sixth consecutive section (50 µm thick) was counted for each region of the spinal cord, with a total of ten sections per region. Across 3 animals this gave a total of 30 sections each for the cervical, thoracic and lumbar regions. Due to the decreased volume of tissue in young animals, every third consecutive section (50 µm thick) was counted with a total of 5 sections per region. This gave a total of 15 sections for each region across 3 animals. Cells were counted by eye using epifluoresence microscopy, so allowing for adjustment of the plane of focus in order to ensure all positively labelled cells in the section (both sides) were accounted for. Data was collated in a Microsoft Excel spreadsheet for statistical analysis. Pooled data for each section area of a region was used to determine the

mean number of positive cells per section in each respective region across all 3 animals. This was repeated for all areas to give the mean values (± SEM, standard error of the mean) of positively labelled neurones in relation to each marker (ChAT and GAD67-GFP) within laminae X and VII, plus the ventral horn, dorsal horn and lateral horn for the cervical, thoracic and lumbar regions. Where co-localised neurones were observed, the proportion of co-localisation was expressed as a percentage of the ChAT-IR and GAD67-GFP-IR population separately. N is used to represent the number of neurones counted and n is used to indicate the number of animals used. The number of sections counted is depicted as nsc. Comparison of the relative abundance of each neurochemically-defined population in lamina X between juvenile and adult mice was conducted using Student's t-test via SPSS.

Neuronal morphology, determined by soma shape and soma size, was measured using the pictures taken from sections with double labelling IHC. The width (X-axis diameter) and length (Y-axis diameter) of somata from a two dimensional perspective were measured using CorelDraw x6 software. The cross sectional area of neuronal soma were then estimated based on the cells being oval (using the average value of the X- and Y-axia diameters).

2.12.2 NTS and medulla oblongata study

ChAT-IR and/or GAD67-GFP-IR neurones in the NTS of adult mice (n = 3) were manually quantified from both sides of the NTS column across 50 µm thick sections under an epiflorescence microscope. Each subnucleus was identified by its location based on literature reports (Ciriello, 1994, Poole et al., 2007, Okada et al., 2008, Ganchrow et al., 2014) (see Figure 4.1).

From each animal, every sixth consecutive section was studied to avoid the risk of double counting the same neurones in adjacent sections. Six sections were counted in total (from each animal); two each representative of the caudal, intermediate and rostral regions of the NTS, and if a section to be investigated was damaged, it was substituted in the analysis by an adjacent section. Due to the limited distribution of the central subnucleus in the NTS, ChAT-IR, GAD67-GFP-IR and nNOS-IR neurones in this area were counted in four sections, from every third consecutive serial section (30 µm thick) from one animal. Data was collated in a Microsoft Excel spreadsheet for statistical analysis. Pooled data for each subnucleus of the NTS was used to determine

the mean number of positive cells per section across all 3 animals. This was repeated for all subnuclei to give the mean values (± SEM) of positively labelled neurones in relation to each marker (ChAT and GAD67-GFP) within each subnucleus of the NTS. Comparison of the relative abundance of each neurochemically-defined population between NTS and area postrema was conducted using Student's t-test via SPSS.

In an attempt to quantify the intensity of ChAT staining within the NTS neurones ChAT immunoreactivity in the NTS was compared against that observed in the dorsal vagal nucleus for the same section of a wild type mouse using DAB staining. The detail of DAB IHC protocol was described in section 2.8 using DAB solution (Sigma). The value obtained from ImageJ software relates only to lightness not darkness. In order to measure darkness, it would have been necessary to convert the captured image to a negative of itself, so that light features became dark and dark features became light. As such it was decided not to convert the images, but instead to measure the lightness of neurones in the original image. Consequently, when comparing the intensity of staining between NTS and dorsal vagal neurones the relative lightness level was reported, based on measurements taken from isolated neurones. By being specific to the staining of selected cells, the approach taken therefore eliminated several possible sources of measurement error, including those that may arise from differences in background staining, and also from multiple cells or processes passing through the measured region.

The numbers of neurones containing ChAT and/or GAD67-GFP in other areas of the medulla oblongata, including the area postrema, reticular formation, dorsal vagal nucleus, hypoglossal nucleus and nucleus ambiguus were manually quantified using the same approach as for the NTS. Specifically, from 3 mice using 50 µm thick sections and an epiflorescent microscpe, with every sixth consecultive section being examined; the total number of sections examined per animal being dependent on the size of the area, for instance 2 sections per animal for the area postrema and 6 sections per animal for the reticular formation. Each area was identified by its location based on reports in the literature (VanderHorst and Ulfhake, 2006, Allen Brain Atlas: Mouse Brain) (see section 4.3).

3 Neurones expressing ChAT and GAD67-GFP in mouse spinal cord focusing on lamina X and VII

3.1 Introduction

A full understanding of the functions of the CNS requires a detailed understanding of neuronal circuitry. One way in which specific neuronal subgroups can be studied in relation to their location and potential function is to utilise neurochemical identification of particular subgroups. In this chapter, we focus on the existence of a subgroup of neurones in the spinal cord which potentially utilise both ACh and GABA, located in lamina X.

The neurotransmitters GABA and ACh play important functional roles in the spinal cord. GABAergic inhibitory interneurons are critical components of local circuits and play significant roles in the dorsal horn and ventral horn (Todd and Maxwell, 2000). Neurons containing immunoreactivity for GABA or the synthesizing enzyme GAD are found in the dorsal horn of the rat and mouse (Kaduri et al., 1987, Todd and McKenzie, 1989, Polgar et al., 2013) with scattered soma in other layers, particularly lamina X surrounding the spinal cord and cerebrospinal fluid contacting neurones in the ependymal layer surrounding the central canal (Kaduri et al., 1987).

The possibility that neurones can co-release both ACh and GABA originated from anatomical studies showing ChAT-IR neurones that also contain GAD (or GABA) in the rat retina, cerebral cortex and basal forebrain (Kosaka et al., 1988), the cat laterodorsal and pedunculopontine tegmental nuclei (Jia et al., 2003), ChAT immunoreactivity has also been observed in GAD67-GFP-IR neurones in the mouse brainstem in the NTS, area postrema, reticular formation and lateral paragigantocellular nucleus (Gotts et al., 2015). In situ hybridisation studies have shown mRNA for both GAD and ChAT is present in cell bodies of the globus pallidus and nucleus basalis of the mouse basal forebrain (Granger et al., 2016).

Functional studies have since determined that ACh and GABA are co-released from starburst amacrine cells in the rabbit retina (Lee et al., 2010), from a population of globus pallidus cells projecting to the mouse cerebral cortex (Saunders et al., 2015a) and from neurons in the mouse forebrain (Saunders et al., 2015b). For a review see Granger et al. 2016.

In the rat spinal cord, a population of ChAT-IR or ChAT-GFP containing cells that also contain GABA or GAD have been observed in lamina III of the dorsal horn (Kosaka et al., 1988, Todd, 1991, Mesnage et al., 2011) where they display morphological and electrophysiological characteristics consistent with interneurones (Mesnage et al.,

2011). In addition, ChAT and GABA (or GAD) immunoreactivity are co-localised in a population of cells surrounding the rat central canal, studied only at the cervical level (Kosaka et al., 1988).

Sources of cholinergic and GABAergic mediated effects on various pathways in the spinal cord are yet to be fully defined. The origin of thes cholinergic and GABAergic inputs may arise from lamina X neurones since evidence suggests that lamina X contains a heterogeneous population of neurones and may contain many unidentified interneurones which provide the source of cholinergic and GABAergic modulation of several pathways (see section 1.6.4). Therefore this study focuses on the presence of a neuronal group in lamina X and adjacent regions that potentially uses both ACh and GABA.

3.2 Aim

The aim of this study is to investigate the existence of co-localisation between ACh and GABA within the cervical, thoracic and lumbar spinal cord regions. Adult and young GAD67-GFP knock-in mice (Tamamaki et al., 2003) are used in combination with IHC. The locations of ChAT/GAD67-GFP co-localised neurones are also determined so that further investigations into the projections and functions of such neurones can be considered utilising juxtacellular labelling from extracellular electrodes in spinal cord slices. Moreover, inputs to the co-localised neurones are explored in order to gain a better understanding into their possible functions.

3.3 Methods

The methods in this chapter are divided into 4 subsections based on the purpose of the experiment conducted, as follows:

3.3.1 Looking for evidence of ChAT and GAD67-GFP co-localisation in the adult and neonatal spinal cords of mice

For the study of ChAT/GAD67-GFP co-localisation defined by this section, adult (4-6 weeks, n = 3) or young (7-14 days postnatal, n = 3) GAD67-GFP knock-in mice of either sex (Tamamaki et al., 2003) were used. To distinguish motoneurones and SPNs from interneurones in the spinal cord, the mice were intraperitoneally injected with Fluorogold (Ambalavanar and Morris, 1989, Anderson and Edwards, 1994). Immunohistochemistry was performed as described previously (see section 2.7), using the combinations of antibodies depicted in Table 3.1. Details regarding the appropriate control and characterization of antibodies used are described in chapter 2 (see Table 2.2). Quantification of co-localisation was performed in laminae X and VII, with the laminae being identified based on the information indicated in the Allen mouse spinal cord atlas (http://mousespinal.brain-map.org/) and literature (Rexed, 1952, Rexed, 1954, Watson and Kayalioglu, 2009) (see Figure 1.1 and 1.2). Other areas in the spinal cord including the ventral horn, dorsal horn and lateral horn were also investigated for the presence of co-localisation. The experimental, quantification and analytical methods used are detailed in section 2.12.1).

Table 3.1: Combinations of antibodies used for quantification of co-localisation study

Target Marker	Primary			Secondary		
	Antibody	**Conc**	**Source**	**Antibody**	**Conc**	**Source**
ChAT	Goat anti-ChAT	1:500	Millipore	Alexa Fluor ® 555 donkey anti- goat	1 : 1000	Invitrogen
GFP	Rabbit anti-GFP	1: 1000	Invitrogen	Alexa Fluor ® 488 donkey anti-rabbit	1: 1000	Invitrogen

3.3.2 Looking at the pattern of intersegmental expression of ChAT-IR and GAD67-GFP-IR cells in lamina X of adult and neonatal mouse spinal cords

The number of ChAT-IR, GAD67-GFP-IR plus ChAT/GAD67-GFP co-localised neurones present in the cervical, thoracic and lumbar cord regions of both adult (n = 3) and young mice (n = 3) were determined using the methodology indicated in section 3.3.1 and 2.12.1.

Since the connection between co-localised neurones and SPNs was of interest, plus given the fact that the thoracic cord region contains the majority of SPNs, the location of co-localised neurones in lamina X of the thoracic cord region was explored to establish the optimal area for subsequent juxtacellular labelling experiments. In order to observe neurones exhibiting ChAT/GAD67-GFP co-localisation, sagittal and transverse serial sections of the spinal cords were examined, as per the methodology indicated in the following sub-sections:

3.3.2.1 Reconstruction of the location of ChAT/GAD67-GFP co-localised neurones

3.3.2.1.1 Transverse serial sections

The upper thoracic cord (approximately T2-T4) of a GAD67-GFP knock-in adult mouse was sectioned serially and transversely at 50 µm, following which the sections were processed for IHC for ChAT and GAD67-GFP as above (Table 3.1). Pictures of serial sections around the central canal regions were taken to observe co-localisation. The location of co-localisation was then three-dimensionally reconstructed using Reconstruct software version 1.1.0.0 (SynapseWeb, 1999).

3.3.2.1.2 Sagittal serial sections

Nearly the whole thoracic spinal cord (approximately from T1 to T12) of a GAD67-GFP knock-in adult mouse was embedded in 10% gelatin and then postfixed with 1% glutaraldehyde in 4% PFA overnight (see section 2.5.4). The embedded cord was then sectioned serially and sagittally at 50 µm and processed using IHC for ChAT and

GAD67-GFP (see Table 3.1). The location of ChAT/GAD67-GFP co-localised neurones in relation to the central canal region throughout the studied thoracic spinal cord was observed and mapped using camera lucida. The locations were then reconstructed using CorelDraw x6 software.

Reconstruct software version 1.1.0.0 was not selected for reconstructing the co-localised neurone locations in the sagittal sections because the whole length of the T1-T12 cord section under investigation was too large for the required level of microscope magnification. Therefore, the camera lucida approach was selected. In addition, since the sagittal and transverse planes provided sufficient information on where the majority of co-localised neurones were located, it was not necessary to extend the study to investigate the horizontal sections.

3.3.3 Morphological analysis of cells that express ChAT and GAD67-GFP in neonatal spinal cords using juxtacellular labelling

3.3.3.1 Animal and tissue preparation

Forty three GAD67-GFP knock-in mice, of both sexes and 7-14 days postnatal, were used. The mice were anaesthetised with an IP injection of 60 mg/kg sodium pentobarbitone. The depth of anaesthesia was assessed by the pinch reflex and when it was absent the ribcage was opened to expose the heart. The right atrium was cut and 20 ml of ice-cold sucrose artificial cerebrospinal fluid (Sucrose aCSF, composition in mM; Sucrose (217), $NaHCO_3$ (26), KCl (3), $MgSO_4$ (2), NaH_2PO4 (2.5), $CaCl_2$ (2), glucose (10)) perfused into the left ventricle. After the perfusion, the animals were decapitated and the vertebral columns were dissected. The spinal cords were removed from the animals and placed in ice-cold sucrose aCSF under continual oxygenation (95% O_2, 5% CO_2). The meninges were carefully removed using fine forceps. A 5% solution of agar in aCSF (composition in mM; NaCl (124), $NaHCO_3$ (26), KCl (3), $MgSO_4$ (2), NaH_2PO_4 (2.5), $CaCl_2$ (2), glucose (10) pH7.4) was heated to boiling point. When the agar solution cooled down, the thoracic and upper lumbar spinal cord was embedded in the agar and then placed on ice until it was set. The embedded spinal cords were cut at 300 µm using Integraslice 7550 PSDS (Campden Instruments) and maintained in oxygenated ice-cold sucrose aCSF throughout the cutting process. The slices were transferred to a holding chamber where they were left to equilibrate in oxygenated aCSF for approximately one hour prior to patching.

3.3.3.2 Patch electrode preparation and tracer agents

Borosilicate glass tubes (1.20 mm outside diameter, 0.94 mm internal diameter and 10 cm in length, model no G120TF-4, Warner Instruments) were pulled by a micropipette puller (model P-97, Sutter Instrument CO, USA) to form the patch electrodes. These pulled electrodes had a tip diameter of approximately 2-3 μm and a resistance of 5-7 MΩ. The electrodes were filled with intracellular solution (pH 7.2, 295 mOsm, composition in mM; K-gluconate (110), EGTA (11), $MgCl_2$ (2), $CaCl_2$ (0.1), HEPES (10), Na_2ATP (2), NaGTP (0.03) using a Microfill (World Precision Instruments, UK)). To enable cell recovery, neurobiotin (1-2%, Vector Laboratories, UK) and/or rhodamine (2%, Invitrogen) were added into the intracellular solution.

3.3.3.3 Juxtacellular labelling

Spinal cord slices were placed in a chamber with a constant flow of oxygenated aCSF; the flow rate of 3-5 ml per minute being provided via a peristaltic pump.

To visualise neurones, an upright microscope (Zeiss Axioskop, Germany) equipped with infrared DIC/phrase contrast, epifluorescence and a CCD camera was used with Q-Capture Pro7 software.

A chloride silver wire was placed into the barrel of the patch clamp electrode, which was subsequently mounted onto an electrode holder (Warner Instrument Corp, USA). pCLAMP version 10.2 (Molecular Devices) was used as the data acquisition package. Master 8 (AMP instruments, Israel) was used to set the time and duration of applied current.

The central canal of the spinal cord was placed in the centre of the field of view at x2.5 and then x10 magnification. Any neurones situated ventral to the central canal that were positive for GFP (being visualised under epifluorescence) were then viewed more closely at x60 magnification, since these were the neuronal targets of the study. Prior to the electrode being placed into the bath solution containing the spinal cord slice, a positive pressure was applied using a 5 ml syringe to prevent debris build up in the tip of the electrode. The electrode was positioned above the slice using the coarse control of manipulator (Luigs & Neumann, Germany). The slice was then viewed again at x10 magnification under infrared DIC while the electrode was lowered towards the region containing the neurone of interest. Next, the target neurone was viewed at x60

magnification and placed in the centre of the field of view. Finally, the electrode was visualised at x60 magnification and its tip placed in the centre of the field of view just above the slice.

In current-clamp mode, the electrode resistance was removed from the recording by adjusting the series resistance dial until the voltage response to a 250 pA pulse became zero. An electrode resistance of between 5 and 7 MΩ was required and the offset moved to zero. A positive pressure was applied before moving the electrode to the surface of the neurone using the fine controls of the manipulator (Luigs & Neumann, Germany). When the electrode was close enough to the neurone a dimple was observed on the surface of the neurone.

To establish a seal, the amplifier was switched to voltage clamp mode and a -25 mV pulse was applied (20 ms, 5 Hz). The positive pressure was removed and as the seal formed the current response to the voltage pulse decreased in accordance to Ohm's law. A constant holding voltage of -60 mV was applied. When the seal resistance increased the current reading was observed until a current of approximately 20 pA - 30 pA was observed, which indicated that the seal resistance was nearly 3 GΩ. A small amount of negative pressure was essential to help create the seal.

The holding potential and current pulse were decreased in I=0 mode. A small amount of holding potential was left on and a current pulse of -50 pA was set to stabilise the neurone. The mode was then switched back to current clamp.

To observe extracellular action potentials a small positive current was applied (0.01 to 0.03 nA) to the cell membrane of the neurones (see Figure 3.1). When an action potential was discerned, a higher positive current of 0.3 to 2.0 nA was then applied to the cell membrane (200 ms ON and 200 ms OFF) for at least 20 minutes to label the neurones (Pinault, 1996, Joshi and Hawken, 2006) . The time and duration of the applied current were set using a Master 8.

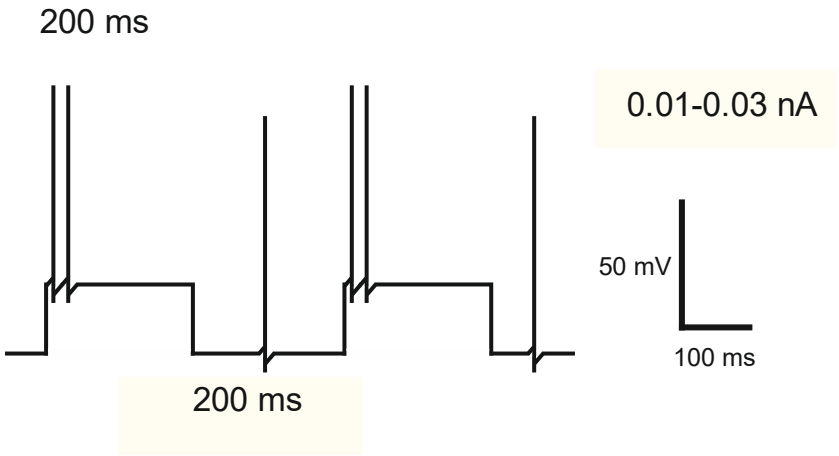

Figure 3.1: Diagrammatic representation of extracellular action potential upon application of a positive current (between 0.01 to 0.03 nA) to the cell membrane of a neurone.

3.3.3.4 Fluorescence IHC for ChAT, GAD67-GFP and neurobiotin following juxtacellular labelling.

Following juxtacellular labelling, electrodes were carefully removed from the filled neurones while applying a gentle positive pressure. The spinal cord slice (300 µm thick) was fixed overnight using a solution of 0.25% glutaraldehyde in 4% PFA. Following fixation, the sections were washed in 0.2 M PB and then incubated for up to a week in solutions of PBS containing 0.05% of thimerosal and 1.5-2% Triton X-100 plus combinations of antibodies as detailed in Table 3.2.

3.3.3.5 Peroxidase IHC

Following the triple labelling fluorescent IHC to detect ChAT, GAD67-GFP and neurobiotin, the 300 µm thick spinal cord slices containing the labelled neurones were further processed using peroxidase IHC to provide a permanent reaction product and to study their morphology and possible projections. The details of the DAB IHC procedure involved was as described in section 2.8 using DAB SK-4100 from Vector Laboratories, with the only difference being that the EAP step incorporated PBS containing 0.3% Triton X-100 and 1:250 of ExtrAvidin Peroxidase (EAP, Sigma).

Table 3.2: Combinations of antibodies used for IHC following juxtacellular labelling.

Target Marker	Primary			Secondary			Tertiary		
	Antibody	Conc	Source	Antibody	Conc	Source	Antibody	Conc	Source
ChAT	Goat anti-ChAT	1:500	Millipore	Alexa Fluor ® 555 donkey anti-goat	1 : 1000	Invitrogen			
GFP	Rabbit anti-GFP	1: 1000	Invitrogen	Alexa Fluor ® 488 donkey anti-rabbit	1: 1000	Invitrogen			
Neurobiotin tracer			Vector Laboratories				Streptavidin pacific blue	1: 1000	Invitrogen

3.3.3.6 Morphology study using camera lucida

For morphological studies, the cell body and processes of DAB-labelled neurones were observed and drawn using camera lucida in conjunction with the Nikon Eclipse E600 microscope.

3.3.4 Assessment of neurochemically-defined afferent inputs on to ChAT/GAD67-GFP co-localised neurones in lamina X

For assessment of the neurochemically-defined afferent inputs onto ChAT/GAD67-GFP co-localised neurones in lamina X, 2 GAD67-GFP adult mice (females) were used. Immunohistochemistry was performed as described previously (see section 2.7), using the combinations of antibodies detailed in Tables 3.3 and 3.4. The numbers of VGLUT1-IR, VGLUT2-IR, GlyT2-IR and GAD67-IR boutons observed in close proximity to the cell body of a co-localised neurone in lamina X were established, and have been presented in section 3.4.5 as the mean ± SEM for boutons observed per 100 µm of co-localised cell body.

Table 3.3: Combinations of antibodies used for triple labelling for ChAT, GFP and either VGLUT1, VGLUT2 or GlyT2 IHC.

Target Marker	Primary			Secondary			Tertiary		
	Antibody	Conc	Source	Antibody	Conc	Source	Antibody	Conc	Source
ChAT	Goat anti ChAT	1:500	Millipore	Alexa Fluor ® 555 donkey anti-goat	1: 1000	Invitrogen			
GFP	Rabbit anti-GFP	1: 1000	Invitrogen	Alexa Fluor ® 488 donkey anti-rabbit	1: 1000	Invitrogen			
VGLUT1	Guinea pig anti-VGLUT1	1:30,000	Millipore	Biotinylated donkey anti- guinea pig	1 : 500	Jackson Immuno-Research Laboratories	Streptavidin pacific blue	1 : 1000	Invitrogen
VGLUT2	Guinea pig anti-VGLUT 2	1:10,000	Millipore	Biotinylated donkey anti- guinea pig	1 : 500	Jackson Immuno-Research Laboratories	Streptavidin pacific blue	1 : 1000	Invitrogen
GlyT2	Guinea pig anti-GlyT2	1:15,000	Millipore	Biotinylated donkey anti- guinea pig	1 : 500	Jackson Immuno-Research Laboratories	Streptavidin pacific blue	1 : 1000	Invitrogen

Table 3.4: Combinations of antibodies used for triple labelling for ChAT, GFP and GAD67 IHC.

Target Marker	Primary			Secondary			Tertiary		
	Antibody	Conc	Source	Antibody	Conc	Source	Antibody	Conc	Source
ChAT	Goat anti ChAT	1:500	Millipore	Biotinylated donkey anti- goat	1 : 500	Jackson Immuno-Research Laboratories	Streptavidin pacific blue	1 : 1000	Invitrogen
GFP	Rabbit anti-GFP	1: 1000	Invitrogen	Alexa Fluor ® 488 donkey anti-rabbit	1: 1000	Invitrogen			
GAD67	Mouse anti-GAD67	1:500	Chemicon International	Alexa Fluor ® 555 donkey anti-mouse	1 : 1000	Invitrogen			

3.4 Results

3.4.1 Adult mice

ChAT and GAD67-GFP immunoreactivity was observed in separate neurones in all studied levels (cervical, thoracic and lumbar) but there was limited co-localisation (see Figure 3.2). The morphology and distribution of ChAT-IR and/or GAD67-GFP-IR neurones, and the locations of neurones expressing co-localisation, within the major discrete areas of the grey matter of the spinal cord (including the ventral horn, dorsal horn, lateral horn, lamina VII and lamina X) were as follows:

3.4.1.1 There are few ChAT/GAD67-GFP co-localised neurones in the ventral horn

ChAT-IR neurones were observed in the motoneurone pool (lamina IX) of the ventral horn, (see Figure 3.2-Ai) in all studied levels; 2048 neurones for cervical (n = 3, nsc = 30), 629 neurones for thoracic (n = 3, nsc = 30) and 1029 neurones for lumbar (n = 3, nsc = 30), see Table 3.5. GAD67-GFP-IR neurones were found throughout the ventral horn (see Figure 3.2-Aii and Table 3.5); 1435 neurones for cervical (n = 3, nsc = 30), 929 neurones for thoracic (n = 3, nsc = 30) and 1441 neurones for lumbar (n = 3, nsc = 30). Both ChAT-IR and GAD67-GFP-IR neurones exhibited oval or elliptical shaped cell bodies; the sizes of which were 18.82 ± 1.59 μm x 31.33 ± 2.30 μm (N = 10) for ChAT-IR neurones and 10.89 ± 0.57 μm x 15.70 ± 1.09 μm (N = 10) for GAD67-GFP-IR neurones. Cross sectional areas of ChAT-IR soma and GAD67-GFP-IR soma were 493.89 μm^2 and 138.84 μm^2 respectively. Only two co-localised neurones were observed, one in a thoracic section of animal 1 and one in a lumbar section of animal 2. The percentage of ChAT-IR neurones that exhibited co-localisation for GAD67-GFP in the cervical, thoracic and lumbar sections was therefore 0% (0/2048), 0.16% (1/629) and 0.10% (1/1029) respectively. Similarly, the percentage of GAD67-GFP-IR neurones which exhibited co-localisation for ChAT in the cervical, thoracic and lumbar sections was 0%, 0.11% and 0.07%, respectively.

Table 3.5: Numbers of ChAT-IR and GAD67-GFP-IR neurones per 50 µm section in the ventral horns of each region of the spinal cord of adult mice (n = 3). Values are presented as mean ± SEM.

Regions	ChAT/GAD67-GFP co-localised neurones	ChAT-IR neurones	GAD67-GFP-IR neurones
Cervical (30 sections)	0	68.27 ± 2.96	47.83 ± 2.72
Thoracic (30 sections)	0.03 ± 0.03	20.97 ± 0.92	30.97 ± 2.04
Lumbar (30 sections)	0.03 ± 0.03	34.30 ± 2.13	48.03 ± 2.28

3.4.1.2 ChAT-IR and GAD67-GFP-IR neurones are present in the dorsal horn and a limited number are co-localised.

Many neurones in the dorsal horn were GAD67-GFP-IR; totalling 5436 neurones for the cervical (n = 3, nsc = 30), 3853 for the thoracic (n = 3, nsc = 30) and 5361 for the lumbar sections (n = 3, nsc = 30) (see Figure 3.2-Bii and Table 3.6). These neurones were small in size (7.96 ± 0.25 µm x 10.26 ± 0.58 µm, N = 10), with a soma cross sectional area of 65.19 μm^2. The dorsal horn also contained a limited number of ChAT-IR neurones; totalling 175, 101 and 142 neurones for the cervical (n = 3, nsc = 30), thoracic (n = 3, nsc = 30) and lumbar (n = 3, nsc = 30) respectively (see Figure 3.2-Bi and Table 3.6). ChAT-IR neurones were located in lamina III of the dorsal horn. The size of the ChAT-IR neurones was 9.88 ± 0.69 µm x 14.29 ± 1.15 µm (N = 10), corresponding to a soma cross sectional area of 114.72 μm^2. Both ChAT-IR and GAD67-GFP-IR neurones exhibited oval or elliptical cell bodies. A limited number of ChAT/GAD67-GFP co-localised neurones were also observed in the dorsal horn; 34 neurones for the cervical (n = 3, nsc = 30), 13 for the thoracic (n = 3, nsc = 30) and 20 for the lumbar sections (n = 3, nsc = 30), with the average number of co-localised neurones observed for both sides of the cord per 50 µm section being 1.13 ± 0.23 for

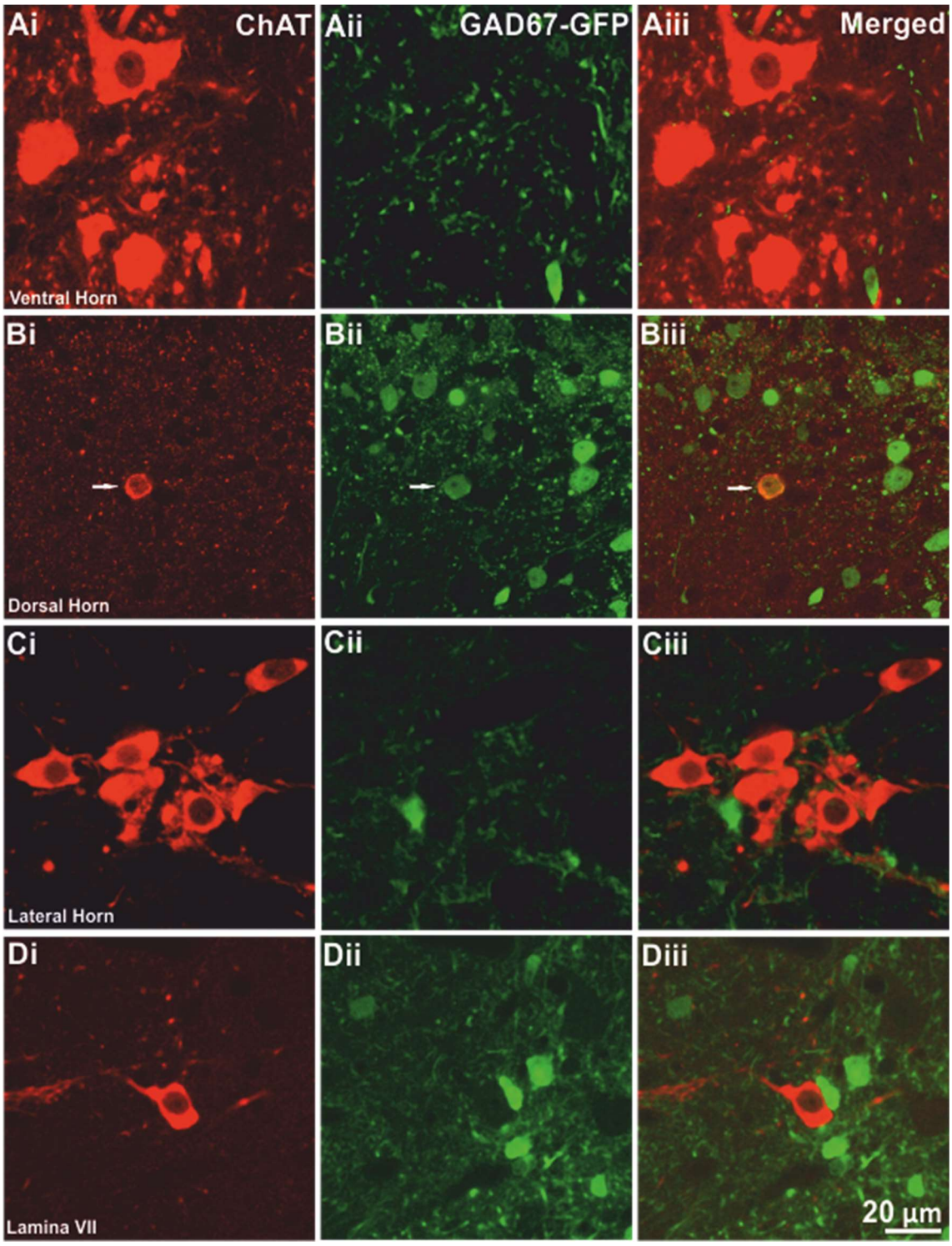

Figure 3.2: Extent of ChAT-IR, GAD67-GFP-IR and ChAT/GAD67-GFP co-localised neurones in the thoracic cord sections of adult mice. Confocal images depict ChAT-IR and/or GAD67-GFP-IR neurones in the ventral horn (Ai and Aii respectively), dorsal horns (Bi and Bii), lateral horn (Ci and Cii) and lamina VII (Di and Dii) of the thoracic cord sections. Arrows (Bi to Biii) indicate ChAT/GAD67-GFP co-localised neurones.

the cervical, 0.43 ± 0.10 for the thoracic and 0.67 ± 0.15 for the lumbar section (see Table 3.6). The percentage of ChAT-IR neurones that contained GAD67-GFP in the cervical, thoracic and lumbar sections was 19.43%, 12.87% and 14.08% respectively. The percentage of GAD67-GFP-IR neurones that contained ChAT for the cervical, thoracic and lumbar sections was 0.63%, 0.34% and 0.37% respectively. The size of the co-localised neurones was 8.45 ± 0.29 µm x 11.85 ± 0.87 µm (N = 10), corresponding to a soma cross sectional area of 80.92 µm^2.

Table 3.6: Numbers of ChAT-IR and/or GAD67-GFP-IR neurones per 50 µm section in the dorsal horns of each region of the spinal cord of adult mice (n = 3).

Regions	ChAT/GAD67-GFP co-localised neurones	ChAT-IR neurones	GAD67-GFP-IR neurones
Cervical (30 sections)	1.13 ± 0.23	5.83 ± 0.58	181.20 ± 10.31
Thoracic (30 sections)	0.43 ± 0.10	3.37 ± 0.28	128.43 ± 4.32
Lumbar (30 sections)	0.67 ± 0.15	4.73 ± 0.42	178.70 ± 7.99

3.4.1.3 Co-localisation was not observed in the lateral horn

SPNs in the lateral horn of the thoracic (Figure 3.2-Ci) (490 neurones, n = 3, nsc = 30) and upper lumbar regions (152 neurones, n = 3, nsc = 13), were positive for ChAT labelling and had oval or elliptical shaped cell bodies. This corresponds to approximately 16.33 ± 1.10 and 11.69 ± 0.96 ChAT-IR neurones being observed on average, for both sides of a 50 µm thick section, in the thoracic and lumbar cord sections respectively (see Table 3.7).These ChAT-IR neurones were medium in size (12.46 ± 0.95 µm x 15.42 ± 5.06 µm, N = 10), with a soma cross sectional area of 152.64 µm^2. By comparison a relatively small number of GAD67-GFP-IR neurones

were observed in the lateral horn (see Table 3.7); 63 neurones in the thoracic sections (n = 3, nsc = 30) and 35 in the lumbar sections (n = 3, nsc = 13). The size of these neurones was 8.40 ± 0.39 μm x 12.47 ± 0.87 μm (N = 10), with a soma cross sectional area of 85.53 μm^2. Co-localisation was not observed in any of the studied sections.

Table 3.7: Numbers of ChAT-IR and GAD67-GFP-IR neurones per 50 μm section in the lateral horns of the thoracic and lumbar regions of the spinal cord of adult mice (n = 3).

Regions	ChAT-IR neurones	GAD67-GFP-IR neurones
Thoracic (30 sections)	16.33 ± 1.10	2.10 ± 0.34
Lumbar (13 sections)	11.69 ± 0.96	2.69 ± 0.35

3.4.1.4 ChAT-IR and GAD67-GFP-IR neurones are present in lamina VII but ChAT/GAD67-GFP co-localised neurones are almost absent in the lamina.

ChAT-IR and GAD67-GFP-IR neurones were observed in lamina VII (Figure 3.2Di and Dii) of all the studied spinal regions; totalling 481, 297 and 283 ChAT-IR neurones, plus 1695, 1300 and 1729 GAD67-GFP-IR neurones being found respectively in the cervical (n = 3, nsc = 30), thoracic (n = 3, nsc = 30) and lumbar sections (n = 3, nsc = 30). Both types of neurone exhibited oval or elliptical cell bodies. The size of ChAT-IR neurones was 14.54 ± 0.91 μm x 21.88 ± 1.30 μm (N = 10), while those of GAD67-GFP-IR neurones was 10.75 ± 0.36 μm x 14.95 ± 0.94 μm (N = 10). The cross sectional areas of the ChAT-IR and GAD67-GFP-IR soma were 260.48 μm^2 and 129.70 μm^2, respectively. A very limited number of ChAT/GAD67-GFP co-localised neurones were observed in the cervical (5 neurones, n = 3, nsc = 30) and lumbar regions (1 neurone, n = 3, nsc = 30)(see Table 3.8). Their size was 10.58 ± 1.23 x 12.95 ± 0.97 (N = 4) with a soma cross sectional area of 108.73 μm^2. The percentage of ChAT-IR neurones

containing GAD67-GFP for the cervical, thoracic and lumbar sections was 1.04%, 0% and 0.35%, respectively. The percentage of GAD67-IR neurones containing ChAT for the cervical, thoracic and lumbar sections was 0.29%, 0% and 0.06%, respectively.

Table 3.8: Numbers of ChAT-IR and/or GAD67-GFP-IR neurones per 50 µm section in lamina VII of each region of the spinal cord of adult mice (n = 3).

Regions	ChAT/GAD67-GFP co-localised neurones	ChAT-IR neurones	GAD67-GFP-IR neurones
Cervical (30 sections)	0.20 ± 0.07	16.03 ± 1.29	56.50 ± 4.07
Thoracic (30 sections)	0	9.90 ± 0.81	43.33 ± 2.54
Lumbar (30 sections)	0.10 ± 0.07	9.43 ± 0.82	57.63 ± 3.30

3.4.1.5 ChAT-IR and GAD67-GFP-IR neurones are present in lamina X and a small number are co-localised.

323 (n = 3, nsc = 30), 428 (n = 3, nsc = 30) and 411 (n = 3, nsc = 30) ChAT-IR neurones were counted in lamina X in cervical, thoracic and lumbar cord sections respectively (Figure 3.3 Ai, Bi and Ci). In addition, these cervical (n = 3, nsc = 30), thoracic (n = 3, nsc = 30) and lumbar cord sections (n = 3, nsc = 30) of lamina X section contained respectively 1015, 972 and 962 GAD67-GFP-IR neurones (Figure 3.3 Aii, Bii and Cii). Both ChAT-IR and GAD67-GFP-IR neurones possessed oval or elliptical cell bodies. The size of the ChAT-IR neurones varied greatly however, ranging from 8 µm to 27 µm for the X-diameter and from 9 µm to 47 µm for the Y-diameter of the somata (raw data from 26 neurones (N = 26) randomly selected from all studied regions of the spinal cords). The average sizes of the ChAT-IR neurones and GAD67-GFP-IR neurones were 13.62 ± 0.95 µm x 19.52 ± 1.68 µm (N = 10) and 11.14 ± 0.36

µm x 15.08 ± 0.57 µm (N = 10) respectively. The cross sectional area of ChAT-IR and GAD67-GFP-IR soma was 215.67 and 135.01 μm^2 respectively. The intensity of the ChAT staining also varied from one neurone to another (see Figure 3.3-Ai, Bi and Ci).

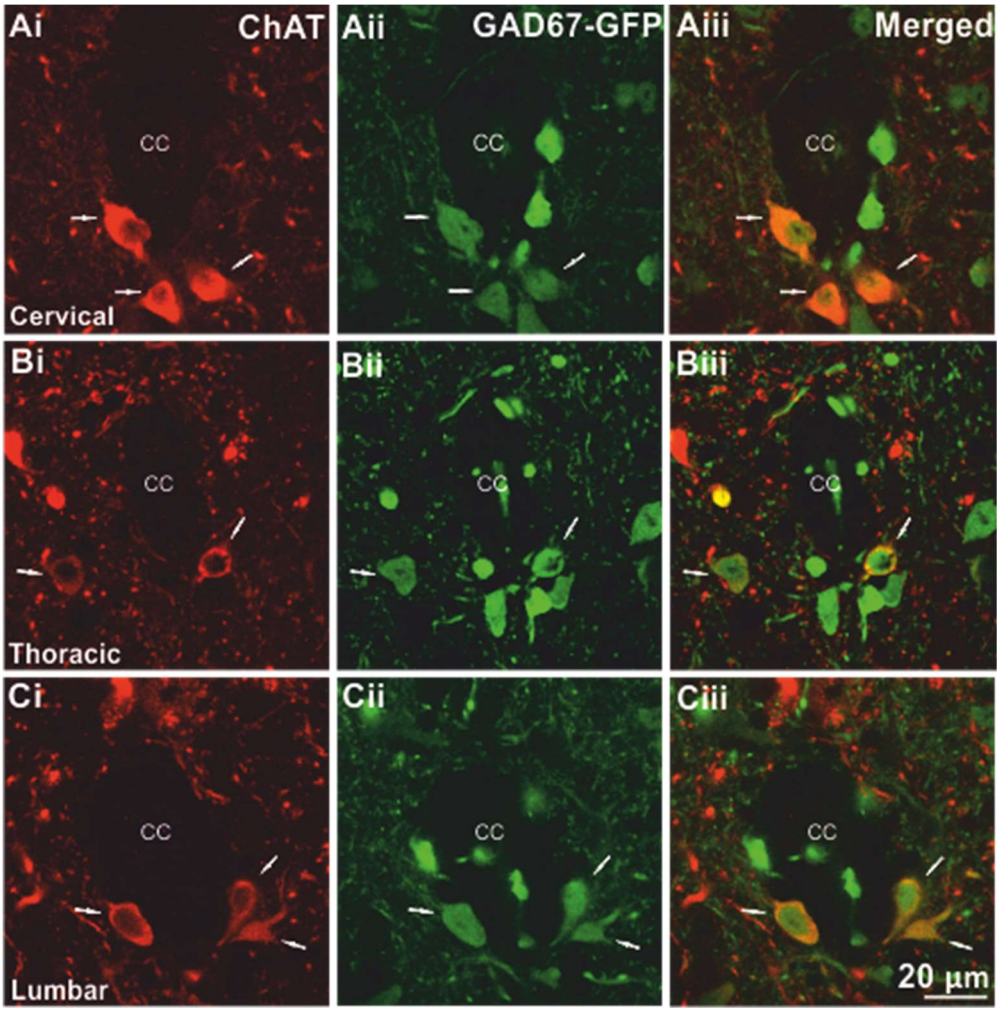

Figure 3.3: Co-localisation of ChAT and GAD67-GFP in lamina X of the adult mice. Confocal images show ChAT/GAD67-GFP co-localisation in lamina X of the cervical, thoracic and lumbar sections (Ai to Aiii, Bi to Biii and Ci to Ciii respectively). Neurones which exhibit co-localisation are indicated by arrows.

The number of ChAT/GAD67-GFP co-localised neurones observed in the cervical, thoracic and lumbar cord sections of lamina X was 121 (n = 3, nsc = 30), 114 (n = 3, nsc = 30) and 134 (n = 3, nsc = 30) respectively. In comparison to other investigated

areas within the spinal cord, lamina X contained the majority of co-localised neurones. The average number of co-localised neurones observed per 50 µm section in lamina X for each region of the spinal cord is shown in Table 3.9. The percentage of ChAT-IR neurones that contained GAD67-GFP for the cervical, thoracic and lumbar sections was 37.46%, 26.64% and 32.60%, respectively. The percentage of GAD67-GFP-IR neurones that contained ChAT-GFP for the cervical, thoracic and lumbar sections was 11.92%, 11.73% and 13.93%, respectively.

The ChAT/GAD67-GFP co-localised neurones were of size 11.35 ± 0.66 µm x 14.68 ± 0.55 (N = 10), with a soma cross sectional area of 133.06 µm^2. They were negative for Fluorogold labelling (see Figure 3.4-Aiii) which indicates that they were neither motoneurones nor preganglionic neurones (Ambalavanar and Morris, 1989). They also appeared to be lightly immunoreactive for both ChAT and GAD67-GFP (see Figure 3.3 and Figure 3.7-B).

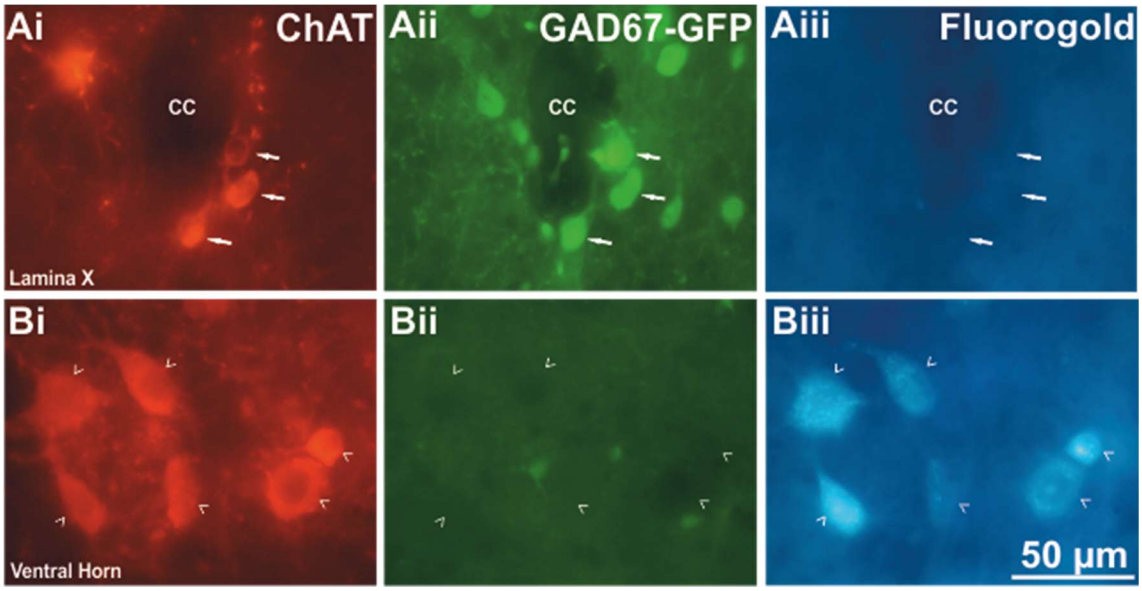

Figure 3.4: ChAT/GAD67-GFP co-localised neurones in lamina X were negative for Fluorogold labelling. Epifluorescent images show ChAT/GAD67-GFP co-localised neurones (indicated by arrows in Ai and Aii) in lamina X which are negative for Fluorogold (Aiii) suggesting that they are neither motoneurones nor preganglionic neurones. Open arrows in Bi mark the presence of ChAT-IR neurones in the ventral horn; these are not co-localised with GAD67-GFP (Bii), but are positive for Fluorogold (Biii) indicating that they are motoneurones.

3.4.1.5.1 The location of ChAT/GAD67-GFP co-localised neurones in lamina X of adult mice

The location of ChAT/GAD67-GFP co-localised neurones in relation to the central canal was mapped from serial transverse sections of the upper thoracic cord region (approximately T2-T4) of a GAD67-GFP knock-in adult mouse using Reconstruct software to create a three dimensional diagram (see Figure 3.5). In addition, serial sagittal sections of a GAD67-GFP knock-in adult mouse were used to map the sites of co-localised neurones throughout nearly the whole thoracic cord region (T1-T12) (see Figure 3.6 and Figure 3.7-A). The results suggested that while the majority of neurones exhibiting co-localisation were located ventral and ventrolateral to the central canal (see Figures 3.5 and 3.6), a small number of such neurones could also be found dorsal to the central canal.

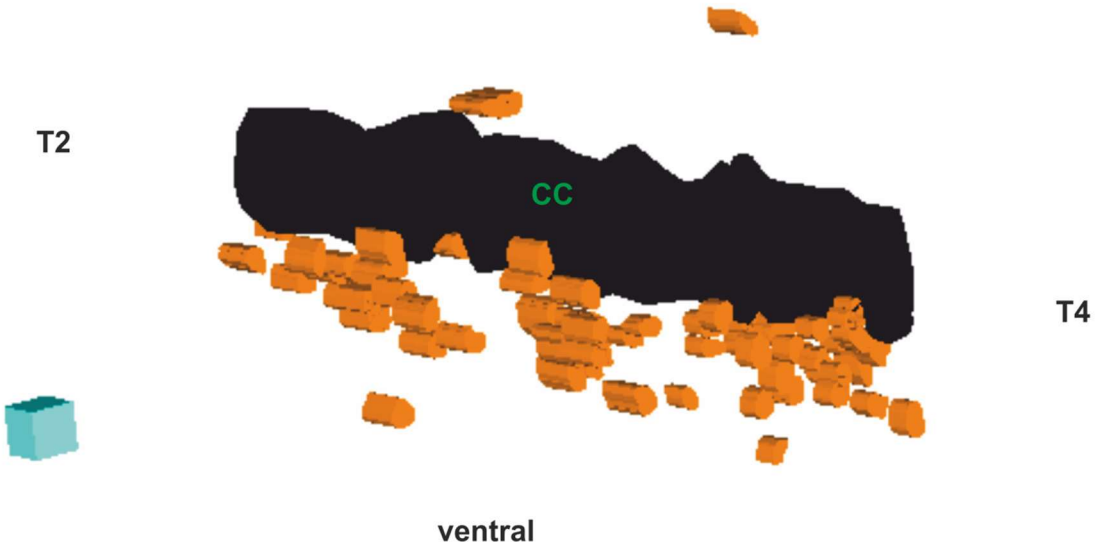

Figure 3.5: Location of ChAT/GAD67-GFP co-localised neurones in relation to the central canal of T2-T4 cord sections. Each orange block represents a co-localised neurone. The blue box represents a 3-D scale bar, 50 µm x 50 µm x 50 µm. (Note: to aid visualisation, the size of each orange block does not represent the actual size of each co-localised neurone but represents the thickness of each studied cord section).

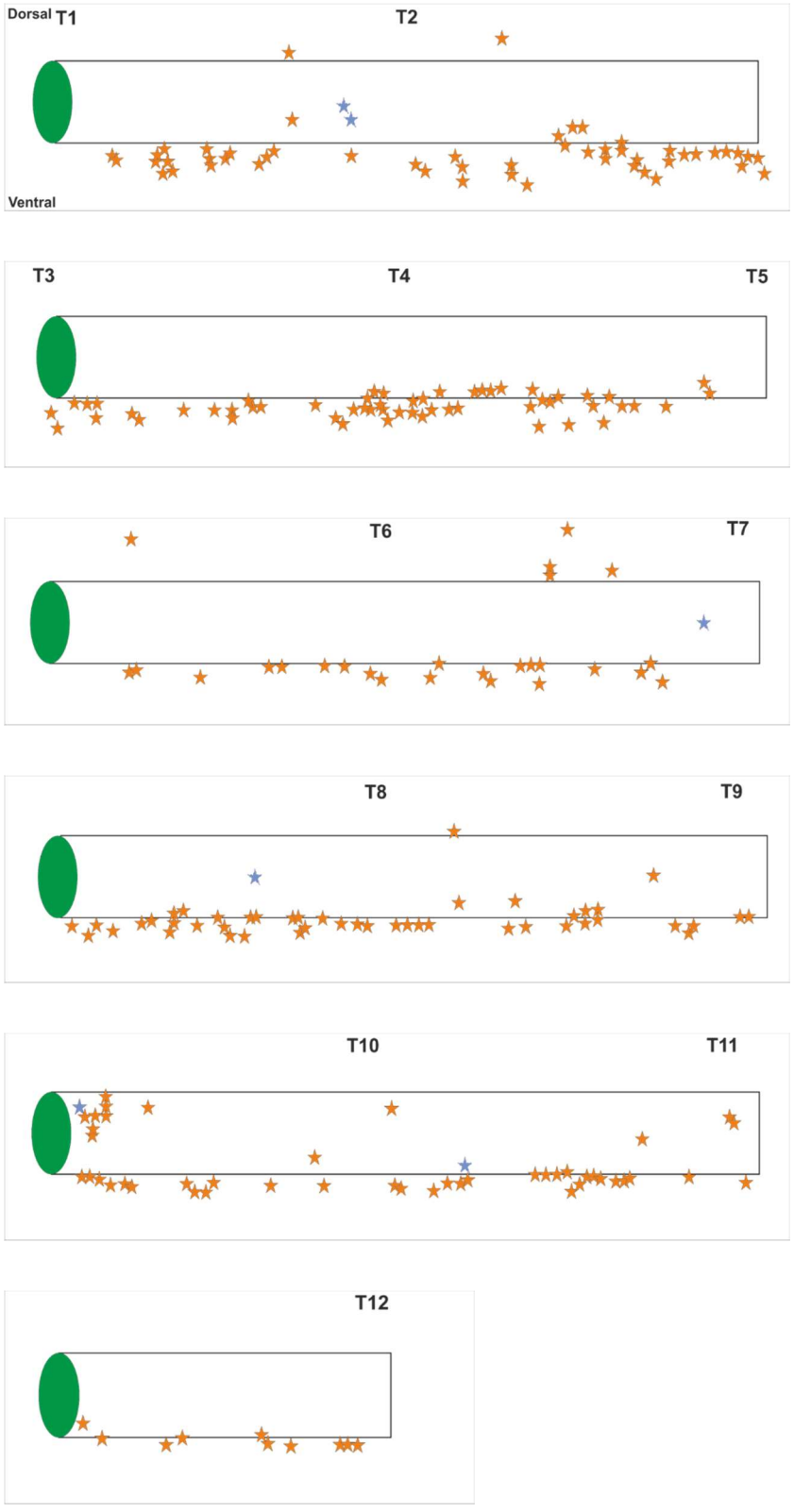

Figure 3.6: Location of ChAT/GAD67-GFP co-localised neurones in serial sagittal sections from T1-T12 of a GAD67-GFP knock-in mouse. An orange star represents a co-localised neurone, while a blue star represents a co-localised neurone located deeper in a section.

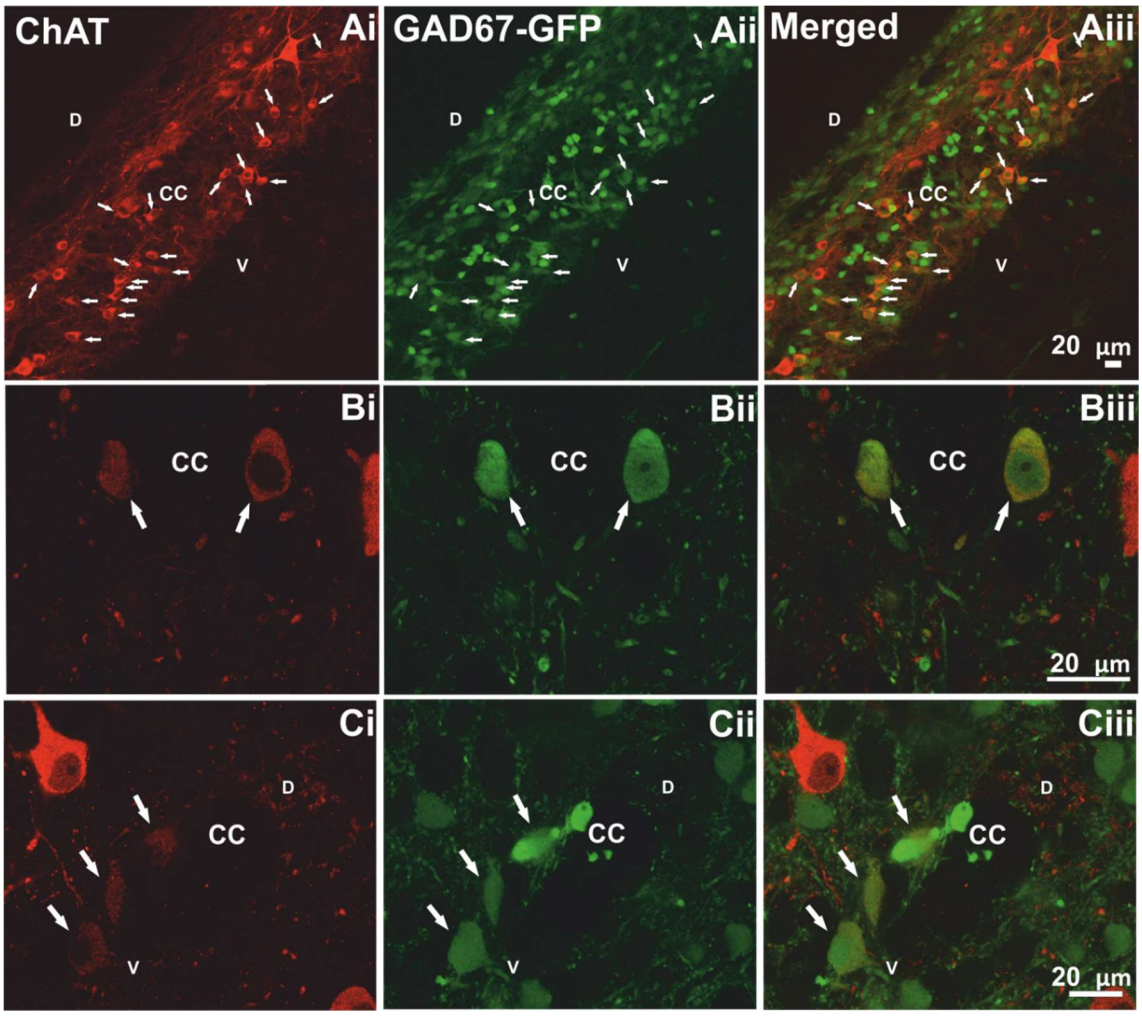

Figure 3.7: Location of co-localised neurones in lamina X in the thoracic cord of adult mice and a young mouse. Concocal images show that the majority of co-localised neurones (indicated by arrows in A) were observed ventral to the central canal in a sagittal thoracic cord section of an adult mouse. B and C show co-localised neurones (indicated by arrows) ventral to the central canal in a transverse thoracic cord section of an adult and a young mouse respectively. CC: central canal; D: dorsal; V: ventral.

Table 3.9: Numbers of ChAT-IR and/or GAD67-GFP-IR neurones per 50 µm section in lamina X of each region of the spinal cord of adult mice (n = 3).

Regions	ChAT/GAD67-GFP co-localised neurones	ChAT-IR neurones	GAD67-GFP-IR neurones
Cervical (30 sections)	4.03 ± 0.41	10.77 ± 0.70	33.83 ± 2.21
Thoracic (30 sections)	3.80 ± 0.31	14.27 ± 0.76	32.40 ± 1.43
Lumbar (30 sections)	4.47 ± 0.27	13.70 ± 0.80	32.07 ± 2.33

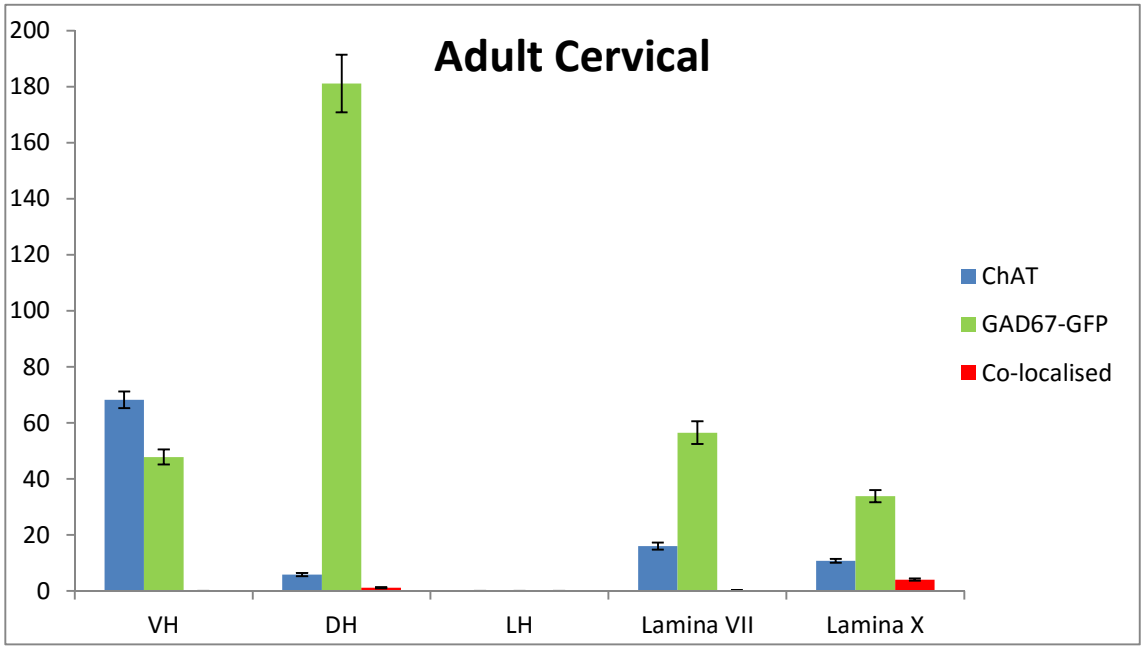

Figure 3.8: Distribution of ChAT, GAD67-GFP and co-localisation in adult cervical spinal cord.

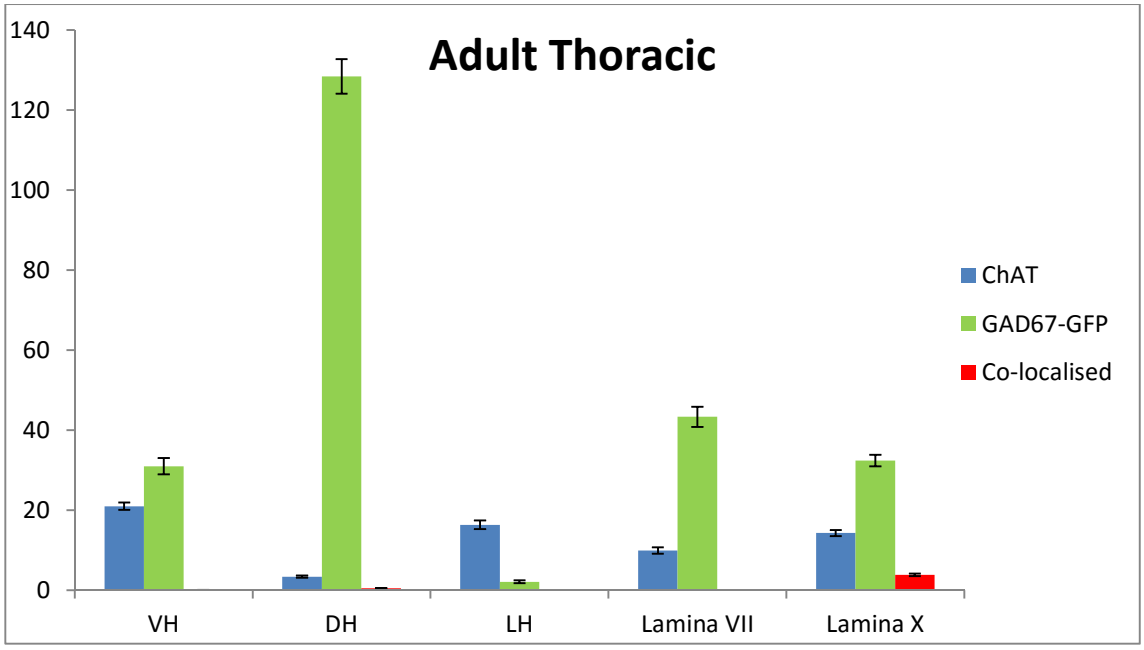

Figure 3.9: Distribution of ChAT, GAD67-GFP and co-localisation in adult thoracic spinal cord.

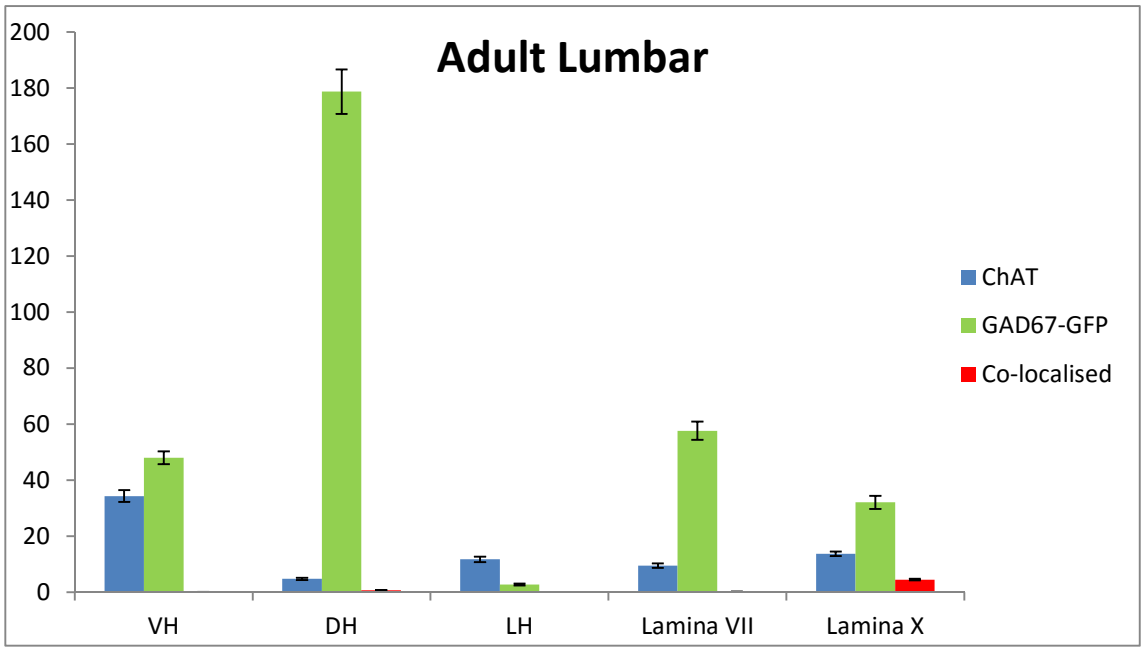

Figure 3.10: Distribution of ChAT, GAD67-GFP and co-localisation in adult lumbar spinal cord.

3.4.2 Young mice

An aim was to trace the axonal projections of ChAT/GAD67-GFP co-localised neurones in lamina X by juxtacellular labelling in spinal cord slices. Since optimal visualisation of slices is performed in young mice with reduced myelination, potential ChAT/GAD67-GFP co-localisation was first examined in these mice.

3.4.2.1 Only one ChAT/GAD67-GFP co-localised neurone was observed in the ventral horn

ChAT-IR neurones were observed predominantly in lamina IX of the ventral horn (see Table 3.10 and Figure 3.11-Ai) for all the studied cord regions; 1234 ChAT-IR neurones for the cervical (n = 3, nsc = 15), 478 for the thoracic (n = 3, nsc = 15) and 813 for the lumbar cord sections (n = 3, nsc = 15). These neurones exhibited oval or elliptical shaped cell bodies of size 24.46 ± 1.44 µm x 32.06 ± 1.96 µm (N = 10), with a soma cross sectional area of 627.32 μm^2. In addition, they were found to be positive for Fluorogold, indicating that they were motoneurones (Ambalavanar and Morris, 1989).

The ventral horn of the cervical, thoracic and lumbar cord sections contained 1204 (n = 3, nsc = 15), 561 (n = 3, nsc = 15) and 884 GAD67-GFP-IR neurones (n = 3, nsc = 15)(see Table 3.10 and Figure 3.11 Aii), respectively. GAD67-GFP-IR neurones in the ventral horn exhibited oval or elliptical shaped cell bodies of size 13.93 ± 0.74 µm x 19.64 ± 0.90 µm (N = 10), with a soma cross sectional area of 221.30 μm^2.

Only one ChAT/GAD67-GFP co-localised neurone was observed in the ventral horn. It was located in a lumbar cord section of animal 2. The percentage of ChAT-IR neurones that contained GAD67-GFP for the lumbar sections (n=3, nsc = 15) was 0.12% and the percentage of GAD67-GFP-IR neurones that contained ChAT was 0.11%.

Table 3.10: Numbers of ChAT-IR and/or GAD67-GFP-IR neurones per 50 µm section in the ventral horns of each region of the spinal cord of young mice (n = 3).

Regions	ChAT/GAD67-GFP co-localised neurones	ChAT-IR neurones	GAD67-GFP-IR neurones
Cervical (15 sections)	0	82.27 ± 5.86	80.27 ± 6.60
Thoracic (15 sections)	0	31.87 ± 1.66	37.40 ± 2.72
Lumbar (15 sections)	0.07 ± 0.07	54.20 ± 3.82	58.93 ± 5.31

3.4.2.2 ChAT-IR and GAD67-GFP-IR neurones are present in the dorsal horn and a limited number are co-localised.

The cervical, thoracic and lumbar dorsal horns contained 214 (n = 3, nsc = 15), 245 (n = 3, nsc = 15) and 224 ChAT-IR neurones (n = 3, nsc = 15), respectively (see Figure 3.11-Bi). These were predominantly located in lamina III of the dorsal horn and possessed oval or elliptical cell bodies. The size of the ChAT-IR neurones was 11.25 ± 0.37 µm x 14.55 ± 0.46 µm (N = 10), with a soma cross sectional area of 130.72 µm^2.

A large number of GAD67-GFP-IR neurones were observed in the dorsal horn (see Figure 3.11-Bii) for all the cord regions; 4806, 3502 and 4118 neurones for the cervical (n = 3, nsc = 15), thoracic (n = 3, nsc = 15) lumbar cord sections (n = 3, nsc = 15), respectively. The size of the GAD67-GFP-IR neurones was 9.69 ± 0.38 µm x 11.81 ± 0.35 µm (N = 10), with a soma cross sectional area of 90.77 µm^2. They exhibited oval or elliptical cell bodies.

A small number of ChAT/GAD67-GFP co-localised neurones were also observed in the dorsal horn of the cervical (26 neurones, n = 3, nsc = 15), thoracic (30 neurones, n = 3, nsc = 15) lumbar cord sections (26 neurones, n = 3, nsc = 15), respectively (see Figure 3.11-Biii and Table 3.11). The percentage of ChAT-IR neurones containing GAD67-

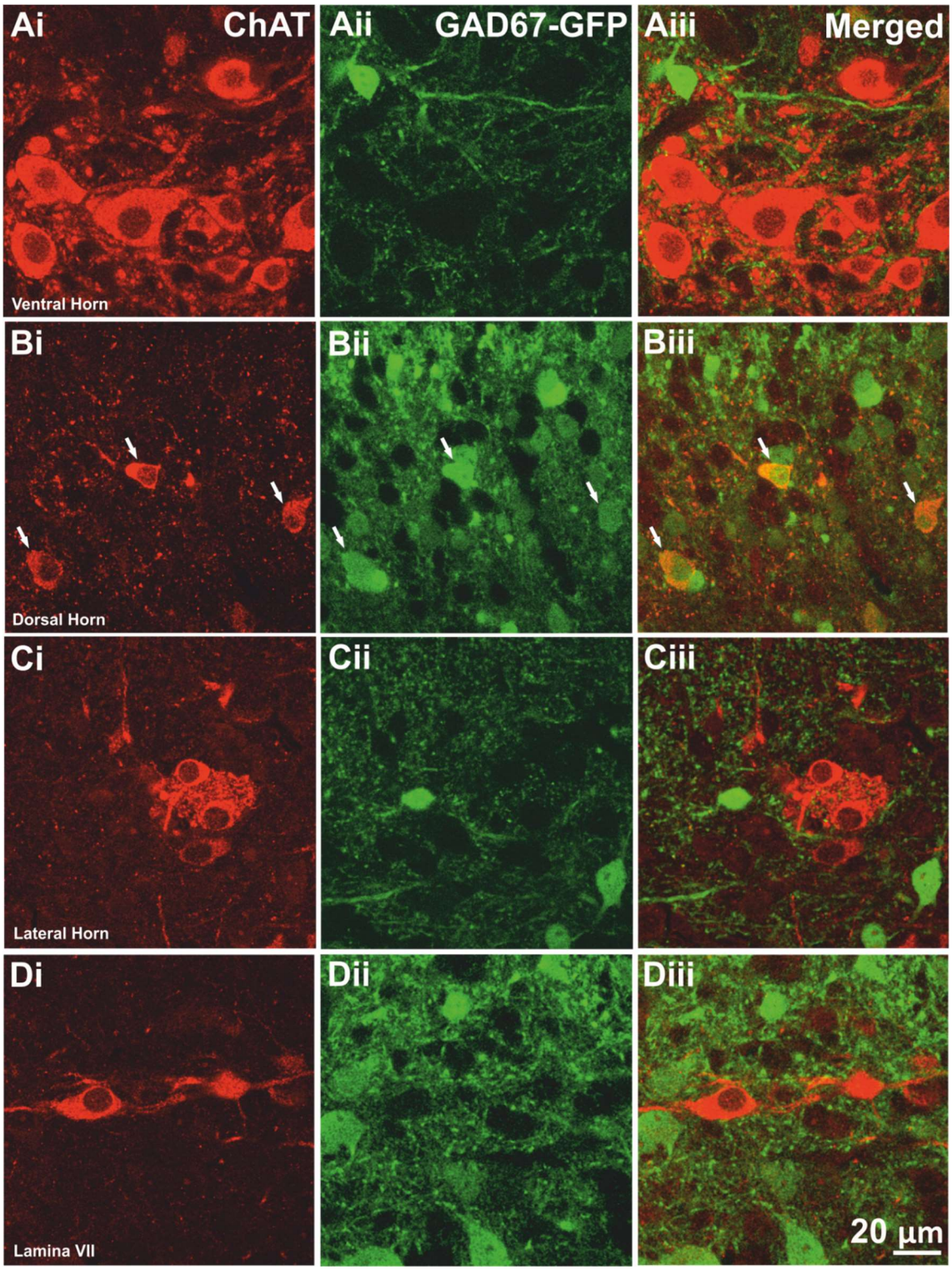

Figure 3.11: ChAT-IR and GAD67-GFP-IR neurones were present in various areas within the spinal cord of young mice. The confocal images present the distribution of ChAT-IR and GAD67-GFP-IR neurones in the ventral horn (Ai, Aii), dorsal horn (Bi, Bii), lateral horn (Ci, Cii) and lamina VII (Di, Dii). ChAT/GAD67-GFP co-localised neurones were observed in the dorsal horn as indicated by the arrows (Biii).

GFP was 12.15%, 12.24% and 11.61% for the cervical, thoracic and lumbar cord sections respectively. The percentage of GAD67-GFP-IR neurones containing ChAT was 0.54%, 0.86% and 0.63% for the cervical, thoracic and lumbar cord sections respectively. The average number of co-localised neurones observed for both sides of the cord per 50 µm section was aproximately 1.73 ± 0.56, 2.00 ± 0.38 and 1.73 ± 0.40 for the cervical, thoracic and lumbar cord sections respectively. The size of the ChAT/GAD67-GFP co-localised neurones was 11.15 ± 0.39 µm x 14.33 ± 0.37 µm (N = 10) with a soma cross sectional area of 127.49 μm^2.

Table 3.11: Numbers of ChAT-IR and/or GAD67-GFP-IR neurones per 50 µm section in the dorsal horns of each region of the spinal cord of young mice (n = 3).

Regions	ChAT/GAD67-GFP co-localised neurones	ChAT-IR neurones	GAD67-GFP-IR neurones
Cervical (15 sections)	1.73 ± 0.56	14.27 ± 2.41	320.40 ± 18.63
Thoracic (15 sections)	2.00 ± 0.38	16.33 ± 1.11	233.47± 11.11
Lumbar (15 sections)	1.73 ± 0.40	14.93 ± 1.33	274.53 ± 14.09

3.4.2.3 ChAT/GAD67-GFP co-localised neurones were not observed in the lateral horns

The lateral horn of the thoracic (n = 3, nsc = 15) and lumbar cord (n = 3, nsc = 7) sections contained 205 and 61 ChAT-IR neurones respectively (Figure 3.11 Ci). The average number of ChAT-IR neurones observed for both sides of the cord per 50 µm section was as shown in Table 3.12. The ChAT-IR neurones (Figure 3.11-Ci) of young mice appeared as a cluster and exhibited oval or elliptical shaped cell bodies of size 14.62 ± 0.51 µm x 18.31 ± 0.87 µm (N = 10), with a soma cross sectional area of

212.95 μm^2. In addition, they were found to be positive for Fluorogold, so indicating that they were preganglionic neurones (Ambalavanar and Morris, 1989).

The number of GAD67-GFP-IR neurones observed in the lateral horn (Figure 3.11-Cii) was markedly less than number of ChAT-IR neurones (see Table 3.12); 43 neurones for the thoracic and 26 for the lumbar sections. The average number of GAD67-GFP-IR neurones observed per 50 μm section was as shown in Table 3.12. The size of the GAD67-GFP-IR neurones was 12.49 ± 0.75 μm x 16.66 ± 2.03 μm (N = 6), with a soma cross sectional area of 166.86 μm^2.

ChAT/GAD67-GFP co-localised neurones were not observed in the lateral horns.

Table 3.12: Numbers of ChAT-IR and GAD67-GFP-IR neurones per 50 μm section in the lateral horns of each region of the spinal cord of young mice (n = 3).

Regions	ChAT-IR neurones	GAD67-GFP-IR neurones
Thoracic (15 sections)	13.67 ± 1.22	2.87 ± 0.72
Lumbar (7 sections)	8.71 ± 2.95	3.71 ± 1.15

3.4.2.4 ChAT-IR and GAD67-GFP-IR neurones were present in lamina VII though only one neurone exhibited co-localisation

Lamina VII of the cervical (n = 3, nsc = 15), thoracic (n = 3, nsc = 15) and lumbar cord sections (n = 3, nsc = 15) contained 156, 151 and 96 ChAT-IR neurones respectively (Figure 3.11-Di). The average number of ChAT-IR neurones observed for both sides of the cord per 50 μm section was as shown in Table 3.13. They possessed oval or elliptical cell bodies of size 15.46 ± 0.59 μm x 23.09 ± 1.28 μm (N = 7), with a soma cross sectional area of 291.83 μm^2.

Lamina VII of the cervical (n = 3, nsc = 15), thoracic (n = 3, nsc = 15) and lumbar cord sections (n = 3, nsc = 15) contained 1199, 988 and 1503 GAD67-GFP-IR neurones respectively (Figure 3.11-Dii). They possessed oval or elliptical cell bodies of size 12.81 ± 0.64 µm x 18.06 ± 1.53 µm (N = 10), with a soma cross sectional area of GAD67-GFP-IR 187.14 μm^2.

Only one ChAT/GAD67-GFP co-localised neurone was observed in lamina VII (see Table 3.13). This was located in a cervical cord section of one animal, animal 2. The percentage of ChAT-IR neurones which contained GAD67-GFP for the cervical sections was therefore 0.64%. Similarly, the percentage of GAD67-GFP-IR neurones that contained ChAT was 0.08%.

Table 3.13: Numbers of ChAT-IR and/or GAD67-GFP-IR neurones per 50 µm section in lamina VII of each region of the spinal cord of young mice (n = 3).

Regions	ChAT/GAD67-GFP co-localised neurones	ChAT-IR neurones	GAD67-GFP-IR neurones
Cervical (15 sections)	0.07 ± 0.07	10.40 ± 0.94	79.93 ± 8.88
Thoracic (15 sections)	0	10.07 ± 1.14	65.87 ± 4.79
Lumbar (15 sections)	0	6.40 ± 1.19	100.20 ± 5.95

3.4.2.5 ChAT-IR and GAD67-GFP-IR neurones are present in lamina X and a small number are co-localised, in similarity to adult mice observations.

Lamina X of the cervical (n = 3, nsc = 15), thoracic (n = 3, nsc = 15) and lumbar cord sections (n = 3, nsc = 15) contained 146, 188 and 243 ChAT-IR neurones respectively

(Figure 3.12-Ai, Bi and Ci). The average number of ChAT-IR neurones observed for both side of the cord across 50 µm section was as shown in Table 3.14. The cell bodies for the ChAT-IR neurones were oval or elliptical in shape. Likewise, GAD67-GFP-IR neurones were observed in the lamina X of all studied cord regions (Figure 3.12-Aii, Bii and Cii) and possessed oval or elliptical cell bodies. Lamina X of the cervical, thoracic and lumbar cord regions contained 780 (n = 3, nsc = 15), 660 (n = 3, nsc = 15) and 761 GAD67-GFP-IR neurones (n = 3, nsc = 15), respectively. The average number of GAD67-GFP-IR neurones observed per 50 µm section was as shown in Table 3.14. The size of the ChAT-IR neurones was 16.17 ± 0.57 µm x 21.60 ± 1.13 µm (N = 10), with a soma cross sectional area of 280.14 μm^2, whereas the size of the GAD67-GFP-IR neurones was 13.21 ± 0.63 µm x 16.17 ± 0.98 µm (N = 10), with a soma cross sectional area of 169.51 μm^2.

ChAT/GAD67-GFP co-localised neurones were observed in lamina X of the young mice (Figure 3.12-Aiii, Biii and Ciii); 60, 35 and 43 neurones for the cervical (n =3, nsc = 15), thoracic (n =3, nsc = 15) and lumbar cord sections (n =3, nsc = 15) respectively. Similar to the findings for the adult animals, it was discerned that the majority of co-localised neurones were in lamina X when compared to other studied areas of the spinal cord, and these co-localised neurones were negative for Fluorogold labelling.

The percentage of of ChAT-IR neurones which contained GAD67-GFP for the cervical, thoracic and lumbar sections was 41.10%, 18.62%, 17.70% respectively, while the percentage of of GAD67-GFP-IR neurones which contained ChAT for the cervical, thoracic and lumbar sections was 7.69%, 5.3% and 5.65% respectively. Aproximately 4 ± 0.26, 2.33 ± 0.43 and 2.87 ± 0.32 co-localised neurones were observed on average for both sides of the cord per 50 µm thick cervical, thoracic and lumbar cord section respectively (see Table 3.14).

The size of ChAT/GAD67-GFP co-localised neurones was 12.68 ± 0.47 µm x 16.90 ± 1.11 µm (N = 10), with a soma cross sectional area of 171.82 μm^2.They also appeared to be lightly immunoreactive for both ChAT and GAD67-GFP (see Figure 3.7-C and Figure 3.12).

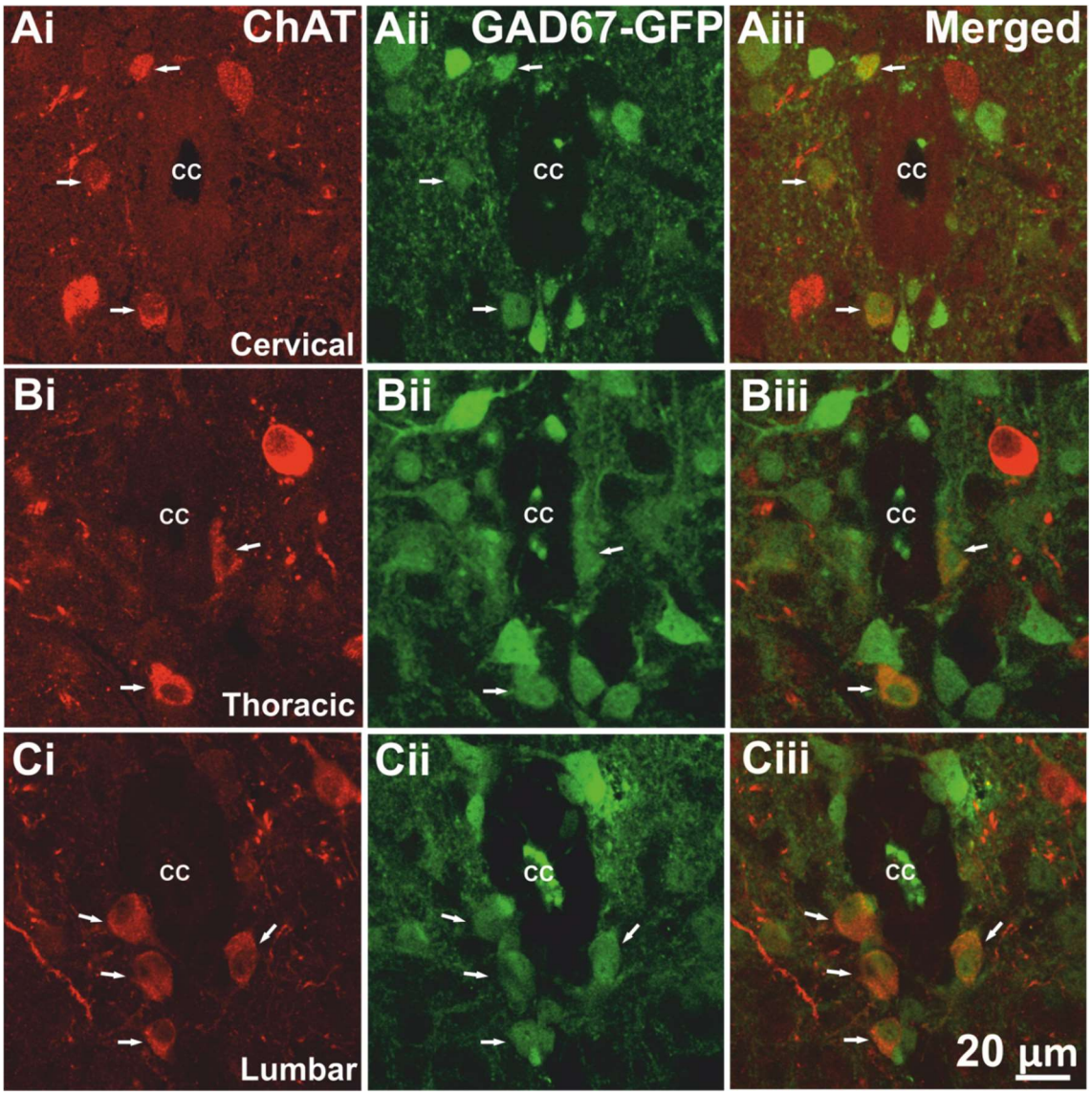

Figure 3.12: Co-localisation of ChAT and GAD67-GFP in lamina X of young mice. ChAT/GAD67-GFP co-localised neurones are observed in the cervical, thoracic and lumbar sections of lamina X (marked respectively as areas in A, B and C in the figure). Neurones which exhibit co-localisation are indicated by arrows. Images taken using confocal microscopy.

Table 3.14: Numbers of ChAT-IR and/or GAD67-GFP-IR neurones per 50 µm section in lamina X of each region of the spinal cord of young mice (n = 3).

Regions	ChAT/GAD67-GFP co-localised neurones	ChAT-IR neurones	GAD67-GFP-IR neurones
Cervical (15 sections)	4 ± 0.26	9.73 ± 0.77	52 ± 5.98
Thoracic (15 sections)	2.33 ± 0.43	12.53 ± 0.82	44 ± 3.21
Lumbar (15 sections)	2.87 ± 0.32	16.20 ± 1.42	50.73 ± 2.69

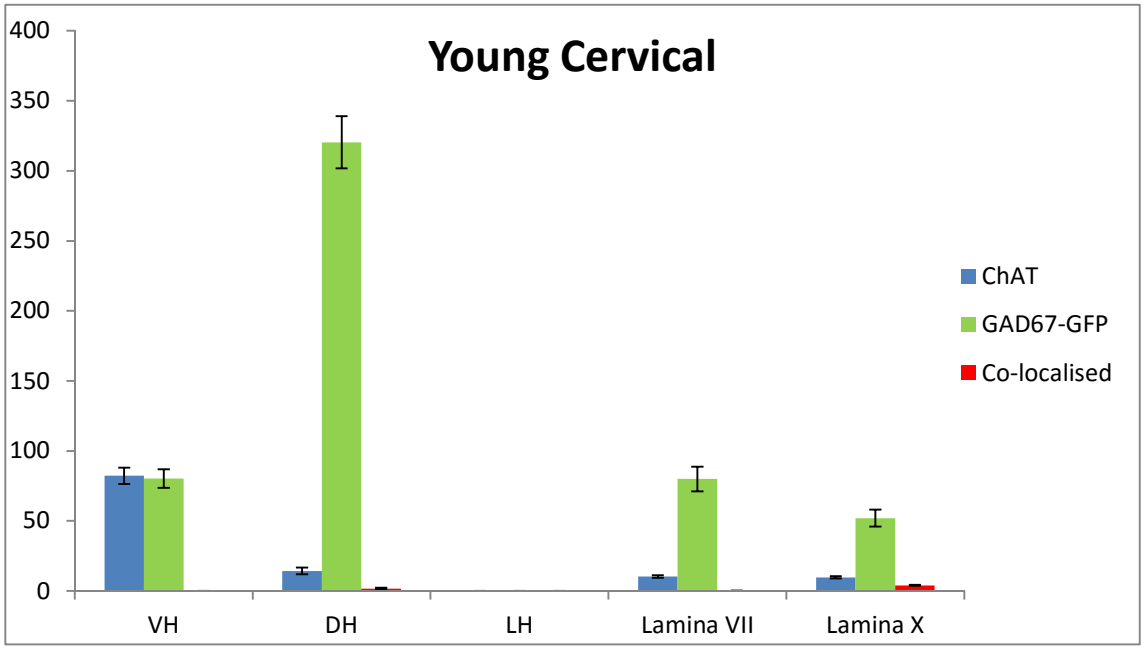

Figure 3.13: Distribution of ChAT, GAD67-GFP and co-localisation in young cervical spinal cord.

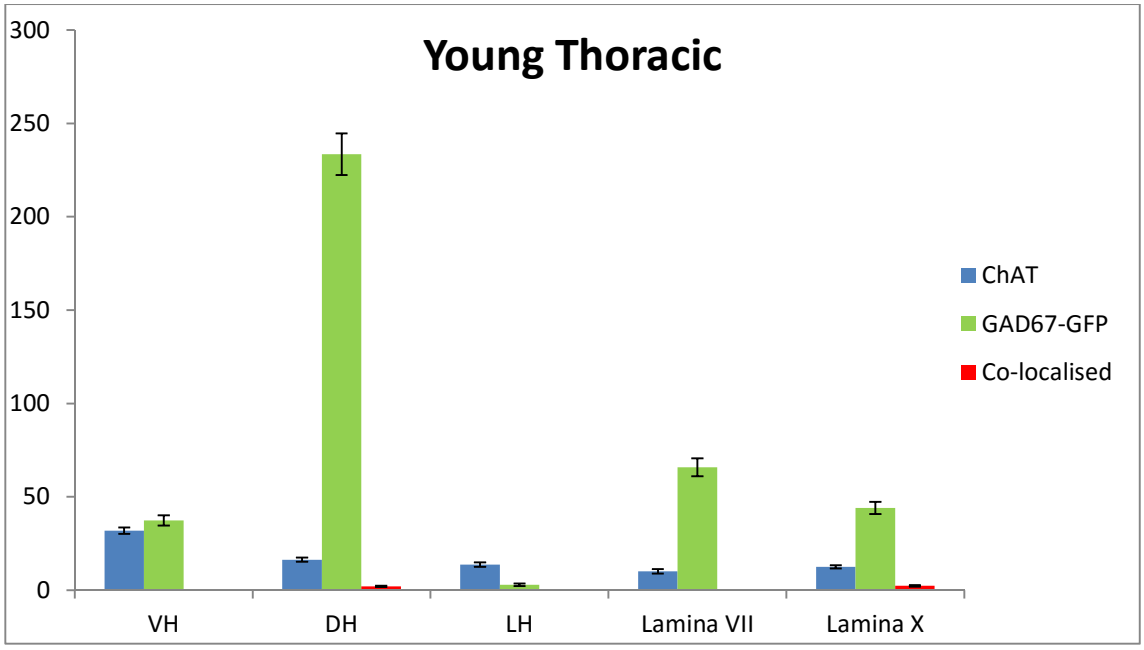

Figure 3.14: Distribution of ChAT, GAD67-GFP and co-localisation in young thoracic spinal cord.

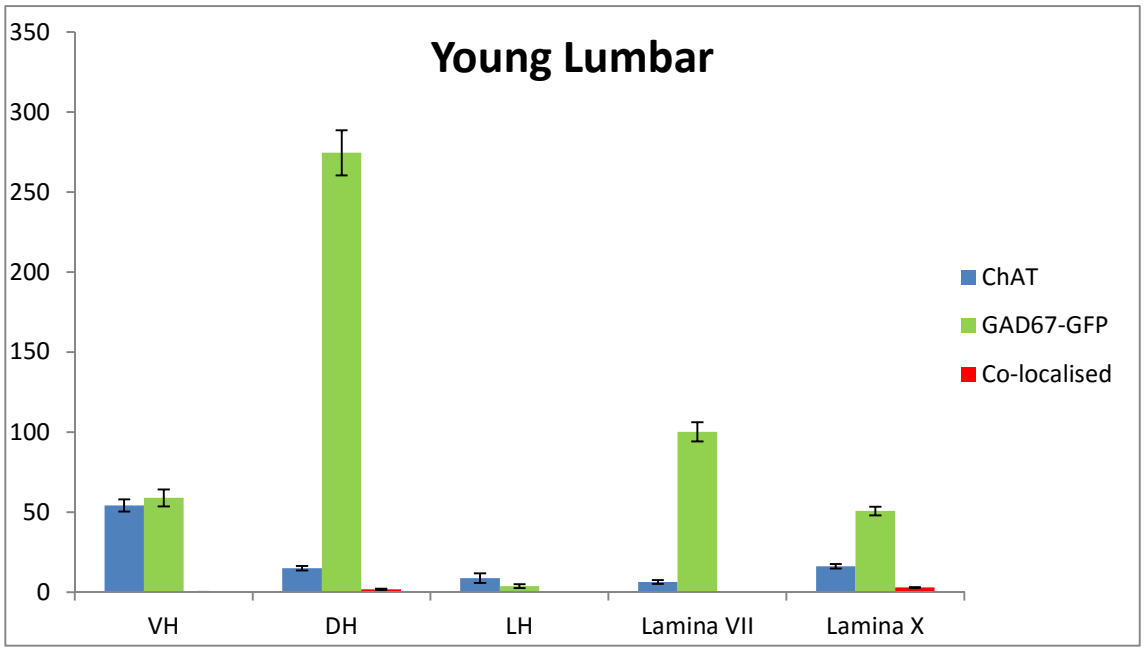

Figure 3.15: Distribution of ChAT, GAD67-GFP and co-localisation in young lumbar spinal cord.

3.4.3 Comparison of the the relative abundance of each neurochemically-defined population in lamina X between juvenile and adult mice.

For the cervical cord, the number of ChAT-IR neurones in lamina X for juvenile mice (9.73 ± 0.77) is not significantly different (p = 0.37) to that for adult mice (10.77 ± 0.70). The number of ChAT/GAD67-GFP co-localised neurones in the two age groups (4 ± 0.26 for juvenile and 4.03 ± 0.41 for adult is also not significantly different (p = 0.95). However, the number GAD67-GFP-IR neurones in lamina X of the cervical cord is significantly different between the two groups (52 ± 5.98 for juvenile and 33.83 ± 2.21 for adult mice, p = 0.01).

For the thoracic cord, the number of ChAT-IR neurones in lamina X for juvenile mice (12.53 ± 0.82) is not significantly different (p = 0.16) to that for adult mice (14.27 ± 0.76). However, the number of GAD67-GFP-IR neurones in the two age groups (44 ± 3.21 for juvenile and 32.4 ± 1.43 for adult mice) is significantly different (p = 0). Similarly, the number of co-localised ChAT/GAD67-GFP neurones in lamina X of the thoracic cord is also significantly different between the juvenile (2.33 ± 0.43) and adult (3.8 ± 0.31) mice (p = 0.01).

For the lumbar cord, the number of ChAT-IR neurones in lamina X for juvenile mice (16.20 ± 1.43) is not significantly different to that for adult mice (13.70 ± 0.80) (p = 0.10). In contrast, the number of GAD67-GFP-IR neurones in the two age groups (50.73 ± 2.69 for juvenile and 32.07± 2.33 for adult mice) is significantly different (p = 0). Similarly, the number of co-localised ChAT/GAD67-GFP neurones in lamina X of the lumbar cord is also significantly different between the juvenile (2.87 ± 0.32) and adult (4.47 ± 0.27) mice (p = 0).

3.4.4 Morphological analysis of cells that express ChAT and GAD67-GFP in neonatal spinal cords using juxtacellular labelling combined with IHC

A total of 130 neurones in lamina X were recorded and 122 of them were processed utilising IHC. Out of these only 34 neurones were either recovered or partially recovered. While the numbers of recovered neurones exhibiting sole immunoreactive labelling for ChAT and GAD67-GFP were 1 and 7 respectively, only one ChAT/GAD67-

GFP co-localised neurone was recorded and recovered. The morphology of the co-localised neurone, plus the ChAT-IR neurones and GAD67-GFP-IR neurones were as follows.

3.4.4.1 Morphology of a ChAT/GAD67-GFP co-localised neurone in lamina X

In lamina X, the ChAT/GAD67-GFP co-localised neurone had an oval or elliptical shaped cell body. The size of the neurone was 12.30 x 13.85 μm (N = 1), with a soma cross sectional area of 134.29 μm^2.

The processes seemed to be relatively small and short, and thus were likely to be locally branching within lamina X. The neurone had some dendrites passing close to the ependymal cells lining the central canal, although one dendrite reached the ventral aspect of lamina X (see Figure 3.16).

3.4.4.2 Morphology of a ChAT-IR neurone in lamina X

In lamina X the ChAT-IR neurone had an oval or elliptical shaped cell body. Its processes branched extensively dorsally, ventrally and laterally within the grey matter. The neurone also sent a dendrite across the ventral aspect of the central canal to the contralateral side (see Figure 3.17). The size of the neurone was 12.40 x 15.55 μm (N = 1), corresponding to a soma cross sectional area of 153.41 μm^2.

3.4.4.3 Morphology of GAD67-GFP-IR neurones in lamina X

In lamina X, GAD67-GFP-IR neurones had an oval or elliptical shaped cell body. The size of the cell body was 8.29 ± 0.49 x 13.42 ± 1.87 μm (N = 7), with a soma cross sectional area of 92.56 μm^2. Only one process was observed which appeared to be very fine, sending local branching within the vicinity of lamina X itself and potentially into the area of the ventral horn (see Figure 3.18*).*

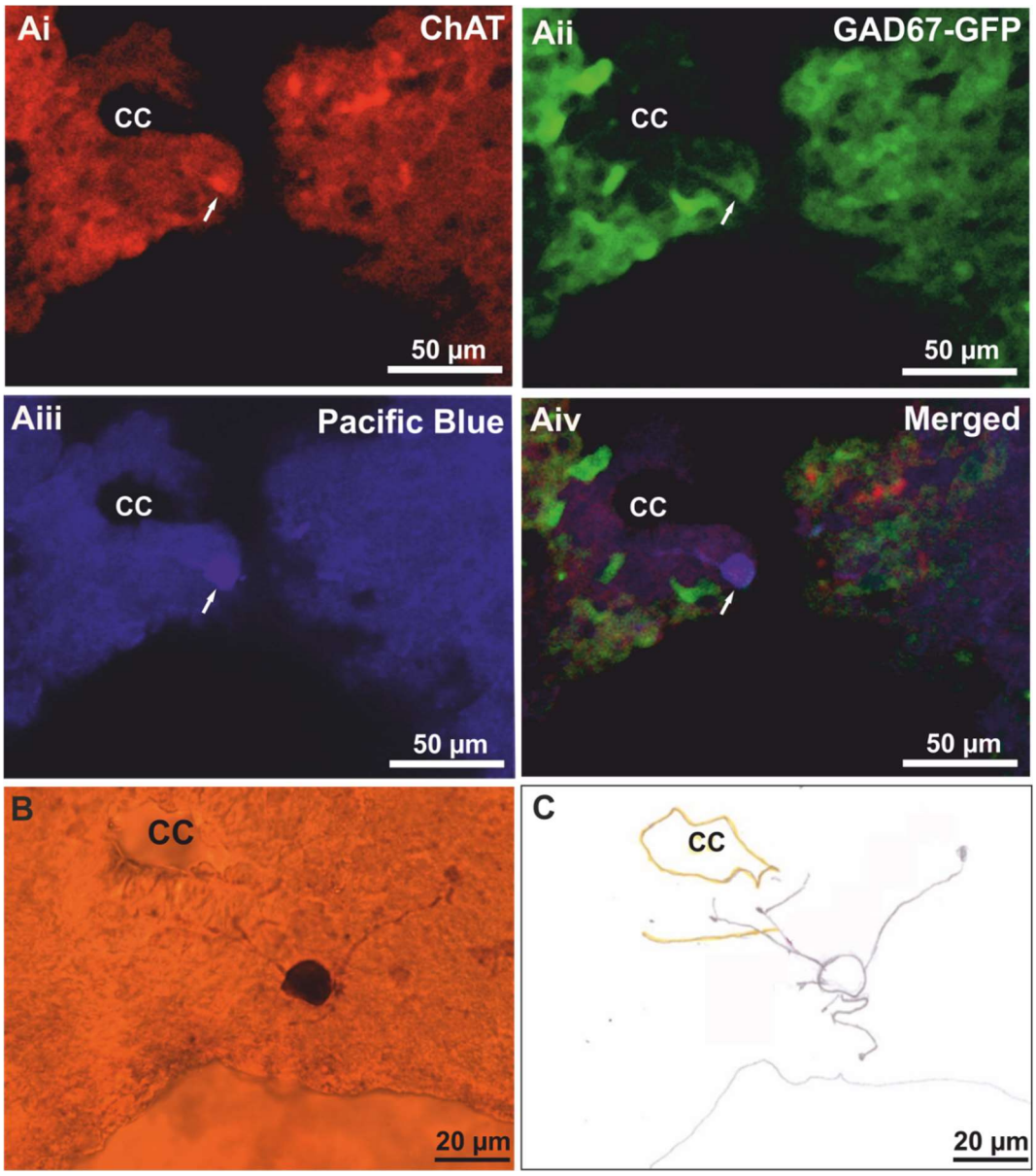

Figure 3.16: Morphological study of a ChAT/ GAD67-GFP co-localised neurone using juxtacellular labelling in combination with IHC. The co-localised neurone (indicated by the arrow in A) was visualised using double labelling fluorescent IHC for ChAT (Ai) and GFP (Aii), with streptavidin pacific blue being used to label the neurobiotin tracer (Aiii). The ChAT staining in Ai is pale due to the low permeability of the antibody into the 300 µm thick spinal cord section. The focal plane which depicted the largest area of the soma was selected for viewing under a confocal microscope (Ai to Aiv). The labelled neurone was then processed using DAB protocol (B) to observe morphology; additionally illustrated in the drawing (C) using camera lucida.

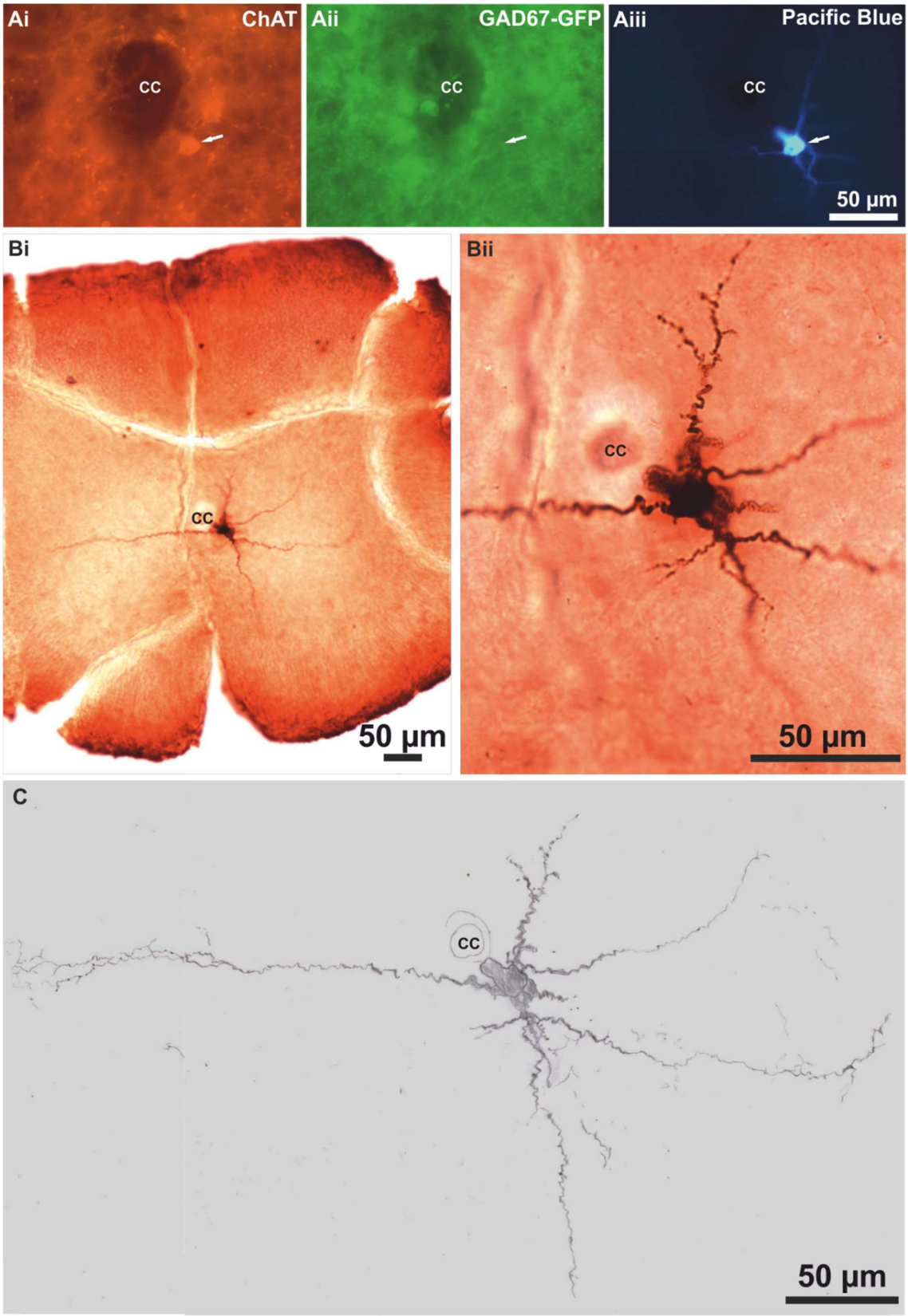

Figure 3.17: Morphological study of a ChAT-IR neurone using juxtacellular labelling in combination with IHC.

Figure 3.17 (continued):

The neurone (indicated by an arrow in A) was visualised with streptavidin pacific blue to label the neurobiotin tracer (Aiii). Double IHC revealed the neurobiotin labelled cell was ChAT-IR (Ai) yet did not contain immunoreactivity for GAD67-GFP (Aii). The labelled neurone was then processed using DAB protocol (Bi at lower magnification and Bii at higher magnification) to observe morphology; as additionally illustrated in the drawing (C) using camera lucida. Images shown are epifluoescent (Ai-Aiii) and brightfield photomicrographs (Bi-Bii).

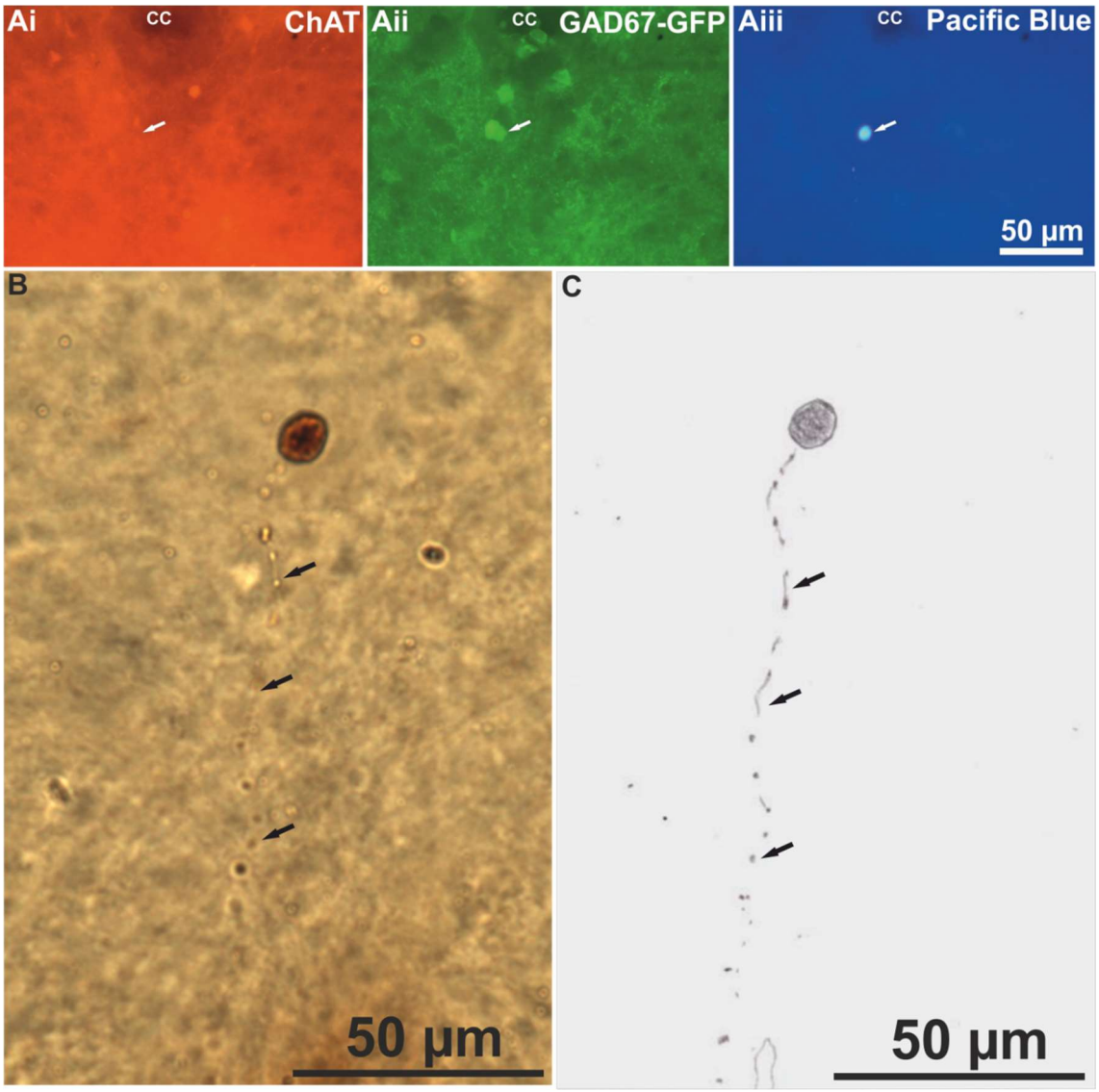

Figure 3.18: Morphological study of a GAD67-GFP-IR neurone labelled juxtacellularly with neurobiotin.

Figure 3.18 (continued):

Double IHC revealed the neurobiotin labelled cell (Aiii) did not contain ChAT immunoreactivity (Ai) yet contained immunoreactivity for GAD67-GFP (Aii). Visualisation of neurobiotin with DAB (B) and mapping using camera lucida (C) revealed a long, fine process (indicated by arrows in B and C) branching within the vicinity of lamina X (arrows). Images shown are epifluoescent (Ai-Aiii) and brightfield photomicrographs (B).

3.4.5 Close apposition between ChAT/GAD67-GFP co-localised neurones in lamina X and glutamatergic, glycinergic and GABAergic terminals.

Possible inputs onto the ChAT/GAD67-GFP co-localised neurones in lamina X were investigated since this knowledge would indicate potential connections between the co-localised neurones and other pathways. Using VGLUT1 and VGLUT2 as markers for glutamatergic terminals, possible projections were explored from glutamatergic terminals to the co-localised neurones of lamina X in adult mice. In addition, GlyT2 was used to label glycinergic terminals, while GAD67 was selected as a marker to label GABAergic terminals.

3.4.5.1 Close apposition between ChAT/GAD67-GFP co-localised neurones in lamina X and glutamatergic terminals

Both VGLUT1-IR and VGLUT2-IR terminals formed close appositions near the somata of ChAT/GAD67-GFP co-localised neurones in lamina X (see Figure 3.19 and 3.20). The average numbers of VGLUT1-IR and VGLUT2-IR terminals were 7.4 ± 3.41 (mean ± SEM) boutons per 100 µm (membrane of co-localised neurone cell body) (N = 2) and 18.23 ± 3.61 per 100 µm (N = 2) respectively.

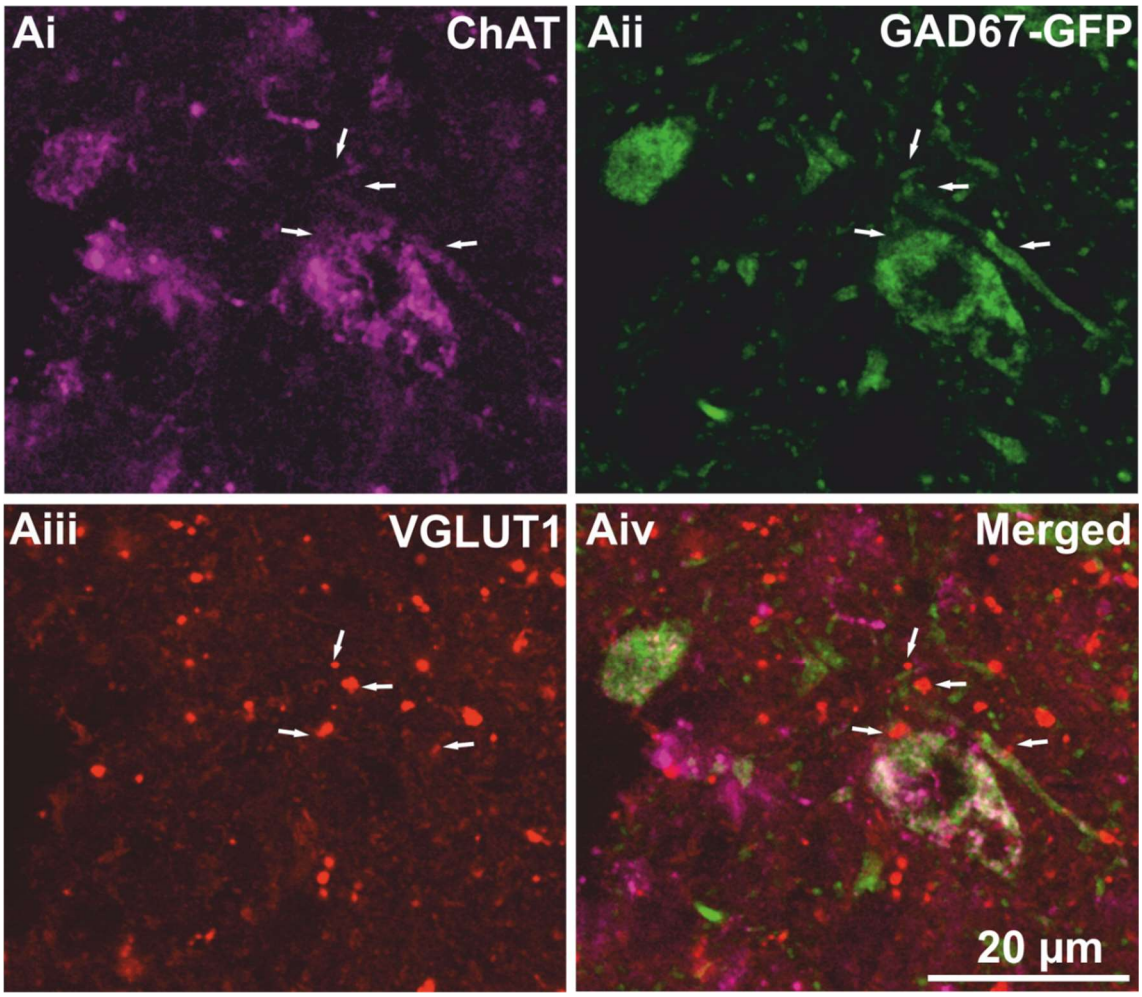

Figure 3.19: VGLUT1-IR terminals form close appositions with ChAT/GAD67-GFP co-localised neurones in lamina X. The arrows indicate the location of VGLUT1-IR terminals in close proximity to the cell body and proximal dendrites of a co-localised neurone. Images show immunoreactivity for ChAT (Ai), GAD67-GFP (Aii), VGLUT1 (Aiii) and the merged image (Aiv). Co-localisation of ChAT and GAD67-GFP appears as white in the merged image. Images acquired by confocal microscopy.

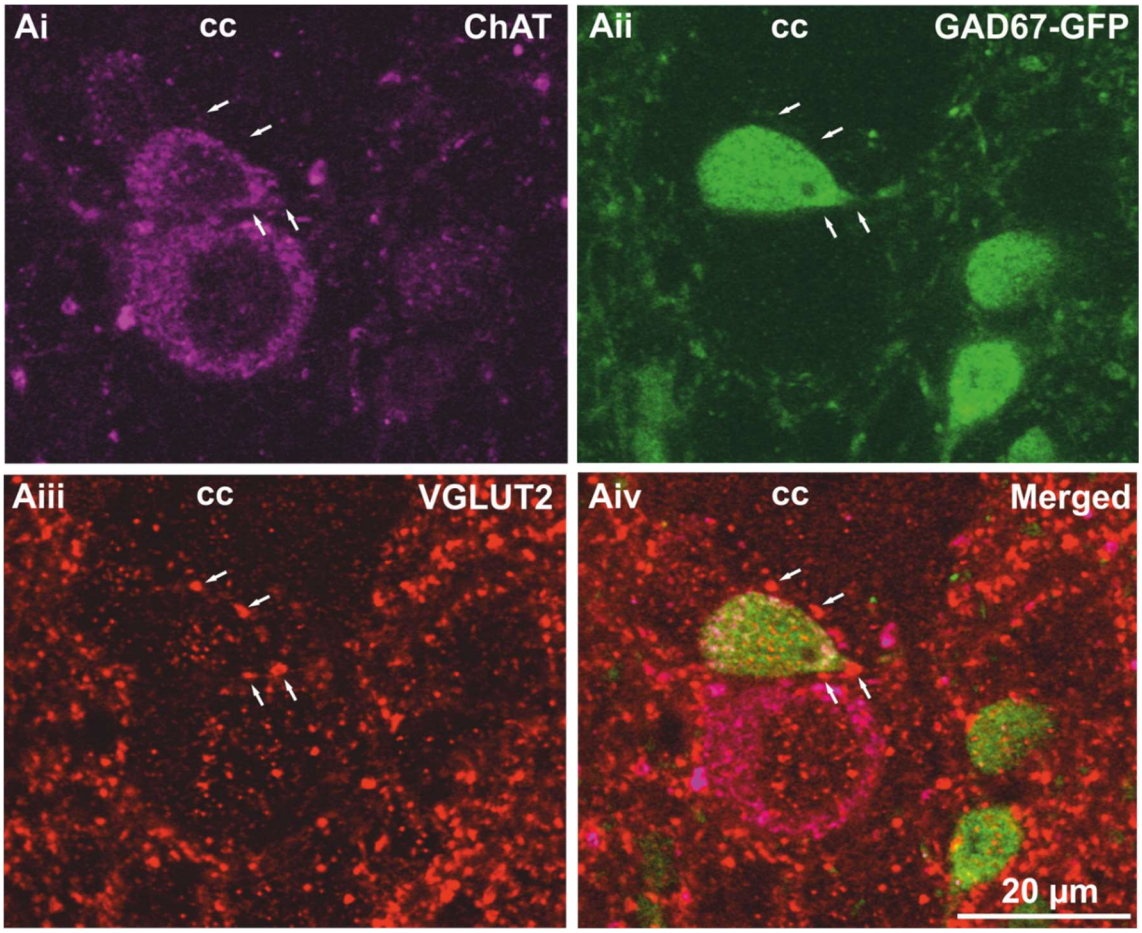

Figure 3.20: VGLUT2-IR boutons form close appositions onto ChAT/GAD67-GFP co-localised neurones in lamina X. The arrows indicate the location of VGLUT2-IR terminals having close proximity to the cell body of a co-localised neurone. CC: central canal. Images acquired by confocal microscopy.

3.4.5.2 Close apposition between ChAT/GAD67-GFP co-localised neurones in lamina X and glycinergic terminals

GlyT2-IR terminals were also found in close proximity to ChAT/GAD67-GFP co-localised neurones in lamina X (see Figure 3.21). The average number of GlyT2-IR terminals was 13.24 ± 1.86 per 100 µm (N = 2).

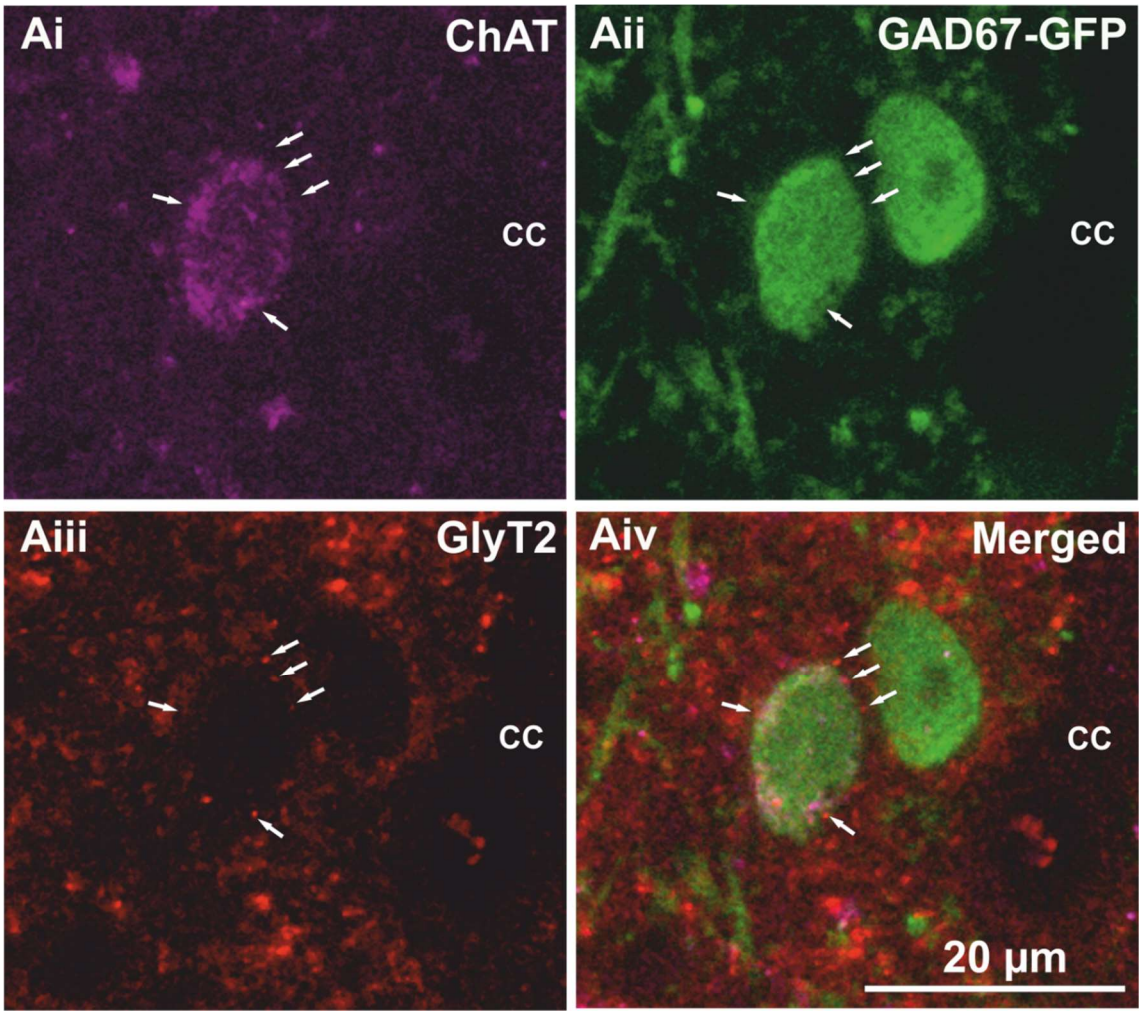

Figure 3.21: GlyT2-IR terminals form close appositions with co-localised neurones in lamina X. The arrows indicate the putative close contacts of GlyT2-IR terminals with the cell body of a co-localised neurone. CC: central canal. Images acquired by confocal microscopy.

3.4.5.3 Close apposition between ChAT/GAD67-GFP co-localised neurones in lamina X and GABAergic terminals

GAD67 was used as a marker for GABAergic terminals. The results suggested that GAD67-IR terminals were in close proximity to ChAT/GAD67-GFP co-localised neurones in lamina X (see Figure 3.22). The average number of GAD67 terminals was 6.26 ± 2.53 per 100 µm (N = 2).

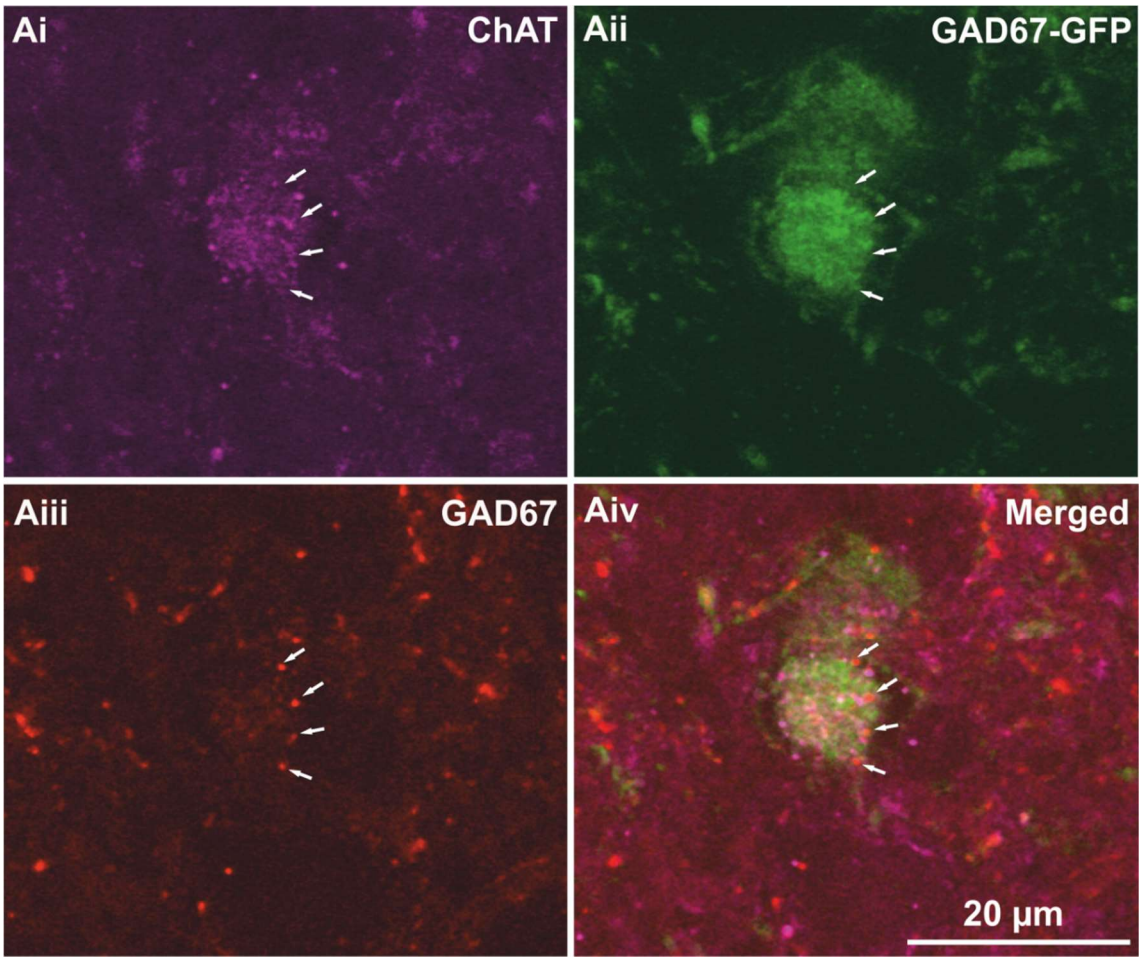

Figure 3.22: GAD67-IR terminals in close proximity with co-localised neurones in lamina X. The arrows indicate the putative contacts of the GAD67-IR terminals onto the cell body of a co-localised neurone. Images acquired by confocal microscopy.

3.5 Discussion

3.5.1 Summary

In this study, small populations of neurones in lamina X and the dorsal horn of cervical, thoracic and lumbar spinal cords of adult mice are described which contain the synthesizing enzymes for both ACh and GABA; with the larger number being contained in lamina X. The majority of co-localised neurones were located ventral and ventrolateral to the central canal. A very limited number of co-localised neurones were observed in lamina VII and the ventral horn of adult spinal cords. Moreover, co-localisation was not observed in the lateral horn of adult mice.

In preparation for morphological and projection studies of these co-localised neurones using juxtacellular labelling under electrophysiological conditions, the spinal cords of young animals were likewise investigated; since the presence of co-localised neurones in the young animals needed to be established prior to undertaking the electrophysiological work. The results from the young animals were similar to those obtained from the adult mice, since lamina X contained the majority of co-localised neurones compared to the other areas. In addition there were a small number of co-localised neurones in the dorsal horn of young mice, while a very limited number of co-localised neurones were discerned in lamina VII and the ventral horn; similar to the observations for adult mice. Co-localised neurones were not observed in the lateral horn of young mice.

Application of juxtacellular labelling, in combination with IHC, revealed the morphology and dendrites of the ChAT/GAD67-GFP co-localised neurones in lamina X of the mouse spinal cord. The axon was not identified, which may possibly be a result of the projections travelling in the sagittal plane and so the associated terminals were not located within the recovered section.

Terminal labelling IHC suggested that the co-localised neurones in lamina X likely received input from VGLUT1-IR, VGLUT2-IR, GlyT2-IR and GAD67-IR terminals.

3.5.2 Co-expression pattern of ChAT/GABA (or GAD) and other neurochemical markers with respect to previous studies

The results of this study indicate the presence of a subgroup of interneurones that are predominantly observed in lamina X of the spinal cord, and which potentially utilise both ACh and GABA.

In the spinal cord, co-expression of ChAT/GABA (Todd, 1991, Mesnage et al., 2011) as well as GABA/glycine (Todd, 1991) have been previously reported in dorsal horn neurones. Kosaka et al. reported the co-localisation of ChAT and GAD (or GABA) in the area lateral to the central canal in lamina X and in the intermediate grey (lamina VII) (Kosaka et al., 1988). The possible co-localisation of ChAT and GABA in neurones ventral to the central canal was proposed by Spike et al. (1993) who found that NADPH diaphorase positive neurones were mostly immunoreactive for GABA (Spike et al., 1993). Working from the postulations of Kosaka (1988) and Todd (1991) that some GABAergic neurones were likely to also produce acetylcholine, Spike et al. also

established that many NADPH diaphorase positive neurones around the central canal additionally exhibited ChAT immunoreactivity. Based on their findings they inferred that coexpression of ChAT and GABA occurred within at least a proportion of NADPH diaphorase neurones in lamina X, although they could not directly demonstrate the ChAT/GABA co-localisation. A study by Miles et al. determined that the ChAT positive interneurones giving rise to the C boutons that innervate ventral horn motoneurones were discretely located lateral to the central canal in lamina X and medial lamina VII, plus that they co-localised with YFP in the transgenic mouse used (Dbx1-YFP) but not with NOS. Moreover, some interneurones around the central canal that did not give rise to C boutons were demonstrated to be ChAT and NOS positive (Miles et al., 2007).

Whilst the aforementioned studies provided strong evidence for the existence of a population of ChAT and GAD co-expressing neurones in lamina X, only Kosaka (1988) showed direct coexpression in the region. By contrast, this study has described a population of GAD67-GFP expressing neurones predominantly located in the ventral aspect of lamina X for which direct evidence of ChAT immunoreactivity has been observed.

3.5.3 Technical Summary

3.5.3.1 Validation of IHC and Fluorogold labelling experiments.

The antibodies used in this study have appropriate control and ChAT, GFP and GAD67 antibodies have been characterised by Chapman et al 2003 (see details in Table 2.2). The validation of the staining of other antibodies have been compared to the literature and found to be reliable to use as desbribed in chapter 2 (see Table 2.2).

In our study, Fluorogold injection (Ambalavanar and Morris, 1989) was made through IP injection to distinguish motoneurones and SPNs from interneurones. Although an adverse aspect of using Fluorogold is that it is non specific to a particular group of neurones and could diffuse from the injection site to be endocytosed by any neurones whose terminals make contact with it (Catapano et al., 2008), the IP injection of Fluorogold has become widely used to distinguish motoneurones and SPNs from interneurones in spinal cord studies (Anderson and Edwards, 1994, Al-Mosawie et al., 2007). In our study, Fluorogold labelling is observed in cholinergic motoneurones of the ventral horn and cholinergic SPNs, but not for cholinergic dorsal horn cells. As such its labelling pattern is believed to be validated for use in this study.

3.5.3.2 Sample size and statistical approaches

Ideally cell populations would be studied in their entirety but there are clear practical limitations to this approach depending on the numbers involved and tissue distribution. Where it is not feasible to study a population, due to time or technical constraints, a representative or sample population can be used to estimate and draw conclusions with regard to the whole population (Nayak, 2010). For the purpose of this study, a statistical comparison between 2 groups was used to determine the similarity of a neurochemically defined population identified in young animals following maturation. Ordinarily sample size calculations precede the experimental phase of a study in order to predict the sample size required to give a meaningful observation (Nayak, 2010). This is useful in reducing the number of animals required for a study and predicting costs when writing grants but can be estimated reasonably accurately on previous experience or following best practices within a field (Dell et al., 2002, Charan and Kantharia, 2013).

As this work was initiated as a speculative study investigating the occurrence and distribution of neurones co-localising ChAT and GAD67-GFP in regions of the medulla and spinal cord of adult mice, power analysis was not performed in advance of experimentation. When it was determined that the juxtacellular labelling method should be used to investigate the connectivity of co-localised neurones in the spinal cord a new technical consideration was introduced. The production of viable spinal cord slices for electrophysiology from adult animals is a difficult process facilitated by the use of neonates instead. This required validating the population to ChAT/GAD67-GFP co-localised neurones observed in the ventral part of lamina X of adult animals are present in the juveniles to be used for electrophysiological investigation. As such, a quantitative description of the differences between this population of neurones in young and old animals was a secondary question considered after the data was collated. Owing to the circumstances, the sample size used was determined through previous experience of similar studies.

3.5.3.3 Problems encountered in labelling the ChAT/GAD67-GFP co-localised neurones via juxtacellular labelling; approach, success rates, quality of fills and quality of immunolabelling

The technique of juxtacellular labelling (Pinault, 1996, Joshi and Hawken, 2006) was utilised to observe the possible projections of co-localised neurones. One problem to obtaining increased numbers of labelled co-localised neurones from the juxtacellular activities was the nature of the selected transgenic mouse line, since it enabled the visualisation of only GABAergic (GAD67-GFP) neurones during the labelling process. Therefore, knowledge of whether the neurones being labelled during the juxtacellular labelling process were co-localised or not could not be determined. After the juxtacellular labelling process, co-localisation could only be confirmed once cell recovery had been completed utilising IHC. As a result, only one co-localised neurone (1/34 neurones = 3%) was labelled in this study from 34 neurones that were recovered. A potential solution for this difficulty would involve current transgenic technologies creating an animal line suitable for the study of neurones co-expressing both enzymes synthesising ACh and GABA, so allowing for detailed studies in relation to their possible function and how they fit in the spinal cord circuits. Saito et al. reported a study involving the use of a double transgenic rat model in which the neurones within the prepositus hypoglossi nucleus expressed both ChAT and vesicular GABA transporter (VGAT) (Saito et al., 2015). This rat model may prove to be a suitable candidate in aiding future studies to investigate the functions of our co-localised neurones.

When undertaking triple labelling to label co-localised neurones along with a neuronal tracer, the availability of secondary antibodies and microscope filters prevented us from using tracer dyes such as rhodamine in addition to neurobiotin. As a result neurobiotin was the sole tracer used to label the neurones. One of the disadvantages to the use of neurobiotin is that it is colourless and cannot be visualised under a fluorescence microscope. Therefore, we could not confirm whether neurones were being filled with the dye during the passing of current.

GAD67-GFP positive cells located in regions of the spinal cord which contained the majority of the small co-localised neurone population were visualized and targeted. Successful recovery of the filled neurones then required triple labelling with IHC for GAD67-GFP, ChAT and neurobiotin. Since only a small percentage of all GAD67-GFP positive neurones in the lamina X also expressed ChAT, this proved to be technically

challenging. Low yields have been described by other researchers when attempting to juxtacellularly fill and then co-label for only a single neurotransmitter, rather than the two that was attempted in this study. For example, with respect to the raphe nuclei, where a very high proportion of cells are known to be serotonergic, only 12.9 % of the juxtacellularly labelled cells were successfully identified as 5-HT immunopositive by Iceman et al. (Iceman et al., 2013). The low yield of recovered and triple co-labelled cells was therefore to be expected.

The quality of fills also plays an important role for cell recovery. The quality of cell attachment, application of appropriate current, labelling time and the viability of the labelled cells, can all act to affect the quality of subsequent immunolabelling (Duque and Zaborszky, 2006).

In relation to cell recovery utilising IHC, given the lack of reported information on the morphology of ChAT/GAD67-GFP co-localised neurones in the spinal cord we did not know which direction their processes were likely to travel within the spinal cord slice. As such, the whole 300 µm thick slice containing a labelled neurone was recovered without further re-sectioning. At this thickness it is difficult for the antibodies to penetrate into the sections, plus there was increased risk of cross reaction from the application of triple labelling, so making it particularly challenging to achieve successful staining through the application of IHC on these slices.

3.5.4 Neurones located within lamina X which co-express the synthesising enzymes for ACh and GABA constitute a novel subgroup of interneurones.

In this study, the majority of neurones which exhibit co-localisation are observed in lamina X of the cervical, thoracic and lumbar cord regions; particularly in the areas ventral and ventrolateral to the central canal. They are negative for Fluorogold labelling which suggests that they are neither motoneurones nor preganglionic neurones; Fluorogold is a retrograde tracer which labels motoneurones and preganglionic neurones (Ambalavanar and Morris, 1989). Therefore, it is proposed that these neurones constitute a novel subgroup of interneurones within the area around the central canal that potentially utilise both ACh and GABA as their neurotransmitters.

3.5.5 Challenges in establishing possible projections of co-localised neurones

The results from the juxtacellular labelling made it clear how difficult it was to target and fill single co-localised cells and the technical difficulties in this are discussed below.

The limited data obtained from juxtacellular labelling was not able to identify the potential targets for projections from these co-localised neurones in lamina X. A possible explanation for the lack of idendification may be that the neurone projections travelled in the sagittal plane and so the associated terminals were not located within the studied section. Furthermore, the relatively small size of the co-localised neurones suggests that their dendrites and axon might reasonably be expected to be fine and small, which in turn would have made observation of their termination sites considerably challenging.

There have been no previous reports on the co-localisation of GABAergic and cholinergic machinery in presynaptic terminals in the spinal cord. Based on our data, combined with the known location of cholinergic boutons in the vicinity of lamina X and adjacent areas as reported by other studies, the co-localised neurones might project to three different regions; Firstly to SPNs in the IML, secondly to the cells surrounding the central canal and thirdly to cells within lamina X.

Small sized cholinergic terminals have been detected in the lateral horn which contains SPNs (Deuchars and Lall, 2015). As previously mentioned in section 1.6.4, in relation to autonomic control, ACh plays an important role in cardiovascular regulation; as evidenced by studies involving anaesthetised rats, where injecting ACh into the IML of the thoracic cord resulted in increased heart rate (McKitrick and Calaresu, 1991). On the other hand, in the rat spinal cord slice, the weak effect of Ach was specifically remarked upon (Gibson and Logan, 1995), and potentially attributed to rapid metabolism of ACh by endogenous cholinesterase. By instead using the enzyme-resistant acetylcholine analogue carbachol, hyperpolarising responses in SPNs were subsequently observed and ascribed to M_2 muscarinic receptor activation.

ChAT-IR fibres possessing a terminal-like appearance were previously observed in the central grey matter in proximity to non-ChAT-IR cells of the ependymal layer by Barber et al. (Barber et al., 1984). Close apposition of cholinergic structures to cells surrounding the central canal in the spinal cord, including ependymal cells and

cerebrospinal fluid contacting cells (CSFcCs), has been observed (Corns et al., 2015). Both ependymal cells and CSFcCs reacted to ACh.

Based on our results from juxtacellular labelling, plus reported evidence indicating that ACh has an effect on neurones within lamina X, the third possible target of projections from the co-localised neurones is likely to be to lamina X itself. According to Bordey et al. (Bordey et al., 1996a) DMPP, a selective nAChR agonist, gave rise to a direct depolarization of SPNs in the CAA, so suggesting that nicotinic excitation of such neurones could influence sympathetic outflow. In addition, DMPP application also depolarised what were seemingly non-SPNs in lamina X (predominantly located in the ventral part of the dorsal commissure and also in the pericanal region), so suggesting that those neurones possessed nAChRs (Bordey et al., 1996b).

In addition, the ventral horn might also constitute a possible target for these co-localised neurones. Although the main source of cholinergic input in the form of C boutons to motoneurones in the ventral horn is reported to originate from cholinergic interneurones lateral to the central canal (Miles et al., 2007), our hypothesis regarding possible projections from the co-localised neurones to the ventral horn cannot be ruled out, since small cholinergic fibres can be observed to have contact onto the motoneurones (Barber et al., 1984).

Therefore, since the exact source of the cholinergic input onto all these regions in the spinal cord remains currently unknown, yet must be from a local source (Barber et al., 1984, Gotts, Unpublished Data), the neurones described here may form part of this innervation.

3.5.6 ChAT/GAD67-GFP co-localised neurones in lamina X likely receive both excitatory and inhibitory inputs; possible origins of VGLUT1, VGLUT2, GlyT2 and GAD67 inputs to co-localised neurones.

The results indicate that the ChAT/GAD67-GFP co-localised neurones in lamina X of the spinal cord likely receive excitatory inputs from terminals immunoreactive for VGLUT1 and VGLUT2. VGLUT1 inputs onto these neurones may originate from primary afferents (Todd et al., 2003, Alvarez et al., 2004) and/or the corticospinal tract (Du Beau et al., 2012), while VGLUT2 terminals are suggested to come from interneurones (Todd et al., 2003, Alvarez et al., 2004) and descending projections (Du

Beau et al., 2012). In addition the co-localised neurones are also likely to receive inhibitory inputs from both GlyT2 and GAD67 terminals as indicated by close apposition of these terminals onto the co-localised neurones. Suggested sources for GABAergic and glycinergic axons are local interneurones (Spike et al., 1993, Mackie et al., 2003). From these observations, it is suggested that ChAT/GAD67-GFP co-localised neurones are interneurones that form part of spinal circuits involved in modulating and integrating roles in different systems, or alternatively they may have a role in the provision of antagonistic feedback within the system in which they are involved, such as in efferent modulation.

It should be noted that the visualisation of possible inputs onto the co-localised neurones was obtained using confocal microscopy. This approach only allows the assertion that terminals are in close apposition to the soma and may represent synaptic inputs. Definitive proof that these close appositions are indeed synapses would require the visualisation of the synaptic contact by electron microscopy.

3.5.7 ChAT/GAD67-GFP co-localised neurones in the dorsal horn

In our study ChAT/GAD67-GFP co-localised neurones were observed in the dorsal horn. Todd (Todd, 1991) reported similar results in which 94% of ChAT-IR neurones within lamina III were also immunoreactive to GABA. Although Todd reported that GABAergic neurones in lamina III of the dorsal horn generally co-express glycine (Todd, 1991), GABA-IR neurones immunoreactive to ChAT constituted a different group (as they were not immunoreactive to glycine), so suggesting that these two neuronal populations possess different roles in sensory circuits.

3.5.8 Functional consideration of co-transmission

One neurone can release more than one neurotransmitter, a trait which is termed co-transmission (Douglas and Poisner, 1966, Burnstock, 1976, Westfall et al., 1978, Sneddon and Burnstock, 1984, Lee et al., 2010, Ishibashi et al., 2013). Co-transmission has been observed and reported in many CNS regions, including GABA-glycine in spinal cord (Jonas et al., 1998, Ishibashi et al., 2013), ACh-GABA in retina (Lee et al., 2010) and ACh-glutamate in the brain (Ren et al., 2011, Guzman et al., 2011). Through co-transmission each neurotransmitter can increase the capability of a

circuit to be involved in numerous distinctive tasks (Lee et al., 2010, Ishibashi et al., 2013). In our study, although the function of ACh-GABA co-transmission of ChAT/GAD67-GFP co-localised neurones in lamina X has not been studied, it is likely that the co-transmission from these neurones not only enhances the ability of the associated circuits but also provides for fast synaptic transmission to the circuits in which they are involved, similar to what occurs in the retina (Lee et al., 2010). Within the spinal cord, each important circuit (motor, sensory or autonomic) has its own distinctive control. However, interconnection between circuits is also required in order for optimal or appropriate responses to be received and discharged. These neurones which exhibit co-localisation in the spinal cord could be a conduit for interconnection within or between these circuits.

It is possible that ChAT/GAD67-GFP co-localised neurones in lamina X are interneurones that have a role in sympatho-motor integration. The key function of the autonomic nervous system is to maintain homeostasis of the body (Deuchars, 2007) . Sympathetic outflow from the spinal cord levels comes from SPNs, which comprise the sole connection between the CNS and the peripheral nervous system. SPNs are innervated by supraspinal inputs (see Figure1.13), with some circuits requiring interneurones in order to establish contact onto SPNs. However, identification of the sympathetic interneurones is challenging due to the spinal cord being heterogeneous with respect to its neuronal cell type population. As a result the locations of interneurones controlling sympathetic activity in laminae V, VII and X, plus in the IML region, have only been established in the last few decades. Along with supraspinal innervation, sympathetic interneurones also receive innervation from afferent pathways, which have a crucial contribution to the maintenance of sympathetic outflow. The observations from our study indicate potential synaptic inputs onto ChAT/GAD67-GFP co-localised neurones in lamina X from various other pathways, including primary afferents (Todd et al., 2003, Alvarez et al., 2004) and/or the corticospinal tract (Du Beau et al., 2012) through VGLUT1 inputs , interneurones (Todd et al., 2003, Alvarez et al., 2004) and descending projections (Du Beau et al., 2012) through VGLUT2-IR terminals, plus inhibitory inputs via both GlyT2-IR and GAD67-IR terminals (Spike et al., 1993, Mackie et al., 2003). ChAT/GAD67-GFP co-localised neurones may therefore be a further subgroup of sympathetic interneurones, one that potentially utilises both ACh and GABA to play a role in sympatho-motor integration.

An alternate hypothesis is that the ChAT/GAD67-GFP co-localised neurones observed in lamina X could be postnatally newborn cells which are in the process of acquiring

their identity as cholinergic cells. This is because the area surrounding the central canal of the spinal cord contains the ependymal cell layer, which is the spinal cell niche (Corns et al., 2015), and as such it is likely that newborn cells would be located in close proximity to this region. The ChAT/GAD67-GFP co-localised neurones might therefore be in a transitional phase, changing from neuroblasts which are GABAergic, as observed from those in subventricular neurogenic zones (Platel et al., 2010), to become cholinergic neurones. As a result these neurones would be lightly immunoreactive for both GAD67-GFP and ChAT. Consistent with this was the finding that there were more GAD67-GFP-IR cells in lamina X of the young mouse compared to the older mouse. However, the number of ChAT and GAD67-GFP dual labelled cells was not significantly different in lamina X between the two age groups. It therefore remains to be determined if either of these cell types are indeed born postnatally.

The ChAT/GAD67-GFP co-localised neurones observed within lamina X in our study constitutes a newly identified subgroup of interneurones that potentially utilise both ACh and GABA. These neurones may play an important role in relation to sympatho-motor integration within spinal cord circuits.

4 Co-expression of ChAT and GAD67-GFP reveals a novel neuronal phenotype in the mouse medulla oblongata

4.1 Rationale

The presence of neurones expressing both ChAT and GAD67-GFP in lamina X throughout the cervical, thoracic and lumbar spinal cord was observed in this study. An aspect of interest pertained to the rostral termination of this group of neurones and whether their presence in the medulla oblongata related to a particular area and thus could provide insight into a possible physiological role. The aim of this chapter was to investigate the distribution, morphology and location of ChAT/GAD67-GFP co-localised neurones, with our preliminary findings leading us to focus primarily on the NTS. Supplemental observations were also made of the co-localisation in other areas within the medulla oblongata.

4.2 Roles and presence of GABA and ACh in the NTS

GABAergic systems play an important part in autonomic pathways and blockade of GABAergic signalling in the NTS broadly impacts cardiovascular (Mei et al., 2003), respiratory (Wasserman et al., 2002) and gastrointestinal regulation (Travagli et al., 2006). IHC for GABA or its synthesizing enzyme GAD67 reveals GABAergic neurones and terminals throughout the NTS (Maqbool et al., 1991, Izzo et al., 1992, Kawai and Senba, 1999, Fong et al., 2005, Okada et al., 2008). Similarly in transgenic animals in which enhanced GFP expression was linked to GAD67 expression, labelled neurones were widespread across the NTS, and the majority were directly activated by solitary tract afferents (Bailey et al., 2008).

A functional cholinergic system has also been described in the NTS. Microinjection of ACh into the rat NTS induces dose-dependent baroreflex-like hypotensive and bradycardic responses (Criscione et al., 1983, Tsukamoto et al., 1994, da Silva et al., 2008), modulates sympathetic and phrenic nerve activity (Furuya et al., 2014) and elicits a swallowing response (Hashim and Bieger, 1987).

Anatomically, some NTS neurones and terminals have been shown to contain the ACh hydrolysing enzyme - AChE (Kobayashi et al., 1978) and the enzyme responsible for synthesizing ACh - ChAT (Helke et al., 1983, Simon et al., 1985, Armstrong et al., 1988, Ruggiero et al., 1990). Two populations of ChAT-IR neurones in the NTS have

been described, one in medial NTS just dorsal to the dorsal vagal nucleus and one surrounding the medial and dorsal borders of the tractus (Armstrong et al., 1988).

Although GAD67-IR (Fong et al., 2005) and ChAT-IR (Ruggiero et al., 1990) neurones have been observed in the rat NTS, to date there has been no report on the co-localisation of the enzymes responsible for synthesising for both ACh and GABA within neurones in this region. A potential reason for this is the difficulty in labelling GABAergic neurones in the brainstem with IHC. We therefore utilised the GAD67-GFP knock-in mouse line and combined this with IHC for ChAT to identify ChAT/GAD67-GFP co-localised neurones in the NTS and other areas of the medulla oblongata.

4.3 Methods

For the study of ChAT/GAD67-GFP co-localisation detailed in this section, adult GAD67-GFP knock-in mice of either sex (4-6 weeks, n = 4) (Tamamaki et al., 2003) and wild type mice (4-6 weeks, n = 1, female) were used. Immunohistochemistry was performed as described previously (see section 2.7), using the combinations of antibodies detailed in Table 3.1. The location of each NTS subnucleus was identified via literature reports as illustrated in Figure 4.1. The experimental, analytical and quantification methods used for these investigations were those detailed in section 2.12.2. As the majority of neurones in the central subnucleus of the NTS use nitric oxide (Wiedner et al., 1995) we utilised triple labelling with neuronal nitric oxide synthase (nNOS) to define the region (Table 4.1). Since ChAT immunoreactivity within the NTS was apparently weak, we attempted to quantitatively determine if the weakness was possibly a result of lower ChAT expression or due to an artefact of our method. To achieve this we compared ChAT immunoreactivity in the NTS against that observed in the dorsal vagal nucleus for the same section of a wild type mouse using DAB staining. Details of the DAB IHC protocol used, involving a DAB solution from Sigma, was as described in section 2.8.

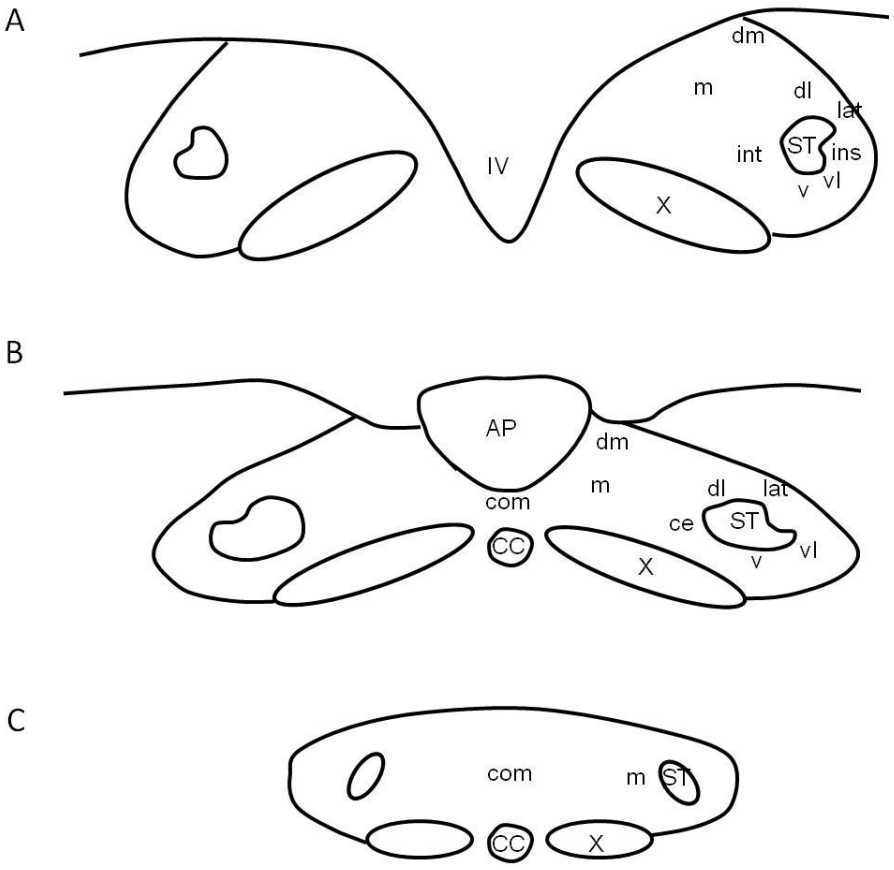

Figure 4.1: Various NTS subnuclei in three NTS regions, corresponding to a) rostral, b) intermediate and c) caudal (Figure adapted from Ciriello, 1994, Poole et al., 2007, Okada et al., 2008, Ganchrow et al., 2014).

NTS subnuclei; ce: central subnucleus; com: commissural subnucleus; dl: dorsolateral subnucleus; dm: dorsomedial subnucleus; ins: interstitial subnucleus; int: intermediate subnucleus; lat: lateral subnucleus; m: medial subnucleus; v: ventral subnucleus; vl: ventrolateral subnucleus.

Other structures; AP: area postrema; CC: central canal; IV: fourth ventricle; ST: solitary tract; X: dorsal vagal nucleus.

Note: In the rostral NTS region (a), subnucleus gelatinosus is included within the region described as medial subnucleus.

Table 4.1: Combinations of antibodies used for the triple labelling study of ChAT, GFP and nNOS in the central subnucleus of the NTS

Target Marker	Primary			Secondary			Tertiary		
	Antibody	Conc	Source	Antibody	Conc	Source	Antibody	Conc	Source
ChAT	Goatanti-ChAT	1:500	Millipore	Alexa Fluor ® 555 donkey anti-goat	1 : 1000	Invitrogen	Streptavidin Alexa Fluor ® 555	1 : 1000	Invitrogen
GFP	Rabbit anti-GFP	1: 1000	Invitrogen	Alexa Fluor ® 488 donkey anti-rabbit	1: 1000	Invitrogen			
nNOS	Mouse anti-nNOS	1: 250	Santa Cruz	Biotinylated horse anti-mouse	1: 500	Vector Laboratories	Streptavidin pacific blue	1: 1000	Invitrogen

Other areas in the medulla oblongata including the area postrema, reticular formation, dorsal vagal nucleus, hypoglossal nucleus and nucleus ambiguus were also investigated for the presence of the ChAT/GAD67-GFP co-localisation; using the same immunohistochemical protocol as that applied to the NTS study. The locations of such nuclei were identified based on information contained within the Allen mouse brain atlas (http://mouse.brain-map.org/) and literature (see Figure 4.2). In accordance with these resources, the area postrema was ascribed to be located at the midpoint of the dorsal surface of the medulla about the level of the obex (VanderHorst and Ulfhake, 2006, Hindmarch et al., 2011) in close apposition to the 4th ventricle (Walberg and Ottersen, 1992). The dorsal vagal nucleus lay in the dorsal aspect of the medulla oblongata (VanderHorst and Ulfhake, 2006, Ai et al., 2007) and dorsal to the hypoglossal nucleus (VanderHorst and Ulfhake, 2006). The nucleus ambiguus was located in the ventrolateral part of the medulla oblongata (VanderHorst and Ulfhake, 2006, Ai et al., 2007). The reticular formation consisted of scattered cells which spanned across the ventrolateral portion of the medulla oblongata (VanderHorst and Ulfhake, 2006). The experimental and quantification methods used for these investigations were those detailed in sections 2.12.2.

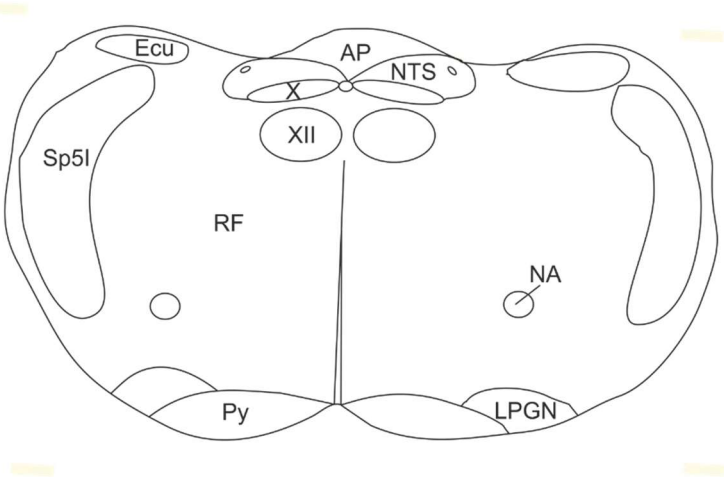

Figure 4.2: Diagram illustrating the approximate location of major nuclei of the medulla oblongata (Figure adapted from VanderHorst and Ulfhake, 2006). AP = area postrema, Ecu = external cuneate nucleus, LPGN = lateral paragigantocellular nucleus, NA = nucleus ambiguus, NTS = nucleus of tractus solitarius, Py = pyramidal tract, RF = reticular formation, Sp5I = interpolar part of spinal trigeminal nucleus, X = dorsal vagal nucleus, XII = hypoglossal nucleus.

4.4 Results

4.4.1 ChAT-IR and GAD67-GFP-IR neurones are present in the NTS and a small number are co-localised.

ChAT-IR neurones could be found throughout the subnuclei of the NTS. The cell bodies of ChAT-IR neurones were oval or elliptical shaped with a size of 12.33 ± 0.49 µm x 15.68 ± 0.8 µm (N = 16 neurones randomly chosen from all NTS subnuclei). The cross sectional area of the ChAT-IR soma was 154.07µm^2. GAD67-GFP-IR neurones were also found throughout the NTS with oval or elliptical shaped cell bodies and with a size of 10.03 ± 0.31 µm x 12.59 ± 0.49 µm (N = 12 neurones randomly chosen from all NTS subnuclei). The cross sectional area of the GAD67-GFP-IR soma was 100.48 µm^2.

A limited number of ChAT/GAD67-GFP co-localised neurones were observed in the NTS (Figure 4.3). These neurones had small cell bodies (8.15 ± 0.48 µm x 12.57 ± 0.67 µm, N = 12). The cross sectional area of the ChAT/GAD67-GFP co-localised

soma was 84.3074 μm^2. The highest percentage of co-localised neurones was found in the intermediate subnucleus (81 co-localised neurones / 610 total number of ChAT-IR and/or GAD67-GFP-IR neurones, 13.28%, number of sections counted (nsc) = 6 sections, n = 3 animals, see Figure 4.3-A), followed by the central subnucleus (19/215, 8.84%, nsc = 6, n = 3, see Figure 4.3-B), the ventrolateral subnucleus (10/330, 3.03%, nsc = 12 , n = 3), the ventral (10/343, 2.92%, nsc = 12, n = 3, see Figure 4.3-C), the dorsomedial (13/556, 2.34%, nsc = 11, n = 3), the dorsolateral (3/247, 1.21%, nsc = 12, n = 3), the medial (6/924, 0.65%, nsc = 18, n = 3) and the commissural (2/479, 0.42%, nsc = 12, n = 3) subnuclei. No co-localised neurones were observed in the lateral (0/141, 0%, nsc = 12, n = 3) or interstitial subnuclei (0/31, 0%, nsc = 6, n = 3). See Table 4.2 for the average number of neurones observed per 50 μm section in each subnucleus of the NTS.

When examined under a confocal microscope, GAD67-GFP staining was observed throughout the cytoplasm and nucleus of the neurones whereas ChAT staining was observed in the cytoplasm (see Figure 4.4-A, B).

4.4.2 DAB IHC labelling for ChAT to assess staining intensity between the NTS and the dorsal vagal nucleus

The intensity of DAB staining for ChAT-IR neurones in the NTS was observed based on a comparison with the intensity level of stained ChAT-IR neurones present in the same sections for the dorsal vagal nucleus, as present in three pictures (see Figure 4.5-Aii (caudal region), Bii (intermediate region) and Cii (rostral region)); the method of DAB staining being that described in section 2.8 and 4.3. The lightness level of neurones was measured for five randomly chosen ChAT-IR neurones of the dorsal vagal nucleus and five randomly chosen NTS ChAT-IR neurones from each picture, using Image J software, with the data obtained being presented in Table 4.3 as mean ± SEM (arbitrary units); the details of the analysis was as described in section 2.12.2. The degree of lightness level for ChAT-IR neurones in all three regions of the NTS was much greater than that for the dorsal vagal nucleus. This means that the ChAT-IR neurones located in all three regions of the NTS exhibit lighter or paler intensity for the ChAT staining when compared to the dorsal vagal nucleus (the higher the number, the lighter the shade of colour and paler the intensity). Moreover, the intensity of staining for ChAT-IR neurones in the rostral region appears to be much darker than that in the caudal and intermediate regions.

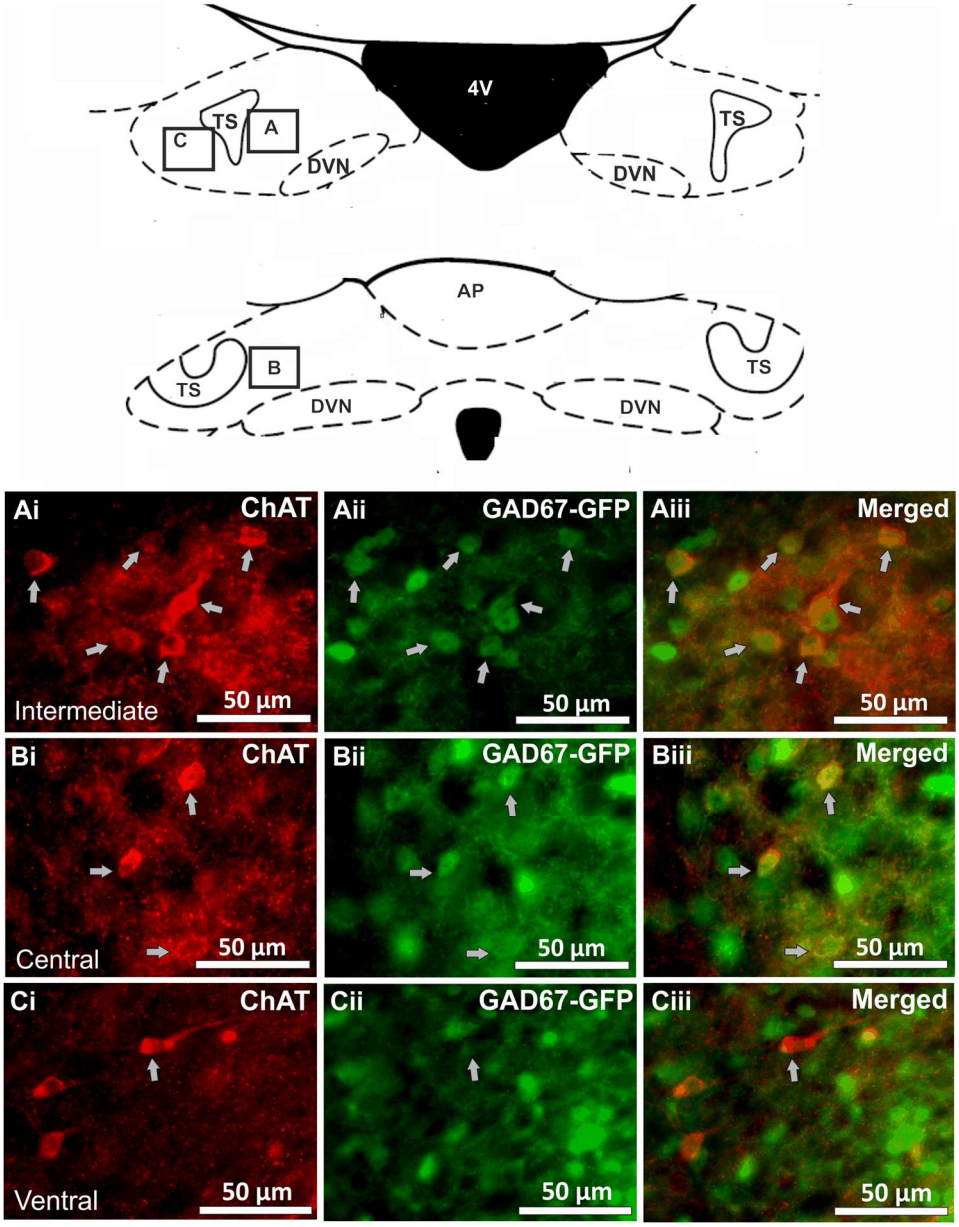

Figure 4.3: Distribution of ChAT-IR and GAD67-GFP cells in rostral and intermediate NTS.

Fluorescent images showing the distribution of ChAT-IR and GAD67-GFP cells in the intermediate (Ai-Aiii), central (Bi-Biii) and ventral (Ci-Ciii) subnuclei of the rostral and intermediate NTS. In all of these NTS subnuclei, double labelled cells containing both ChAT-IR (Ai, Bi and Ci) and GAD67-GFP (Aii, Bii and Cii) can be observed (Aiii, Biii and Ciii). Arrows indicate double labelled neurones. The schematic diagram is adapted from Paxinos and Watson (Paxinos and Watson, 1997) and indicates the approximate position of the subnuclei.

Table 4.2: The number of ChAT-IR and/or GAD67-GFP-IR neurones in each subnuclei of the NTS (per 50 µm section) in 3 animals (n = 3). nsc = number of sections counted. Values are presented as mean ± SEM.

NTS subnucleus	Side	ChAT/GAD67-GFP co-localised neurones Mean ± SEM	ChAT-IR neurones Mean ± SEM	GAD67-GFP-IR neurones Mean ± SEM	ChAT-IR neruones total number	GAD67-GFP-IR neurones total number	Co-localised neurones total number
Intermediate	Right	6.8 ± 1.9	17.5 ± 4.3	37.3 ± 8.2	105	224	41
(n = 3, nsc = 6)	Left	6.7 ± 2.2	16.7 ± 3.3	30.2 ± 6.4	100	181	40
Central	Right	1.0 ± 0.7	2.2 ± 1.3	16.3 ±2.6	13	98	6
(n = 3, nsc = 6)	Left	2.2 ± 1.4	2.8 ± 1.6	14.5 ± 2.0	17	87	13
Ventrolateral	Right	0.3 ± 0.1	1.6 ± 0.7	13.3 ± 3.1	19	160	4
(n = 3, nsc = 12)	Left	0.5 ± 0.3	1.8 ± 0.7	10.8 ± 2.3	21	130	6
Ventral	Right	0.4 ± 0.2	1.1 ± 0.4	13.8 ± 3.3	13	166	5
(n = 3, nsc = 12)	Left	0.4 ± 0.2	1.0 ± 0.5	12.7 ± 2.3	12	152	5
Dorsomedial	Right	0.6 ± 0.3	4.4 ± 1.7	18.9 ± 3.9	48	208	6
(n = 3, nsc = 11)	Left	0.6 ± 0.6	4.6 ± 2.1	22.6 ± 5.9	51	249	7
Dorsolateral	Right	0.3 ± 0.2	2.2 ± 1.0	10.2 ± 3.4	26	122	3
(n = 3, nsc = 12)	Left	0.0 ± 0.0	0.9 ± 0.4	7.3 ± 1.5	11	88	0
Medial	Right	0.2 ± 0.1	2.1 ± 0.6	25.4 ± 4.0	37	458	6
(n = 3, nsc = 18)	Left	0.2 ± 0.1	1.3 ± 0.3	22.6 ± 3.8	23	406	7
Commissural (n = 3, nsc = 12)		0.2 ± 0.1	5.0 ± 2.0	34.9 ± 9.1	60	419	2
Lateral	Right	0.0 ± 0.0	0.1 ± 0.1	5.9 ± 1.6	1	71	0
(n = 3, nsc = 12)	Left	0.0 ± 0.0	0.1 ± 0.1	5.7 ± 2.0	1	68	0
Interstitial	Right	0.0 ± 0.0	0.7 ± 0.5	3.3 ± 0.8	4	0	0
(n = 3, nsc = 6)	Left	0.0 ± 0.0	0.0 ± 0.0	1.2 ± 0.5	20	7	0

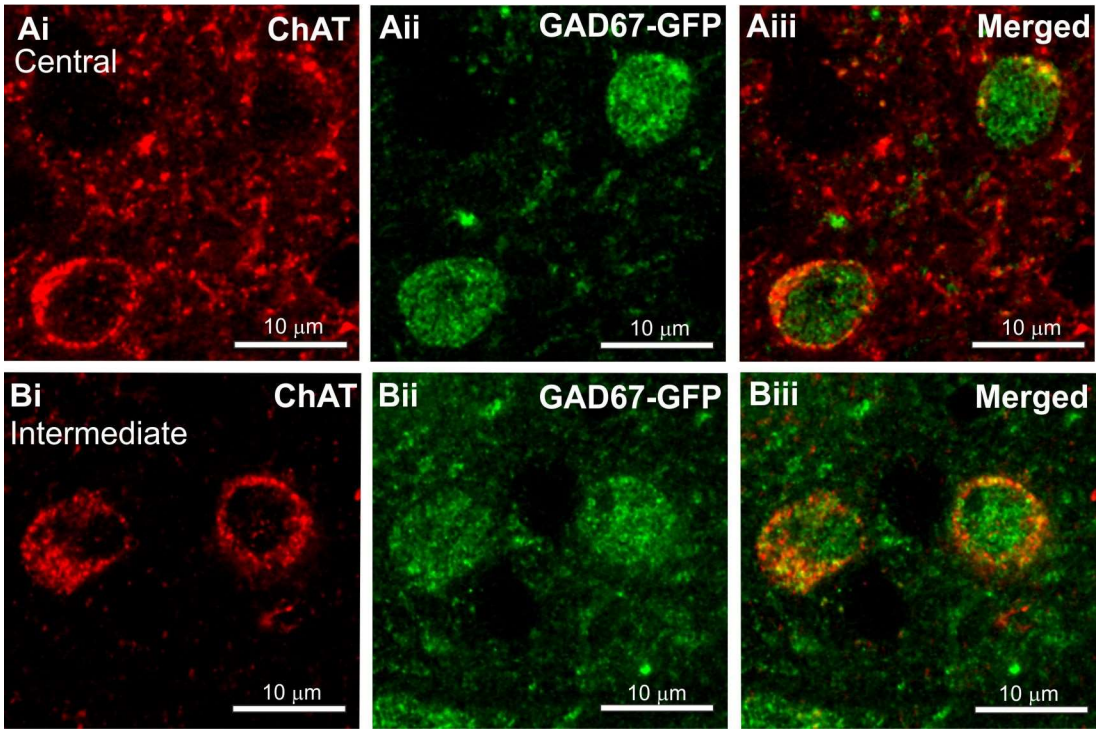

Figure 4.4: Examples of ChAT/GAD67-GFP co-localised neurones in the central and intermediate subnuclei of the NTS. Confocal images showing ChAT-IR staining is localised to the cytoplasm of the neurones in the central (Ai) and intermediate (Bi) subnuclei of the NTS whereas GAD67-GFP is present in the nucleus and the cytoplasm (Aii, Bii).

Table 4.3: The relative lightness level for ChAT staining of neurones between the dorsal vagal nucleus and the NTS (AU = Arbitrary Unit). The greater the number, the lighter (paler) the shade of colour. Note: for each region, 5 dorsal vagal neurones and 5 NTS neurones were measured using Image J software.

NTS Regions	DAB IHC	
	dorsal vagal nucleus (AU)	NTS (AU)
Caudal	92.05 ± 9.46	169.82 ± 2.92
Intermediate	95.47 ± 3.36	140.05 ± 1.47
Rostral	67.50 ± 5.43	127.44 ± 2.80

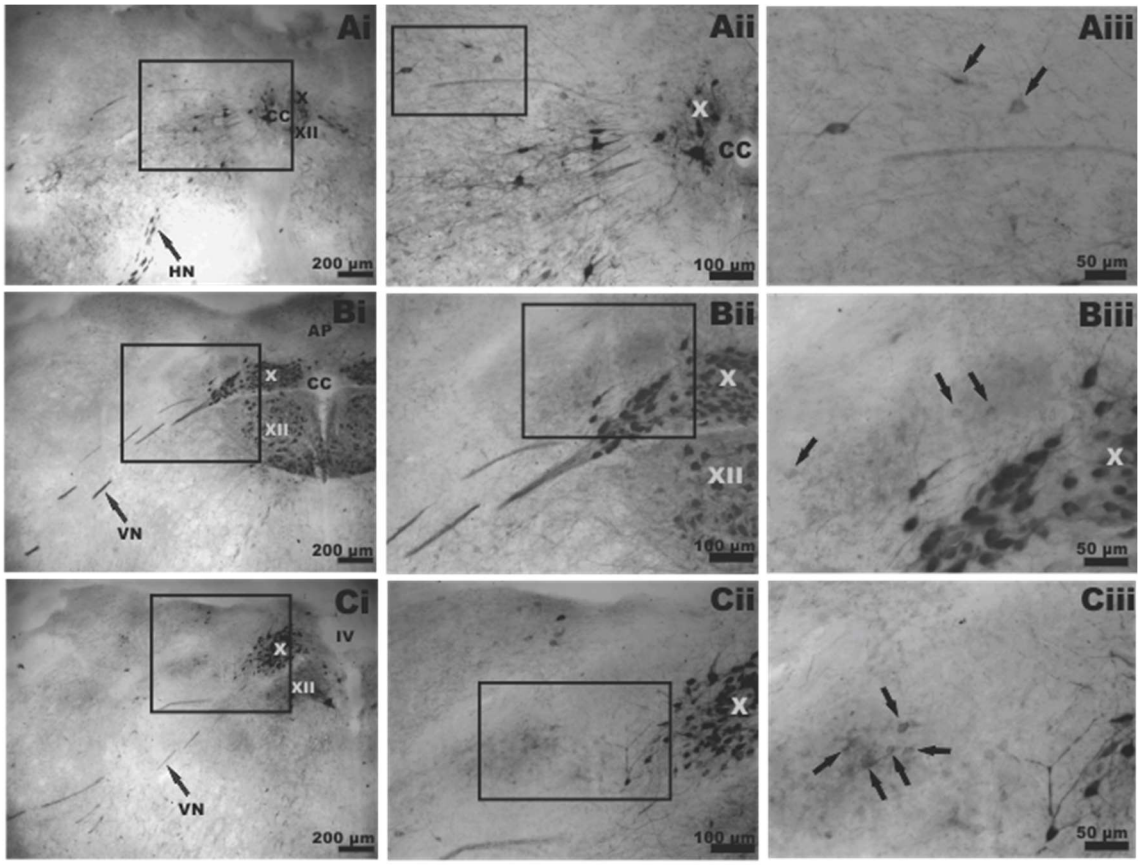

Figure 4.5: ChAT-IR neurones in the dorsal vagal nucleus, hypoglossal nucleus and the NTS in the medulla oblongata, visualised using DAB IHC. Ai, Bi and Ci indicate sections corresponding to the caudal, intermediate and rostral regions of the NTS respectively. Magnified views of the outline areas for the medial, central, and intermediate subnuclei of the NTS in Ai, Bi and Ci are shown in Aii, Bii and Cii respectively. The marked area in Aii, Bii and Cii have been further magnified as shown in Aiii, Biii and Ciii respectively. ChAT-IR neurones located in the caudal, intermediate and rostral regions of the NTS exhibit lighter intensities for the ChAT staining when compared to the dorsal vagal nucleus. AP: area postrema; CC: central canal; HN: hypoglossal nerve; IV: fourth ventricle; VN: vagus nerve; X: dorsal vagal nucleus; XII: hypoglossal nucleus.

4.4.3 ChAT/GAD67-GFP co-localised neurones in the central subnucleus of the NTS do not contain nNOS

Nitric oxide is the neurotransmitter of the majority of premotor neurones in the central subnucleus of the NTS (Wiedner et al., 1995). However, although ChAT/GAD67-GFP co-localised neurones were in close proximity to nNOS-IR neurones, they were not observed to contain nNOS immunoreactivity in the central subnucleus (see Figure 4.6-Ai to Aiii) or any other subnuclei in the NTS (see Figure 4.6-Bi to Biii).

4.4.4 Area postrema

In the area postrema, ChAT-IR and GAD67-GFP-IR neurones were observed (see Figure 4.7). The ChAT-IR or GAD67-GFP-IR neurones in the region both had oval or elliptical shaped cell bodies, the sizes of which were 9.35 ± 0.43 μm x 12.77 ± 0.96 μm (N = 5) for ChAT-IR neurones and 9.26 ± 0.24 μm x 13.49 ± 0.60 μm (N = 5) for GAD67-GFP-IR neurones. The cross sectional areas of the ChAT-IR and GAD67-GFP-IR soma were 96.09 and 101.64 μm^2.

A number of neurones in the area postrema were ChAT/GAD67-GFP co-localised (see Figure 4.7-Ai to Aiii, Bi to Biii); the size of these neurones was 10.50 ± 0.49 μm x 14.20 ± 0.97 μm) (N = 5). The cross sectional area of the ChAT/GAD67-GFP co-localised soma was 119.81 μm^2. The mean number of co-localised neurones per 50 μm section was 8.83 ± 5.12 (nsc = 6 sections, n = 3). The percentage of co-localised neurones in all ChAT-IR and/or GAD67-GFP-IR neurones in the area postrema is 4.55% (53/1164 neurones, nsc = 6, n = 3).

4.4.5 Comparison of the the relative abundance of each neurochemically-defined population between NTS and area postrema.

The number of ChAT/GAD67-GFP co-localised neurones in the NTS and area postrema (15.10 ± 7.60 for NTS and 8.83 ± 5.12 for area postrema) is not significantly different ($p = 0.57$). Similarly, the number of ChAT-IR neurones for NTS (58.30 ± 18.32) is not significantly different ($p = 0.48$) to that for the area postrema (38.67 ± 17.03). The

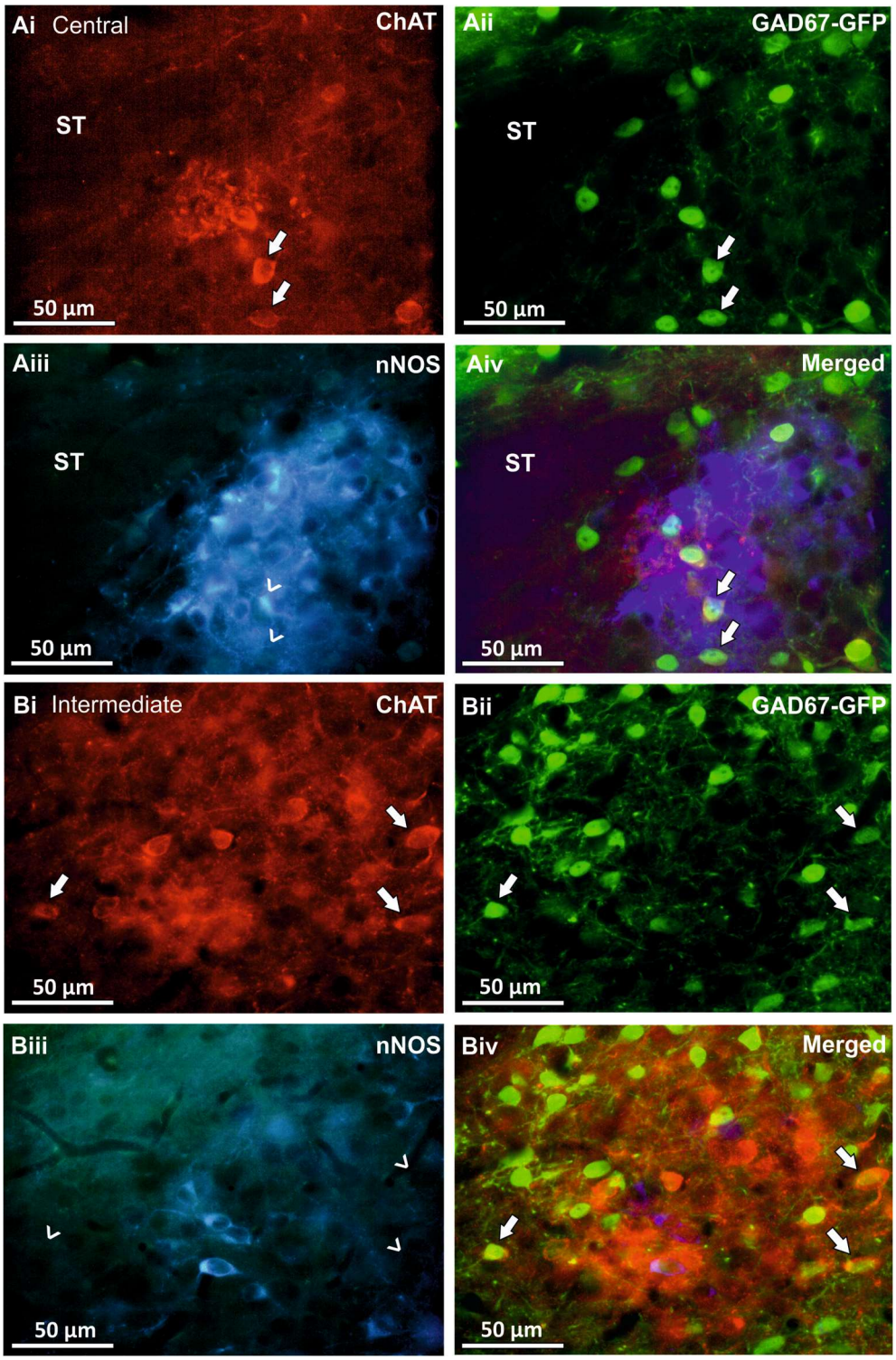

Figure 4.6: ChAT/GAD67-GFP co-localised neurones in the NTS do not contain nNOS immunoreactivity. Fluorescent images illustrating that neurones in the central (Ai-Aiv) and intermediate (Bi-Biv) subnuclei of the NTS are ChAT/GAD67-GFP co-localised (arrows), but do not contain nNOS immunoreactivity (open arrows).

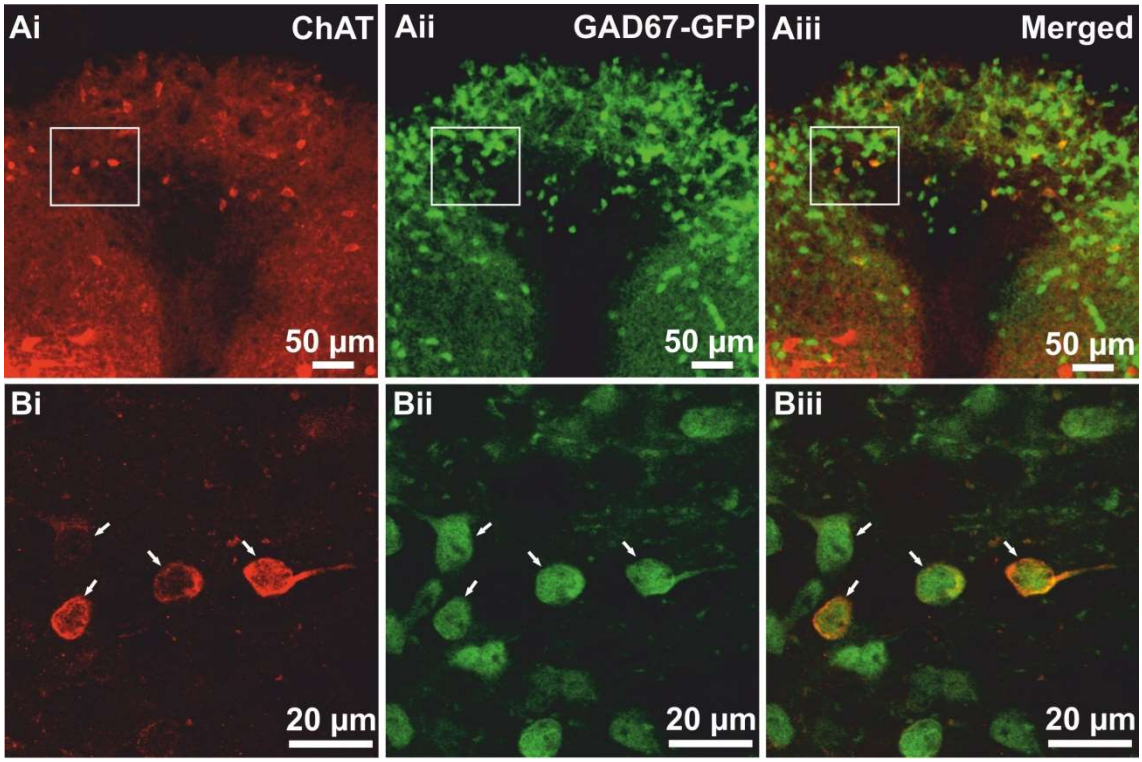

Figure 4.7: All ChAT-IR neurones in the area postrema contain GAD67-GFP. Confocal images showing ChAT-IR and GAD67-GFP-IR neurones are found in the area postrema (Ai, Aii). Magnified views of the marked area in A are shown in B illustrates neurones that are immunoreactive to both ChAT (Ai, Bi) and GAD67-GFP (Aii, Bii) (Arrows indicate co-localised neurones).

number GAD67-GFP-IR neurones between the two areas (329.40 ± 74.00 for NTS and 155.33 ± 52.10 for area postrema, p = 0.12) is also not significantly different.

4.4.6 Reticular formation and its adjacent regions

ChAT/GAD67-GFP co-localised neurones could also be found throughout the reticular formation. The size of these neurones was 12.06 ± 0.41 µm x 15.03 ± 0.73 µm (N = 4) (see Figure 4.8-Ai to Aiv). The cross sectional area of the ChAT/GAD67-GFP co-localised soma was 144.11 µm^2. The mean number of co-localised neurones per 50 µm section was 5.56 ± 1.29 and 5 ± 1.10 for the right and left side of the section respectively (nsc = 18 sections, n = 3), which was approximately 2% (190/>8903) of

the total ChAT-IR and/or GAD67-GFP-IR neurones. ChAT/GAD67-GFP co-localised neurones were also observed in the lateral paragigantocellular nucleus (see Figure 4.8-Bi, Bii and Biv). These were 11.09 ± 0.94 µm x 20.03 ± 1.42 µm in size (N = 5) (see Figure 4.8-Bi to Biv). The cross sectional area of these ChAT/GAD67-GFP co-localised soma was 190.18 µm^2. In the intermediate reticular formation and the lateral paragigantocellular nucleus occasional ChAT/GAD67-GFP co-localised neurones were also observed to be nNOS-IR (see Figure 4.8-A, B).

4.4.7 The dorsal vagal nucleus

In the dorsal vagal nucleus, a large number of neurones are ChAT-IR (see Figure 4.9-Ai). These neurones were large in size (16.45 ± 1.07 µm x 23.87 ± 0.98 µm, N = 10) and possessed an oval or elliptical shaped cell body, typical of vagal preganglionic neurones. The cross sectional area of the ChAT-IR soma was 319.25 µm^2. The dorsal vagal nucleus also contained occasional GAD67-GFP-IR neurones (see Figure 4.9-Aii), which similarly exhibited oval or elliptical shaped cell bodies, but were smaller in size (10.08 ± 0.58 µm x 13.86 ± 0.94 µm, N = 10). The cross sectional area of the GAD67-GFP-IR soma was 112.55 µm^2. No ChAT/GAD67-GFP co-localised neurones were observed in the dorsal vagal nucleus.

4.4.8 The hypoglossal nucleus

Many neurones in the hypoglossal nucleus were intensely ChAT-IR. These neurones were large in size (18.94 ± 0.94 µm x 25.42 ± 0.83 µm, N = 10) (see Figure 4.9-Bi). The cross sectional area of the ChAT-IR soma was 386.43 µm^2. The hypoglossal nucleus also contained a limited number of GAD67-GFP-IR neurones (see Figure 4.9-Bii). Co-localisation for ChAT and GAD67-GFP was not observed in the hypoglossal nucleus.

4.4.9 Nucleus ambiguus

The nucleus ambiguus contained intensely ChAT-IR neurones whose sizes, at 17.94 ± 0.98 µm x 20.40 ± 1.25 µm (N = 5), were relatively large. The cross sectional area of the ChAT-IR soma was 288.66 µm^2. Smaller GAD67-GFP-IR neurones (9.66 ± 0.64 µm x 13.06 ± 0.89 µm, N = 5) were also found in this area. The cross sectional area of

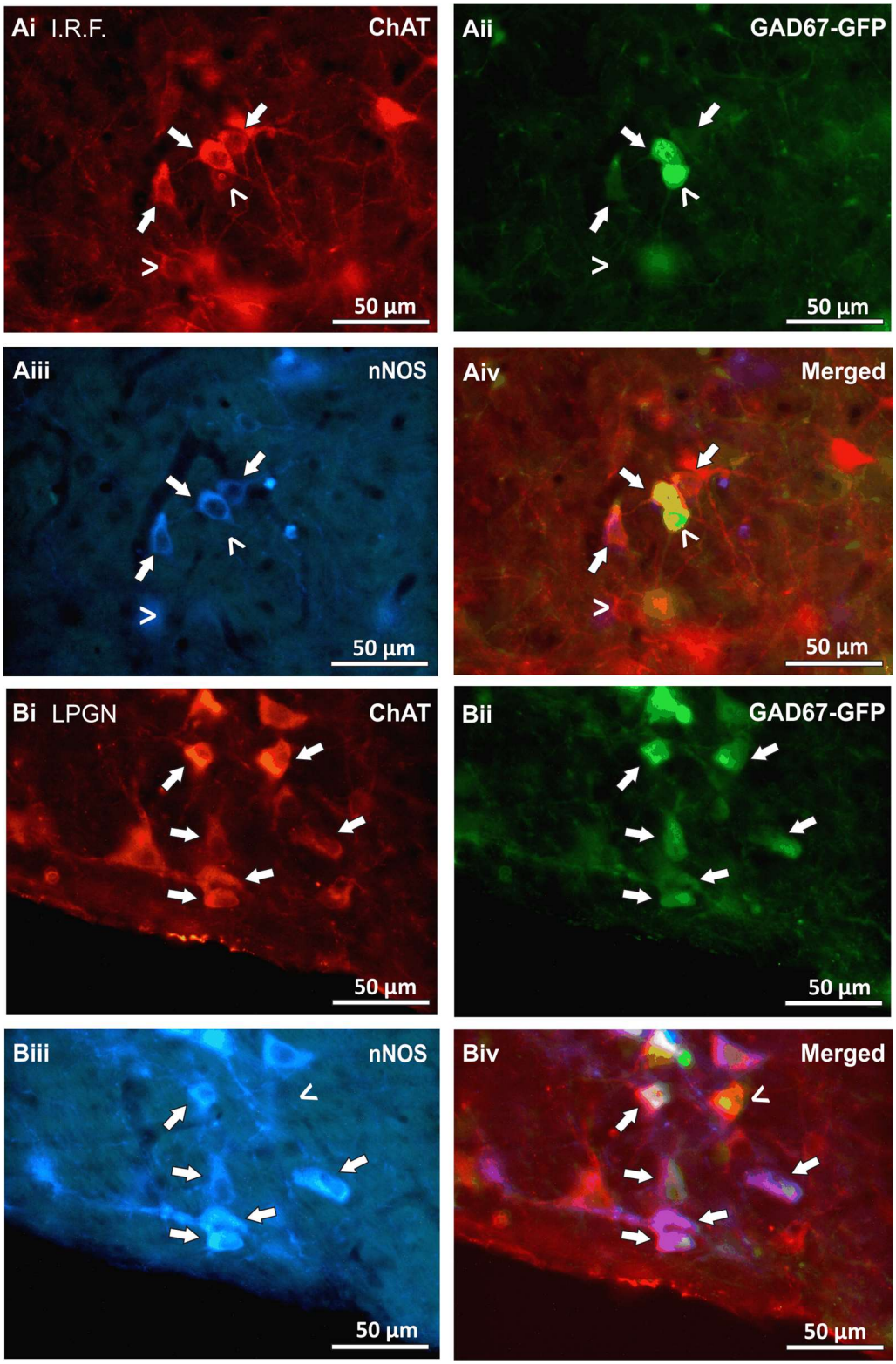

Figure 4.8: ChAT/GAD67-GFP co-localised neurones are observed in the intermediate reticular formation and the lateral paragigantocellular nucleus, some of which contain nNOS immunoreactivity.

Figure 4.8 (continued):

Fluorescent images showing that neurones in intermediate reticular formation (IRF) (A) and the lateral paragigantocellular nucleus (LPGN) (B) are immunoreactive to both ChAT (Ai, Bi) and GAD67-GFP (Aii, Bii) (arrows). Some of these co-localised neurones are also nNOS-IR (Aiii, Biii). Open arrows in A show neurones that are not double and/or triple labelled. Open arrows in B show a neurone that is not triple labelled.

the GAD67-GFP-IR soma was 101.37 μm^2. Co-localisation of ChAT and GAD67-GFP was not observed (see Figure 4.9-Ci to Ciii).

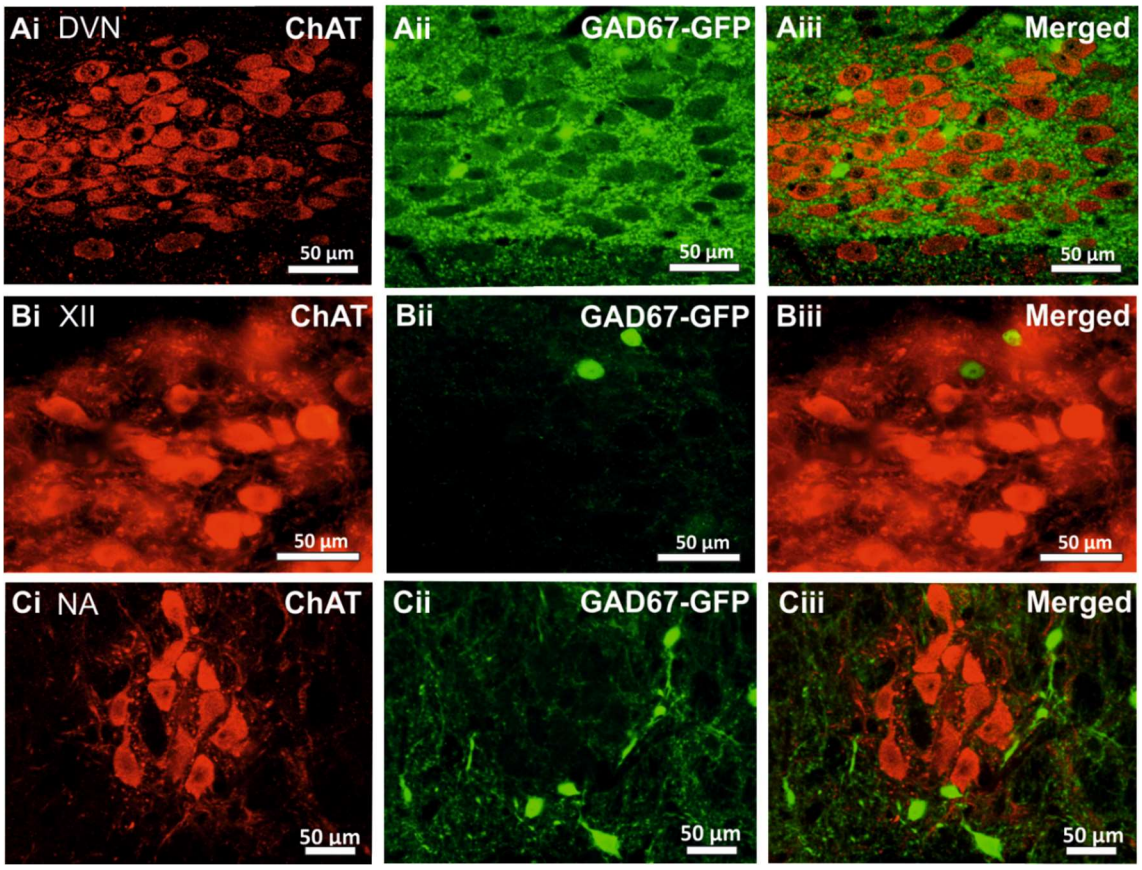

Figure 4.9: No ChAT/GAD67-GFP co-localised neurones in the dorsal vagal nucleus, the hypoglossal nucleus or the nucleus ambiguus. Confocal (A and C) and fluorescent images (B) showing ChAT-IR and GAD67-GFP-IR neurones are present in the dorsal vagal nucleus (Ai, Aii), hypoglossal nucleus (Bi, Bii) and the nucleus ambiguus (Ci, Cii) and yet do not co-localise in these areas (Aiii, Biii, Ciii).

4.5 Discussion

This study describes subpopulations of neurones containing enzymes responsible for the production of both ACh and GABA in areas of the medulla oblongata involved in autonomic control. ChAT/GAD67-GFP co-localised neurones were observed in the NTS, area postrema and the reticular formation of the mouse brainstem. Whilst neurones containing both ChAT and GAD (or GABA) immunoreactivity have previously been observed in neurones in the rat retina, cerebral cortex, basal forebrain and spinal cord (Kosaka et al., 1988), hypoglossal nucleus (Davidoff and Schulze, 1988), turtle retina (Nguyen and Grzywacz, 2000), and the tegmental nuclei of the cat (Jia et al., 2003), these are the first such populations described throughout the medulla oblongata.

4.5.1 ChAT-IR and GAD67-GFP-IR neurones in the NTS

A very small number of ChAT/GAD67-GFP co-localised neurones was located throughout the NTS (with the exception of the lateral and interstitial subnuclei). The largest populations of co-localised neurones were observed in the intermediate and central subnuclei of the NTS. Their small size may correlate to the small cells with local axonal arborisation and no axonal projections (Okada et al., 2006, Kawai and Senba, 1999) which include GABAergic neurones (Kawai and Senba, 1999) suggesting a potential role in integrating input information in local circuits of the NTS.

Tracing studies have shown that the intermediate subnucleus of the NTS receives afferent input from the tongue (Hayakawa et al., 2001), soft palate, pharynx and larynx (Altschuler et al., 1989, Broussard and Altschuler, 2000) and contains pharyngeal premotor neurones. The central subnucleus of the NTS receives the majority of the sensory afferent inputs from the oesophagus (Altschuler et al., 1989) and contains oesophageal premotor neurones that project to the nucleus ambiguus. The small populations of ChAT/GAD67-GFP co-localised neurones in the intermediate and central subnuclei of the NTS may therefore play a role in the integration of several visceral sensory inputs that contribute to the reflex control of swallowing, gagging and phonation.

The vast majority of premotor neurones in the central subnucleus of the NTS that project to the nucleus ambiguus use nitric oxide as a neurotransmitter (Wiedner et al.,

1995). The fact that the ChAT/GAD67-GFP co-localised neurones in the central subnucleus of the NTS do not contain nNOS immunoreactivity may suggest these neurones are the small proportion of local interneurones that do not contain NOS. Indeed, it has been suggested that GABA interneurones in the intermediate and central subnuclei of the NTS inhibit the premotor neurones involved in the pharyngeal and oesophageal stages of swallowing (Wang and Bieger, 1991, Dong et al., 2000).

It therefore seems likely that in the NTS ChAT/GAD67-GFPco-localised neurones are involved in circuitry mediating autonomic reflexes. Future studies may therefore investigate whether these co-localised neurones receive direct innervation from afferents or are otherwise involved in reflex arcs through their outputs.

4.5.2 ChAT-IR and GAD67-GFP-IR neurones in the area postrema

ChAT/GAD67-GFP co-localised neurones were observed in the area postrema and they contributed to a small percentage (4.55%, 53/1164) of all the ChAT-IR and/or GAD67-GFP-IR neurones in this area. The area postrema is a circumventricular organ located outside the blood brain barrier and a vital player in the control of autonomic functions. It receives blood borne information from the vasculature in addition to input from the vagus nerve, carotid sinus and other brain areas and projects to autonomic centres including the NTS, nucleus ambiguus, dorsal vagal nucleus and RVLM (Price et al., 2008). Previously GABA-IR (Walberg and Ottersen, 1992) and ChAT-IR (Tago et al., 1989) neurones have been observed in the rat area postrema but this is the first study to show a population of neurones which contain enzymes responsible for both ACh and GABA synthesis. The area postrema offers an attractive area in which to study the brainstem ChAT/GAD67-GFP neurones since all ChAT-IR neurones also contained GAD67-GFP. Transgenic mice in which ChAT neurones are labelled (Kolisnyk et al., 2013, Krasteva et al., 2012) would therefore enable specific targeting of these cells.

4.5.3 ChAT-IR and GAD67-GFP-IR neurones in the reticular formation

The reticular formation contains neurones involved in a wide range of autonomic and regulatory processes including ingestive responses and a role in organising rhythmic oromotor behaviours (St John, 1986, Inoue et al., 1994, Travers et al., 1997). We

observed 2% of neurones in this area were ChAT/GAD67-GFP co-localised, a subpopulation of which also contained nNOS immunoreactivity. Previously, Travers et al. (Travers et al., 2005) have shown that 6.7% of pre-oromotor neurones in the intermediate reticular formation contained both ChAT and NOS immunoreactivity and suggested that they may represent a subset of GABAergic neurones. This study has shown that there is indeed such a population of triple labelled neurones in the reticular formation, although their function remains to be determined.

4.5.4 Unravelling functions of ChAT/GAD67-GFP co-localised neurones.

A significant hurdle to unravelling the functions of the dual labelled neurones identified here are their small numbers and limited intensity of immunolabelling. However, current transgenic technologies may render these neurones amenable to further investigation, for example, the GAD67-GFP knock-in mice used in this study could feasibly be crossed with another line of mice bred to express a complementary reporter such as mCherry under control of the ChAT promoter (Nagode et al., 2011, Nelson et al., 2014). It is possible that transgenic technologies may also enable selective expression of optogenetic proteins within these cells thus permitting selective activation/inhibition (Nagode et al., 2011) in future functional investigations. Indeed, recent technology has introduced transgenic mice for intersectional targeting of specific neurone populations for expression of neural sensors and effectors (Madisen et al., 2015), an approach that would be ideal for revealing the functions of dual expressing neurones such as these ChAT/GAD67-GFP co-localised neurones. Such approaches to reveal functions of these and other cell classes may therefore provide improved understanding of autonomic microcircuitry in the medulla oblongata.

4.6 Conclusion

Small populations of neurones in the NTS, area postrema, reticular formation and lateral paragigantocellular nucleus in the mouse medulla oblongata contain the synthesizing enzymes for both ACh and GABA. In all areas in the brainstem the function of these neurones is currently unknown.

5 General Discussion

5.1 ChAT/GAD67-GFP co-localised neurones are observed in the spinal cord and medulla oblongata

In this study we have demonstrated that a population of neurones located in the ventral portion of the lamina X coexpress the enzymes ChAT and GAD67 suggesting they could potentially corelease acetylcholine and GABA. These clusters of ChAT/GAD67-GFP co-localised neurones were observed in cervical, thoracic and lumbar regions of the spinal cord implying they possess a more versatile role in the circuitry of the spinal cord than previously hypothesised. We also investigated the coexpression of ChAT and GAD67 enzymes in the medulla oblongata nuclei associated with autonomic function, particularly the NTS, for which co-localisation was observed predominantly in the intermediate and central subnucleus of the NTS.

ACh (Perry et al., 1999) and GABA (Krnjevic and Schwartz, 1967, Iversen and Kelly, 1975, Clark et al., 1992, Liu et al., 1993, Gadea and Lopez-Colome, 2001) are major neurotransmitters within the CNS. In our study, ChAT-IR or GAD67-GFP-IR neurones were observed throughout the spinal cord and medulla oblongata.

Observations on the co-existence of ACh and GABA within the same neurones in the spinal cord and medulla oblongata are limited. Neurones containing both ChAT and GAD (or GABA) have only been reported in the cervical cord regions (Kosaka et al., 1988)(see section 1.6.4) and in the dorsal horn (Kosaka et al., 1988, Todd, 1991, Mesnage et al., 2011) of the spinal cord. In the medulla oblongata, neurones expressing both ChAT and GABA have only been found in the hypoglossal nucleus (Davidoff and Schulze, 1988). However, neurones of the hypoglossal nucleus are typically large motoneurones (Ladewig et al., 2003), and it is well established that motoneurones throughout the CNS are cholinergic (Barber et al., 1984, Connaughton et al., 1986, Johann et al., 2011, Zhou et al., 2014). Although the apparent presence of smaller GABAergic interneurones within the hypoglossal nucleus has been reported (Takasu et al., 1987, Takasu and Hashimoto, 1988). Given the absence of additional supporting evidence for the co-localisation of ChAT and GABA in hypoglossal motoneurones it is reasonable to suppose that the coexpression observed by Davidoff and Schulze could be an artefact of inappropriate GABA staining.

Given the overall lack of reports on the co-existence of these two major neurotransmitters in neurones within the spinal cord and medulla oblongata, establishing the presence, morphology and location of such neurones within these regions is essential prior to undertaking further investigations into their roles.

With respect to the spinal cord, Kosaka (Kosaka et al 1988) discerned the presence of ChAT and GAD (or GABA) co-localised neurones in the central canal cluster cells and partition cells of the rat cervical spinal cord (Kosaka et al., 1988). Our study reports on the observation of neurones containing enzymes which synthesise both ACh and GABA in the cervical, thoracic and lumbar spinal cord regions of GAD67-GFP knock-in mice, utilising IHC for ChAT and GAD67-GFP. The majority of ChAT/GAD67-GFP co-localised neurones were found in lamina X of the cervical, thoracic and lumbar cord regions. A smaller number of such co-localised neurones was additionally observed in the dorsal horn, which was also consistent with the reports of Kosaka et al. (Kosaka et al., 1988), Todd (Todd, 1991) and Mesnage et al. (Mesnage et al., 2011).

In our study the presence of ChAT/GAD67-GFP co-localised neurones was discerned throughout the rostrocaudal axis, extending from the cervical to the lumbar spinal cords. Such co-localised neurones in the spinal cord may be involved in integrating different systems, or providing antagonistic feedback within a single system. Given the fact that co-localised neurones were found to be present in the cervical, thoracic and lumbar cord segments, the hypothesis regarding the potential for integration of sympathetic and motor systems within the thoracic cord (Chizh et al., 1998) still remains a worthy line of investigation. Based on our observations, plus the limited information on the co-existence of ACh and GABA within the medulla (as previously mentioned), the distribution of ChAT/GAD67-GFP co-localised neurones was further investigated to determine whether it extended to reach the medulla oblongata; with a particular focus on the NTS due to its significance as a primary integration location for the autonomic nervous system (Loewy, 1990b). ChAT/GAD67-GFP co-localised neurones were observed in the NTS, the majority of which were in the intermediate and central subnucleus. Although the function of these neurones currently remains unknown, it seems probable that they may be involved in circuitry which mediates autonomic reflexes; as GABA interneurons in the intermediate and central subnuclei of the NTS have been previously suggested to inhibit premotor neurones involved in the pharyngeal and oesophageal stages of swallowing (Wang and Bieger, 1991, Dong et al., 2000).

For the cervical and lumbar cord levels, the presence of co-localised neurones may represent a pathway for coordinating other systems with motor output. Further studies to deduce these parallel functions are required. The role of these co-localised neurones in the integration of neuronal activity with motor output may in principle be the same across the regions, with level specificity pertaining to the system that is being integrated. If this is the case the role of these co-localised neurones for sympatho-motor coordination within the thoracic region continues to be a viable hypothesis.

ChAT/GAD67-GFP co-localised neurones were found in the area postrema. Indeed, all ChAT-IR neurones in the area postrema were co-localised with GAD67-GFP. ChAT/GAD67-GFP co-localised neurones were also found in the reticular formation. No co-localised neurones were observed in the hypoglossal nucleus.

5.2 ChAT/GAD67-GFP co-localised neurones contribute to the neuronal cell type heterogeneity in lamina X

The location of the majority of ChAT/GAD67-GFP co-localised neurones within lamina X was studied in order to aid us in establishing a specific area in which to perform subsequent juxtacellular labelling analyses. Our results showed that most of the ChAT/GAD67-GFP co-localised neurones in the thoracic spinal cord were located ventral and ventrolateral to the central canal.

The reason behind selection of the thoracic spinal cord for our investigation into the location of ChAT/GAD67-GFP co-localised neurones was that SPNs in the IML of mice are only present in T1-L2 spinal cord levels (Anderson et al., 2009, Sengul and Watson, 2012, Sengul et al., 2012). The thoracic cord was therefore the most suitable region of study, because in order to establish all the possible projections of ChAT/GAD67-GFP co-localised neurones, the SPNs needed to be present in all the studied spinal cord slices. A further aim of the study was to provide for increased understanding regarding potential connections associated with autonomic circuits within the spinal cord.

The lamina X of the spinal cord exhibits heterogeneity in relation to neuronal cell types. These include cholinergic central canal cluster cells (Barber et al., 1984), cholinergic

SPNs (in the CAA) (Barber et al., 1984), cholinergic medial partition neurones (Miles et al., 2007), GABAergic interneurones in the CAA (Deuchars et al., 2005), neurones co-expressing both ChAT and GAD (or GABA) in the cervical spinal cord (Kosaka et al., 1988), and V2 interneurones (Al-Mosawie et al., 2007); where V2 interneurones consist of several subpopulations, some of which are propriospinal cells which are active during locomotion.

There is also variation in relation to projections. For example the cholinergic central canal cluster cells within lamina X contribute short range intersegmental propriospinal projections to various laminae (Sherriff and Henderson, 1994) and may have a neuromodulatory function. Other neuronal cell types in lamina X and adjacent regions can give rise to long ascending projections targeting various brainstem regions particularly into the paramedian medullar and/or pontine reticular formation (Nahin et al., 1983), plus also to the cerebellum (Sengul et al., 2015). While the majority of the neuronal cell types are located either lateral and/or dorsal to the central canal (and/or in lamina VII) (see Figure 5.1), our ChAT/GAD67-GFP co-localised neurones which potentially use both ACh and GABA as their neurotransmitters are predominantly situated ventral and ventrolateral to the central canal, so making lamina X even more heterogeneous in relation to cell types.

Although Kosaka et al. (Kosaka et al., 1988) reported over a decade ago on the presence of ChAT and GAD (or GABA) co-expressing neurones amongst the central canal cluster cells and partition cells of the cervical spinal cord, these were respectively located lateral to the central canal in lamina X and in the intermediate grey (lamina VII). The ChAT/GAD67-GFP co-localised neurones in our study represent a novel observation since they are located ventral and ventrolateral to the central canal of the thoracic spinal cord. By virtue of the difference in location, the ChAT/GAD67-GFP co-localised neurones from our study may constitute a different subgroup of neurones from those of Kosaka et al.; although another possible explanation that can not be discounted at this time is that the rostrocaudal distribution of such co-localised neurones within lamina X varies based on spinal cord level, and so our findings could correspond to the same population as reported by Kosaka et al., but with a shift in position relative to the central canal relating to the change of study area from cervical to thoracic spinal cord segments.

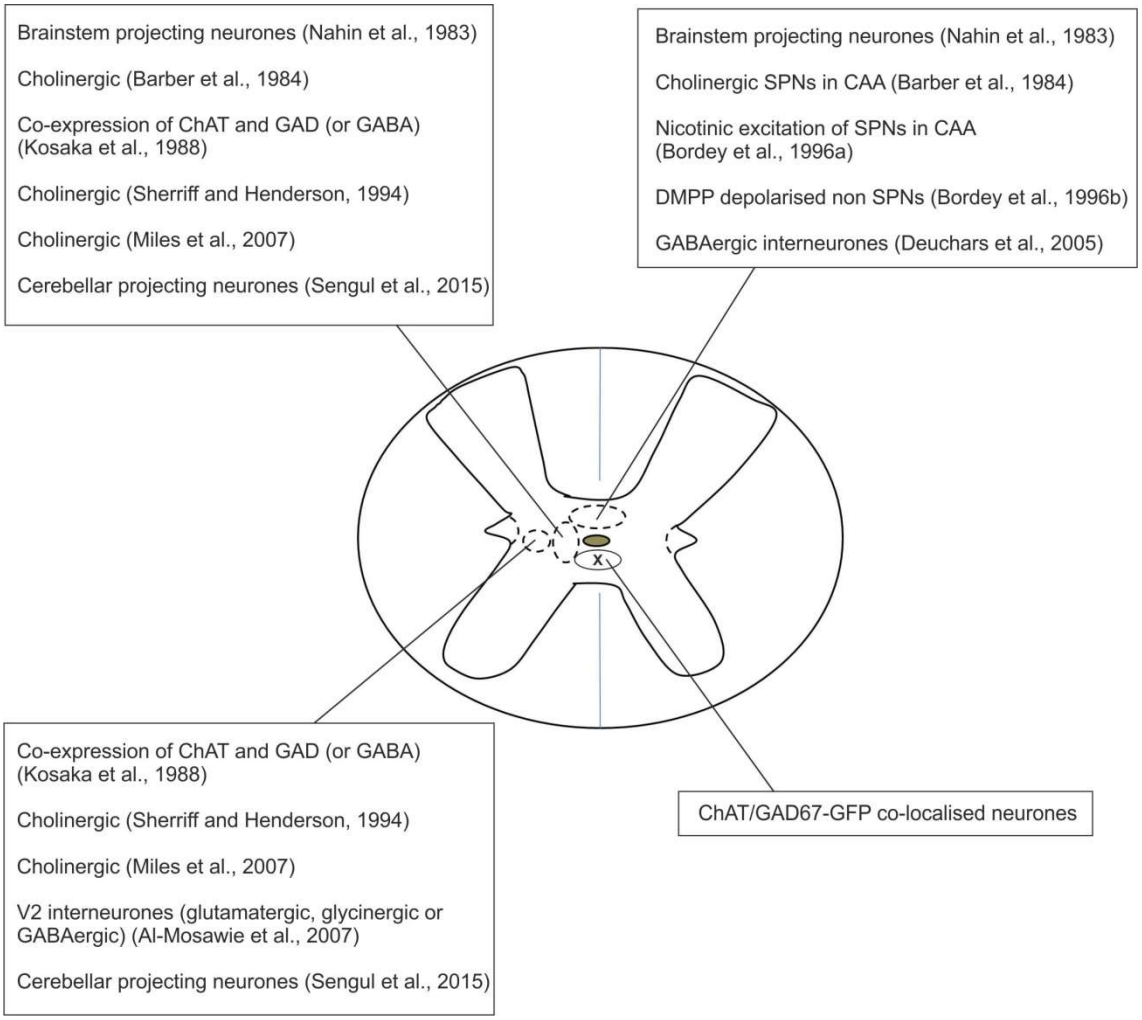

Figure 5.1: Cell types and cholinergic receptor mediated effects reported in lamina X and adjacent regions. The majority of ChAT/GAD67-GFP co-localised neurones observed in our study are located ventral and ventrolateral to the central canal (marked by X).

5.3 Functional significance of ACh and GABA transmission

ChAT/GAD67-GFP co-localised neurones found in both the spinal cord and the medulla oblongata might have similar roles. A clear function of the co-transmission between ACh and GABA is demonstrated by starburst amacrine cells in the retina mediating fast transmission in two different circuits (Lee et al., 2010), those of motion and direction. In relation to our study, although the function of ACh-GABA co-transmission of ChAT/GAD67-GFP co-localised neurones located in the spinal cord

and medulla oblongata is currently unknown, it is likely that the co-transmission from these neurones may provide for fast synaptic transmission to the circuits in which they play a role. In the medulla oblongata ChAT/GAD67-GFP co-localised neurones are observed in areas involved in autonomic control, including the NTS, area postrema and reticular formation. As a result it is possible that these co-localised neurones may be involved in autonomic-efferent modulation. With regard to the spinal cord, the locations of interneurones controlling sympathetic activity in laminae V, VII and X, and in the intermediolateral cell column region, have been reported. In addition to supraspinal innervation, sympathetic interneurones also receive innervation from afferent pathways, which have a crucial contribution to the maintenance of sympathetic outflow (Deuchars, 2007, Deuchars and Lall, 2015). Since the majority of ChAT/GAD67-GFP co-localised neurones in this study were found in lamina X, it is possible that a role of these ChAT/GAD67-GFP co-localised neurones are as interneurones involved in sympathetic activity. The observations from this study also suggested synaptic inputs onto ChAT/GAD67-GFP co-localised neurones from other pathways, including primary afferents (Todd et al., 2003, Alvarez et al., 2004) and/or the corticospinal tract (Du Beau et al., 2012) through VGLUT1 inputs, interneurones (Todd et al., 2003, Alvarez et al., 2004) and descending projections (Du Beau et al., 2012) through VGLUT2 terminals, and inhibitory inputs via both GlyT2 and GAD67 terminals. ChAT/GAD67-GFP co-localised neurones may therefore be a subgroup of sympathetic interneurones that utilises both ACh and GABA to play a role in sympatho-motor integration.

The function of neurones in the spinal cord that contain both ACh and GABA has been well demonstrated for the dorsal horn. A primary driver behind a study by Mesnage et al. (Mesnage et al., 2011) into cholinergic neurones of the dorsal horn was the major role played by endogenous Ach in sensory modulation. The study used ChAT: EGFP transgenic mice, which express enhanced GFP (EGFP) in cholinergic neurones, in combination with IHC and electrophysiology. According to their results, the dorsal horn contained ChAT interneurones in very low abundance. Most of those observed (95.5% ± 1.0%) were immunoreactive for GABA. Based on observations of processes running in the dorsal direction, plus dendrites and axon that extended through more than one spinal cord segment in a rostrocaudal direction, as determined via intrinsic fluorescence and intracellular labelling, these cholinergic interneurones were indicated as being the predominant group of neurones constituting the cholinergic plexus in lamina IIi. Through utilisation of electrophysiological techniques to record from ChAT:EGFP neurones in spinal slices from young adult mice (21 to 30 days postnatal), and application of depolarizing current pulses of increasing intensity, 10 neurones (out

of 15 tested) exhibited a repetitive firing pattern, 7 of which additionally exhibited rebound spikes following hyperpolarization. Based on their results Mesnage et al. suggested that while the numbers of these cholinergic dorsal horn interneurones were very low, their morphology and properties may allow them to collect segmental information in the dorsal horn and to be involved in modulating this information over different cord segments. The similarities of these ChAT neurones in lamina III and those we describe in lamina X are that they are rare and contain GABA (or GAD67). Although the cholinergic neurones we observe may not be a subpopulation of the cholinergic central cluster cells as described by Barber et al. (1984), based on the limited evidence we have our ChAT/GAD67-GFP co-localised neurones might project locally to other neurone populations within lamina X. However, this would not confine their actions to lamina X as they may influence the function of externally projecting neurones such as SPN in the CAA.

5.4 Technical consideration and limitations

5.4.1 Sensitivity and specificity of the immunohistochemical method and animals used in the study

Immunolabelling for GABA is difficult to achieve for various reasons (Zhao et al., 2013), including that it does not appear to fix readily and as such fixatives containing glutaraldehyde at elevated concentrations of 0.5 – 2.5 % have been recommended in order to preserve GABA by quickly binding it to the tissue (Zhao et al., 2013) . In addition, since it is a small molecule containing a single amino acid (Iversen and Kelly, 1975, Bowery and Smart, 2006), it has low antigenicity. Moreover, the use of Triton X-100 is not recommended as it reduces the intensity of staining (Zhao et al., 2013). Despite the remedial processes adopted to improve GABA immunolabelling, the level of labelled cell bodies remains low and so not sufficient for precise determinations (Zhao et al., 2013).

In the past, the detection of GABAergic neurones proved to be challenging. In the research field, antibodies raised against GABA (Hodgson et al., 1985, Kosaka et al., 1988, Davidoff and Schulze, 1988, Caffe et al., 1996) or against the GAD enzyme (McLaughlin et al., 1975, Ribak et al., 1976, Ruggiero et al., 1985, Kosaka et al., 1988, Gritti et al., 1993, Caffe et al., 1996) have been widely used; although to detect GABA in the soma of neurones it is typically necessary to inject animals with colchicine

(Kosaka et al., 1988, Barber et al., 1982). Since the antibodies available in our lab which have been raised against GAD and GABA (without injecting colchicine) can only detect GABAergic terminals but not the somata under normal IHC condition, this study has used GAD67-GFP knock-in mice (Tamamaki et al., 2003). This type of mouse has been extensively used in studies by other researchers (Edwards et al., 2014, Gotts et al., 2015), the reasons for which are detailed in section 2.1.1 and 2.1.2. Furthermore, due to differences in expression during development, while around 50% of GAD65-GFP cells in the GAD65-GFP mouse line indicate the presence of GABA during the embryonic period, the level rises to approximately 70% at 21 days postnatal. Hence the GAD65-GFP mouse line appears to have limitations in regards to its viability for studies into GABAergic neurones during mouse development. Since our strudy required the use of neonate mice, the GAD67-GFP knock-in mouse line is therefore more suited for our work than the GAD65-GFP mouse line (Lopez-Bendito et al., 2004).

To label ChAT-IR neurones, an antibody raised against the ChAT enzyme is widely used (Jia et al., 2003, Barber et al., 1984, Stornetta et al., 2013, Gotts et al., 2015) and accepted as being the most reliable marker for cholinergic neurones (Bradford, 1986). Since the ChAT enzyme is synthesized and present in cell bodies (Bradford, 1986), there was therefore no difficulty in the present study to label the cell bodies (or occasionally even the terminals) of ChAT-IR neurones using the antibody raised against ChAT. The specificity of the ChAT antibody used in this study was determined by experimental testing in the spinal cord, from which it was found to label known cholinergic regions of the spinal cord, such as ventral horn motoneurons, SPN of the IML, central canal cluster cells and lamina III dorsal horn neurones (Barber et al., 1984, Todd, 1991). Moreover, other regions not previously reported as containing cholinergic neurones were similarly discerned to be negative for ChAT-immunoreactivity in our tests. The ChAT antibody used was the same as that used by Chapman et al. (2013).

5.4.2 Juxtacellular labelling vs other methods

For observation of the possible projections from ChAT/GAD67-GFP co-localised neurones, juxtacellular labelling in combination with IHC seemed to be a more suitable method than other approaches such as tracing techniques. While the application of tracing agents in combination with IHC presents problems that would be difficult to overcome, given the relatively small numbers and pale intensity of immunolabelled ChAT/GAD67-GFP co-localised neurones, juxtacellular labelling, on the other hand,

allows a single neurone to be individually labelled, so making it a more suitable technique when the neurones of interest are only found in low numbers and possess pale immunostaining.

Each technique carries its own advantages and disadvantages with appropriate selection determined by the objectives of an experiment. Whilst intracellular recording may give fills with better labelling of axons and dendrites (Pilowsky and Makeham, 2001) it is a very difficult procedure to carry out on small neurones. Conversely, the whole-cell patch-clamp technique enables recording of small cells but the dialysis of intracellular components affects the capacity to gain stable, long term recordings of some currents (Horn and Marty, 1988) and may affect the immunohistochemical staining of cytosolic components (Puche et al., 2004). Despite not experiencing the high success rate previously reported for juxtacellular labelling (Pinault, 1996)(see section 3.5.3.3 and 3.5.5), the ability to individually label cells (per juxtacellular labelling) without the trauma of going “whole-cell” combined with increased ease of electrode withdrawal undoubtedly contributes to preservation of cellular integrity and thus aids recovery. A compromise between these two approaches may be the combination of a “perforated” patch approach coupled with a cell permeant dye as demonstrated by Puche et al.(Puche et al., 2004). Here they combined the use of a perforated patch approach for “intracellular-like” recordings without compromising second messenger systems with a cell permeant dye for single neurone labelling. Upon entering the cell, the dye (Cell Tracker Green CMFDA) is converted by endogenous esterases and glutathione-S-transferase into an impermeant, fluorescent state. The use of this dye would also be well suited to juxtacellular labelling. Moreover, cells labelled with the permeant dye can be further processed via IHC for investigations utilising electron microscopy (MolecularProbes, 2001).

While juxtacellular labelling is a suitable tool for studying morphology and projection, the full labelling of axon is dependent on the quality of entrainment and labelling time (Duque and Zaborszky, 2006). In addition, although labelled neurones from juxtacellular labelling may be studied using electron microscopy (Duque and Zaborszky, 2006) good preservation of the ultrastructural morphology of labelled cells can be a challenge to achieve, due to the longer times required for the labelling process prior to the application of the fixative agent which preserves the tissue of the spinal cord slices (Notter et al., 2014) before the subsequent electron microscopic analysis.

5.4.3 Animals: juveniles and adults

The reason for investigating the presence of ChAT/GAD67-GFP co-localised neurones within lamina X of the spinal cord in young GAD67-GFP knock-in mice after having undertaken the study in adult animals, was that in order to apply the juxtacellular labelling technique spinal cord slices from young animals were required. Once the presence of ChAT/GAD67-GFP co-localised neurones in the lamina X of young mice was confirmed, juxtacellular labelling could be subsequently performed.

In relation to the preparation of spinal cord slices for electrophysiological studies, healthier tissue slices tend to be obtained from young animals; one reason for this is that tissue from young animals is more resistant to anoxia than that from adult animals (Gibb and Edwards, 1994, Mitra and Brownstone, 2012). As a result, young animals tend to be used for juxtacellular labelling. Gibb and Edwards (Gibb and Edwards, 1994) indicated that animals aged less than 3 weeks were the most suitable for these types of studies, generally though, for both mice and rats, spinal cord slices have been most commonly prepared from animals that are between the first and second week postnatal (Thurbon et al., 1998, Carlin et al., 2000, Deuchars et al., 2005). Visualisation of neuronal cell bodies during the juxtacellular labelling process is additionally aided by the fact that in young animals myelination is not complete (Gibb and Edwards, 1994, Mitra and Brownstone, 2012).

In order to understand the development of the spinal circuitry, studies involving the use of spinal cord slices from adult animals (Graham et al., 2003, Yasaka et al., 2007, Yasaka et al., 2010, Hughes et al., 2012, Hadzipasic et al., 2014) have the advantage that postnatal maturation should be complete but the preparation of adult spinal cord slices yielding viable neurones are more difficult to achieve (Mitra and Brownstone, 2012). Time is crucial for each step of the preparation process, such as in respect of the period spanning dissection to tissue removal and placement into cold solution (Gibb and Edwards, 1994). For adult animals the vertebral columns are harder than those from young animals, so resulting in longer preparation times (Gibb and Edwards, 1994), which likely has an adverse impact on the chances of neuronal survival. To increase the probability of obtaining improved levels of viable neurones from preparations involving adult spinal cord slices a special protocol is required, which incorporates additional chemical compositions (Mitra and Brownstone, 2012). The reason for this is that tissue from adult animals is less resistant to anoxia than that from young animals (Gibb and Edwards, 1994, Mitra and Brownstone, 2012), possibly due to the cells having higher metabolic demands, plus also exhibits more myelination

(Mitra and Brownstone, 2012). Increased myelination causes the tissue to be less permeable to oxygen and therefore less tolerant to insults during the preparation process. The use of a protocol involving polyethylene glycol seemingly mitigates the amount of neuronal loss attributable to insult (Mitra and Brownstone, 2012).

While it is suggested that neurogenesis of GABAergic neurones in each lamina of the mouse spinal cord varies, the majority of GABAergic neurones are typically generated before embryonic day 14.5 (Huang et al., 2013). For the cholinergic system, it is indicated that the expression of ChAT mRNA (detected through the use of northern blot analysis and ISH) in the rat spinal cord increases from birth until adulthood, with a significant rise occurring at day 1 postnatal, when the majority of synapses will have already been formed (Ibanez et al., 1991). As a result, it is therefore appropriate for our study to undertake juxtacellular labelling on the spinal cord slices from young animals, in order to investigate the morphology and projection of ChAT/GAD67-GFP co-localised neurones, because the majority of GABAergic neurone and cholinergic neurone generation will be complete and mature at the age that we use.

It is believed that the populations of ChAT/GAD67-GFP co-localised neurones reported in this study for young and old mice are the same on the basis of their co-localisation with the two markers plus their location within the ventral aspect of lamina X. Whilst other groups of ChAT/GABA co-localised neurones have been reported within the spinal cord (Todd et al., 2003, Mesnage et al., 2011), particularly in the dorsal horn, we believe their locations are sufficiently anatomically distinct so as to be dismissed as possible sources of misidentification error for the neurones we have discerned. Moreover, these other neurone populations also appear to be present in both young (Mesnage et al., 2011) and adult animals (Todd, 1991), therefore suggesting that they do not migrate during maturation and so remain as distinct populations.

In order to be certain that the population of neurones we observe in the adult and young animals are the same, costaining for other markers unique to the population would be required or demonstration that they have the same efferent projection. An effective method to label the ChAT/GAD67-GFP co-localised neurones as a unique population would be to identify a transcription factor expressed during development that directly dictates the coexpression of these two enzymes. This approach would necessitate a detailed developmental study building upon what is already known regarding GABAergic (Cheng et al., 2005, Glasgow et al., 2005) and cholinergic neurone cell fate (Zagoraiou et al., 2009, Cho et al., 2014) in the CNS. Validating the outcomes of such a study would also be facilitated by the generation and

characterisation of a new line of transgenic mouse, which may use intersectional genetics to label only cells that express GAD67 and ChAT (Madisen et al., 2015, Saito et al., 2015).

Cell physiology is another possible identifier but this can change from young to old depending on whether the cells undergo postnatal maturation.

5.4.4 Animal model: wild type vs transgenic type

Prior to the juxtacellular labelling method being considered, double labelled IHC analyses for VAChT and either GAD67 or GABA or VGAT was first undertaken on the spinal cord and medulla oblongata from both adult wild type and GAD67-GFP mice. The sections were then visualised through the use of both epifluorescent and confocal microscopy to observe the possible projections of co-localised neurones. Unfortunately, these investigations were not able to provide positive confirmation of the projections from such neurones. Consequently, juxtacellular labelling was employed in order to trace the projections of the co-localised neurones in this study.

It should be possible to identify co-localised ChAT/GAD terminals by using antibodies against VGAT and VAChT which would label the boutons specifically. However this approach would not identify the neurone supplying the bouton, plus it would require the use of electron microscopy to confirm true co-localisation as opposed spatial co-localisation (boutons in close proximity to each other leading to a false positive result). If used in conjunction with soma immunolabelling, the method would in theory indicate the neurone from which the bouton arises and demonstrate at least spatial co-localisation of the vesicular markers. For our purpose though, this would require somatic staining for ChAT and GABA/GAD plus terminal stains for VGAT and VAChT, a process that would require each immunoreaction to work specifically and have its own identifiable fluorophore in order to prevent the signals mixing. The next issue that arises would be on how to trace a co-labelled bouton back to a specific neuron or group of neurons when there is abundant labelling of cells and fibres. The use of a transgenic mouse, such as the GAD67-GFP knock-in mice used in this study, would aid some aspects of this scenario, especially where reliable immunohistochemical detection of GABA has proven difficult. However, the problem still remains of discerning individual neurones and their projections amidst the others that are labelled. We elected to use juxtacellular labelling to overcome some of these obstacles, by

individually labelling neurons in the area of interest and then identifying them through the subsequent application of immunohistochemistry to allow us to trace the specific projection from a ChAT/GAD67-GFP co-localised neurone. A refinement to this procedure is the selection of GAD67-GFP knock-in mice for the juxtacellular labelling experiments, since their use aids identification of the appropriate cell population to target. As ChAT/GAD67-GFP co-localised neurones are a subpopulation of the GFP-expressing neurones it should make the process more efficient than “blindly” labelling neurones in the ventral part of lamina X region. It also provides somatic and terminal labelling for GAD67-GFP, which combined with the juxtacellular label would allow the projection of a single neurone to be traced. Positive confirmation for ChAT co-localisation could then be achieved via ChAT- or VAChT-immunoreactivity.

Due to the difficulties in labelling the cell bodies of GABAergic neurones as discussed above, wild type animals were not suitable for use in relation to quantification studies, where the number of neuronal cell bodies needed to be counted. Instead, GAD67-GFP knock-in mice were selected for quantification work.

5.5 Limitation of animals used in the study and future study

Although the result from our study utilising juxtacellular labelling suggested that ChAT/GAD67-GFP co-localised neurones might project to lamina X, or in the vicinity of lamina X, only one juxtacellularly labelled neurone from 34 neurones recovered contained both ChAT and GAD67-GFP. A problem of obtaining these labelled co-localised neurones was the nature of selected transgenic mouse line that was available and most suitable at that time, in respect to which GABAergic neurones could only be visualised during the labelling process. Confirmation of co-localisation was then possible only once cell recovery had been completed utilising IHC subsequent to the juxtacellular labelling process.

Recent developments in transgenic technology involving creation of a more suitable double transgenic animal model would likely overcome such limitation. Recently Saito et al. reported a study involving the use of a double transgenic rat model in which the neurones within the prepositus hypoglossi nucleus expressed both ChAT and VGAT (Saito et al., 2015). This rat model may be a more suitable candidate in aiding future studies to examine the functions of neurones co-expressing both the ACh and GABA

synthesising enzyme within the spinal cord and medulla oblongata, since the neurones expressing both ChAT and VGAT in these transgenic rats can be visualised during juxtacellular labelling and/or electrophysiological studies, so potentially facilitating increased numbers of labelled and/or recorded ChAT/VGAT neurones to be obtained. Once the projection of such neurones is confirmed, which establish the systems modulated by their output, studies regarding the function of these neurones would then be pursued.

Our reports suggest that studying the possible inputs from VGLUT1, VGLUT2, GlyT2 and GAD67 terminals onto ChAT/GAD67-GFP co-localised neurones in lamina X could be beneficial future investigations. Such work would help identify the neuronal populations that influence the activity of ChAT/GAD67-GFP co-localised neurones, plus may resolve the physiological role of ChAT/GAD67 co-localised neurones and the pathway by which the systems they interact with are linked.

5.6 Conclusion

For the first time this study provides a complete anatomical report regarding the neurones containing enzymes responsible for the production of both ACh and GABA throughout the spinal cord and medulla oblongata. Within the spinal cord the majority of such neurones were observed in lamina X of the cervical, thoracic and lumbar cord regions. A smaller number of co-localised neurones was also found in the dorsal horn. The location of these co-localised neurones relative to the central canal within lamina X was also investigated, in order to narrow the specific area in which subsequent juxtacellular labelling would be focussed. Results indicated that the majority of the co-localised neurones were located ventral and ventrolateral to the central canal. To trace the axonal projections of ChAT/GAD67-GFP co-localised neurones in lamina X, the juxtacellular labelling method was selected for spinal cord slices. Since the use of young mice with reduced myelination provides for optimal slice visualisation, potential ChAT/GAD67-GFP co-localisation in young animals was first examined prior to juxtacellular labelling being undertaken. In the young animals the presence of co-localised neurones was predominantly observed in lamina X, similar to that observed for adult animals. A smaller number of co-localised neurones were additionally observed in the dorsal horn of the young mice. On application of juxtacellular labelling, the result obtained suggested the processes of a co-localised neurone to be seemingly relatively small and short, likely locally branching within lamina X. The neurone

appeared to have some dendrites that passed close to the ependymal cells lining the central canal, although one dendrite reached the ventral aspect of lamina X. The axon of the neurone, based on morphology, seemed to be located in lamina X. The possible inputs onto ChAT/GAD67-GFP co-localised neurones were also investigated, the results of which suggested that co-localised neurones in lamina X receive inputs from VGLUT1-IR, VGLUT2-IR, GlyT2-IR and GAD67-IR terminals. Having observed the presence of neurones expressing both ChAT and GAD67-GFP throughout the lamina X of the cervical, thoracic and lumbar spinal cord, the presence of such co-expression could additionally be observed along the rostrocaudal axis, extending to reach the medulla oblongata. The areas of the medulla oblongata containing such co-localised neurones were the NTS, area postrema and reticular formation; corresponding to regions known to be involved in autonomic control. Although the function of these co-localised neurones is currently unknown, a complete anatomical knowledge regarding their morphology, location, possible projection and inputs has been explored and reported in this study, providing a foundation of knowledge upon which future research into the roles of such neurones within the circuits of the spinal cord and medulla oblongata can be based.

References

Abraira, V. E. & Ginty, D. D. 2013. The sensory neurons of touch. *Neuron,* 79**,** 618-39.

Ai, J., Epstein, P. N., Gozal, D., Yang, B., Wurster, R. & Cheng, Z. J. 2007. Morphology and topography of nucleus ambiguus projections to cardiac ganglia in rats and mice. *Neuroscience,* 149**,** 845-60.

Al-Mosawie, A., Wilson, J. M. & Brownstone, R. M. 2007. Heterogeneity of V2-derived interneurons in the adult mouse spinal cord. *Eur J Neurosci,* 26**,** 3003-15.

Alexander, S. P., Davenport, A. P., Kelly, E., Marrion, N., Peters, J. A., Benson, H. E., Faccenda, E., Pawson, A. J., Sharman, J. L., Southan, C. & Davies, J. A. 2015a. The Concise Guide to PHARMACOLOGY 2015/16: G protein-coupled receptors. *Br J Pharmacol,* 172**,** 5744-869.

Alexander, S. P., Peters, J. A., Kelly, E., Marrion, N., Benson, H. E., Faccenda, E., Pawson, A. J., Sharman, J. L., Southan, C. & Davies, J. A. 2015b. The Concise Guide to PHARMACOLOGY 2015/16: Ligand-gated ion channels. *Br J Pharmacol,* 172**,** 5870-903.

Allen brain atlas: Mouse brain. Available: http://mouse.brain-map.org/ [Accessed 13th March 2016].

Allen brain atlas: Mouse spinal cord. Available: http://mousespinal.brain-map.org [Accessed 13th March 2016].

Altschuler, S. M., Bao, X. M., Bieger, D., Hopkins, D. A. & Miselis, R. R. 1989. Viscerotopic representation of the upper alimentary tract in the rat: sensory ganglia and nuclei of the solitary and spinal trigeminal tracts. *J Comp Neurol,* 283**,** 248-68.

Alvarez, F. J., Villalba, R. M., Zerda, R. & Schneider, S. P. 2004. Vesicular glutamate transporters in the spinal cord, with special reference to sensory primary afferent synapses. *J Comp Neurol,* 472**,** 257-80.

Ambalavanar, R. & Morris, R. 1989. Fluoro-Gold injected either subcutaneously or intravascularly results in extensive retrograde labelling of CNS neurones having axons terminating outside the blood-brain barrier. *Brain Res,* 505**,** 171-5.

Anderson, C. R. & Edwards, S. L. 1994. Intraperitoneal injections of Fluorogold reliably labels all sympathetic preganglionic neurons in the rat. *J Neurosci Methods,* 53**,** 137-41.

Anderson, C. R., Keast, J. R. & Mclachlan, E. M. 2009. Spinal Autonomic Preganglionic Neurons: the visceral efferent system of the spinal cord. *In:* Watson, C., Paxinos, G. & Kayalioglu, G. (eds.) *The Spinal Cord.* Amsterdam: Academic Press.

Armstrong, D. M., Rotler, A., Hersh, L. B. & Pickel, V. M. 1988. Localization of choline acetyltransferase in perikarya and dendrites within the nuclei of the solitary tracts. *J Neurosci Res,* 20**,** 279-90.

Arvidsson, U., Riedl, M., Elde, R. & Meister, B. 1997. Vesicular acetylcholine transporter (VAChT) protein: a novel and unique marker for cholinergic neurons in the central and peripheral nervous systems. *J Comp Neurol,* 378**,** 454-67.

Audet, M. & Bouvier, M. 2012. Restructuring G-protein- coupled receptor activation. *Cell,* 151**,** 14-23.

Awapara, J., Landua, A. J., Fuerst, R. & Seale, B. 1950. Free gamma-aminobutyric acid in brain. *J Biol Chem,* 187**,** 35-9.

Bacon, S. J., Zagon, A. & Smith, A. D. 1990. Electron microscopic evidence of a monosynaptic pathway between cells in the caudal raphe nuclei and sympathetic preganglionic neurons in the rat spinal cord. *Exp Brain Res,* 79**,** 589-602.

Bailey, T. W., Appleyard, S. M., Jin, Y. H. & Andresen, M. C. 2008. Organization and properties of GABAergic neurons in solitary tract nucleus (NTS). *J Neurophysiol,* 99**,** 1712-22.

Ballion, B., Branchereau, P., Chapron, J. & Viala, D. 2002. Ontogeny of descending serotonergic innervation and evidence for intraspinal 5-HT neurons in the mouse spinal cord. *Brain Res Dev Brain Res,* 137**,** 81-8.

Bannatyne, B. A., Edgley, S. A., Hammar, I., Jankowska, E. & Maxwell, D. J. 2003. Networks of inhibitory and excitatory commissural interneurons mediating crossed reticulospinal actions. *Eur J Neurosci,* 18**,** 2273-84.

Baptista, V., Zheng, Z. L., Coleman, F. H., Rogers, R. C. & Travagli, R. A. 2005. Characterization of neurons of the nucleus tractus solitarius pars centralis. *Brain Res,* 1052**,** 139-46.

Barber, R. P., Phelps, P. E., Houser, C. R., Crawford, G. D., Salvaterra, P. M. & Vaughn, J. E. 1984. The morphology and distribution of neurons containing choline acetyltransferase in the adult rat spinal cord: an immunocytochemical study. *J Comp Neurol,* 229**,** 329-46.

Barber, R. P., Vaughn, J. E. & Roberts, E. 1982. The cytoarchitecture of GABAergic neurons in rat spinal cord. *Brain Res,* 238**,** 305-28.

Belin, M. F., Nanopoulos, D., Didier, M., Aguera, M., Steinbusch, H., Verhofstad, A., Maitre, M. & Pujol, J. F. 1983. Immunohistochemical evidence for the presence of gamma-aminobutyric acid and serotonin in one nerve cell. A study on the raphe nuclei of the rat using antibodies to glutamate decarboxylase and serotonin. *Brain Res,* 275**,** 329-39.

Benes, F. M. & Berretta, S. 2001. GABAergic interneurons: implications for understanding schizophrenia and bipolar disorder. *Neuropsychopharmacology,* 25**,** 1-27.

Bilgen, M. & Al-Hafez, B. 2006. Comparison of spinal vasculature in mouse and rat: investigations using MR angiography. *Neuroanatomy,* 5**,** 12-16.

Bittencourt, J. C. & Elias, C. F. 1998. Melanin-concentrating hormone and neuropeptide EI projections from the lateral hypothalamic area and zona incerta to the medial septal nucleus and spinal cord: a study using multiple neuronal tracers. *Brain Res,* 805**,** 1-19.

Bittencourt, J. C., Presse, F., Arias, C., Peto, C., Vaughan, J., Nahon, J. L., Vale, W. & Sawchenko, P. E. 1992. The melanin-concentrating hormone system of the rat brain: an immuno- and hybridization histochemical characterization. *J Comp Neurol,* 319**,** 218-45.

Borden, L. A., Dhar, T. G., Smith, K. E., Branchek, T. A., Gluchowski, C. & Weinshank, R. L. 1994. Cloning of the human homologue of the GABA transporter GAT-3 and identification of a novel inhibitor with selectivity for this site. *Receptors Channels,* 2**,** 207-13.

Bordey, A., Feltz, P. & Trouslard, J. 1996a. Nicotinic actions on neurones of the central autonomic area in rat spinal cord slices. *J Physiol,* 497 (Pt 1)**,** 175-87.

Bordey, A., Feltz, P. & Trouslard, J. 1996b. Patch-clamp characterization of nicotinic receptors in a subpopulation of lamina X neurones in rat spinal cord slices. *J Physiol,* 490 (Pt 3)**,** 673-8.

Borges, L. F. & Iversen, S. D. 1986. Topography of choline acetyltransferase immunoreactive neurons and fibers in the rat spinal cord. *Brain Res,* 362**,** 140-8.

Bormann, J. 2000. The 'ABC' of GABA receptors. *Trends Pharmacol Sci,* 21**,** 16-9.

Bouche, N., Fait, A., Bouchez, D., Moller, S. G. & Fromm, H. 2003. Mitochondrial succinic-semialdehyde dehydrogenase of the gamma-aminobutyrate shunt is required to restrict levels of reactive oxygen intermediates in plants. *Proc Natl Acad Sci U S A,* 100**,** 6843-8.

Bowery, N. G., Bettler, B., Froestl, W., Gallagher, J. P., Marshall, F., Raiteri, M., Bonner, T. I. & Enna, S. J. 2002. International Union of Pharmacology. XXXIII. Mammalian gamma-aminobutyric acid(B) receptors: structure and function. *Pharmacol Rev,* 54**,** 247-64.

Bowery, N. G., Doble, A., Hill, D. R., Hudson, A. L., Shaw, J. S., Turnbull, M. J. & Warrington, R. 1981. Bicuculline-insensitive GABA receptors on peripheral autonomic nerve terminals. *Eur J Pharmacol,* 71**,** 53-70.

Bowery, N. G. & Smart, T. G. 2006. GABA and glycine as neurotransmitters: a brief history. *Br J Pharmacol,* 147 Suppl 1**,** S109-19.

Bradaia, A., Seddik, R., Schlichter, R. & Trouslard, J. 2005. The rat spinal cord slice: Its use in generating pharmacological evidence for cholinergic transmission using the alpha7 subtype of nicotinic receptors in the central autonomic nucleus. *J Pharmacol Toxicol Methods,* 51**,** 243-52.

Bradford, H. F. 1986. *Chemical Neurobiology: An Introduction to Neurochemistry,* New York, W.H. Freeman and Company.

Brekke, E., Morken, T. S. & Sonnewald, U. 2015. Glucose metabolism and astrocyte-neuron interactions in the neonatal brain. *Neurochem Int,* 82**,** 33-41.

Briatore, F., Patrizi, A., Viltono, L., Sassoe-Pognetto, M. & Wulff, P. 2010. Quantitative organization of GABAergic synapses in the molecular layer of the mouse cerebellar cortex. *PLoS One,* 5**,** e12119.

Briscoe, J. & Ericson, J. 2001. Specification of neuronal fates in the ventral neural tube. *Curr Opin Neurobiol,* 11**,** 43-9.

Brooke, R. E., Pyner, S., Mcleish, P., Buchan, S., Deuchars, J. & Deuchars, S. A. 2002. Spinal cord interneurones labelled transneuronally from the adrenal gland by a GFP-herpes virus construct contain the potassium channel subunit Kv3.1b. *Auton Neurosci,* 98**,** 45-50.

Broussard, D. L. & Altschuler, S. M. 2000. Brainstem viscerotopic organization of afferents and efferents involved in the control of swallowing. *Am J Med,* 108 Suppl 4a**,** 79S-86S.

Brown, A. G. & Iggo, A. 1967. A quantitative study of cutaneous receptors and afferent fibres in the cat and rabbit. *J Physiol,* 193**,** 707-33.

Brown, A. G., Rose, P. K. & Snow, P. J. 1978. Morphology and organization of axon collaterals from afferent fibres of slowly adapting type I units in cat spinal cord. *J Physiol,* 277**,** 15-27.

Brucke, F. T. V. 1937. The cholinesterase in sympathetic ganglia. *J Physiol,* 89**,** 429-37.

Burnstock, G. 1976. Do some nerve cells release more than one transmitter? *Neuroscience,* 1**,** 239-48.

Burt, A. M. 1993. *Textbook of Neuroanatomy,* Philadelphia, W.B. Saunders Company.

Cabot, J. B., Alessi, V., Carroll, J. & Ligorio, M. 1994. Spinal cord lamina V and lamina VII interneuronal projections to sympathetic preganglionic neurons. *J Comp Neurol,* 347**,** 515-30.

Caffe, A. R., Hawkins, R. K. & De Zeeuw, C. I. 1996. Coexistence of choline acetyltransferase and GABA in axon terminals in the dorsal cap of the rat inferior olive. *Brain Res,* 724**,** 136-40.

Carlin, K. P., Jiang, Z. & Brownstone, R. M. 2000. Characterization of calcium currents in functionally mature mouse spinal motoneurons. *Eur J Neurosci,* 12**,** 1624-34.

Carlton, S. M. & Hayes, E. S. 1990. Light microscopic and ultrastructural analysis of GABA-immunoreactive profiles in the monkey spinal cord. *J Comp Neurol,* 300**,** 162-82.

Caspary, T. & Anderson, K. V. 2003. Patterning cell types in the dorsal spinal cord: what the mouse mutants say. *Nat Rev Neurosci,* 4**,** 289-97.

Catapano, L. A., Magavi, S. S. & Macklis, J. D. 2008. Neuroanatomical tracing of neuronal projections with Fluoro-Gold. *Methods Mol Biol,* 438**,** 353-9.

Caulfield, M. P. 1993. Muscarinic receptors--characterization, coupling and function. *Pharmacol Ther,* 58**,** 319-79.

Caulfield, M. P. & Birdsall, N. J. 1998. International Union of Pharmacology. XVII. Classification of muscarinic acetylcholine receptors. *Pharmacol Rev,* 50**,** 279-90.

Chang, Y., Wang, R., Barot, S. & Weiss, D. S. 1996. Stoichiometry of a recombinant GABAA receptor. *J Neurosci,* 16**,** 5415-24.

Changeux, J. P., Kasai, M. & Lee, C. Y. 1970. Use of a snake venom toxin to characterize the cholinergic receptor protein. *Proc Natl Acad Sci U S A,* 67**,** 1241-7.

Chapman, R. J., Lall, V. K., Maxeiner, S., Willecke, K., Deuchars, J. & King, A. E. 2013. Localization of neurones expressing the gap junction protein Connexin45 within the adult spinal dorsal horn: a study using Cx45-eGFP reporter mice. *Brain Struct Funct,* 218**,** 751-65.

Charan, J. & Kantharia, N. D. 2013. How to calculate sample size in animal studies? *J Pharmacol Pharmacother,* 4**,** 303-6.

Chatzidaki, A. & Millar, N. S. 2015. Allosteric modulation of nicotinic acetylcholine receptors. *Biochem Pharmacol,* 97**,** 408-17.

Cheng, L., Samad, O. A., Xu, Y., Mizuguchi, R., Luo, P., Shirasawa, S., Goulding, M. & Ma, Q. 2005. Lbx1 and Tlx3 are opposing switches in determining GABAergic versus glutamatergic transmitter phenotypes. *Nat Neurosci,* 8**,** 1510-5.

Chessler, S. D., Simonson, W. T., Sweet, I. R. & Hammerle, L. P. 2002. Expression of the vesicular inhibitory amino acid transporter in pancreatic islet cells: distribution of the transporter within rat islets. *Diabetes,* 51**,** 1763-71.

Chizh, B. A., Headley, P. M. & Paton, J. F. 1998. Coupling of sympathetic and somatic motor outflows from the spinal cord in a perfused preparation of adult mouse in vitro. *J Physiol,* 508 (Pt 3)**,** 907-18.

Cho, H. H., Cargnin, F., Kim, Y., Lee, B., Kwon, R. J., Nam, H., Shen, R., Barnes, A. P., Lee, J. W., Lee, S. & Lee, S. K. 2014. Isl1 directly controls a cholinergic neuronal identity in the developing forebrain and spinal cord by forming cell type-specific complexes. *PLoS Genet,* 10**,** e1004280.

Ciriello, J., Hochstenbach, S.L. & Roder, S. 1994. Central Projections of Baroreceptor and Chemoreceptor Afferent Fibers in the Rat. *In:* Barraco, I. R. (ed.) *Nucleus of the Solitary Tract.* Boca Raton: CRC Press.

Clark, F. M. & Proudfit, H. K. 1991. The projection of locus coeruleus neurons to the spinal cord in the rat determined by anterograde tracing combined with immunocytochemistry. *Brain Res,* 538**,** 231-45.

Clark, J. A., Deutch, A. Y., Gallipoli, P. Z. & Amara, S. G. 1992. Functional expression and CNS distribution of a beta-alanine-sensitive neuronal GABA transporter. *Neuron,* 9**,** 337-48.

Collingridge, G. L., Olsen, R. W., Peters, J. & Spedding, M. 2009. A nomenclature for ligand-gated ion channels. *Neuropharmacology,* 56**,** 2-5.

Connaughton, M., Priestley, J. V., Sofroniew, M. V., Eckenstein, F. & Cuello, A. C. 1986. Inputs to motoneurones in the hypoglossal nucleus of the rat: light and electron microscopic immunocytochemistry for choline acetyltransferase, substance P and enkephalins using monoclonal antibodies. *Neuroscience,* 17**,** 205-24.

Contreras, R. J., Beckstead, R. M. & Norgren, R. 1982. The central projections of the trigeminal, facial, glossopharyngeal and vagus nerves: an autoradiographic study in the rat. *J Auton Nerv Syst,* 6**,** 303-22.

Coons, A. H., Creech, H. J. & Jones, R. N. 1941. Immunological properties of an antibody containing a fluorescent group. *Proc Soc Exp Biol Med,* 47**,** 200-202.

Coons, A. H. & Kaplan, M. H. 1950. Localization of antigen in tissue cells. *J Exp Med,* 91**,** 1-13.

Coons, A. H., Leduc, E. H. & Connolly, J. M. 1955. Studies on antibody production. I: A method for the histochemical demonstration of specific antibody and its application to a study of the hyperimmune rabbit. *J Exp Med,* 102**,** 49-60.

Coote, J. H., Macleod, V. H., Fleetwood-Walker, S. & Gilbey, M. P. 1981. The response of individual sympathetic preganglionic neurones to microelectrophoretically applied endogenous monoamines. *Brain Res,* 215**,** 135-45.

Corns, L. F., Atkinson, L., Daniel, J., Edwards, I. J., New, L., Deuchars, J. & Deuchars, S. A. 2015. Cholinergic Enhancement of Cell Proliferation in the Postnatal Neurogenic Niche of the Mammalian Spinal Cord. *Stem Cells*.

Costa, E., Guidotti, F., Moroni, F. & Peralta, E. 1979. Glutamic Acid as a Transmitter Precursor and as a Transmitter. *In:* Filer, L. J. (ed.) *Glutamic Acid: Advances in Biochemistry and Physiology.* New York: Raven Press.

Criscione, L., Reis, D. J. & Talman, W. T. 1983. Cholinergic mechanisms in the nucleus tractus solitarii and cardiovascular regulation in the rat. *Eur J Pharmacol,* 88**,** 47-55.

Curtis, D. R., Game, C. J., Lodge, D. & Mcculloch, R. M. 1976. A pharmacological study of Renshaw cell inhibition. *J Physiol,* 258**,** 227-42.

D'errico, P., Boido, M., Piras, A., Valsecchi, V., De Amicis, E., Locatelli, D., Capra, S., Vagni, F., Vercelli, A. & Battaglia, G. 2013. Selective vulnerability of spinal and cortical motor neuron subpopulations in delta7 SMA mice. *PLoS One,* 8**,** e82654.

Da Silva, L. G., Dias, A. C., Furlan, E. & Colombari, E. 2008. Nitric oxide modulates the cardiovascular effects elicited by acetylcholine in the NTS of awake rats. *Am J Physiol Regul Integr Comp Physiol,* 295**,** R1774-81.

Dale, H. 1935. Pharmacology and Nerve-endings (Walter Ernest Dixon Memorial Lecture): (Section of Therapeutics and Pharmacology). *Proceedings of the Royal Society of Medicine* 28**,** 319-332.

Dale, H. H. 1914. The action of certain esters and ethers of choline, and their relation to muscarine. *J Pharmacol Exp Ther* 6**,** 147-190.

Davidoff, M. S. & Schulze, W. 1988. Coexistence of GABA- and choline acetyltransferase (ChAT)-like immunoreactivity in the hypoglossal nucleus of the rat. *Histochemistry,* 89**,** 25-33.

Dell, R. B., Holleran, S. & Ramakrishnan, R. 2002. Sample size determination. *ILAR J,* 43**,** 207-13.

Deuchars, S. A. 2007. Multi-tasking in the spinal cord--do 'sympathetic' interneurones work harder than we give them credit for? *J Physiol,* 580**,** 723-9.

Deuchars, S. A. 2015. How sympathetic are your spinal cord circuits? *Exp Physiol,* 100**,** 365-71.

Deuchars, S. A., Brooke, R. E., Frater, B. & Deuchars, J. 2001. Properties of interneurones in the intermediolateral cell column of the rat spinal cord: role of the potassium channel subunit Kv3.1. *Neuroscience,* 106**,** 433-46.

Deuchars, S. A. & Lall, V. K. 2015. Sympathetic preganglionic neurons: properties and inputs. *Compr Physiol,* 5**,** 829-69.

Deuchars, S. A., Milligan, C. J., Stornetta, R. L. & Deuchars, J. 2005. GABAergic neurons in the central region of the spinal cord: a novel substrate for sympathetic inhibition. *J Neurosci,* 25**,** 1063-70.

Dias, N. & Stein, C. A. 2002. Antisense Oligonucleotides: Basic Concepts and Mechanisms. *Molecular Cancer Therapeutics,* 1**,** 347-355.

Djouhri, L. 2016. Adelta-fiber low threshold mechanoreceptors innervating mammalian hairy skin: A review of their receptive, electrophysiological and cytochemical properties in relation to Adelta-fiber high threshold mechanoreceptors. *Neurosci Biobehav Rev,* 61**,** 225-38.

Dong, H., Loomis, C. W. & Bieger, D. 2000. Distal and deglutitive inhibition in the rat esophagus: role of inhibitory neurotransmission in the nucleus tractus solitarii. *Gastroenterology,* 118**,** 328-36.

Douglas, W. W. & Poisner, A. M. 1966. Evidence that the secreting adrenal chromaffin cell releases catecholamines directly from ATP-rich granules. *J Physiol,* 183**,** 236-48.

Du Beau, A., Shakya Shrestha, S., Bannatyne, B. A., Jalicy, S. M., Linnen, S. & Maxwell, D. J. 2012. Neurotransmitter phenotypes of descending systems in the rat lumbar spinal cord. *Neuroscience,* 227**,** 67-79.

Duque, A. & Zaborszky, L. 2006. Juxtacellular Labeling of Individual Neurons In Vivo: From Electrophysiology to Synaptology. *In:* Zaborszky, L., Wouterlood, F. & Lanciego, J. (eds.) *Neuroanatomical Tract-Tracing 3.* Springer US.

Eckenstein, F. & Sofroniew, M. V. 1983. Identification of central cholinergic neurons containing both choline acetyltransferase and acetylcholinesterase and of central neurons containing only acetylcholinesterase. *J Neurosci,* 3**,** 2286-91.

Eckenstein, F. & Thoenen, H. 1982. Production of specific antisera and monoclonal antibodies to choline acetyltransferase: characterization and use for identification of cholinergic neurons. *Embo j,* 1**,** 363-8.

Eckenstein, F. & Thoenen, H. 1983. Cholinergic neurons in the rat cerebral cortex demonstrated by immunohistochemical localization of choline acetyltransferase. *Neurosci Lett,* 36**,** 211-15.

Edwards, I. J., Dallas, M. L., Poole, S. L., Milligan, C. J., Yanagawa, Y., Szabo, G., Erdelyi, F., Deuchars, S. A. & Deuchars, J. 2007. The neurochemically diverse intermedius nucleus of the medulla as a source of excitatory and inhibitory synaptic input to the nucleus tractus solitarii. *J Neurosci,* 27**,** 8324-33.

Edwards, I. J., Lall, V. K., Paton, J. F., Yanagawa, Y., Szabo, G., Deuchars, S. A. & Deuchars, J. 2014. Neck muscle afferents influence oromotor and cardiorespiratory brainstem neural circuits. *Brain Struct Funct,* 220**,** 1421-36.

Elliott, T. R. 1904. On the action of adrenalin. *Proc Physiol Soc***,** xx-xxi.

Erickson, J. D., Varoqui, H., Schafer, M. K., Modi, W., Diebler, M. F., Weihe, E., Rand, J., Eiden, L. E., Bonner, T. I. & Usdin, T. B. 1994. Functional identification of a vesicular acetylcholine transporter and its expression from a "cholinergic" gene locus. *J Biol Chem,* 269**,** 21929-32.

Ericson, J., Briscoe, J., Rashbass, P., Van Heyningen, V. & Jessell, T. M. 1997a. Graded sonic hedgehog signaling and the specification of cell fate in the ventral neural tube. *Cold Spring Harb Symp Quant Biol,* 62**,** 451-66.

Ericson, J., Rashbass, P., Schedl, A., Brenner-Morton, S., Kawakami, A., Van Heyningen, V., Jessell, T. M. & Briscoe, J. 1997b. Pax6 controls progenitor cell identity and neuronal fate in response to graded Shh signaling. *Cell,* 90**,** 169-80.

Erlander, M. G., Tillakaratne, N. J., Feldblum, S., Patel, N. & Tobin, A. J. 1991. Two genes encode distinct glutamate decarboxylases. *Neuron,* 7**,** 91-100.

Ewins, A. J. 1914. Acetylcholine, a New Active Principle of Ergot. *Biochem J,* 8**,** 44-9.

Fagerlund, M. J. & Eriksson, L. I. 2009. Current concepts in neuromuscular transmission. *Br J Anaesth,* 103**,** 108-14.

Farrar, M. J., Rubin, J. D., Diago, D. M. & Schaffer, C. B. 2015. Characterization of blood flow in the mouse dorsal spinal venous system before and after dorsal spinal vein occlusion. *J Cereb Blood Flow Metab,* 35**,** 667-75.

Feldberg, W. & Vogt, M. 1948. Acetylcholine synthesis in different regions of the central nervous system. *J Physiol,* 107**,** 372-81.

Fong, A. Y., Stornetta, R. L., Foley, C. M. & Potts, J. T. 2005. Immunohistochemical localization of GAD67-expressing neurons and processes in the rat brainstem: subregional distribution in the nucleus tractus solitarius. *J Comp Neurol,* 493**,** 274-90.

Fornai, F., Ferrucci, M., Lenzi, P., Falleni, A., Biagioni, F., Flaibani, M., Siciliano, G., Giannessi, F. & Paparelli, A. 2014. Plastic changes in the spinal cord in motor neuron disease. *Biomed Res Int,* 2014**,** 670756.

Friese, A., Kaltschmidt, J. A., Ladle, D. R., Sigrist, M., Jessell, T. M. & Arber, S. 2009. Gamma and alpha motor neurons distinguished by expression of transcription factor Err3. *Proc Natl Acad Sci U S A,* 106**,** 13588-93.

Furuya, W. I., Bassi, M., Menani, J. V., Colombari, E., Zoccal, D. B. & Colombari, D. S. 2014. Differential modulation of sympathetic and respiratory activities by cholinergic mechanisms in the nucleus of the solitary tract in rats. *Exp Physiol,* 99**,** 743-58.

Fykse, E. M., Christensen, H. & Fonnum, F. 1989. Comparison of the properties of gamma-aminobutyric acid and L-glutamate uptake into synaptic vesicles isolated from rat brain. *J Neurochem,* 52**,** 946-51.

Gadea, A. & Lopez-Colome, A. M. 2001. Glial transporters for glutamate, glycine, and GABA: II. GABA transporters. *J Neurosci Res,* 63**,** 461-8.

Gaiarsa, J. L., Mclean, H., Congar, P., Leinekugel, X., Khazipov, R., Tseeb, V. & Ben-Ari, Y. 1995. Postnatal maturation of gamma-aminobutyric acidA and B-mediated inhibition in the CA3 hippocampal region of the rat. *J Neurobiol,* 26**,** 339-49.

Gamboa-Esteves, F. O., Kaye, J. C., Mcwilliam, P. N., Lima, D. & Batten, T. F. 2001a. Immunohistochemical profiles of spinal lamina I neurones retrogradely labelled from the nucleus tractus solitarii in rat suggest excitatory projections. *Neuroscience,* 104**,** 523-38.

Gamboa-Esteves, F. O., Lima, D. & Batten, T. F. 2001b. Neurochemistry of superficial spinal neurones projecting to nucleus of the solitary tract that express c-fos on chemical somatic and visceral nociceptive input in the rat. *Metab Brain Dis,* 16**,** 151-64.

Gamboa-Esteves, F. O., Tavares, I., Almeida, A., Batten, T. F., Mcwilliam, P. N. & Lima, D. 2001c. Projection sites of superficial and deep spinal dorsal horn cells in the nucleus tractus solitarii of the rat. *Brain Res,* 921**,** 195-205.

Ganchrow, D., Ganchrow, J. R., Cicchini, V., Bartel, D. L., Kaufman, D., Girard, D. & Whitehead, M. C. 2014. Nucleus of the solitary tract in the C57BL/6J mouse: Subnuclear parcellation, chorda tympani nerve projections, and brainstem connections. *J Comp Neurol,* 522**,** 1565-96.

Geerling, J. C., Shin, J. W., Chimenti, P. C. & Loewy, A. D. 2010. Paraventricular hypothalamic nucleus: axonal projections to the brainstem. *J Comp Neurol,* 518**,** 1460-99.

Gibb, A. J. & Edwards, F. A. 1994. Patch-clamp recording from cells in sliced tissues. *In:* Ogden, D. (ed.) *Microelectrode Technique: The Plymouth Workshop Handbook.* Cambridge: The Company of Biologists Limited.

Gibson, I. C. & Logan, S. D. 1995. Effects of muscarinic receptor stimulation of sympathetic preganglionic neurones of neonatal rat spinal cord in vitro. *Neuropharmacology,* 34**,** 309-18.

Glasgow, S. M., Henke, R. M., Macdonald, R. J., Wright, C. V. & Johnson, J. E. 2005. Ptf1a determines GABAergic over glutamatergic neuronal cell fate in the spinal cord dorsal horn. *Development,* 132**,** 5461-9.

Gotti, C., Zoli, M. & Clementi, F. 2006. Brain nicotinic acetylcholine receptors: native subtypes and their relevance. *Trends Pharmacol Sci,* 27**,** 482-91.

Gotts, J. Unpublished Data. University of Leeds.

Gotts, J., Atkinson, L., Edwards, I. J., Yanagawa, Y., Deuchars, S. A. & Deuchars, J. 2015. Co-expression of GAD67 and choline acetyltransferase reveals a novel neuronal phenotype in the mouse medulla oblongata. *Auton Neurosci*, 2015 May 16. pii: S1566-0702(15)00053-3. doi: 10.1016/j.autneu.2015.05.003.

Graham, B. A., Schofield, P. R., Sah, P. & Callister, R. J. 2003. Altered inhibitory synaptic transmission in superficial dorsal horn neurones in spastic and oscillator mice. *J Physiol,* 551**,** 905-16.

Graham, R. C., Jr. & Karnovsky, M. J. 1966. The early stages of absorption of injected horseradish peroxidase in the proximal tubules of mouse kidney: ultrastructural cytochemistry by a new technique. *J Histochem Cytochem,* 14**,** 291-302.

Granger, A. J., Mulder, N., Saunders, A. & Sabatini, B. L. 2016. Cotransmission of acetylcholine and GABA. *Neuropharmacology,* 100**,** 40-6.

Gritti, I., Mainville, L. & Jones, B. E. 1993. Codistribution of GABA- with acetylcholine-synthesizing neurons in the basal forebrain of the rat. *J Comp Neurol,* 329**,** 438-57.

Gross, M. K., Dottori, M. & Goulding, M. 2002. Lbx1 specifies somatosensory association interneurons in the dorsal spinal cord. *Neuron,* 34**,** 535-49.

Grossmann, K. S., Giraudin, A., Britz, O., Zhang, J. & Goulding, M. 2010. Genetic dissection of rhythmic motor networks in mice. *Prog Brain Res,* 187**,** 19-37.

Grudt, T. J. & Perl, E. R. 2002. Correlations between neuronal morphology and electrophysiological features in the rodent superficial dorsal horn. *J Physiol,* 540**,** 189-207.

Guan, Z. L., Ding, Y. Q., Li, J. L. & Lu, B. Z. 1998. Substance P receptor-expressing neurons in the medullary and spinal dorsal horns projecting to the nucleus of the solitary tract in the rat. *Neurosci Res,* 30**,** 213-8.

Guzman, M. S., De Jaeger, X., Raulic, S., Souza, I. A., Li, A. X., Schmid, S., Menon, R. S., Gainetdinov, R. R., Caron, M. G., Bartha, R., Prado, V. F. & Prado, M. A. 2011. Elimination of the vesicular acetylcholine transporter in the striatum reveals regulation of behaviour by cholinergic-glutamatergic co-transmission. *PLoS Biol,* 9**,** e1001194.

Hadzipasic, M., Tahvildari, B., Nagy, M., Bian, M., Horwich, A. L. & Mccormick, D. A. 2014. Selective degeneration of a physiological subtype of spinal motor neuron in mice with SOD1-linked ALS. *Proc Natl Acad Sci U S A,* 111**,** 16883-8.

Hantman, A. W., Van Den Pol, A. N. & Perl, E. R. 2004. Morphological and physiological features of a set of spinal substantia gelatinosa neurons defined by green fluorescent protein expression. *J Neurosci,* 24**,** 836-42.

Harrison, M., O'brien, A., Adams, L., Cowin, G., Ruitenberg, M. J., Sengul, G. & Watson, C. 2013. Vertebral landmarks for the identification of spinal cord segments in the mouse. *Neuroimage,* 68**,** 22-9.

Hashim, M. A. & Bieger, D. 1987. Excitatory action of 5-HT on deglutitive substrates in the rat solitary complex. *Brain Res Bull,* 18**,** 355-63.

Hayakawa, T., Takanaga, A., Maeda, S., Seki, M. & Yajima, Y. 2001. Subnuclear distribution of afferents from the oral, pharyngeal and laryngeal regions in the nucleus tractus solitarii of the rat: a study using transganglionic transport of cholera toxin. *Neurosci Res,* 39**,** 221-32.

Heise, C. & Kayalioglu, G. 2009a. Cytoarchitecture of the Spinal Cord. *In:* Watson, C., Paxinos, G. & Kayalioglu, G. (ed.) *The Spinal Cord.* Amsterdam: Academic Press.

Heise, C. & Kayalioglu, G. 2009b. Spinal Cord Transmitter Substances. *In:* Watson, C., Paxinos, G. & Kayalioglu G. (ed.) *The Spinal Cord.* Amsterdam: Academic Press.

Helke, C. J., Handelmann, G. E. & Jacobowitz, D. M. 1983. Choline acetyltransferase activity in the nucleus tractus solitarius: regulation by the afferent vagus nerve. *Brain Res Bull,* 10**,** 433-6.

Hell, J. W., Edelmann, L., Hartinger, J. & Jahn, R. 1991. Functional reconstitution of the gamma-aminobutyric acid transporter from synaptic vesicles using artificial ion gradients. *Biochemistry,* 30**,** 11795-800.

Hell, J. W., Maycox, P. R. & Jahn, R. 1990. Energy dependence and functional reconstitution of the gamma-aminobutyric acid carrier from synaptic vesicles. *J Biol Chem,* 265**,** 2111-7.

Hell, J. W., Maycox, P. R., Stadler, H. & Jahn, R. 1988. Uptake of GABA by rat brain synaptic vesicles isolated by a new procedure. *EMBO J,* 7**,** 3023-9.

Helms, A. W. & Johnson, J. E. 2003. Specification of dorsal spinal cord interneurons. *Curr Opin Neurobiol,* 13**,** 42-9.

Hindmarch, C. C., Fry, M., Smith, P. M., Yao, S. T., Hazell, G. G., Lolait, S. J., Paton, J. F., Ferguson, A. V. & Murphy, D. 2011. The transcriptome of the medullary area postrema: the thirsty rat, the hungry rat and the hypertensive rat. *Exp Physiol,* 96**,** 495-504.

Hodgson, A. J., Penke, B., Erdei, A., Chubb, I. W. & Somogyi, P. 1985. Antisera to gamma-aminobutyric acid. I. Production and characterization using a new model system. *J Histochem Cytochem,* 33**,** 229-39.

Holstege, J. C., Van Dijken, H., Buijs, R. M., Goedknegt, H., Gosens, T. & Bongers, C. M. 1996. Distribution of dopamine immunoreactivity in the rat, cat and monkey spinal cord. *J Comp Neurol,* 376**,** 631-52.

Horn, R. & Marty, A. 1988. Muscarinic activation of ionic currents measured by a new whole-cell recording method. *J Gen Physiol,* 92**,** 145-59.

Hosoya, Y., Nadelhaft, I., Wang, D. & Kohno, K. 1994. Thoracolumbar sympathetic preganglionic neurons in the dorsal commissural nucleus of the male rat: an immunohistochemical study using retrograde labeling of cholera toxin subunit B. *Exp Brain Res,* 98**,** 21-30.

Hsu, S. M. & Raine, L. 1981. Protein A, avidin, and biotin in immunohistochemistry. *J Histochem Cytochem,* 29**,** 1349-53.

Huang, J., Chen, J., Wang, W., Wei, Y. Y., Cai, G. H., Tamamaki, N., Li, Y. Q. & Wu, S. X. 2013. Birthdate study of GABAergic neurons in the lumbar spinal cord of the glutamic acid decarboxylase 67-green fluorescent protein knock-in mouse. *Front Neuroanat,* 7**,** 42.

Huang, S. N., Minassian, H. & More, J. D. 1976. Application of immunofluorescent staining on paraffin sections improved by trypsin digestion. *Lab Invest,* 35**,** 383-90.

Hughes, D. I., Mackie, M., Nagy, G. G., Riddell, J. S., Maxwell, D. J., Szabo, G., Erdelyi, F., Veress, G., Szucs, P., Antal, M. & Todd, A. J. 2005. P boutons in lamina IX of the rodent spinal cord express high levels of glutamic acid decarboxylase-65 and originate from cells in deep medial dorsal horn. *Proc Natl Acad Sci U S A,* 102**,** 9038-43.

Hughes, D. I., Sikander, S., Kinnon, C. M., Boyle, K. A., Watanabe, M., Callister, R. J. & Graham, B. A. 2012. Morphological, neurochemical and electrophysiological features of parvalbumin-expressing cells: a likely source of axo-axonic inputs in the mouse spinal dorsal horn. *J Physiol,* 590**,** 3927-51.

Hunt, S. P. & Rossi, J. 1985. Peptide- and non-peptide-containing unmyelinated primary afferents: the parallel processing of nociceptive information. *Philos Trans R Soc Lond B Biol Sci,* 308**,** 283-9.

Ibanez, C. F., Ernfors, P. & Persson, H. 1991. Developmental and regional expression of choline acetyltransferase mRNA in the rat central nervous system. *J Neurosci Res,* 29**,** 163-71.

Iceman, K. E., Richerson, G. B. & Harris, M. B. 2013. Medullary serotonin neurons are CO2 sensitive in situ. *J Neurophysiol,* 110**,** 2536-44.

Ikegaki, N., Saito, N., Hashima, M. & Tanaka, C. 1994. Production of specific antibodies against GABA transporter subtypes (GAT1, GAT2, GAT3) and their application to immunocytochemistry. *Brain Res Mol Brain Res,* 26**,** 47-54.

Inoue, T., Chandler, S. H. & Goldberg, L. J. 1994. Neuropharmacological mechanisms underlying rhythmical discharge in trigeminal interneurons during fictive mastication. *J Neurophysiol,* 71**,** 2061-73.

Ishibashi, H., Yamaguchi, J., Nakahata, Y. & Nabekura, J. 2013. Dynamic regulation of glycine-GABA co-transmission at spinal inhibitory synapses by neuronal glutamate transporter. *J Physiol,* 591**,** 3821-32.

Ishizuka, N., Mannen, H., Hongo, T. & Sasaki, S. 1979. Trajectory of group Ia afferent fibers stained with horseradish peroxidase in the lumbosacral spinal cord of the cat: three dimensional reconstructions from serial sections. *J Comp Neurol,* 186**,** 189-211.

Itouji, A., Sakai, N., Tanaka, C. & Saito, N. 1996. Neuronal and glial localization of two GABA transporters (GAT1 and GAT3) in the rat cerebellum. *Brain Res Mol Brain Res,* 37**,** 309-16.

Iversen, L. L. & Kelly, J. S. 1975. Uptake and metabolism of gamma-aminobutyric acid by neurones and glial cells. *Biochem Pharmacol,* 24**,** 933-8.

Izzo, P. N., Sykes, R. M. & Spyer, K. M. 1992. gamma-Aminobutyric acid immunoreactive structures in the nucleus tractus solitarius: a light and electron microscopic study. *Brain Res,* 591**,** 69-78.

Jankowska, E. & Lindstrom, S. 1972. Morphology of interneurones mediating Ia reciprocal inhibition of motoneurones in the spinal cord of the cat. *J Physiol,* 226**,** 805-23.

Jessell, T. M. 2000. Neuronal specification in the spinal cord: inductive signals and transcriptional codes. *Nat Rev Genet,* 1**,** 20-9.

Jia, H. G., Yamuy, J., Sampogna, S., Morales, F. R. & Chase, M. H. 2003. Colocalization of gamma-aminobutyric acid and acetylcholine in neurons in the laterodorsal and pedunculopontine tegmental nuclei in the cat: a light and electron microscopic study. *Brain Res,* 992**,** 205-19.

Johann, S., Dahm, M., Kipp, M., Zahn, U. & Beyer, C. 2011. Regulation of choline acetyltransferase expression by 17 beta-oestradiol in NSC-34 cells and in the spinal cord. *J Neuroendocrinol,* 23**,** 839-48.

Jonas, P., Bischofberger, J. & Sandkuhler, J. 1998. Corelease of two fast neurotransmitters at a central synapse. *Science,* 281**,** 419-24.

Joshi, S. & Hawken, M. J. 2006. Loose-patch-juxtacellular recording in vivo--a method for functional characterization and labeling of neurons in macaque V1. *J Neurosci Methods,* 156**,** 37-49.

Jursky, F. & Nelson, N. 1995. Localization of glycine neurotransmitter transporter (GLYT2) reveals correlation with the distribution of glycine receptor. *J Neurochem,* 64**,** 1026-33.

Kaduri, A. J., Magoul, R., Lescaudron, L., Campistron, G. & Calas, A. 1987. Immunocytochemical approach of GABAergic innervation of the mouse spinal cord using antibodies to GABA. *J Hirnforsch,* 28**,** 349-55.

Kalia, M., Fuxe, K., Hokfelt, T., Johansson, O., Lang, R., Ganten, D., Cuello, C. & Terenius, L. 1984. Distribution of neuropeptide immunoreactive nerve terminals within the subnuclei of the nucleus of the tractus solitarius of the rat. *J Comp Neurol,* 222**,** 409-44.

Kalia, M. & Mesulam, M. M. 1980. Brain stem projections of sensory and motor components of the vagus complex in the cat: I. The cervical vagus and nodose ganglion. *J Comp Neurol,* 193**,** 435-65.

Kalia, M. & Sullivan, J. M. 1982. Brainstem projections of sensory and motor components of the vagus nerve in the rat. *J Comp Neurol,* 211**,** 248-65.

Karunaratne, A., Hargrave, M., Poh, A. & Yamada, T. 2002. GATA proteins identify a novel ventral interneuron subclass in the developing chick spinal cord. *Dev Biol,* 249**,** 30-43.

Kaupmann, K., Huggel, K., Heid, J., Flor, P. J., Bischoff, S., Mickel, S. J., Mcmaster, G., Angst, C., Bittiger, H., Froestl, W. & Bettler, B. 1997. Expression cloning of GABA(B) receptors uncovers similarity to metabotropic glutamate receptors. *Nature,* 386**,** 239-46.

Kawai, Y. & Senba, E. 1999. Electrophysiological and morphological characterization of cytochemically-defined neurons in the caudal nucleus of tractus solitarius of the rat. *Neuroscience,* 89**,** 1347-55.

Kaye, R. G., Saldanha, J. W., Lu, Z. L. & Hulme, E. C. 2011. Helix 8 of the M1 muscarinic acetylcholine receptor: scanning mutagenesis delineates a G protein recognition site. *Mol Pharmacol,* 79**,** 701-9.

Kingsley, R. E. 2000. *Concise Text of Neuroscience,* Baltimore, Lippincott Williams & Wilkins.

Kish, P. E., Fischer-Bovenkerk, C. & Ueda, T. 1989. Active transport of gamma-aminobutyric acid and glycine into synaptic vesicles. *Proc Natl Acad Sci U S A,* 86**,** 3877-81.

Kobayashi, R. M., Palkovits, M., Hruska, R. E., Rothschild, R. & Yamamura, H. I. 1978. Regional distribution of muscarinic cholinergic receptors in rat brain. *Brain Res,* 154**,** 13-23.

Kolisnyk, B., Guzman, M. S., Raulic, S., Fan, J., Magalhaes, A. C., Feng, G., Gros, R., Prado, V. F. & Prado, M. A. 2013. ChAT-ChR2-EYFP mice have enhanced motor endurance but show deficits in attention and several additional cognitive domains. *J Neurosci,* 33**,** 10427-38.

Kosaka, T., Tauchi, M. & Dahl, J. L. 1988. Cholinergic neurons containing GABA-like and/or glutamic acid decarboxylase-like immunoreactivities in various brain regions of the rat. *Exp Brain Res,* 70**,** 605-17.

Krasteva, G., Hartmann, P., Papadakis, T., Bodenbenner, M., Wessels, L., Weihe, E., Schutz, B., Langheinrich, A. C., Chubanov, V., Gudermann, T., Ibanez-Tallon, I. & Kummer, W. 2012. Cholinergic chemosensory cells in the auditory tube. *Histochem Cell Biol,* 137**,** 483-97.

Krnjevic, K. & Schwartz, S. 1967. The action of gamma-aminobutyric acid on cortical neurones. *Exp Brain Res,* 3**,** 320-36.

Kruse, A. C., Hu, J., Pan, A. C., Arlow, D. H., Rosenbaum, D. M., Rosemond, E., Green, H. F., Liu, T., Chae, P. S., Dror, R. O., Shaw, D. E., Weis, W. I., Wess, J. & Kobilka, B. K. 2012. Structure and dynamics of the M3 muscarinic acetylcholine receptor. *Nature,* 482**,** 552-6.

Ladewig, T., Kloppenburg, P., Lalley, P. M., Zipfel, W. R., Webb, W. W. & Keller, B. U. 2003. Spatial profiles of store-dependent calcium release in motoneurones of the nucleus hypoglossus from newborn mouse. *J Physiol,* 547**,** 775-87.

Lagerback, P. A. & Kellerth, J. O. 1985. Light microscopic observations on cat Renshaw cells after intracellular staining with horseradish peroxidase. II. The cell bodies and dendrites. *J Comp Neurol,* 240**,** 368-76.

Lamotte, C. 1977. Distribution of the tract of Lissauer and the dorsal root fibers in the primate spinal cord. *J Comp Neurol,* 172**,** 529-61.

Lamotte, C. C. & Shapiro, C. M. 1991. Ultrastructural localization of substance P, met-enkephalin, and somatostatin immunoreactivity in lamina X of the primate spinal cord. *J Comp Neurol,* 306**,** 290-306.

Lang-Lazdunski, L., Matsushita, K., Hirt, L., Waeber, C., Vonsattel, J. P., Moskowitz, M. A. & Dietrich, W. D. 2000. Spinal cord ischemia. Development of a model in the mouse. *Stroke,* 31**,** 208-13.

Langley, J. N. 1921. *The Autonomic Nervous System,* Cambridge, W. Heffer and Sons.

Lee, S., Kim, K. & Zhou, Z. J. 2010. Role of ACh-GABA cotransmission in detecting image motion and motion direction. *Neuron,* 68**,** 1159-72.

Light, A. R. & Perl, E. R. 1979. Spinal termination of functionally identified primary afferent neurons with slowly conducting myelinated fibers. *J Comp Neurol,* 186**,** 133-50.

Lin, H., Heo, B. H., Kim, W. M., Kim, Y. C. & Yoon, M. H. 2015. Antiallodynic effect of tianeptine via modulation of the 5-HT7 receptor of GABAergic interneurons in the spinal cord of neuropathic rats. *Neurosci Lett,* 598**,** 91-5.

Lipmann, F. 1953. Development of the acetylation problem: a personal account. *Nobel Lecture*.

Lipton, M. A. & Barron, E. S. 1946. On the mechanism of the anaerobic synthesis of acetylcholine. *J Biol Chem,* 166**,** 367-80.

Liu, Q. R., Lopez-Corcuera, B., Mandiyan, S., Nelson, H. & Nelson, N. 1993. Molecular characterization of four pharmacologically distinct gamma-aminobutyric acid transporters in mouse brain [corrected]. *J Biol Chem,* 268**,** 2106-12.

Llewellyn-Smith, I. J., Marina, N., Manton, R. N., Reimann, F., Gribble, F. M. & Trapp, S. 2015. Spinally projecting preproglucagon axons preferentially innervate sympathetic preganglionic neurons. *Neuroscience,* 284**,** 872-87.

Loewi, O. 1921. Pfluger's Arch. *Ges Physiol,* cxcix**,** 239.

Loewy, A. D. 1990a. Anatomy of the Autonomic Nervous System: An Overview. *In:* Loewy, A. D. & Spyer, K. M. (eds.) *Central Regulation of Autonomic Functions.* New York: Oxford University Press.

Loewy, A. D. 1990b. Central Autonomic Pathways. *In:* Loewy, A. D. & Spyer, K. M. (eds.) *Central Regulation of Autonomic Functions.* New York: Oxford University Press.

Loewy, A. D. & Burton, H. 1978. Nuclei of the solitary tract: efferent projections to the lower brain stem and spinal cord of the cat. *J Comp Neurol,* 181**,** 421-49.

Longstaff, A. 2005. *Neuroscience*, Taylor & Francis.

Lopez-Bendito, G., Sturgess, K., Erdelyi, F., Szabo, G., Molnar, Z. & Paulsen, O. 2004. Preferential origin and layer destination of GAD65-GFP cortical interneurons. *Cereb Cortex,* 14**,** 1122-33.

Lopez-Corcuera, B., Liu, Q. R., Mandiyan, S., Nelson, H. & Nelson, N. 1992. Expression of a mouse brain cDNA encoding novel gamma-aminobutyric acid transporter. *J Biol Chem,* 267**,** 17491-3.

Lu, D. C., Niu, T. & Alaynick, W. A. 2015. Molecular and cellular development of spinal cord locomotor circuitry. *Front Mol Neurosci,* 8**,** 25.

Lu, Y. & Perl, E. R. 2003. A specific inhibitory pathway between substantia gelatinosa neurons receiving direct C-fiber input. *J Neurosci,* 23**,** 8752-8.

Lu, Y. & Perl, E. R. 2005. Modular organization of excitatory circuits between neurons of the spinal superficial dorsal horn (laminae I and II). *J Neurosci,* 25**,** 3900-7.

Lukas, R. J., Changeux, J. P., Le Novere, N., Albuquerque, E. X., Balfour, D. J., Berg, D. K., Bertrand, D., Chiappinelli, V. A., Clarke, P. B., Collins, A. C., Dani, J. A., Grady, S. R., Kellar, K. J., Lindstrom, J. M., Marks, M. J., Quik, M., Taylor, P. W. & Wonnacott, S. 1999. International Union of Pharmacology. XX. Current status of the nomenclature for nicotinic acetylcholine receptors and their subunits. *Pharmacol Rev,* 51**,** 397-401.

Luo, W., Enomoto, H., Rice, F. L., Milbrandt, J. & Ginty, D. D. 2009. Molecular identification of rapidly adapting mechanoreceptors and their developmental dependence on ret signaling. *Neuron,* 64**,** 841-56.

Mackie, M., Hughes, D. I., Maxwell, D. J., Tillakaratne, N. J. & Todd, A. J. 2003. Distribution and colocalisation of glutamate decarboxylase isoforms in the rat spinal cord. *Neuroscience,* 119**,** 461-72.

Madisen, L., Garner, A. R., Shimaoka, D., Chuong, A. S., Klapoetke, N. C., Li, L., Van Der Bourg, A., Niino, Y., Egolf, L., Monetti, C., Gu, H., Mills, M., Cheng, A., Tasic, B., Nguyen, T. N., Sunkin, S. M., Benucci, A., Nagy, A., Miyawaki, A., Helmchen, F., Empson, R. M., Knopfel, T., Boyden, E. S., Reid, R. C., Carandini, M. & Zeng, H. 2015. Transgenic mice for intersectional targeting of neural sensors and effectors with high specificity and performance. *Neuron,* 85**,** 942-58.

Maeda, M., Ohba, N., Nakagomi, S., Suzuki, Y., Kiryu-Seo, S., Namikawa, K., Kondoh, W., Tanaka, A. & Kiyama, H. 2004. Vesicular acetylcholine transporter can be a morphological marker for the reinnervation to muscle of regenerating motor axons. *Neurosci Res,* 48**,** 305-14.

Maqbool, A., Batten, T. F. & Mcwilliam, P. N. 1991. Ultrastructural Relationships Between GABAergic Terminals and Cardiac Vagal Preganglionic Motoneurons and Vagal Afferents in the Cat: A Combined HRP Tracing and Immunogold Labelling Study. *Eur J Neurosci,* 3**,** 501-513.

Marnay, A. & Nachmansohn, D. 1937. Cholinesterase in voluntary frog's muscle. *J Physiol,* 89**,** 359-67.

Marshall, F. H., Jones, K. A., Kaupmann, K. & Bettler, B. 1999. GABAB receptors - the first 7TM heterodimers. *Trends Pharmacol Sci,* 20**,** 396-9.

Mason, D. Y. & Sammons, R. 1978. Alkaline phosphatase and peroxidase for double immunoenzymatic labelling of cellular constituents. *J Clin Pathol,* 31**,** 454-60.

Matos, L. L., Trufelli, D. C., De Matos, M. G. & Da Silva Pinhal, M. A. 2010. Immunohistochemistry as an important tool in biomarkers detection and clinical practice. *Biomark Insights,* 5**,** 9-20.

Matsumoto, M., Xie, W., Inoue, M. & Ueda, H. 2007. Evidence for the tonic inhibition of spinal pain by nicotinic cholinergic transmission through primary afferents. *Mol Pain,* 3**,** 41.

Maxwell, D. J., Christie, W. M., Short, A. D. & Brown, A. G. 1990. Direct observations of synapses between GABA-immunoreactive boutons and muscle afferent terminals in lamina VI of the cat's spinal cord. *Brain Res,* 530**,** 215-22.

Maxwell, L., Maxwell, D. J., Neilson, M. & Kerr, R. 1996. A confocal microscopic survey of serotoninergic axons in the lumbar spinal cord of the rat: co-localization with glutamate decarboxylase and neuropeptides. *Neuroscience,* 75**,** 471-80.

Mchanwell, S. & Watson, C. 2009. Localization of Motoneurons in the Spinal Cord. *In:* Watson, C., Paxinos, G. & Kayalioglu, G. (ed.) *The Spinal Cord.* Amsterdam: Academic Press.

Mcintire, S. L., Reimer, R. J., Schuske, K., Edwards, R. H. & Jorgensen, E. M. 1997. Identification and characterization of the vesicular GABA transporter. *Nature,* 389**,** 870-6.

Mckitrick, D. J. & Calaresu, F. R. 1991. Cardiovascular responses to combined microinjection of substance P and acetylcholine in the intermediolateral nucleus of the rat. *J Auton Nerv Syst,* 32**,** 69-75.

Mclaughlin, B. J. 1972. Propriospinal and supraspinal projections to the motor nuclei in the cat spinal cord. *J Comp Neurol,* 144**,** 475-500.

Mclaughlin, B. J., Barber, R., Saito, K., Roberts, E. & Wu, J. Y. 1975. Immunocytochemical localization of glutamate decarboxylase in rat spinal cord. *J Comp Neurol,* 164**,** 305-21.

Meeley, M. P., Ruggiero, D. A., Ishitsuka, T. & Reis, D. J. 1985. Intrinsic gamma-aminobutyric acid neurons in the nucleus of the solitary tract and the rostral ventrolateral medulla of the rat: an immunocytochemical and biochemical study. *Neurosci Lett,* 58**,** 83-9.

Mei, L., Zhang, J. & Mifflin, S. 2003. Hypertension alters GABA receptor-mediated inhibition of neurons in the nucleus of the solitary tract. *Am J Physiol Regul Integr Comp Physiol,* 285**,** R1276-86.

Menetrey, D. & Basbaum, A. I. 1987. Spinal and trigeminal projections to the nucleus of the solitary tract: a possible substrate for somatovisceral and viscerovisceral reflex activation. *J Comp Neurol,* 255**,** 439-50.

Menetrey, D. & De Pommery, J. 1991. Origins of Spinal Ascending Pathways that Reach Central Areas Involved in Visceroception and Visceronociception in the Rat. *Eur J Neurosci,* 3**,** 249-259.

Mesnage, B., Gaillard, S., Godin, A. G., Rodeau, J. L., Hammer, M., Von Engelhardt, J., Wiseman, P. W., De Koninck, Y., Schlichter, R. & Cordero-Erausquin, M. 2011. Morphological and functional characterization of cholinergic interneurons in the dorsal horn of the mouse spinal cord. *J Comp Neurol,* 519**,** 3139-58.

Miles, G. B., Hartley, R., Todd, A. J. & Brownstone, R. M. 2007. Spinal cholinergic interneurons regulate the excitability of motoneurons during locomotion. *Proc Natl Acad Sci U S A,* 104**,** 2448-53.

Miller, P. S. & Smart, T. G. 2010. Binding, activation and modulation of Cys-loop receptors. *Trends Pharmacol Sci,* 31**,** 161-74.

Milligan, C. J., Buckley, N. J., Garret, M., Deuchars, J. & Deuchars, S. A. 2004. Evidence for inhibition mediated by coassembly of GABAA and GABAC receptor subunits in native central neurons. *J Neurosci,* 24**,** 7241-50.

Mitra, P. & Brownstone, R. M. 2012. An in vitro spinal cord slice preparation for recording from lumbar motoneurons of the adult mouse. *J Neurophysiol,* 107**,** 728-41.

Molecularprobes 2001. CellTracker™ Probes for Long-Term Tracing of Living Cells.

Moreira, I. S. 2014. Structural features of the G-protein/GPCR interactions. *Biochim Biophys Acta,* 1840**,** 16-33.

Mtui, E. P., Anwar, M., Gomez, R., Reis, D. J. & Ruggiero, D. A. 1993. Projections from the nucleus tractus solitarii to the spinal cord. *J Comp Neurol,* 337**,** 231-52.

Mueller, A. L., Chesnut, R. M. & Schwartzkroin, P. A. 1983. Actions of GABA in developing rabbit hippocampus: an in vitro study. *Neurosci Lett,* 39**,** 193-8.

Muennich, E. A. & Fyffe, R. E. 2004. Focal aggregation of voltage-gated, Kv2.1 subunit-containing, potassium channels at synaptic sites in rat spinal motoneurones. *J Physiol,* 554**,** 673-85.

Muller, T., Brohmann, H., Pierani, A., Heppenstall, P. A., Lewin, G. R., Jessell, T. M. & Birchmeier, C. 2002. The homeodomain factor lbx1 distinguishes two major programs of neuronal differentiation in the dorsal spinal cord. *Neuron,* 34**,** 551-62.

Nachmansohn, D. & Berman, M. 1946. Studies on choline acetylase; on the preparation of the coenzyme and its effect on the enzyme. *J Biol Chem,* 165**,** 551-63.

Nachmansohn, D. & Machado, A. L. 1943. The formation of acetylcholine. A new enzyme: "Choline acetylase". *J Neurophysiol,* 6**,** 397-403.

Nagode, D. A., Tang, A. H., Karson, M. A., Klugmann, M. & Alger, B. E. 2011. Optogenetic release of ACh induces rhythmic bursts of perisomatic IPSCs in hippocampus. *PLoS One,* 6**,** e27691.

Nahin, R. L., Madsen, A. M. & Giesler, G. J., Jr. 1983. Anatomical and physiological studies of the gray matter surrounding the spinal cord central canal. *J Comp Neurol,* 220**,** 321-35.

Nakane, P. K. & Pierce, G. B., Jr. 1966. Enzyme-labeled antibodies: preparation and application for the localization of antigens. *J Histochem Cytochem,* 14**,** 929-31.

Nayak, B. K. 2010. Understanding the relevance of sample size calculation. *Indian J Ophthalmol,* 58**,** 469-70.

Nelson, A. B., Bussert, T. G., Kreitzer, A. C. & Seal, R. P. 2014. Striatal cholinergic neurotransmission requires VGLUT3. *J Neurosci,* 34**,** 8772-7.

Newton, B. W. & Hamill, R. W. 1989. Immunohistochemical distribution of serotonin in spinal autonomic nuclei: I. Fiber patterns in the adult rat. *J Comp Neurol,* 279**,** 68-81.

Nguyen, L. T. & Grzywacz, N. M. 2000. Colocalization of choline acetyltransferase and gamma-aminobutyric acid in the developing and adult turtle retinas. *J Comp Neurol,* 420**,** 527-38.

Nicholas, A. P., Zhang, X. & Hokfelt, T. 1999. An immunohistochemical investigation of the opioid cell column in lamina X of the male rat lumbosacral spinal cord. *Neurosci Lett,* 270**,** 9-12.

Notter, T., Panzanelli, P., Pfister, S., Mircsof, D. & Fritschy, J. M. 2014. A protocol for concurrent high-quality immunohistochemical and biochemical analyses in adult mouse central nervous system. *Eur J Neurosci,* 39**,** 165-75.

Okada, T., Tashiro, Y., Kato, F., Yanagawa, Y., Obata, K. & Kawai, Y. 2008. Quantitative and immunohistochemical analysis of neuronal types in the mouse caudal nucleus tractus solitarius: focus on GABAergic neurons. *J Chem Neuroanat,* 35**,** 275-84.

Okada, T., Yoshioka, M., Inoue, K. & Kawai, Y. 2006. Local axonal arborization patterns of distinct neuronal types in the caudal nucleus of the tractus solitarius. *Brain Res,* 1083**,** 134-44.

Oliva, A. A., Jr., Jiang, M., Lam, T., Smith, K. L. & Swann, J. W. 2000. Novel hippocampal interneuronal subtypes identified using transgenic mice that express green fluorescent protein in GABAergic interneurons. *J Neurosci,* 20**,** 3354-68.

Olsen, R. W. & Sieghart, W. 2008. International Union of Pharmacology. LXX. Subtypes of gamma-aminobutyric acid(A) receptors: classification on the basis of subunit composition, pharmacology, and function. Update. *Pharmacol Rev,* 60**,** 243-60.

Papke, R. L., Bencherif, M. & P., L. 1996. An evaluation of neuronal nicotinic acetylcholine receptor activation by quaternary nitrogen compounds indicates that choline is selective for the alpha 7 subtype. *Neurosci Lett,* 213**,** 201-4.

Pawlowski, S. A., Gaillard, S., Ghorayeb, I., Ribeiro-Da-Silva, A., Schlichter, R. & Cordero-Erausquin, M. 2013. A novel population of cholinergic neurons in the macaque spinal dorsal horn of potential clinical relevance for pain therapy. *J Neurosci,* 33**,** 3727-37.

Paxinos, G. & Watson, C. 1997. The rat brain in stereotaxic coordinates, Compact. *San Diego: Academic Press. Figure,* 1**,** 25-30.

Pechura, C. M. & Liu, R. P. 1986. Spinal neurons which project to the periaqueductal gray and the medullary reticular formation via axon collaterals: a double-label fluorescence study in the rat. *Brain Res,* 374**,** 357-61.

Perry, E., Walker, M., Grace, J. & Perry, R. 1999. Acetylcholine in mind: a neurotransmitter correlate of consciousness? *Trends Neurosci,* 22**,** 273-80.

Perry, E. K., Tomlinson, B. E., Blessed, G., Bergmann, K., Gibson, P. H. & Perry, R. H. 1978. Correlation of cholinergic abnormalities with senile plaques and mental test scores in senile dementia. *Br Med J,* 2**,** 1457-9.

Petras, J. M. & Cummings, J. F. 1972. Autonomic neurons in the spinal cord of the Rhesus monkey: a correlation of the findings of cytoarchitectonics and sympathectomy with fiber degeneration following dorsal rhizotomy. *J Comp Neurol,* 146**,** 189-218.

Pierani, A., Moran-Rivard, L., Sunshine, M. J., Littman, D. R., Goulding, M. & Jessell, T. M. 2001. Control of interneuron fate in the developing spinal cord by the progenitor homeodomain protein Dbx1. *Neuron,* 29**,** 367-84.

Pilowsky, P. M. & Makeham, J. 2001. Juxtacellular labeling of identified neurons: kiss the cells and make them dye. *J Comp Neurol,* 433**,** 1-3.

Pinault, D. 1996. A novel single-cell staining procedure performed in vivo under electrophysiological control: morpho-functional features of juxtacellularly labeled thalamic cells and other central neurons with biocytin or Neurobiotin. *J Neurosci Methods,* 65**,** 113-36.

Pituello, F. 1997. Neuronal specification: generating diversity in the spinal cord. *Curr Biol,* 7**,** R701-4.

Platel, J. C., Stamboulian, S., Nguyen, I. & Bordey, A. 2010. Neurotransmitter signaling in postnatal neurogenesis: The first leg. *Brain Res Rev,* 63**,** 60-71.

Plotkin, M. D., Snyder, E. Y., Hebert, S. C. & Delpire, E. 1997. Expression of the Na-K-2Cl cotransporter is developmentally regulated in postnatal rat brains: a possible mechanism underlying GABA's excitatory role in immature brain. *J Neurobiol,* 33**,** 781-95.

Polak, J. M. & Van Noorden, S. 2003. *Introduction to Immunocytochemistry,* Trowbridge BIOS scientific Publishers Limited.

Polgar, E., Durrieux, C., Hughes, D. I. & Todd, A. J. 2013. A quantitative study of inhibitory interneurons in laminae I-III of the mouse spinal dorsal horn. *PLoS One,* 8**,** e78309.

Polgar, E., Hughes, D. I., Riddell, J. S., Maxwell, D. J., Puskar, Z. & Todd, A. J. 2003. Selective loss of spinal GABAergic or glycinergic neurons is not necessary for development of thermal hyperalgesia in the chronic constriction injury model of neuropathic pain. *Pain,* 104**,** 229-39.

Poole, S. L., Deuchars, J., Lewis, D. I. & Deuchars, S. A. 2007. Subdivision-specific responses of neurons in the nucleus of the tractus solitarius to activation of mu-opioid receptors in the rat. *J Neurophysiol,* 98**,** 3060-71.

Portillo, F., Pasaro, R. & Delgado-Garcia, J. M. 1986. Spinal projections of brainstem respiratory related neurons in the cat as revealed by retrograde fluorescent markers. *Rev Esp Fisiol,* 42**,** 483-8.

Price, C. J., Hoyda, T. D. & Ferguson, A. V. 2008. The area postrema: a brain monitor and integrator of systemic autonomic state. *Neuroscientist,* 14**,** 182-94.

Price, T. J., Hargreaves, K. M. & Cervero, F. 2006. Protein expression and mRNA cellular distribution of the NKCC1 cotransporter in the dorsal root and trigeminal ganglia of the rat. *Brain Res,* 1112**,** 146-58.

Puche, A. C., Heyward, P. & Shipley, M. T. 2004. Transmembrane dye labeling and immunohistochemical staining of electrophysiologically characterized single neurons. *J Neurosci Methods,* 137**,** 235-40.

Purves, D., Augustine, G.J., Fitzpatrick, D., Hall, W.C., Lamantia, A.S., Mcnamara, J.O. & White, L.E. 2008. *Neuroscience,* 4th edn. Sunderland (MA), Sinauer Associates Inc.

Radian, R., Ottersen, O. P., Storm-Mathisen, J., Castel, M. & Kanner, B. I. 1990. Immunocytochemical localization of the GABA transporter in rat brain. *J Neurosci,* 10**,** 1319-30.

Ramerstorfer, J., Furtmuller, R., Sarto-Jackson, I., Varagic, Z., Sieghart, W. & Ernst, M. 2011. The GABAA receptor alpha+beta- interface: a novel target for subtype selective drugs. *J Neurosci,* 31**,** 870-7.

Ren, J., Qin, C., Hu, F., Tan, J., Qiu, L., Zhao, S., Feng, G. & Luo, M. 2011. Habenula "cholinergic" neurons co-release glutamate and acetylcholine and activate postsynaptic neurons via distinct transmission modes. *Neuron,* 69**,** 445-52.

Rexed, B. 1952. The cytoarchitectonic organization of the spinal cord in the cat. *J Comp Neurol,* 96**,** 414-95.

Rexed, B. 1954. A cytoarchitectonic atlas of the spinal cord in the cat. *J Comp Neurol,* 100**,** 297-379.

Ribak, C. E., Vaughn, J. E. & Saito, K. 1978. Immunocytochemical localization of glutamic acid decarboxylase in neuronal somata following colchicine inhibition of axonal transport. *Brain Res,* 140**,** 315-32.

Ribak, C. E., Vaughn, J. E., Saito, K., Barber, R. & Roberts, E. 1976. Immunocytochemical localization of glutamate decarboxylase in rat substantia nigra. *Brain Res,* 116**,** 287-98.

Roberts, E. & Frankel, S. 1950. gamma-aminobutyric acid in brain: its formation from glutamic acid. *J Biol Chem,* 187**,** 55-63.

Roelink, H., Porter, J. A., Chiang, C., Tanabe, Y., Chang, D. T., Beachy, P. A. & Jessell, T. M. 1995. Floor plate and motor neuron induction by different concentrations of the amino-terminal cleavage product of sonic hedgehog autoproteolysis. *Cell,* 81**,** 445-55.

Roghani, A., Feldman, J., Kohan, S. A., Shirzadi, A., Gundersen, C. B., Brecha, N. & Edwards, R. H. 1994. Molecular cloning of a putative vesicular transporter for acetylcholine. *Proc Natl Acad Sci U S A,* 91**,** 10620-4.

Ross, C. A., Ruggiero, D. A. & Reis, D. J. 1985. Projections from the nucleus tractus solitarii to the rostral ventrolateral medulla. *J Comp Neurol,* 242**,** 511-34.

Rousseau, S. J., Jones, I. W., Pullar, I. A. & Wonnacott, S. 2005. Presynaptic alpha7 and non-alpha7 nicotinic acetylcholine receptors modulate [3H]d-aspartate release from rat frontal cortex in vitro. *Neuropharmacology,* 49**,** 59-72.

Rudolph, U. & Knoflach, F. 2011. Beyond classical benzodiazepines: novel therapeutic potential of GABAA receptor subtypes. *Nat Rev Drug Discov,* 10**,** 685-97.

Ruggiero, D. A., Giuliano, R., Anwar, M., Stornetta, R. & Reis, D. J. 1990. Anatomical substrates of cholinergic-autonomic regulation in the rat. *J Comp Neurol,* 292**,** 1-53.

Ruggiero, D. A., Meeley, M. P., Anwar, M. & Reis, D. J. 1985. Newly identified GABAergic neurons in regions of the ventrolateral medulla which regulate blood pressure. *Brain Res,* 339**,** 171-7.

Sagne, C., El Mestikawy, S., Isambert, M. F., Hamon, M., Henry, J. P., Giros, B. & Gasnier, B. 1997. Cloning of a functional vesicular GABA and glycine transporter by screening of genome databases. *FEBS Lett,* 417**,** 177-83.

Saha, S. 2005. Role of the central nucleus of the amygdala in the control of blood pressure: descending pathways to medullary cardiovascular nuclei. *Clin Exp Pharmacol Physiol,* 32**,** 450-6.

Saito, Y., Zhang, Y. & Yanagawa, Y. 2015. Electrophysiological and morphological properties of neurons in the prepositus hypoglossi nucleus that express both ChAT and VGAT in a double-transgenic rat model. *Eur J Neurosci,* 41**,** 1036-48.

Sapir, T., Geiman, E. J., Wang, Z., Velasquez, T., Mitsui, S., Yoshihara, Y., Frank, E., Alvarez, F. J. & Goulding, M. 2004. Pax6 and engrailed 1 regulate two distinct aspects of renshaw cell development. *J Neurosci,* 24**,** 1255-64.

Sardella, T. C., Polgar, E., Garzillo, F., Furuta, T., Kaneko, T., Watanabe, M. & Todd, A. J. 2011. Dynorphin is expressed primarily by GABAergic neurons that contain galanin in the rat dorsal horn. *Mol Pain,* 7**,** 76.

Saunders, A., Granger, A. J. & Sabatini, B. L. 2015b. Corelease of acetylcholine and GABA from cholinergic forebrain neurons. *Elife,* 4.

Saunders, A., Oldenburg, I. A., Berezovskii, V. K., Johnson, C. A., Kingery, N. D., Elliott, H. L., Xie, T., Gerfen, C. R. & Sabatini, B. L. 2015a. A direct GABAergic output from the basal ganglia to frontal cortex. *Nature,* 521**,** 85-9.

Schofield, P. R., Darlison, M. G., Fujita, N., Burt, D. R., Stephenson, F. A., Rodriguez, H., Rhee, L. M., Ramachandran, J., Reale, V., Glencorse, T. A. & Et Al. 1987. Sequence and functional expression of the GABA A receptor shows a ligand-gated receptor super-family. *Nature,* 328**,** 221-7.

Schon, F. & Kelly, J. S. 1975. Selective uptake of (3H)beta-alanine by glia: association with glial uptake system for GABA. *Brain Res,* 86**,** 243-57.

Scremin, O. U. 2009. The Spinal Cord Blood Vessels. *In:* Watson, C., Paxinos, G. & Kayalioglu, G. (eds.) *The Spinal Cord* Amsterdam: Academic Press.

Seddik, R., Schlichter, R. & Trouslard, J. 2006. Modulation of GABAergic synaptic transmission by terminal nicotinic acetylcholine receptors in the central autonomic nucleus of the neonatal rat spinal cord. *Neuropharmacology,* 51**,** 77-89.

Seddik, R., Schlichter, R. & Trouslard, J. 2007. Corelease of GABA/glycine in lamina-X of the spinal cord of neonatal rats. *Neuroreport,* 18**,** 1025-9.

Sengul, G., Fu, Y., Yu, Y. & Paxinos, G. 2015. Spinal cord projections to the cerebellum in the mouse. *Brain Struct Funct,* 220**,** 2997-3009.

Sengul, G., Puchalski, R. B. & Watson, C. 2012. Cytoarchitecture of the spinal cord of the postnatal (P4) mouse. *Anat Rec (Hoboken),* 295**,** 837-45.

Sengul, G. & Watson, C. 2012. Spinal cord. *In:* Watson, C., Paxinos, G. & Puelles, L. (ed.) *The Mouse Nervous System.* London: Elsevier Inc.

Shapiro, R. E. & Miselis, R. R. 1985. The central neural connections of the area postrema of the rat. *J Comp Neurol,* 234**,** 344-64.

Sherriff, F. E. & Henderson, Z. 1994. A cholinergic propriospinal innervation of the rat spinal cord. *Brain Res,* 634**,** 150-4.

Sherriff, F. E., Henderson, Z. & Morrison, J. F. 1991. Further evidence for the absence of a descending cholinergic projection from the brainstem to the spinal cord in the rat. *Neurosci Lett,* 128**,** 52-6.

Shi, S. R., Cote, R. J. & Taylor, C. R. 1997. Antigen retrieval immunohistochemistry: past, present, and future. *J Histochem Cytochem,* 45**,** 327-43.

Simon, H., Hornbruch, A. & Lumsden, A. 1995. Independent assignment of antero-posterior and dorso-ventral positional values in the developing chick hindbrain. *Curr Biol,* 5**,** 205-14.

Simon, J. R., Dimicco, S. K., Dimicco, J. A. & Aprison, M. H. 1985. Choline acetyltransferase and glutamate uptake in the nucleus tractus solitarius and dorsal motor nucleus of the vagus: effect of nodose ganglionectomy. *Brain Res,* 344**,** 405-8.

Sine, S. M. & Engel, A. G. 2006. Recent advances in Cys-loop receptor structure and function. *Nature,* 440**,** 448-55.

Singer, S. J. 1959. Preparation of an electron-dense antibody conjugate. *Nature,* 183**,** 1523-4.

Smith, G. B. & Olsen, R. W. 1995. Functional domains of GABAA receptors. *Trends Pharmacol Sci,* 16**,** 162-8.

Sneddon, P. & Burnstock, G. 1984. Inhibition of excitatory junction potentials in guinea-pig vas deferens by alpha, beta-methylene-ATP: further evidence for ATP and noradrenaline as cotransmitters. *Eur J Pharmacol,* 100**,** 85-90.

Snell, R. S. 2010. *Clinical Neuroanatomy* .7th edn. Philadelphia, Lippincott Williams & Wilkins.

Song, Z. M., Hu, J., Rudy, B. & Redman, S. J. 2006. Developmental changes in the expression of calbindin and potassium-channel subunits Kv3.1b and Kv3.2 in mouse Renshaw cells. *Neuroscience,* 139**,** 531-8.

Spike, R. C., Todd, A. J. & Johnston, H. M. 1993. Coexistence of NADPH diaphorase with GABA, glycine, and acetylcholine in rat spinal cord. *J Comp Neurol,* 335**,** 320-33.

St John, W. M. 1986. Influence of reticular mechanisms upon hypoglossal, trigeminal and phrenic activities. *Respir Physiol,* 66**,** 27-40.

Stedman, E. & Stedman, E. 1937. The mechanism of the biological synthesis of acetylcholine: The isolation of acetylcholine produced by brain tissue in vitro. *Biochem J,* 31**,** 817-27.

Sternberger, L. A., Hardy, P. H., Jr., Cuculis, J. J. & Meyer, H. G. 1970. The unlabeled antibody enzyme method of immunohistochemistry: preparation and properties of soluble antigen-antibody complex (horseradish peroxidase-antihorseradish peroxidase) and its use in identification of spirochetes. *J Histochem Cytochem,* 18**,** 315-33.

Stornetta, R. L. & Guyenet, P. G. 1999. Distribution of glutamic acid decarboxylase mRNA-containing neurons in rat medulla projecting to thoracic spinal cord in relation to monoaminergic brainstem neurons. *J Comp Neurol,* 407**,** 367-80.

Stornetta, R. L., Macon, C. J., Nguyen, T. M., Coates, M. B. & Guyenet, P. G. 2013. Cholinergic neurons in the mouse rostral ventrolateral medulla target sensory afferent areas. *Brain Struct Funct,* 218**,** 455-75.

Strack, A. M., Sawyer, W. B., Hughes, J. H., Platt, K. B. & Loewy, A. D. 1989a. A general pattern of CNS innervation of the sympathetic outflow demonstrated by transneuronal pseudorabies viral infections. *Brain Res,* 491**,** 156-62.

Strack, A. M., Sawyer, W. B., Marubio, L. M. & Loewy, A. D. 1988. Spinal origin of sympathetic preganglionic neurons in the rat. *Brain Res,* 455**,** 187-91.

Strack, A. M., Sawyer, W. B., Platt, K. B. & Loewy, A. D. 1989b. CNS cell groups regulating the sympathetic outflow to adrenal gland as revealed by transneuronal cell body labeling with pseudorabies virus. *Brain Res,* 491**,** 274-96.

Stradleigh, T. W. & Ishida, A. T. 2015. Fixation strategies for retinal immunohistochemistry. *Prog Retin Eye Res,* 48**,** 181-202.

Su, J., Yin, J., Qin, W., Sha, S., Xu, J. & Jiang, C. 2015. Role for pro-inflammatory cytokines in regulating expression of GABA transporter type 1 and 3 in specific brain regions of kainic acid-induced status epilepticus. *Neurochem Res,* 40**,** 621-7.

Synapseweb. 1999. *Laboratory of Synapse Structure and Function, The University of Texas at Austin* [Online]. Available: http://synapses.clm.utexas.edu/tools/reconstruct/reconstruct.stm [Accessed 13th March 2016].

Tago, H., Mcgeer, P. L., Mcgeer, E. G., Akiyama, H. & Hersh, L. B. 1989. Distribution of choline acetyltransferase immunopositive structures in the rat brainstem. *Brain Res,* 495**,** 271-97.

Takasu, N. & Hashimoto, P. H. 1988. Morphological identification of an interneuron in the hypoglossal nucleus of the rat: a combined Golgi-electron microscopic study. *J Comp Neurol,* 271**,** 461-71.

Takasu, N., Nakatani, T., Arikuni, T. & Kimura, H. 1987. Immunocytochemical localization of gamma-aminobutyric acid in the hypoglossal nucleus of the macaque monkey, Macaca fuscata: a light and electron microscopic study. *J Comp Neurol,* 263**,** 42-53.

Tamamaki, N., Yanagawa, Y., Tomioka, R., Miyazaki, J., Obata, K. & Kaneko, T. 2003. Green fluorescent protein expression and colocalization with calretinin, parvalbumin, and somatostatin in the GAD67-GFP knock-in mouse. *J Comp Neurol,* 467**,** 60-79.

Tanabe, Y. & Jessell, T. M. 1996. Diversity and pattern in the developing spinal cord. *Science,* 274**,** 1115-23.

Tavares, I. & Lima, D. 1994. Descending projections from the caudal medulla oblongata to the superficial or deep dorsal horn of the rat spinal cord. *Exp Brain Res,* 99**,** 455-63.

Thurbon, D., Luscher, H. R., Hofstetter, T. & Redman, S. J. 1998. Passive electrical properties of ventral horn neurons in rat spinal cord slices. *J Neurophysiol,* 80**,** 2485-502.

Tillakaratne, N. J., De Leon, R. D., Hoang, T. X., Roy, R. R., Edgerton, V. R. & Tobin, A. J. 2002. Use-dependent modulation of inhibitory capacity in the feline lumbar spinal cord. *J Neurosci,* 22**,** 3130-43.

Tillakaratne, N. J., Mouria, M., Ziv, N. B., Roy, R. R., Edgerton, V. R. & Tobin, A. J. 2000. Increased expression of glutamate decarboxylase (GAD(67)) in feline lumbar spinal cord after complete thoracic spinal cord transection. *J Neurosci Res,* 60**,** 219-30.

Todd, A. J. 1991. Immunohistochemical evidence that acetylcholine and glycine exist in different populations of GABAergic neurons in lamina III of rat spinal dorsal horn. *Neuroscience,* 44**,** 741-6.

Todd, A. J. 2010. Neuronal circuitry for pain processing in the dorsal horn. *Nat Rev Neurosci,* 11**,** 823-36.

Todd, A. J., Hughes, D. I., Polgar, E., Nagy, G. G., Mackie, M., Ottersen, O. P. & Maxwell, D. J. 2003. The expression of vesicular glutamate transporters VGLUT1 and VGLUT2 in neurochemically defined axonal populations in the rat spinal cord with emphasis on the dorsal horn. *Eur J Neurosci,* 17**,** 13-27.

Todd, A. J. & Maxwell, D. J. 2000. GABA in the mammalian spinal cord. *In:* Martin, D. L. & Olsen, R. W. (eds.) *GABA in the Nervous System: The View at Fifty Years.* Philadelphia: Lippincott Williams & Wilkins.

Todd, A. J. & Mckenzie, J. 1989. GABA-immunoreactive neurons in the dorsal horn of the rat spinal cord. *Neuroscience,* 31**,** 799-806.

Todd, A. J. & Sullivan, A. C. 1990. Light microscope study of the coexistence of GABA-like and glycine-like immunoreactivities in the spinal cord of the rat. *J Comp Neurol,* 296**,** 496-505.

Torvik, A. 1956. Afferent connections to the sensory trigeminal nuclei, the nucleus of the solitary tract and adjacent structures; an experimental study in the rat. *J Comp Neurol,* 106**,** 51-141.

Travagli, R. A., Hermann, G. E., Browning, K. N. & Rogers, R. C. 2006. Brainstem circuits regulating gastric function. *Annu Rev Physiol,* 68**,** 279-305.

Travers, J. B., Dinardo, L. A. & Karimnamazi, H. 1997. Motor and premotor mechanisms of licking. *Neurosci Biobehav Rev,* 21**,** 631-47.

Travers, J. B., Yoo, J. E., Chandran, R., Herman, K. & Travers, S. P. 2005. Neurotransmitter phenotypes of intermediate zone reticular formation projections to the motor trigeminal and hypoglossal nuclei in the rat. *J Comp Neurol,* 488**,** 28-47.

Trifonov, S., Houtani, T., Kase, M., Toida, K., Maruyama, M., Yamashita, Y., Shimizu, J. & Sugimoto, T. 2012. Lateral regions of the rodent striatum reveal elevated glutamate decarboxylase 1 mRNA expression in medium-sized projection neurons. *Eur J Neurosci,* 35**,** 711-22.

Tsukamoto, K., Yin, M. & Sved, A. F. 1994. Effect of atropine injected into the nucleus tractus solitarius on the regulation of blood pressure. *Brain Res,* 648**,** 9-15.

Udenfriend, S. 1950. Identification of gamma-aminobutyric acid in brain by the isotope derivative method. *J Biol Chem,* 187**,** 65-9.

Unwin, N. 2005. Refined structure of the nicotinic acetylcholine receptor at 4A resolution. *J Mol Biol,* 346**,** 967-89.

Unwin, N. 2013. Nicotinic acetylcholine receptor and the structural basis of neuromuscular transmission: insights from Torpedo postsynaptic membranes. *Q Rev Biophys,* 46**,** 283-322.

Unwin, N., Toyoshima, C. & Kubalek, E. 1988. Arrangement of the acetylcholine receptor subunits in the resting and desensitized states, determined by cryoelectron microscopy of crystallized Torpedo postsynaptic membranes. *J Cell Biol,* 107**,** 1123-38.

Usdin, T. B., Eiden, L. E., Bonner, T. I. & Erickson, J. D. 1995. Molecular biology of the vesicular ACh transporter. *Trends Neurosci,* 18**,** 218-24.

Van Der Kooy, D. & Koda, L. Y. 1983. Organization of the projections of a circumventricular organ: the area postrema in the rat. *J Comp Neurol,* 219**,** 328-38.

Vanderhorst, V. G. & Ulfhake, B. 2006. The organization of the brainstem and spinal cord of the mouse: relationships between monoaminergic, cholinergic, and spinal projection systems. *J Chem Neuroanat,* 31**,** 2-36.

Voytenko, L. P., Lushnikova, I. V., Savotchenko, A. V., Isaeva, E. V., Skok, M. V., Lykhmus, O. Y., Patseva, M. A. & Skibo, G. G. 2015. Hippocampal GABAergic interneurons coexpressing alpha7-nicotinic receptors and connexin-36 are able to improve neuronal viability under oxygen-glucose deprivation. *Brain Res,* 1616**,** 134-45.

Walberg, F. & Ottersen, O. P. 1992. Neuroactive amino acids in the area postrema. An immunocytochemical investigation in rat with some observations in cat and monkey (Macaca fascicularis). *Anat Embryol (Berl),* 185**,** 529-45.

Wallace, B. G. 1981. Distribution of AChE in cholinergic and non-cholinergic neurons. *Brain Res,* 219**,** 190-5.

Wang, Y. T. & Bieger, D. 1991. Role of solitarial GABAergic mechanisms in control of swallowing. *Am J Physiol,* 261**,** R639-46.

Wasserman, A. M., Ferreira, M., Jr., Sahibzada, N., Hernandez, Y. M. & Gillis, R. A. 2002. GABA-mediated neurotransmission in the ventrolateral NTS plays a role in respiratory regulation in the rat. *Am J Physiol Regul Integr Comp Physiol,* 283**,** R1423-41.

Watanabe, S., Sanuki, R., Sugita, Y., Imai, W., Yamazaki, R., Kozuka, T., Ohsuga, M. & Furukawa, T. 2015. Prdm13 regulates subtype specification of retinal amacrine interneurons and modulates visual sensitivity. *J Neurosci,* 35**,** 8004-20.

Watson, C. & Kayalioglu, G. 2009. The Organization of the Spinal Cord. *In:* Watson, C., Paxinos, G. & Kayalioglu, G. (eds.) *The Spinal Cord.* Amsterdam: Academic Press.

Watson, C., Paxinos, G., Kayalioglu, G. & Heise, C. 2009. Atlas of the Mouse Spinal Cord. *In:* Watson, C., Paxinos, G. & Kayalioglu, G. (eds.) *The Spinal Cord.* Amsterdam: Academic Press.

Weber, U. J., Bock, T., Buschard, K. & Pakkenberg, B. 1997. Total number and size distribution of motor neurons in the spinal cord of normal and EMC-virus infected mice--a stereological study. *J Anat,* 191 (Pt 3)**,** 347-53.

Wenningmann, I. & Dilger, J. P. 2001. The kinetics of inhibition of nicotinic acetylcholine receptors by (+)-tubocurarine and pancuronium. *Mol Pharmacol,* 60**,** 790-6.

Westfall, D. P., Stitzel, R. E. & Rowe, J. N. 1978. The postjunctional effects and neural release of purine compounds in the guinea-pig vas deferens. *Eur J Pharmacol,* 50**,** 27-38.

Whatley, V. J., Mihic, S. J., Allan, A. M., Mcquilkin, S. J. & Harris, R. A. 1994. gamma-aminobutyric $acid_A$ receptor function is inhibited by microtubule depolymerization. *J Biol Chem,* 269**,** 19546-52.

Wiedner, E. B., Bao, X. & Altschuler, S. M. 1995. Localization of nitric oxide synthase in the brain stem neural circuit controlling esophageal peristalsis in rats. *Gastroenterology,* 108**,** 367-75.

Wilson, J. M., Rempel, J. & Brownstone, R. M. 2004. Postnatal development of cholinergic synapses on mouse spinal motoneurons. *J Comp Neurol,* 474**,** 13-23.

Wilson, L. & Maden, M. 2005. The mechanisms of dorsoventral patterning in the vertebrate neural tube. *Dev Biol,* 282**,** 1-13.

Wingo, W. J. & Awapara, J. 1950. Decarboxylation of L-glutamic acid by brain. *J Biol Chem,* 187**,** 267-71.

Woolf, C. J. & Fitzgerald, M. 1986. Somatotopic organization of cutaneous afferent terminals and dorsal horn neuronal receptive fields in the superficial and deep laminae of the rat lumbar spinal cord. *J Comp Neurol,* 251**,** 517-31.

Wootz, H., Fitzsimons-Kantamneni, E., Larhammar, M., Rotterman, T. M., Enjin, A., Patra, K., Andre, E., Van Zundert, B., Kullander, K. & Alvarez, F. J. 2013. Alterations in the motor neuron-renshaw cell circuit in the Sod1(G93A) mouse model. *J Comp Neurol,* 521**,** 1449-69.

Wuchert, F., Ott, D., Murgott, J., Rafalzik, S., Hitzel, N., Roth, J. & Gerstberger, R. 2008. Rat area postrema microglial cells act as sensors for the toll-like receptor-4 agonist lipopolysaccharide. *J Neuroimmunol,* 204**,** 66-74.

Xu, Y., Lopes, C., Wende, H., Guo, Z., Cheng, L., Birchmeier, C. & Ma, Q. 2013. Ontogeny of excitatory spinal neurons processing distinct somatic sensory modalities. *J Neurosci,* 33**,** 14738-48.

Yamamura, H. I. & Snyder, S. H. 1972. Choline: high-affinity uptake by rat brain synaptosomes. *Science,* 178**,** 626-8.

Yamamura, H. I. & Snyder, S. H. 1973. High affinity transport of choline into synaptosomes of rat brain. *J Neurochem,* 21**,** 1355-74.

Yasaka, T., Kato, G., Furue, H., Rashid, M. H., Sonohata, M., Tamae, A., Murata, Y., Masuko, S. & Yoshimura, M. 2007. Cell-type-specific excitatory and inhibitory circuits involving primary afferents in the substantia gelatinosa of the rat spinal dorsal horn in vitro. *J Physiol,* 581**,** 603-18.

Yasaka, T., Tiong, S. Y., Hughes, D. I., Riddell, J. S. & Todd, A. J. 2010. Populations of inhibitory and excitatory interneurons in lamina II of the adult rat spinal dorsal horn revealed by a combined electrophysiological and anatomical approach. *Pain,* 151**,** 475-88.

Zagoraiou, L., Akay, T., Martin, J. F., Brownstone, R. M., Jessell, T. M. & Miles, G. B. 2009. A cluster of cholinergic premotor interneurons modulates mouse locomotor activity. *Neuron,* 64**,** 645-62.

Zhao, C., Eisinger, B. & Gammie, S. C. 2013. Characterization of GABAergic neurons in the mouse lateral septum: a double fluorescence in situ hybridization and immunohistochemical study using tyramide signal amplification. *PLoS One,* 8**,** e73750.

Zhou, L., Wang, Z. Y., Lian, H., Song, H. Y., Zhang, Y. M., Zhang, X. L., Fan, R. F., Zheng, L. F. & Zhu, J. X. 2014. Altered expression of dopamine receptors in cholinergic motoneurons of the hypoglossal nucleus in a 6-OHDA-induced Parkinson's disease rat model. *Biochem Biophys Res Commun,* 452**,** 560-6.

Zhou, Y., Holmseth, S., Guo, C., Hassel, B., Hofner, G., Huitfeldt, H. S., Wanner, K. T. & Danbolt, N. C. 2012. Deletion of the gamma-aminobutyric acid transporter 2 (GAT2 and SLC6A13) gene in mice leads to changes in liver and brain taurine contents. *J Biol Chem,* 287**,** 35733-46.

Zhou, Y., Yamamoto, M. & Engel, J. D. 2000. GATA2 is required for the generation of V2 interneurons. *Development,* 127**,** 3829-38.

Zimmermann, H. 2008. ATP and acetylcholine, equal brethren. *Neurochem Int,* 52**,** 634-48.

Zoccal, D. B., Furuya, W. I., Bassi, M., Colombari, D. S. & Colombari, E. 2014. The nucleus of the solitary tract and the coordination of respiratory and sympathetic activities. *Front Physiol,* 5**,** 238.